Title
Design and Optimization of a Biomanufacturing-Driven Reference Mission Architecture for the Human Exploration of Mars

Author
Berliner, Aaron Jacob

Publication Date
2022

Peer reviewed|Thesis/dissertation

Design and Optimization of a Biomanufacturing-Driven Reference Mission Architecture for the Human Exploration of Mars

by

Aaron Jacob Berliner

A dissertation submitted in partial satisfaction of the

requirements for the degree of

Joint Doctor of Philosophy
with The University of California, San Francisco

in

Bioengineering

in the

Graduate Division

of the

University of California, Berkeley

Committee in charge:

Professor Adam P. Arkin, Chair
Professor Douglas Clark
Professor William Collins
Professor Anthony Hunt

Summer 2022

Design and Optimization of a Biomanufacturing-Driven Reference Mission Architecture for the Human Exploration of Mars

Abstract

Design and Optimization of a Biomanufacturing-Driven Reference Mission Architecture for the Human Exploration of Mars

by

Aaron Jacob Berliner

Joint Doctor of Philosophy
with The University of California, San Francisco in Bioengineering

University of California, Berkeley

Professor Adam P. Arkin, Chair

Despite a myriad of national space agencies, industrial partners, university laboratories, and policy groups preparing for human exploration of the Martian surface, there remains a need for a single reference mission architecture (RMA) that models and captures the vast design parameter space, and hence the complexities, of a Mars human exploration operation. The available literature often focuses on shorter-term, opposition-class exploration missions of approximately 30 days of surface operations, instead of the more probable, longer-term, conjunction-class exploration missions of approximately 500 days of surface operations. A critical aspect of these longer duration missions is determining the food, medicine, and materials that are necessary to support a crew over the specified lengthy time-period. In the following dissertation I demonstrate the progress towards the development of a biomanufactory-driven RMA. A crewed mission to and from Mars may include an exciting array of enabling biotechnologies that leverage inherent mass, power, and volume advantages over traditional abiotic approaches. I begin this dissertation by articulating the scientific and engineering goals and constraints, along with example systems, that guide the design of a surface biomanufactory. Extending past arguments for exploiting stand-alone elements of biology, I argue for an integrated biomanufacturing plant replete with modules for microbial *in situ* resource utilization, production, and recycling of food, pharmaceuticals, and biomaterials required for sustaining future intrepid astronauts. Here I also discuss aspirational technology trends in each of these target areas in the context of human and robotic exploration missions. I then formalize the mathematical framework for modeling a biomanufacturing system developing the resources for sustaining a human exploration mission on the surface of Mars by establishing mission goals, extending the Equivalent System Mass framework for comparision of missions, develop the framework for modeling a Martian resource inventory in terms of supplies both produced via ISRU processes and transported as cargo from Earth, and develop the framework required for sustaining a human crew in terms

of essential resources. Using this collection of frameworks, I develop a software framework to implement and integrate process models that can be experimentally validated by the collaborations of the Center for the Utilization for Biological Engineering in Space, beginning with the crop cultivation models for food consumption and pharmaceutical development for astronauts. Finally, I presents an argument for how Space Bioprocess Engineering drives sustainability on- and off-World. Although *raison d'etre* of Space Bioprocess Engineering is the design, realization, and management of biologically-driven technologies for supporting offworld human exploration, it has the potential to offer transformative solutions to the global community in pursuit of the United Nations Sustainable Development Goals. Here we address the growing sentiment that investment in spacefaring enterprises should be redirected towards sustainability programs. In outlining the Earth-benefits of dual-use Space Bioprocess Engineering technologies, we both show that continued investment is justified and offer insight into specific R&D strategies.

To My Father,
Who I laid to Earth in sound.

To My Mother,
Who gave me the stars in song.

To My Mentor,
With whom that distance I sojourn in symphony.

Contents

Contents ii

List of Figures iv

List of Tables xv

1 Introduction 4
- 1.1 Background and Motivation . . . 4
- 1.2 Thesis Statement . . . 5
- 1.3 Thesis Outline . . . 6

2 Space Bioprocess Engineering on the Horizon 10
- 2.1 An Inclusive Mandate To Leverage SBE . . . 11
- 2.2 Specialization of SBE Metrics and Methods . . . 13
- 2.3 Training of SBE Minds . . . 19
- 2.4 Moving Forward . . . 20

3 Perspective: Towards a Biomanufactory on Mars 22
- 3.1 Feasibility, Needs, and Mission Architecture . . . 22
- 3.2 Food and Pharmaceutical Synthesis . . . 24
- 3.3 *In situ* Materials Manufacturing . . . 27
- 3.4 *In situ* Resource Utilization . . . 29
- 3.5 Loop Closure and Recycling . . . 31
- 3.6 Discussion and Roadmap . . . 33

4 Mathematical Formulations For Mission Design, Comparison, and Optimization 37
- 4.1 Towards an Extension of Equivalent System Mass . . . 37
- 4.2 Extending ESM for Long-Duration Mission Profiles . . . 40
- 4.3 Towards xESM Analysis and Optimization Under Uncertainty . . . 47
- 4.4 Future Work . . . 49
- 4.5 Methods . . . 50

5 Computational Methods and Construction of echusOverlook Software 52

5.1 Introduction to Mission Design Software . . . 53
5.2 Preliminary eO Software Design and Overview . . . 55
5.3 Software Overview . . . 58
5.4 Results . . . 60

6 Case Study 1: Photovoltaics-Driven Power Production on Mars 67
6.1 Power Production on Mars . . . 67
6.2 Results . . . 69
6.3 Discussion . . . 72

7 Case Study 2: Nitrogen Accountancy in Space Agriculture 75

8 Case Study 3: Evaluating the cost of pharmaceutical purification in space 85
8.1 The need for a pharmaceutical foundry in space . . . 86
8.2 The bottleneck of space foundries: purification . . . 87
8.3 Space economics . . . 88
8.4 Materials & Methods . . . 90
8.5 Results & Discussion . . . 95

9 Futures: Biomanufacturing for Space Exploration - What to Take, When to Make, How to Break Even 109
9.1 Off-world Biomanufacturing Approaches . . . 111
9.2 Integrating Biomanufacturing with Mission-Architecture . . . 116
9.3 Paths to Realization of Emerging Technologies . . . 119
9.4 Outlook . . . 120

10 Futures: Space Bioprocess Engineering Drives Sustainability On- and Off-World 121

11 Appendix 129
11.1 SI: xESM . . . 130
11.2 SI: Case Study 1 . . . 132
11.3 SI: Case Study 3 . . . 162
11.4 SI: Space Biomanufacturing . . . 166
11.5 SI: Sustainability . . . 193

Bibliography 196

List of Figures

0.1 NNX17AJ31G TreeMap Visualization 3
0.2 Y5 Spring Review Group Photo 3

1.1 Artist's rendering of a crewed Martian biomanufactory powered by photovoltaics, fed via atmospheric ISRU, and capable of food and pharmaceutical synthesis (FPS), *in situ* manufacturing (ISM), and biological loop closure (LC). Artwork by Davian Ho. 5

2.1 **Overview of Space Bioprocess Engineering challenges, components, and platforms. (a)** Venn Diagram-based definition of Space Bioprocess Engineering (SBE) as an interdisciplinary field. **(b)** NASA's space technology grand challenges[514] key by shape and colored by group. **(c)** Possible SBE components separated by colors for *in situ* resource utilization (ISRU), food and pharmaceutical synthesis (FPS), *in situ* manufacturing (ISM), and loop closure (LC), with the biological processes inherent to each represented below in circles. **(d)** Platform evolution for biological experiments starting with Earth-orbit CubeSats and proceeding through the ISS, Mars-and-Luna-based rovers, to Lunar and cis-Lunar based human and autonomous systems via the Artemis program. 12
2.2 **Overview of space systems bioengineering (SBE) performance metrics and the SBE-specific Design, Build, Test, Learn (DBTL) cycle.** The SBE performance metrics in **(a)** are shaded to correspond to the top level core constraints and engineering targets within the **(b)** DBTL cycle. 15
2.3 **Conceptual undergraduate SBE program**. The SBE program is broken in three segments: core STEM courses, introduction to space ecosystem courses, and track specialization courses for tracks in bioengineering, astronautics, planetary science & astronomy, and systems engineering. 19

3.1 Proposed surface operations are drawn from inventories of *in situ* resources (red) such as ice, atmosphere, regolith, and sunlight. Atmospheric feedstocks of carbon and nitrogen are biologically fixed via the ISRU (*in situ* resource utilization) biomanufactory components (including abiotic processes, purple), providing the source of biopolymer manufacturing via the ISM (*in situ* manufacturing) component (grey) and food via the FPS (food and pharmaceutical synthesis) component (green), which are used for astronaut consumption and utilization during mission operations. Waste from each of these elements is collected and fed into the LC (loop closure) element (pink) to maximize efficiency and reduce the cost of supply logistics from Earth. 23

3.2 FPS (green) system breakdown for biomanufactory elements of **(A)** crops, **(B)** a biopharmaceutical, and **(C)** functional food production. In all cases, growth reactors require power (electrical current symbol) and light (γ). **(A)** Crop biomass and oxygen gas (O_2) are produced from hydroponically grown plants using seeds and media ({M}) derived from supply cargo. The reactor is also supplied with an ammonium (NH_4^+) nitrogen source and CO_2 carbon source from ISRU processes. **(B)** In a similar fashion, medicine can be produced from genetically modified crops such as lettuce. **(C)** Functional foods such as nutritional supplements are produced via autotrophic growth of *A. platensis*. In all cases, biomass is produced, collected, and inedible biomass is distributed to the LC module for recycling. . . 25

3.3 ISM systems breakdown for biomanufactory elements of biopolymer production and 3D-printing. 3D printed parts are fabricated from bioproduced plastics. Biopolyesters such as PHB, along with corresponding waste products, are formed in cargo-supplied reactors with the aid of microorganisms. A variety of available carbon feedstocks can serve as substrates for aerobic auto-, hetero-, or mixotrophic microorganisms such as *C. necator*, *Methylocystis parvus* and *Halomonadaceae*. All three microbes are capable of using C_2 feedstocks (like acetate), while *C. necator* and *Methylocystis* can also use C_1 feedstocks. The former utilizes a combination of CO_2 and H_2 (large dotted line), while only *M. parvus* can leverage CH_4 (small dotted line). 28

3.4 ISRU (purple in Fig. 3.1) system breakdown of biomanufactory elements. **(A)** Carbon fixation with the autotrophic bacteria *Sporomusa ovata* or *Cupriavidus necator* through electrosynthesis or lithoautotrophic fixation of C_1-carbon (cathodes or H_2 as the electron donor). **(B)** Microbial nitrogen fixation with diazotrophic bacteria like *Rhodopseudomonas palustris* growing photoheterotrophically. **(C)** Regolith (Reg) enrichment using the perchlorate-reducing microbe *Azospira suillum*. Black lines represent material and energy flows related to biological consumption and production. Orange lines indicate additional power supply to the system. 30

3.5 LC-based (pink) anaerobic digestion of mission waste such as inedible plant matter, microbial biomass, human, and other wastes produce methane, volatile fatty acids (VFAs), and digestate rich with key elemental nutrients (N, P, K), thereby supplementing ISRU operation. 32

3.6 Proposed roadmap from 2021 to 2052 in $\log_2$-scale time of Earth-based developments (black) and their relationships to ISS (gold), lunar (blue), and Martian (red) missions. Missions range in status from currently operational, to enroute, planned, and proposed. Reference Mission Architecture (RMA)-S is a 30-sol mission, and RMA-L are missions with more than 500 sols of surface operations. RMA-L1 is the mission target for deployment of a biomanufactory. An arrival at target location is denoted with a symbol to indicate its type as orbiter, rover, lander, helicopter, support, or crewed operations. Circled letters are colored by location and correspond to specific milestones or opportunities for biomanufactory development. 33

4.1 Transit Diagram of proposed Mission Architecture. In **Profile** 1(grey), **(A)** a crewed transit ship is launched directly from the surface of Earth and **(B)** lands on the surface of Mars where **(C)** the crew assembles the cargo in a habitat and carries out **(D)** surface operations until **(E)** the crew launches from their initial transit ship from the surface of Mars into space and **(F)** lands back on the surface of Earth. In **Profile** 2(purple), **(A)** cargo transit ships without crew are launched directly from the surface of Earth and **(B)** land on the surface of Mars where cargo can be unloaded. In the case of reusable rocket systems[449], **(C)** the cargo rockets can be launched from Mars and returned to Earth. Once all the cargo has been loaded onto the surface of Mars, **(D)** a crewed transit ship is launched directly from the surface of Earth and **(E)** lands on the surface of Mars where (F) the crew assembles the cargo in a habitat and carries out **(G)** surface operations until **(H)** the crew launches from their initial transit ship from the surface of Mars into space and **(I)** lands back on the surface of Earth. In **Profile** 3(green), a number of **(A)** cargo transit ships without crew are launched directly from the surface of Earth and either **(B)** supply a previously interplanetary rocket then **(C)** return to the surface of Earth or **(D)** travel to the surface of Mars where **(E)** cargo can be unloaded. In the case of reusable rocket systems, **(F)** the cargo rockets can be launched from Mars and returned to Earth. Once all the cargo has been loaded on the surface of Mars, **(G)** a crewed transit ship is launched directly from the surface of Earth to Earth Orbit **(H)** where it rendezvous with an interplanetary rocket which **(I)** travels to Martian orbit. The crew **(J)** then boards a descent vehicle and lands on the surface of Mars where **(K)** the crew assembles the cargo in a habitat and carries out **(L)** surface operations until **(M)** the crew launches from their initial transit ship from the surface of Mars into **(N)** Martian orbit where they again rendezvous with their interplanetary rocket which travels to **(O)** Earth orbit at which point they board a descent rocket in which they **(P)** finally return to the surface of Earth. 39

4.2 xESM equation for Profile 3 (Figure 4.1) with terms decomposed by subsystem. **(a)** Breakdown of inventory transfers across mission timeline colored by mission segment. **(b)** The generalized xESM equation colored by mission segment. **(c)** Expanded xESM equation with colored by mission segment with a non-exhaustive set of specific segment-dependent relationships elucidated. 42

4.3 Comparison of ESM and xESM metrics for whole system mass scenarios. **(a)** Log-scale comparison of mission segment mass for increasing mission assembly. **Case 0** is a baseline inventory for the flight from Earth orbit to Mars orbit (tr_1) and back (tr_2), while life support for a 500 day Mars orbit (tr_3) is added in **Case 1**. The mission in **Case 2** includes descent (des), Mars surface operations (sf), and ascent (asc). All inventory for sf is predeployed (pd) in **Case 3**. As the mission grows, both the mass required and the difference between xESM and ESM increases. The final case shows falling xESM with the removal of sf inventory from tr_1 and des. **(b)** Inventory difference between xESM and ESM in raw mass, volume, power, cooling, and crewtime across each mission segment, before the application of location and equivalency factors. **(c)** Raw inventory difference between xESM and ESM displayed across the four cases. 44

4.4 Comparison of ESM and xESM metrics focused on the stored food cost. **(a)** Log-scale comparison of mission segment mass for different food strategies. **Case 2s** is the food cost of Case 2 in Figure 4.3. **Case 2b** reduces the amount of stored food for sf from 500 days to 70 days, assuming a hypothetical future agriculture system could grow the difference. In **Case 3b**, the sf inventory is predeployed, and grown food also sustains the majority of sf. The ESM differences between 2s and 2b and between 2s and 3b show the rough mass requirement for the design and development of such an agricultural system. **(b)** Raw inventory difference between xESM and ESM mass, volume, power, cooling, and crewtime across each mission segment, before the application of location and equivalency factors. **(c)** Raw inventory difference between xESM and ESM displayed across the three cases. 45

5.1 eO Meeting Attendees 56

5.2 Feedback from a form distributed to stakeholders to gauge the interest for in eO. 57

5.3 **Overview or echusOverlook software.** Design of eO **(a)** user journey/story with **(b)** system architecture. 59

5.4 **Technoeconomic Validation of eO against the NASA ALSSAT**. **(a)** Visual depiction of transition matrix for closed loop "bring everything" scearnio. **(b)** Bar chart demonstrating eO calculation and comparison of 4 scenarios in terms of the standard ESM metric using a breakdown of ESM by components such as Mass, Volume, Power, Cooling, and Crew Time. **(c)** Bar chart with same comparisons as (b) using ESM fraction. **(d)** Bar chart demonstrating eO calculation and comparison of 4 scenarios in terms of the standard ESM metric using a breakdown of ESM by material composition in terms of metal, plastic electronics, water, etc. **(e)** Bar chart with same comparisons as (d) using ESM fraction. (f) Bar chart comparison of subsystems for each scenario. 63

5.5 Process simulation in terms of **(a)** representation of systems & states, **(b)** dynamics, and a preliminary **(c** technoeconomic analysis. 65

6.1 **Overview and calculation of spectral flux using atmospheric data.** **(A)** Sunlight incident on the solar cells is mediated by orbital geometry and local atmospheric composition of gases, ice, and dust. **(B, C, and D)** Temperature, partial pressure of atmospheric gases and concentration and effective radii of ice and dust particles as a function of altitude above the surface. **(E)** Information flow in the calculation scheme. Dotted lines represent functions used for calculations; solid lines represent data used as parameters. MCD, Mars Climate Database; LRT, LibRadtran. **(F)** Total (black), direct (blue), and diffuse (red) solar flux at Jezero Crater at solar noon averaged over the course of a typical Martian year. In **(B)**, **(C)**, **(D)**, and **(F)**, solid lines represent yearly averages and shaded regions represent the standard deviation due to seasonal variation. 68

6.2 **Theoretical efficiencies of PV and PEC devices.** Detailed-balance efficiency limits as a function of bandgap energies for **(A)** single-junction, **(B)** two-junction, **(C)** three-junction photovoltaic devices. **(D, and E)** Solar-to-chemical (STC) efficiency for two-junction water splitting PEC devices producing molecular hydrogen with 0 mV (D) and 700 mV (E) overvoltage. **(F)** STC efficiency and optimal bandgaps for two-junction H_2-generating PEC devices as a function of overvoltage. Coloring in **(A)** and **(F)** correspond to contour coloring in **(B, C)** and **(D, E)** respectively. Average flux at solar noon at Jezero Crater is used as the reference solar spectrum. 70

6.3 **PV and PEC production rates.** **(A)** Average and **(B)** daily maximum solar flux (black, left axis) and surface temperature (purple, right axis) as function of **(A)** time of day and **(B)** time of year. **(C, E)** average and **(D, F)** daily maximum production capacity of power **(C, D)** and H_2 **(E, F)** using 3-junction PV and 2-junction PEC cells as described in the main text. Solid lines in **(A, C, E)** correspond to averages; shaded areas represent the standard deviation due to seasonal variation. Jezero Crater is used as the location for plots. 71

6.4 **Solar productivity across the Martian surface.** **(A)** Average daily solar power production capacity across the Martian surface. **(B)** Total carry-along mass required for power production using the PV+E generation system. Black dashed line corresponds to breakeven location with nuclear power generation. **(C)** Carry-along mass breakdown for locations in **(B)** for each power generation option. Black dashed line corresponds to breakeven with nuclear power generation. Optimal **(D)** top, **(E)** middle, **(F)** bottom bandgaps for the 3-junction PV array. 73

7.1 Mars-based Agriculture Overview. **(a)** Scheme for deploying agriculture systems on Mars using ISRU with an expansion of potential crops within habitat and their index within extended MEC model. The expansion of crop systems includes example groupings of crops with hydroponic reactor logistics. **(b)** Systems diagram for crop growth reactor taking in media ($\{M\}$), ammonium (NH_4^+), water (H_2O), carbon dioxide (CO_2), light (γ), and power ($\textcircled{\sim}$) to produce some crop (in this case lettuce), pharmaceuticals, and biowaste. **(c)** Graphical breakdown of and interaction between MEC Lettuce model variables. **D.** Total crop biomass $\hat{m}_{\mathrm{T}}$ (blue) and crop growth rate $\hat{\dot{m}}_B$ (gold) for Dry Bean, Lettuce, Peanut, Rice, Soybean, Sweet Potato, Tomato, Wheat, White Potato at $\Phi_\gamma = 500$ [$\mu\mathrm{mol}_\gamma\,\mathrm{m}^{-2}\,\mathrm{s}^{-1}$], $c_{\mathrm{CO2}} = 1200$ [$\mu\mathrm{mol}_{\mathrm{CO2}}\,\mathrm{mol}_{\mathrm{air}}^{-1}$]. **E.** Contours of biomass accumulation for each crop terminating at each crop's harvest time t_{M} across Φ_γ and c_{CO2}. 77

7.2 Total crop biomass $\hat{m}_{\mathrm{T}}$ (blue) and crop growth rate $\hat{\dot{m}}_B$ (gold) for Dry Bean, Lettuce, Peanut, Rice, Soybean, Sweet Potato, Tomato, Wheat, White Potato at $\Phi_\gamma = 500$ [$\mu\mathrm{mol}_\gamma\,\mathrm{m}^{-2}\,\mathrm{s}^{-1}$], $c_{\mathrm{CO2}} = 1200$ [$\mu\mathrm{mol}_{\mathrm{CO2}}\,\mathrm{mol}_{\mathrm{air}}^{-1}$]. 78

7.3 Contours of biomass accumulation for each crop terminating at each crop's harvest time t_{M} across Φ_γ and c_{CO2}. 79

7.4 **(a)** Measured areal ("per area") biomass and MEC model prediction. The MEC output was calculated with Φ_γ of $225\,\mathrm{mol}\gamma\,\mathrm{m}^{-2}\,s^{-1}$ and c_{CO2} of $525\,\mathrm{ppm}$. **(b)** Measured percentage of total nitrogen by weight in plants over time. Only one measurement could be performed at $20\,\mathrm{d}_{\mathrm{AE}}$. **(c)** Nitrogen productivity calculated from two measured quantities, biomass and nitrogen content. Error bars represent propagated error. **(d)** Relative change (RC, $\underline{\Delta}c$), of measured molar concentration, $c(t)$, of ammonia and nitrate, and their calculated sum, to initially charged concentration, $c(t_0)$, in NSS reservoirs over time for each N condition, where $\underline{\Delta}c \equiv [c(t) - c(t_0)]/c(t_0)$. Error bars represent 1 SD. $N = 3$ for each data point. **(e)** Lettuce in different conditions at $27\,\mathrm{d}_{\mathrm{AE}}$. The range marked in grey is the specified harvest time, t_{M}, [range-units = single]3035AE [17]. Error bars represent 1 SD. $N = [5, 10]$ for each data point. Solid lines represent measurements; dotted lines are derived/calculated values 82

8.1 Monoclonal antibody production consists generically of product accumulation, clarification, initial purification, formulation, and fill & finish. Here we investigate six technologies for the capture step within the first purification step in a space mission context using extended equivalent system mass. The manufacturing origin of the capture reagent is denoted as either **(A)** abiotic or **(B)** biotic. . . . 90

8.2 An illustration of the reference mission architecture in which **(A)** a crewed ship is launched from the surface of Earth and lands on Mars and **(B)** assembles a pre-deployed habitat on the Martian surface to perform operations before **(C)** a return transit to Earth on the same ship. Pharmaceutical needs are supported by flown stores until partway through surface operations, at which point needs are met by pharmaceuticals produced using *in situ* resource utilization. Production is initiated prior to the need window to ensure adequate stocks are generated by the time it is needed. Rocket artwork adapted from Musk, 2017[394]. Habitat artwork by Davian Ho. 92

8.3 **(A)** Scheduling optimization for the establishment of base case scenarios for each unit procedure. The value for number of batches corresponding to the minimum equivalent system mass for each unit procedure, as indicated by black circle markers. Key operational parameters impacted by mission scheduling (shown using the VIN procedure) include **(B)** unit underutilization or vacancy, **(C)** equipment underutilization or vacancy, in this case represented by the centrifuge as the bottleneck, **(D)** the number of use cycles, and **(E)** the total quantity of monoclonal antibody (mAb) per mission and per surface operation (sf). CHM, pre-packed chromatography; SPN, spin column; MAG, magnetic bead; VIN, plant virus-based nanoparticle; ELP, elastin-like polypeptide; OLE, oilbody-oleosin. 96

8.4 Base case equivalent system mass results broken down by **(A)** mass (M), volume (V), power (P), and labor time (T) constituents, **(B)** transit to Mars (tr_1), surface operations (sf), and return transit (tr2) mission segments, and **(C)** labor (L), equipment (E), raw materials (R), and consumables (C) cost category for the six tested Protein A-based monoclonal antibody affinity capture step unit procedures segregated by abiotic (white background) and biotic (grey background) technologies. Also shown are the **(D)** labor and operation times, **(E)** number of use cycles, and **(F)** number of units required for each unit procedure to meet the reference mission demand. CHM, pre-packed chromatography; SPN, spin column; MAG, magnetic bead; VIN, plant virus-based nanoparticle; ELP, elastin-like polypeptide; OLE, oilbody-oleosin. 97

8.5 **(A)** Process mass intensity (PMI) evaluation of the unit procedures broken down by raw materials (R) and consumables (C) contributions. **(B)** Cycle volume for each unit procedure. CHM, pre-packed chromatography; SPN, spin column; MAG, magnetic bead; VIN, plant virus-based nanoparticle; ELP, elastin-like polypeptide; OLE, oilbody-oleosin. 99

8.6 Specific equivalent system mass (per unit mass monoclonal antibody produced) broken down by labor (L), equipment (E), raw materials (R), and consumables (C) cost categories as a function of feed monoclonal antibody (mAb) concentration for **(A)** CHM, **(B)** SPN, **(C)** MAG, **(D)** VIN, **(E)** ELP, and **(F)** OLE. CHM, pre-packed chromatography; SPN, spin column; MAG, magnetic bead; VIN, plant virus-based nanoparticle; ELP, elastin-like polypeptide; OLE, oilbody-oleosin. . 100

8.7 Specific equivalent system mass (per unit mass monoclonal antibody produced) broken down by labor (L), equipment (E), raw materials (R), and consumables (C) cost categories as a function of mission production demand for monoclonal antibody for **(A)** CHM, **(B)** SPN, **(C)** MAG, **(D)** VIN, **(E)** ELP, and **(F)** OLE. CHM, pre-packed chromatography; SPN, spin column; MAG, magnetic bead; VIN, plant virus-based nanoparticle; ELP, elastin-like polypeptide; OLE, oilbody-oleosin. 101

8.8 Evaluation of extended equivalent system mass values in various mission configurations broken down by labor (L), equipment (E), raw materials (R), and consumables (C) cost categories cost category and mass (M), volume (V), power (P), and labor time (T) constituents for CHM, **(A, G)**, SPN, **(B, H)**, MAG, **(C, I)**, VIN, **(D, J)**, ELP **(E, K)**, and OLE, **(F, L)**. Configurations include the base case scenario of manufacturing resources flown with the crew for pharmaceutical production on the surface and return transit (Base), and alternatives in which the manufacturing resources are flown prior to the crew in pre-deployment, (+)pd, the production window is limited to surface operations, (-)tr_2, and a combination of the two previously stated alternatives, (+)pd (-)tr_2. CHM, pre-packed chromatography; SPN, spin column; MAG, magnetic bead; VIN, plant virus-based nanoparticle; ELP, elastin-like polypeptide; OLE, oilbody-oleosin. 103

8.9 Changes in extended equivalent system mass values with different capacity centrifuge models broken down by labor (L), equipment (E), raw materials (R), and consumables (C) cost categories and mass (M), volume (V), power (P), and labor time (T) constituents for SPN **(A, E)**, VIN **(B, F)**, ELP **(C, G)**, and OLE **(D, H)**. SPN, spin column; VIN, plant virus-based nanoparticle; ELP, elastin-like polypeptide; OLE, oilbody-oleosin. 104

8.10 Changes in extended equivalent system mass values with reusability of purification technology broken down by labor (L), equipment (E), raw materials (R), and consumables (C) cost categories and mass (M), volume (V), power (P), and labor time (T) constituents for CHM **(A, C)**, and ELP **(B, D)**. (-)Reuse considers the technology as single-use and accordingly discards the unit procedure cleaning operations; (+) Reuse considers additional reuse cycles of the technology. CHM, pre-packed chromatography; ELP, elastin-like polypeptide. 105

9.1 **Approaches to in situ biomanufacturing dependent on off-world cases.** The context-specific off-world cases 1-4 are defined in **a**, mapped as quadrants on qualitative spectra for the availability of *in situ* resources and logistic resupply. The surface-accessible *in situ* resources for the Moon and Mars are compared in **b** in form of gases and solids, broken down into elemental compositions (SNOPs: sulfur, nitrogen, oxygen, phosphorus). Biomanufacturing concepts-of-operations (CONOPS), outlined in **c**, are color-coded for the operational mode: outgoing from initial cargo (black lines), CONOPS can rely on either loop-closure (LC, blue lines), *in situ* resource utilization (ISRU, orange lines), or both (LC+ISRU, green lines). 112

9.2 **Breakdown of inventory elements dependent on mission scenario.** Panel **a** provides an overview of parameters for exemplar mission-design scenarios: 'A' and 'B' correspond to single sorties (N) to the Moon and Mars respectively using standard surface operation duration[17], while 'C' and 'D' correspond to multi-sortie campaigns with the same 5,400 days of total surface operation as in 'E'. These parameters can be used to calculate the ESM cost and include equivalency factors for Volume (V_{eq}), Power (P_{eq}), Cooling (C_{eq}), Crew-Time (CT_{eq}), and Location (L_{eq}). Panels **b** – **e** visualize the inventory breakdown by component (**b**), system element (**c**), and material composition (**d** & **e**), respectively: the bar-charts in panels **b** – **d** show the breakdown in ESM units (on the left, in mass [kg]), and the fractional breakdown of each scenario (on the right, unit-less). The bar-charts in panel **e** visualize the absolute (left, in mass [kg]) and fractional (right, unit-less) inventory breakdown of material composition. ESM = Equivalent Systems Mass[314] – for more information see the BOX, as well as the SI. 115

9.3 **Breakdown of available routes for bioproduction of inventory elements from carbon dioxide—either as in situ or recovered resource.** Connecting lines represent possible paths for carbon-compound conversion of intermediates to products. Usability of different feedstocks is tied to nutritional mode of the microbial host organism (more than one nutritional mode is possible for certain organisms). Classes of products are assigned to respective microbes in respect of their metabolism as well as not represented 'shadow-characteristics' of the chassis (e.g., aerobic/anaerobic, prokaryotic/eukaryotic, metabolic rate, robustness, etc.), rather than ability to (naturally) derive the respective compounds. While metabolic engineering theoretically allows almost any bio-available compound to be produced in any organism, the effort required for realization can be excessive. For example, oxygen-dependent pathways will hardly be functional in obligate anaerobes without extensive modifications. Likewise, correct folding of proteins with high post-translational modifications in prokaryotes is unlikely. Products may or may not comprise some of the initial feedstocks, hence consecutive runs through this chart to up-cycle carbon are conceivable. 118

10.1 **Space Bioprocess Engineering technologies in the context of NASA's Space Technology Grand Challenges (STGCs) and United Nations Sustainability Development Goals (SDGs).** Specific exemplar technologies developed in service to the STGCs (shades of grey) are described in relationship to corresponding SDGs (shades of pink). More more information and references, see Table S1 in the SI. 123
10.2 **NASA-funded SBE Technology Return on Investment**. A contour plot is provided showing the financial return on investment (ROI) in $Billions as a function of the NASA ROI $:$ and the SBE fraction of the NASA budget of current $26B. The solid white line corresponds sustainability budget of $44B and the dashed white line corresponds the the ROI of sustainability investments at 13:1 [$:$]. 124

S1 **(A)** all parameters available for query in the MCD; **(B.)** example query to MCD; **(C.)** i. plot of surface temperature vs areocentric longitude for local time t = 9:00; ii. plot of surface temperature vs local time for LATITUDE = LONGITUDE = 0; iii. cylindrical projection of surface temperature; **(D.)** Plot of solar longitude vs sol number, demonstrating the eccentricity of Mars's orbit and the approximate season, with northern summer solstice occurring when Ls = 90 and northern winter solstice when Ls = 270. 132
S2 Albedo and zMOL (height above the Martian datum) maps. 135
S3 Left shows the calculated mu parameter as a scalar across geospace for $L_s = 0$. Right shows the spectral flux for lat=0, t=12 noon, and $L_s = 0$. 136
S4 Calculated Annual-Mean TOA Solar Flux distributed across Latitude 137
S5 Refractive Indices for Dust (top) and Clouds (Bottom). 138
S6 Sample Visualization of variables in `.netCDF` Mie output file for dust. 141
S7 Initial (problem) and final (solution) configurations for the RedSun software on the UC Berkeley cluster. 145
S8 Two Junction Photovoltaic Power Production and Optimal Bandgaps distributed over the Martian Grid 150
S9 Three Junction Photovoltaic Power Production and Optimal Bandgaps distributed over the Martian Grid 151
S10 Two Junction Photoelectrochemical H_2 Production and Optimal Bandgaps distributed over the Martian Grid 152
S11 Optimal Bandgap Distributions. 153
S12 **Power generation systems options.** Habitat power systems and ammonia, propellant, and bioplastics production can be powered by nuclear power generation (KRUSTY), photovoltaics with battery storage (PV+B), photovoltaics with H2 energy storage from hydrolysis (PV+E), or photoelectrochemical H2 generation and storage (PEC). 154

S13 **Carry-along mass for different power generation scenarios.** Carry-along mass across the Martian surface for PV+B, PV+E, and PEC power generation systems. PV+B and PEC systems cannot reach parity with nuclear power generation in terms of carry along mass (no locations at which the projected mass of the PV+B or PEC systems is less than the projected mass of the nuclear system). 155

S14 Schematic of deterministic unit procedure model construction grouped by operation, cost category, and equivalent system mass (ESM) constituent. 162

S15 **Alternate visualization of scenario-dependent inventory-breakdown.** The parameter description of exemplar mission-design scenarios is given in panel **a**: scenarios 'A' and 'B' correspond to single sorties (N) to the Moon and Mars respectively using standard surface-operation duration[17], while scenarios 'C' and 'D' correspond to multi-sortie campaigns with the same (total) 5,400 days of surface operation as for scenario 'E'. These parameters can be used to calculate the ESM cost and include equivalency factors for Volume (V_{eq}), Power (P_{eq}), Cooling (C_{eq}), Crew-Time (CT_{eq}), and Location (L_{eq}). A comparison of ESM and carry-along mass (both in kg) is presented in the scatter-plot **b**; the dotted line represents a 1:1 correspondence between ESM and carry-along mass to show the trade-offs in systems grouped by element in terms of non-standard mass components (volume, power, etc.) contributing to cost as compared to only mass. Color-coding of **b** corresponds to the bar-charts in **c**, where the carry-along and ESM are broken down by material-composition. Note that the carry-along and/or ESM for each scenario are plotted on a log scale. The maximum visible edge of each bar in a stack represents the corresponding component's carry-along or ESM value. . . . 192

List of Tables

2.1 Constraints on past and current experimental platforms including Small Satellites (light blue), Space Stations (medium blue), Rovers (dark blue), planned Lunar Habitation (light red), and Martian Habitation (red). The shade of color darkens with increasing complexity and cost. The specific sources can be found in the SI. 17

5.1 Comparison of Life Support Systems Software Packages 54

5.2 Mission desgin metrics. **For T/I/S-RL:** T and I are the TRL and IRL values in range $[1, 9]$, n is the number of subsystems, m is the mass of the subsystem, and S is the SRL value. **For ESM, xESM:** M is the calculated mass, $\mathcal{A}$ is the set of subsystems, $\mathcal{M}$ is the set of mission segments, M_i, V_i, P_i, C_i are the initial mass [kg], volume [m^3], power requirement [kW$_e$], and cooling requirement [kg/kW$_{\text{th}}$], D is the duration of the mission segment [sol], T_i is the crew-time requirement based on an astronaut crew-member (CM) [CM-h/sol], M_{eq} is the stowage factor for accounting for additional structural masses for a subsystem such as shelving [kg/kg], V_{eq} is the mass equivalency factor for the pressurized volume support infrastructure [kg/m^3], P_{eq} is the mass equivalency factor for the power generation support infrastructure [kg/kW$_e$], C_{eq} is the mass equivalency factor for the cooling infrastructure [kg/kW$_{\text{th}}$], T_{eq} is the mass equivalency factor for the crew-time [kg/CM-h], and L_{eq} is the location factor for the mission segment [kg/kg] which accounts for the cost to transport mass from one location in space to another. Mass equivalency factors (V_{eq}, P_{eq}, C_{eq}, T_{eq}) are used to convert the non-mass parameters to mass. **For IMLEO:**, $\mathcal{M}$ is the set of mission segments to LEO. **For SCM:** C is the systems complexity value, L is the level number, N is the number of nodes, and S is the number of subsystems. 62

8.1 List of Protein A-based monoclonal antibody capture step unit procedures included for analysis. ^{A} abiotic technology; ^{B} biotic technology 94

S1 xESM Parameters 131

S2 Initial grid dimensions. 134

S3 Initial atmospheric grid variables sourced from MCD. 134

S4 Initial planetary grid variables sourced from MCD. 135

S5 Initial solar grid variables. 137

S6 Dimensions and variables in `.netCDF` Mie output file. 140
S7 Electrochemical equivalency factor parameters. 146
S8 Comparison of optimal bandgaps for different optimization strategies 149
S9 Additional PV/Power Parameters and Conversion Factors. 157
S10 Example commercially approved monoclonal antibody (mAb) therapies of relevance to human health in space that have been considered in the determination of the reference mission pharmaceutical demand. Need basis is defined per the listed indication and FDA label. Demand estimates are derived by multiplying the FDA-approved need basis by the crew size and the duration of the demand. Asterisk (*) denotes an antibody drug conjugate. 162
S11 Unit procedure assumptions for maximal feed stream volume and monoclonal antibody (mAb) binding capacity. * based on 2 mL unit volume; actual feed stream volume added is based on the amount of stock solution required and thus mAb quantity in the feed stream. α reduced from 2 mL maximal to account for volume needed for salt solution addition (0.4 mL) and required 1:1 volume ratio of ELP:mAb. γ reduced from 2 mL maximal to account for required 1:20 volume ratio of OLE:mAb. 163
S12 Labor time standardizations applied to common operations across unit procedures. 163
S13 Equivalency factor values used to generate equivalent system mass values from constituents of mass, volume, power, cooling, and labor. 163
S14 Optimal number of batches per mission in the base case scenario for each unit procedure, as determined via minimization of equivalent system mass. 164
S15 Mars surface mission equivalency factor values used by Zabel[581] of a space greenhouse. 164
S16 Optimal number of effective batches per mission in the mAb stream composition scenario analysis conditions for each unit procedure, as determined via minimization of equivalent system mass. 164
S17 Optimal number of batches per mission in the mAb demand scenario analysis conditions for each unit procedure, as determined via minimization of equivalent system mass. 164
S18 List of centrifuge models used in the alternative centrifuge scenario. 165
S19 Optimal number of effective batches per mission in the centrifuge model alternative scenario conditions for each analyzed unit procedure, as determined via minimization of equivalent system mass. 165
S20 Parameter description of exemplar scenarios—scenarios 'A' and 'B' correspond to single sorties ($N = 1$) to Moon and Mars respectively using standard surface operation duration[17], while scenarios 'C' and 'D' correspond to multi-sortie campaigns with the same 5,400 days of surface operation as the single-sortie scenario 'E'. All scenarios consider a crew-strength of four astronauts. These parameters can be used to calculate the ESM cost and include equivalency factors for volume (V_{eq}), power (P_{eq}), cooling (C_{eq}), crew-time (CT_{eq}), and location (L_{eq}). 167

S21 ESM parameters for all inventory items broken down by system and subsystem for each scenario described in Table S20. Parameters included are mass M [kg], V [m^3], power P [kW], cooling C [kW], and crew-time CT [hr][17, 317]. The ESM values correspond to a single sortie $S_{\text{num}} = 1$. (ORU = Orbital Replacement Unit) 168
S21 ESM parameters for all inventory items broken down by system and subsystem for each scenario described in Table S20. Parameters included are mass M [kg], V [m^3], power P [kW], cooling C [kW], and crew-time CT [hr][17, 317]. The ESM values correspond to a single sortie $S_{\text{num}} = 1$. (ORU = Orbital Replacement Unit) 169
S21 ESM parameters for all inventory items broken down by system and subsystem for each scenario described in Table S20. Parameters included are mass M [kg], V [m^3], power P [kW], cooling C [kW], and crew-time CT [hr][17, 317]. The ESM values correspond to a single sortie $S_{\text{num}} = 1$. (ORU = Orbital Replacement Unit) 170
S21 ESM parameters for all inventory items broken down by system and subsystem for each scenario described in Table S20. Parameters included are mass M [kg], V [m^3], power P [kW], cooling C [kW], and crew-time CT [hr][17, 317]. The ESM values correspond to a single sortie $S_{\text{num}} = 1$. (ORU = Orbital Replacement Unit) 171
S21 ESM parameters for all inventory items broken down by system and subsystem for each scenario described in Table S20. Parameters included are mass M [kg], V [m^3], power P [kW], cooling C [kW], and crew-time CT [hr][17, 317]. The ESM values correspond to a single sortie $S_{\text{num}} = 1$. (ORU = Orbital Replacement Unit) 172
S21 ESM parameters for all inventory items broken down by system and subsystem for each scenario described in Table S20. Parameters included are mass M [kg], V [m^3], power P [kW], cooling C [kW], and crew-time CT [hr][17, 317]. The ESM values correspond to a single sortie $S_{\text{num}} = 1$. (ORU = Orbital Replacement Unit) 173
S21 ESM parameters for all inventory items broken down by system and subsystem for each scenario described in Table S20. Parameters included are mass M [kg], V [m^3], power P [kW], cooling C [kW], and crew-time CT [hr][17, 317]. The ESM values correspond to a single sortie $S_{\text{num}} = 1$. (ORU = Orbital Replacement Unit) 174
S21 ESM parameters for all inventory items broken down by system and subsystem for each scenario described in Table S20. Parameters included are mass M [kg], V [m^3], power P [kW], cooling C [kW], and crew-time CT [hr][17, 317]. The ESM values correspond to a single sortie $S_{\text{num}} = 1$. (ORU = Orbital Replacement Unit) 175
S21 ESM parameters for all inventory items broken down by system and subsystem for each scenario described in Table S20. Parameters included are mass M [kg], V [m^3], power P [kW], cooling C [kW], and crew-time CT [hr][17, 317]. The ESM values correspond to a single sortie $S_{\text{num}} = 1$. (ORU = Orbital Replacement Unit) 176
S21 ESM parameters for all inventory items broken down by system and subsystem for each scenario described in Table S20. Parameters included are mass M [kg], V [m^3], power P [kW], cooling C [kW], and crew-time CT [hr][17, 317]. The ESM values correspond to a single sortie $S_{\text{num}} = 1$. (ORU = Orbital Replacement Unit) 177

S21 ESM parameters for all inventory items broken down by system and subsystem for each scenario described in Table S20. Parameters included are mass M [kg], V [m^3], power P [kW], cooling C [kW], and crew-time CT [hr][17, 317]. The ESM values correspond to a single sortie $S_{\text{num}} = 1$. (ORU = Orbital Replacement Unit) 178
S21 ESM parameters for all inventory items broken down by system and subsystem for each scenario described in Table S20. Parameters included are mass M [kg], V [m^3], power P [kW], cooling C [kW], and crew-time CT [hr][17, 317]. The ESM values correspond to a single sortie $S_{\text{num}} = 1$. (ORU = Orbital Replacement Unit) 179
S22 Estimation of inventory items into exemplar classes broken down by system and subsystem for each scenario described in Table S20. Classes include: Structural Metal, Plastic, Electronics, Fabric, Glass, Rubber, Ceramics, Gas, Biomass, Water, Other. (ORU = Orbital Replacement Unit) 179
S22 Estimation of inventory items into exemplar classes broken down by system and subsystem for each scenario described in Table S20. Classes include: Structural Metal, Plastic, Electronics, Fabric, Glass, Rubber, Ceramics, Gas, Biomass, Water, Other. (ORU = Orbital Replacement Unit) 180
S22 Estimation of inventory items into exemplar classes broken down by system and subsystem for each scenario described in Table S20. Classes include: Structural Metal, Plastic, Electronics, Fabric, Glass, Rubber, Ceramics, Gas, Biomass, Water, Other. (ORU = Orbital Replacement Unit) 181
S22 Estimation of inventory items into exemplar classes broken down by system and subsystem for each scenario described in Table S20. Classes include: Structural Metal, Plastic, Electronics, Fabric, Glass, Rubber, Ceramics, Gas, Biomass, Water, Other. (ORU = Orbital Replacement Unit) 182
S22 Estimation of inventory items into exemplar classes broken down by system and subsystem for each scenario described in Table S20. Classes include: Structural Metal, Plastic, Electronics, Fabric, Glass, Rubber, Ceramics, Gas, Biomass, Water, Other. (ORU = Orbital Replacement Unit) 183
S22 Estimation of inventory items into exemplar classes broken down by system and subsystem for each scenario described in Table S20. Classes include: Structural Metal, Plastic, Electronics, Fabric, Glass, Rubber, Ceramics, Gas, Biomass, Water, Other. (ORU = Orbital Replacement Unit) 184
S22 Estimation of inventory items into exemplar classes broken down by system and subsystem for each scenario described in Table S20. Classes include: Structural Metal, Plastic, Electronics, Fabric, Glass, Rubber, Ceramics, Gas, Biomass, Water, Other. (ORU = Orbital Replacement Unit) 185
S22 Estimation of inventory items into exemplar classes broken down by system and subsystem for each scenario described in Table S20. Classes include: Structural Metal, Plastic, Electronics, Fabric, Glass, Rubber, Ceramics, Gas, Biomass, Water, Other. (ORU = Orbital Replacement Unit) 186

S23 Qualitative comparison of biotic vs. abiotic *in situ* (bio)manufacturing approaches across different destinations in the Solar-system (excluding cis-Lunar, which can be considered as an in-between of Earth Orbit and destination Moon). 191
S24 **Space Bioprocess Engineering technologies in the context of NASA's Space Technology Grand Challenges (STGCs) and United Nations Sustainability Development Goals (SDGs).** Extended Version. 195

Acknowledgments

"Well, here we are."

I want to thank the co-investigators of CUBES: Craig Criddle and Robert Waymouth at Stanford University; Somen Nandi and Karen McDonald at the University of California Davis; Amor Menezes at the University of Florida; Bruce Bugbee and Lance Seefeldt at Utah State University; Douglas Clark, Devin Coleman-Derr, Ali Mesbah, Peidong Yang at the University of California Berkeley. I thank them for their patience in putting up with me over the past five years of constantly sending emails, sounding the alarms for quarterly reports, pestering them for materials and presentation prep, and generally being the nuisance that was demanded by my tenure as the *major domo* of a large research center. I thank Gwyneth Terry for her help in showing me the ropes of how to be an effective administrator.

I thank the many bosses who helped me reach Berkeley: Larry Peck, Andrew Hessel, Eli Groban, and John Hogan. I thank them for firing me when they knew they had to and putting up with my tantrums. I thank them for knowing that I live by "may the bridges I burn light my way" and for handing me the torch and grinning in the flames.

I thank my advisor and mentor Adam Arkin who believed that we could build a space center. I thank Adam for initially and playfully derisively handing me the title of *major domo*. I thank him for knowing why I wore it so proudly. I thank him for his willingness to tell me what I needed to hear, even when I struggled to hear it. Mostly, I thank him for allowing me to pour myself – body, mind, and soul – into CUBES – without becoming hollowed.

I thank the professors at Berkeley across a myriad of the disciplines that I failed to master. I thank Bill Collins for his patience as I tried to corrupt radiative transfer in the service of Martian Terraforming. I thank Lee Bernstein for his mistake in revealing the dark corners of the national laboratories that dream of deflecting asteroids with nuclear ordnance. I thank Karl van Bibber for allowing me to serve as the brass-knuckles of nuclear policy. I thank Alex Bayen for listening to me yammer on about new space bioprocess engineering opportunities.

I thank my friends. I thank Darrel Hall for his special way of keeping me up at night when the city slept, and ideas would burst into life. I thank him for keeping me going in an alkaline cloud of chalk from equations scribbled hastily on blackboards. I thank Sophia Ewens for putting up with me when I called her late at night to talk about these ideas. I thank Andrew McDonough for answering those 2AM calls to listen to me kvetch on a number of topics – and for continuing to listen from across a dinner table in the south of France – with only mild judginess crinkling his face. I thank Djordie Markovic for summoning me to Serbia when I got lost on Mars and very desperately needed a reminder of my friends on Earth.

I thank my peers across the Arkin Laboratory, CUBES, and UC Berkeley. I thank Kelly Wetmore whose work brought me to Berkeley. I thank Jacob Hilzinger, and Kelly Wetmore for their company at the many lunches where I oscillated between depressingly zoning out and shoveling Imm Thai food into my mouth; I thank them for dragging me kicking and screaming to enjoy a weekend of

skiing in Tahoe. I thank Jake for finding my phone when I lost it tumbling down the mountain; I thank Kelly for reminding me of this more often than I'd like, and adding a note about the humor that found its way – gondola to gondola – of all who saw and pointed. I thank my graduate student peers across the myriad of CUBES institutions: Matt McNulty, Kyle Sander, Anthony Abel, Nils Averesch, and Kevin Yates; I thank them for putting up with my crazed 2AM phone calls and emails about our papers and projects. I thank them for knowing how to treat me with kid-gloves when I needed it, and when to destroy a paper or presentation when I *really* needed it. I thank my two roommates: George Makrygiorgos and Jake Hecla; I thank them for putting up with me as I crashed out on our couch watching Jeopardy! or burned dinner. I thank George for his invitation to Greece and for meeting me boatside with a warm souvlaki under the summer sun; for convincing me to dance my way to a dislocated shoulder on the Athenian shores and into the crown as the King of Mykonos. I thank Jake Hecla for his knowing smirk as I tried and failed to imagine methods for capturing high atmosphere muons. I thank him for his partnership in developing coursework for nuclear engineering history, policy, and spacefaring – and for his company while screaming at emails.

I thank my undergraduate students of the *Child Labor Force*: Mia Mirkovic, Avery Hill, Davian Ho, Isaac Lipsky, Cami Casale, Gretchen Vengerova, Adam Chois, Farrah Kaiyom, Zain Chuadry, and Spencer Zezulka. I thank Mia for being my first student when I had no idea how to manage and for establishing the basis of Crucible. I thank Avery for expertly fibbing her way into the group and proving that economics and molecular biology can be happily married. I thank Isaac for pestering me when he was a freshmen waiter on the Pacifica waters – and mostly for sticking with me to the bitter end despite my many, many pestering texts and calls. I thank Spencer for realizing my dream of life in the torus of accretion disks. I thank them all for their patience with me as a leader as a blustered and bluffed my way through trying to manage their brilliance and passion as I shamelessly diverted their energies for my own gain. I especially thank Davian Ho for all the above, and for his trust in me; for his agency and love in rendering graphics that realized my vision in multicolored inks, for his fingers coding echusOverlook, for calling me a boomer, and knowing that "boomers gotta boom." I thank the whole of the CLF for joining in on our movie nights or potluck dinners – and for their trust and their friendship and their belief in me in poor exchange for allowing me to believe in them.

I thank my family: my brothers, Alex and Anthony, and my sister Carmen for calling me to ask why I was still a student. I thank my mother for calling me and knowing to not ask. I thank them now and hope they'll stop asking.

I thank my partner Emily Crawford for her patience and love across the past 5 years when I was a poor and frustrated graduate slave – and all the years before—and with great optimism – the years ahead.

"If it can be done, it will be done. We can transform Mars and build it like you would build a cathedral, as a monument to humanity and the universe both. We can do it, so we will do it. So –" he held up a palm, as if satisfied that the analysis had been supported by the data in the graph – as if he had examined the periodic table, and found that it still held true – *"we might as well start."*

Center for the Utilization of Biological Engineering in Space

Even before NASA reached the Moon, endeavors to design mission specifications were being drafted with step required to reach the surface of Mars[545, 59, 434]. Decades later in 2004, the President Bush unveiled a plan to return to the moon and on to Mars[68]. Now in 2021, the United States of America still dreams of reaching Mars[337].

For decades, NASA has continued to develop a wide array of technologies for advancing human space exploration. In late 2017, and under the premise that biological systems can provide utility in space[372, 371], NASA funded a proposal for the establishment of a Space Technology Research Institute (STRI) called the Center for the Utilization of Biological Engineering in Space (CUBES) to support biomanufacturing for deep space exploration that realizes the inherent mass, power, and volume advantages of space biotechnology over traditional abiotic approaches[209]. I begin my dissertation with this chapter on CUBES, prior to even the introduction and background of science, as homage to the importance of institutional management which makes such science possible. Here, I offer a brief explanation of CUBES in order to (1) establish an envelope of the institution and mandate that scopes the following dissertation; (2) establish the relationship of CUBES with respect to NASA; and (3) give credit to the many scientists and engineers who have build our center.

This center was tasked with advancing the practicality of deploying an integrated, multi-function, multi-organism biological system on a Mars mission through multidisciplinary re-

search culminating in a biomanufacturing demonstration of materials, pharmaceuticals, and food. The primary tasks[209] for CUBES are

1. *In situ* microbial media and feedstock division (MMFD), which harnesses Mars atmospheric and regolith resources for downstream biological use;

2. *In situ* manufacture of mission products, which creates outputs like propellants and building materials that are fundamental enablers of any long-duration space mission;

3. *In situ* food and pharmaceutical synthesis, which allows these long-duration space missions to be manned, and uses plants and microbes that provide food, nutrients and medicine;

4. Systems design and integration, to optimally allocate and utilize Mars resources, to tightly integrate and automate internal processes, and to satisfactorily achieve performance per mission specifications.

CUBES was designed in alignment with the 2015 NASA Technology Roadmaps, especially TA07 Human Exploration Destination Systems. TA07 includes TA7.1 In Situ Resource Utilization (the MMFD, BBMD, and FPSD will all use such inputs), TA7.2 Sustainability and Supportability (the MMFD, BBMD, and FPSD will all use sustainable resource recycling), TA7.4 Habitat Systems (CUBES will develop a semi-autonomous proof-of-concept biomanufacturing demonstration), and TA7.6 Cross-Cutting Systems (the BBMD additive manufacturing technology will be designed for scaling assembly). Additionally, CUBES will facilitate the development of technologies in TA06 Human Health, Life Support, and Habitation Systems by enabling long-duration, deep-space human exploration through the minimization of resupply consumables and increased Earth independence via Martian in situ resource utilization, synthetic biology, and biomanufacturing. The FPSD will address TA6.3 Human Health and Performance, and the MMFD will address TA6.1 Environmental Control, Life Support Systems and Habitation Systems, and TA6.4 Environmental Monitoring, Safety, and Emergency Response through remediation of toxic perchlorate in the Martian regolith.

As of the writing of this report in completion of this dissertation, CUBES has published ∼68 papers (all of which can be openly accessed via our website here) and which we have visualized categorically in the Figure below. An analysis of 47 of the referable papers (via WebOfScience) reports 540 citations with an average citation of 11.49/paper – and a CUBES H-Index of 9. Moving into the CUBES no-cost-extension and next phase of CUBES-II we expect to add another ∼5-10 publications to our dossier in the coming months.

As we wrap up CUBES, we have officially sunsetted our popular seminar series (schedule available here). Over the course of 5 years, we are proud to have offered ∼60 seminars drawn from both internal CUBES researchers and external experts in the space and biomanufacturing community. All seminar materials have been achieved and can be accessed here.

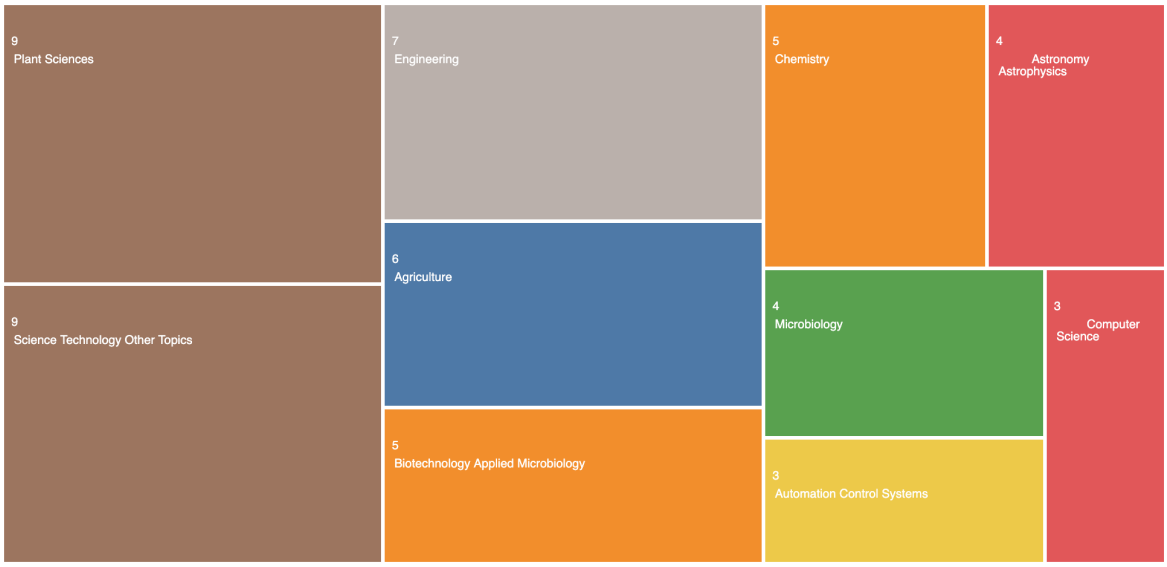

Figure 0.1: NNX17AJ31G TreeMap Visualization

Figure 0.2: Y5 Spring Review Group Photo

Chapter 1

Introduction

1.1 Background and Motivation

In over a century of grand visions for the human exploration of Mars, the notion of footsteps in red sand have padded from science fiction story devices[458] to the *raison d'être* of national organizations. Motivational appeals have been cast in a variety of languages; some have argued that we must go as a matter of pure science in an effort to probe the untouched geology for clues to the early solar system or the origins of life. Others have argued that we must go to answer the challenge of climbing the highest mountain, and others still have argued that we must go as a means to forge a new future. While motivations vary, we are certain that meeting the grand scientific and technical challenges required to enable human exploration of Mars represents a call to the better angels of our nature and will usher in new paradigms in discovery, development, and society.

Extended human stay in space or upon the surface of alien worlds like Mars introduces new mission elements that require innovation[394]; among these are the biotechnological elements[371, 372, 401] that support human health, reduce costs, and increase operational resilience. The potential for a Mars mission in the early 2030s[147] underscores the urgency of developing a roadmap for advantageous space biotechnologies.

A major limiting factor of space exploration is the cost of launching goods into space[557]. The replicative capacity of biology reduces mission launch cost by producing goods on-demand using *in situ* resources[444], recycling waste products[221], and interacting with other biological processes for stable ecosystem function[194]. This trait not only lowers initial launch costs, but also minimizes the quantity and frequency of resupply missions that would otherwise be required due to limited food and pharmaceutical shelf-life[156] on deep space missions. Biological systems also provide robust utility via genetic engineering, which can provide solutions to unforeseen problems and lower inherent risk[371, 40]. For example, organisms can be engineered on-site to produce a pharmaceutical to treat an unexpected medical condition when rapid supply from Earth would be infeasible[366]. A so-called "biomanufactory" for deep space missions[370] based on *in situ* resource utilization and com-

Figure 1.1: Artist's rendering of a crewed Martian biomanufactory powered by photovoltaics, fed via atmospheric ISRU, and capable of food and pharmaceutical synthesis (FPS), *in situ* manufacturing (ISM), and biological loop closure (LC). Artwork by Davian Ho.

posed of integrated biologically-driven subunits capable of producing food, pharmaceuticals, and biomaterials (Fig. 1.1) will greatly reduce launch and resupply cost, and is therefore critical to the future of human-based space exploration[371, 401].

1.2 Thesis Statement

In an effort to address the aforementioned challenges for human exploration of Mars – across the contexts of spacefaring, space bioprocess engineering, and mission design – we summarize our over arching hypothesis as

> **The optimal set of technologies and operational strategies for sustaining a long-duration human exploration mission on Mars is driven by the design, optimization, deployment, and management of a surface biomanufactory.**

Given that the overarching hypothesis of the CUBES program is that biological engineering technologies can provide utility for long-term human exploration missions on Mars, my proposed project is the design and optimization of a biomanufacturing-driven RMA for the human exploration of Mars. In essence, what follows is a collection of models of various systems designed[1] (1) to demonstrate and physical or engineering principle; (2) to prove data consistency with or discriminate among theories; (3) to predict future behaviors or response

[1] These goals of constructing a model, generally, are the guidelines of my PI Adam Arkin

to perturbation; and (5) to design or optimize a system. The reason underlying research questions that guide the construction and integration of these models are

1. How can we model the parametric constraints on and tradeoffs among bioprocesses such that they meet or exceed mission need and are engineered to minimize the risk of failure under different orbital, crew, and landing site scenarios?

2. What are the critical system parameters for demonstrating the feasibility and advantages of biological engineering on a human exploration mission to Mars?

3. Do any requirements for long term exploration exceed the feasible system parameters?

1.3 Thesis Outline

In an effort to most efficaciously present the progress towards address the overall hypothesis and the accompanying research questions, the following dissertation is organized as followings.

Chapter 2 explores the future of Space Bioprocess Engineering (SBE) as an emerging multi-disciplinary field to design, realize, and manage biologically-driven technologies specifically with the goal of supporting life on long term space missions. SBE considers synthetic biology and bioprocess engineering under the extreme constraints of the conditions of space. A coherent strategy for the long term development of this field is lacking. In this Perspective we describe the need for an expanded mandate to explore biotechnological needs of the future missions. We then identify several key parameters – metrics, deployment and training – which together form a pathway towards the successful development and implementation of SBE technologies of the future.

Chapter 3 presents a perspective that articulates the scientific and engineering goals and constraints, along with example systems, that guide the design of a surface biomanufactory. Extending past arguments for exploiting stand-alone elements of biology, we argue for an integrated biomanufacturing plant replete with modules for microbial *in situ* resource utilization, production, and recycling of food, pharmaceuticals, and biomaterials required for sustaining future intrepid astronauts. We also discuss aspirational technology trends in each of these target areas in the context of human and robotic exploration missions.

Chapter 4 presents the progress towards formalizing the mathematical framework for modeling a biomanufacturing system developing the resources for sustaining a human exploration mission on the surface of Mars by establishing mission goals, extending the Equivalent System Mass framework for comparision of missions, develop the framework for modeling a Martian resource inventory in terms of supplies both produced via ISRU processes and transported as cargo from Earth, and develop the framework required for sustaining a human crew in terms of essential resources. NASA mission systems proposals are often compared using an equivalent system mass (ESM) framework, wherein all elements of a technology to deliver an effect – its components, operations and logistics of delivery – are converted to effective

masses, which has a known cost scale in space operations. To date, ESM methods and the tools for system comparison largely fail to consider complexities stemming from multiple transit and operations stages, such as would be required to support a crewed mission to Mars, and thus do not account for different mass equivalency factors during each period and the inter-dependencies of the costs across the mission segments. Further, ESM does not account well for the differential reliabilities of the underlying technologies. The uncertainty in the performance of a technology should incur an equivalent mass penalty for technology options that might otherwise provide a mass advantage. Here we draw attention to the importance of addressing these limitations and formulate the basis of an extension of ESM that allows for a direct method for analyzing, optimizing, and comparing different mission systems. We outline a preliminary example of applying extended ESM (xESM) through a technoeconomic calculation of crop-production technologies as an illustrative case for developing offworld biomanufacturing systems.

Chapter 5 presents the computational methods and construction of echusOverlook (eO) software. eO is a tool for designing, exploring, and optimizing a biologically driven RMA for human exploration of Mars

Chapter 6 presents the first RMA case-study for evaluating the photovoltaics-driven power production on Mars. A central question surrounding possible human exploration of Mars is whether crewed missions can be supported by available technologies using *in situ* resources. Here, we show that photovoltaics-based power systems would be adequate and practical to sustain a crewed outpost for an extended period over a large fraction of the planet's surface. Climate data were integrated into a radiative transfer model to predict spectrally-resolved solar flux across the Martian surface. This informed detailed balance calculations for solar cell devices that identified optimal bandgap combinations for maximizing production capacity over a Martian year. We then quantified power systems, manufacturing, and agricultural demands for a six-person mission, which revealed that photovoltaics-based power generation would require <10 t of carry-along mass, outperforming alternatives over ∼50% of Mars' surface.

Chapter 7 presents the second RMA case-study for Nitrogen accountancy in space agriculture. Food production and pharmaceutical synthesis are critical biotechnologies to enable human exploration of Mars because they reduce mass and volume requirements through scalable and modular agriculture in closed-loop systems. The NASA-sponsored modified energy cascade (MEC) model used to evaluate crop growth is insufficient as a tool to support exploration missions in its monocrop architecture, incomplete material balances on key crop cultivation and life support resources like nitrogen, and lack of the rigorous physical inventory accounting that is required to evaluate mission costs. We expand the MEC model to account for nitrogen dependence across an array of crops and validate our model with experimental fitting of parameters. By adding nitrogen limitations, the extended MEC model accounts for potential interruptions in feedstock supply. Furthermore, we use sensitivity analysis to distil key consequential parameters that may be the focus of future experimental efforts. Finally, the integration of physical system inventories enables comparisons in the choice of architecture and technology.

Chapter 8 presents the 3rd RMA case-study for evaluating the cost of pharmaceutical purification for a long-duration space exploration medical foundry. There are medical treatment vulnerabilities in longer-duration space missions present in the current International Space Station crew health care system with risks, arising from spaceflight-accelerated pharmaceutical degradation and resupply lag times. Bioregenerative life support systems may be a way to close this risk gap by leveraging *in situ* resource utilization (ISRU) to perform pharmaceutical synthesis and purification. Recent literature has begun to consider biological ISRU using microbes and plants as the basis for pharmaceutical life support technologies. However, there has not yet been a rigorous analysis of the processing and quality systems required to implement biologically produced pharmaceuticals for human medical treatment. In this work, we use the equivalent system mass (ESM) metric to evaluate pharmaceutical purification processing strategies for longer-duration space exploration missions. Monoclonal antibodies, representing a diverse therapeutic platform capable of treating multiple space-relevant disease states, were selected as the target products for this analysis. We investigate the ESM resource costs (mass, volume, power, cooling, and crew time) of an affinity-based capture step for monoclonal antibody purification as a test case within a manned Mars mission architecture. We compare six technologies (three biotic capture methods and three abiotic capture methods), optimize scheduling to minimize ESM for each technology, and perform scenario analysis to consider a range of input stream compositions and pharmaceutical demand. We also compare the base case ESM to scenarios of alternative mission configuration, equipment models, and technology reusability. Throughout the analyses, we identify key areas for development of pharmaceutical life support technology and improvement of the ESM framework for assessment of bioregenerative life support technologies.

Chapter 9 demonstrates the impact and value of space-based biomanufacturing. Here we identify specific off-world scenarios where the concept is most applicable, as well as the vital inventories that can be made available thereby. This will serve to increase capabilities of human operations beyond Earth-orbit and allow for extended mission-design through greater autonomy while minimizing risks through redundancy. We sketch the potential routes and systems to arrive at these goals in the form of specialized microbial cell factories that can most meaningfully leverage the resources available along the journey. The strategic vision presented here relies heavily on synthetic biology, integrates with major plans for *in situ* resource utilization, and highlights applications that engineered biology is uniquely suited to address. We finish by advocating for the research and development investments that need to be made in order to significantly increase readiness of these technologies over the coming decade. This dovetails with current efforts to return humans to the Moon – with Mars on the horizon. Besides ensuring the feasibility and sustainability of crewed Space exploration and habitation, the advancement of these technologies may spawn a new scalable microgravity-based biotechnology industry that contributes to the creation of a circular economy on Earth.

Chapter 10 presents an argument for how Space Bioprocess Engineering drives sustainability on- and off-World. Although *raison d'etre* of Space Bioprocess Engineering is the design, realization, and management of biologically-driven technologies for supporting off-world human exploration, it has the potential to offer transformative solutions to the global

community in pursuit of the United Nations Sustainable Development Goals. Here we address the growing sentiment that investment in spacefaring enterprises should be redirected towards sustainability programs. In outlining the Earth-benefits of dual-use Space Bioprocess Engineering technologies, we both show that continued investment is justified and offer insight into specific R&D strategies.

Chapter 2

Space Bioprocess Engineering on the Horizon

Space Bioprocess Engineering (SBE) is an emerging multi-disciplinary field to design, realize, and manage biologically-driven technologies specifically with the goal of supporting life on long term space missions. SBE considers synthetic biology and bioprocess engineering under the extreme constraints of the conditions of space. A coherent strategy for the long term development of this field is lacking. In this Perspective we describe the need for an expanded mandate to explore biotechnological needs of the future missions. We then identify several key parameters – metrics, deployment and training – which together form a pathway towards the successful development and implementation of SBE technologies of the future.

The following chapter can also found here: A.J. Berliner, I. Lipsky, D. Ho, J. Hilzinger, G. Vengerova, M. McNulty, K. Yates, N.J.H Averesch, C.S. Cockell, L.C Seefeldt, C.S. Criddle, S. Nandi, K.A. McDonald, A.A. Menezes, A. Mesbah, A.P. Arkin. **Space Bioprocess Engineering on the Horizon**. *Communications Engineering*. (2022). DOI: 10.1038/s44172-022-00012-9.

Biotechnologies may have mass, power and volume advantages compared to abiotic approaches for critical mission elements for long-term crewed space exploration[371, 401]. While there has been progress in demonstration and evaluation of these benefits for specific examples in this field such as for food production, and waste recycling, there is only just emerging possible consensus on the scope of the application of biosynthetic and biotransformative technologies to space exploration. Additionally, there is almost no formal definition of the scope, performance needs and metrics, and technology development cycle for these systems. It is time to formally establish the field of Space Bioprocess Engineering (SBE) to build this nascent community, train the workforce and develop the critical technologies for planned deep-space missions. SBE (Fig. 2.1a) borrows elements from a number of related fields such as the synthetic biology design process from Bioengineering, astronaut sustainability[580, 565] and mission design from Astronautics[232, 147], environmental-context and constraints from the Space Sciences, and living systems habitability and distribution concepts from

Astrobiology[180]. SBE represents an extension of the standard astronautics paradigm in meeting NASA's Space Technology Grand Challenges (STGCs) for expanding the human presence in space, managing resources in space, and enabling transformative space exploration and scientific discovery[514, 372] (Fig. 2.1b). Aspirational realizations of SBE would feature prominently in establishment of in-orbit test-facilities, interplanetary waystations, lunar habitats, and a biomanufactory on the surface of Mars[44]. Differentiated from traditional efforts in space systems engineering, these SBE systems would encapsulate elements from *in situ* resource utilization (ISRU) for the production of biological feedstocks such as fixed carbon and nitrogen for use as inputs for plant, fungal, and microbial production systems[90, 302], fertilizers for downstream use by plants[444]; *in situ* (bio)manufacturing (ISM) to produce materials requisite to forge useful tools and replacement parts[554], food and pharmaceutical synthesis (FPS) via plant, fungal and microbial engineering for increased productivity and resilience in space conditions, production of nutrients and protective/therapeutic agents for sustaining healthy astronauts[76, 367]; and life-support loop closure (LC) for minimizing waste and regenerating life-support functions and biomanufacturing. Maximizing the productivity of the biomanufacturing elements increases the delivery-independent operating time of a biofoundry in space while minimizing cost and risk.[435] (Fig. 2.1c). Ultimately, efforts must be mounted to: (1) update the *mandate* to include SBE as a tool for enabling human exploration; (2) specialize the *metrics and methods* that guide SBE technology life-cycle and development; (3) further develop the *means* by which SBE technologies are designed for ground-based testing and matured on offworld platforms (Fig. 2.1d); and (4) train the *minds* entering the spacefaring workforce to better understand the leverage the SBE advantages and capabilities.

2.1 An Inclusive Mandate To Leverage SBE

While previous strategic surveys such as NASA's Journey to Mars program[403] the 2018 Biological and Physical Sciences (BPS) Decadal Survey[2] have acknowledged that plants and microbes may be integral parts of life support and recycling systems, but can present challenges to the environmental operation of engineering systems in space due to contamination and other inherent drawbacks. However, no such survey has coherently called for the development of the science and technology to engineer these organisms and their biotransformative processes in support of space exploration. The SBE community requires a mandate that identifies mission designs and elements for which engineering biosystems would be most appropriate, and defines the productivity, risk and efficiency targets for these systems in an integrated context with other mission elements and in fair comparison to abiotic approaches. This will require integration of SBE resources and knowledge across government, industry, and academia. Previous biological strategies should now specifically call for (1) definition of the physical engineering constraints on the production systems and development of optimized reactor/processing systems for these elements; (2) quantitative assessment of the bioengineering required to meet performance goals in space given the special physiology

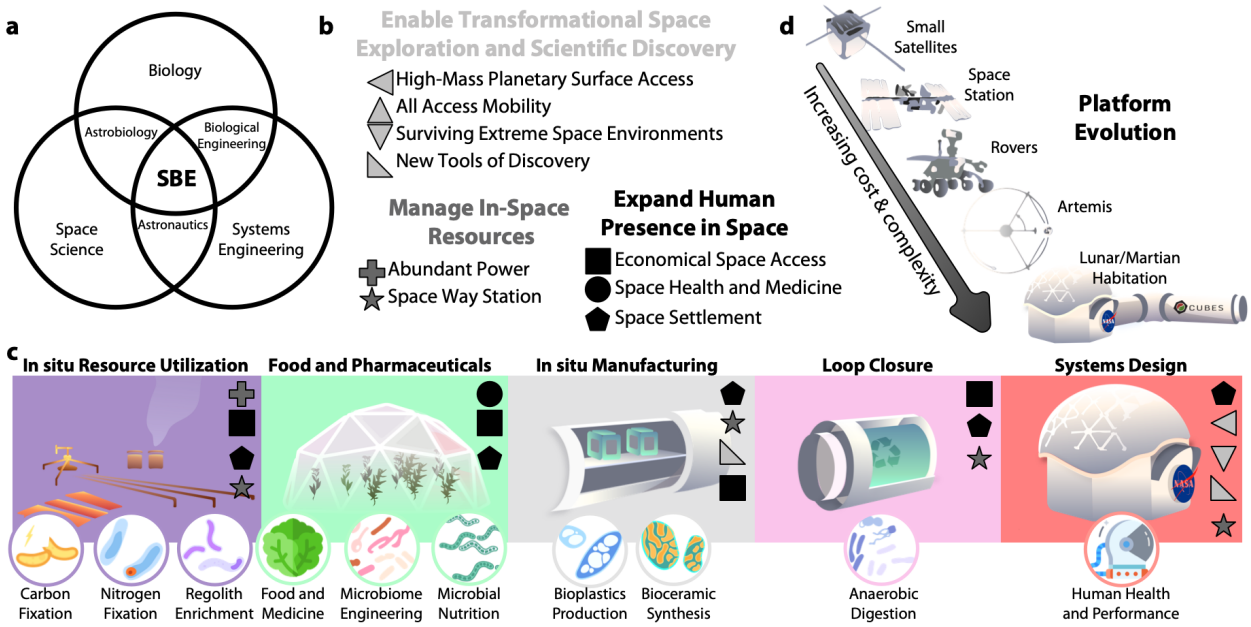

Figure 2.1: Overview of Space Bioprocess Engineering challenges, components, and platforms. (a) Venn Diagram-based definition of Space Bioprocess Engineering (SBE) as an interdisciplinary field. **(b)** NASA's space technology grand challenges[514] key by shape and colored by group. **(c)** Possible SBE components separated by colors for *in situ* resource utilization (ISRU), food and pharmaceutical synthesis (FPS), *in situ* manufacturing (ISM), and loop closure (LC), with the biological processes inherent to each represented below in circles. **(d)** Platform evolution for biological experiments starting with Earth-orbit CubeSats and proceeding through the ISS, Mars-and-Luna-based rovers, to Lunar and cis-Lunar based human and autonomous systems via the Artemis program.

required in an offworld environment; and (3) development of efficient tooling for offworld genetic engineering along with the proper containment and clean-up protocols.

Such a mandate would result in: (1) a deeper, more mechanistic understanding of the growth and phenotypic characteristics of organisms operating in space-based bioprocesses taking into account issues of differences in gravity, radiation, light, water quality; new applications of these organisms off-planet; (3) new reactors, bioprocess control designs and product processing/delivery technologies accounting for these conditions and the specific constraints of scaling and operational simplicity in space. The development of open, publicly accessible data and tools would enable rigorous comparison among biotechnologies and abiotic (physical and chemical) approaches, and across mission-scenarios of higher-fidelity. Ideally, this should create interative sub-communities that may collaborate and compete on different approaches to meet bioengineering goals and metricize results against the mission specifications.

SBE is an emerging engineering discipline and there are long but feasible routes from discovery, through invention to application. Furthermore, SBE is multidisciplinary and its utility within the larger space community demands specialized cross-training of diverse teams. It in such situations agencies like the Department of Energy (DOE) have found it effective

to ensure there is specific funding to support longer-term team science to accomplish ambitious scientific and technical goals. The Industrial Assessment Centers (IACs) program is one longest-running DOE programs (started in 1976) and has provided nearly 20,000 no-cost assessments for small- and medium-sized manufacturers and more than 147,000 recommendations in an effort to reduce greenhouse gas emissions without compromising U.S. manufacturing's competitive edge globally[144]. Conversely, successful examples for demonstrating the effect of fostering multidisciplinary centers for space-based biotechnology can be found in NASA's Center for the Utilization of Biological Engineering in Space (CUBES, https://cubes.space/), or ESA's Micro-Ecological Life Support System Alternative (MELiSSA, https://www.melissafoundation.org/) program – with the capabilities to design, prototype, and ultimately translate biological technologies to space while training the necessary workforce. Such centers are tasked with the development of initial concept trade studies; defining requirements; managing life-support interfaces; evaluating ground integration, operations, and maintenance; coordinating mission operations; and supporting and sustaining engineering and logistics[350, 92]. However, these programs are generally restricted to shorter operation timelines – and would benefit from a longer horizon. This is especially true for SBE as biological developments generally require a longer timeframe for integration in industrial endeavors.

2.2 Specialization of SBE Metrics and Methods

Response to the proposed expanded mandate above requires careful consideration of the space-specific performance metrics that SBE must fulfill. Payload volume, mass, and power requirements are made as small as possible and are limited in envelope by their carrier system. One of the most compelling aspects of biotechnology is the ability of such systems to adapt to these constraints relative to certain industrial alternatives. To efficiently evaluate and deploy novel biotechnologies, SBE experiments should begin with standardized unit operations that clearly define the desired biological function. This allows for a standardized experimental framework to test modular biotechnologies not only within the system to be engineered, but also within and between research groups. To define the minimal basis set of unit operations for a given mission, test and optimize the biotechnologies for each unit operation, and integrate each unit operation into a stable system, we propose to adopt the methods from standard bioengineering in the form of a Design-Build-Test-Learn (DBTL) cycle[112] (Fig. 2.2).

Performance Metrics

The design phase of the DBTL cycle begins with the establishment of core constraints and engineering targets that can be explored by standardizing the high-priority performance metrics ({Modularity, Recyclability, Supportability, Autonomy, Sustainability})- which we argue gain special weight in space- from which downstream technoeconomic and life-cycle analysis

decisions can be explored (Fig. 2.2a). *Modularity* assesses the agility of a system in responding to product changeovers and demand variations to maximize flexible biomanufacturing – de-risking on-demand biological production. *Recyclability* assesses the extent to which wastes and byproducts can be recycled and bioprocesses can be reused/repaired to minimize overall consumable requirements – de-risking circular bioprocessing. *Supportability* assesses system self-sufficiency to maximize self-reliance and minimize logistic resupply requirements from Earth – de-risking unplanned mission extension. *Autonomy* assesses the extent to which optimal system performance can be realized under unknown and transient offworld conditions, as well as potential system faults/failures, with minimal human intervention to maximize the system resilience – de-risking robust and fault-tolerant biomanufacturing. *Sustainability* assesses the flow of environmental assets to minimize environmental footprint and maximize resource efficiency – further de-risking the potential for negative impacts to planetary protection.

The space-specific constraints on performance include: (1) an exceptionally strong weighting on a low mass/volume/power footprint for the integrated bioprocess; (2) limited logistic supply of materials and a narrow band of specifically chosen feedstocks; (3) added emphasis on simplicity of set-up, operation and autonomous function to free up astronaut time; (4) mission-context de-risking against cascading failure; (5) strong requirements for efficiency and closed-loop function to maximize efficient resource use and minimize waste products; (5) a critical need for modularity and 'maintainability' so that parts can be swapped easily, new functions added easily, and repairs can be done without logistical support beyond the crew; (6) an increased dependence on other mission elements such as provision of water, gases, astronaut wastes, power, and other raw materials such a regolith which may vary in abundance, quality, and composition in unpredictable ways; (7) the need to design sustainable and supportable operation across long time horizons without logistical support beyond the bounds of the local mission; (8) increased ability to operate in more extreme environments including low gravity, high radiation, low nutrient input, and other stressors; (9) process compatibility among common media and operational modes to allow for easy process integration and risk-reduction through redundancy of systems; and (10) further consideration and development of biocontainment of engineered organisms to prevent (or at least mitigate) unexpected dispersal of unwanted living systems in pristine or tightly controlled environments[338, 521, 308].

Ideally, this combination of performance metrics provides informative constraints on biology and technology choices. Feedstock, loop-closure, environmental parameters and product needs will constrain the minimal set of organisms to develop and test for growth rate, optimal cultivation, robustness and resilience to space conditions and shelf-life, safety and genetic tractability, product yield, titer and rate, feedstock utilization, ease of biocontainment, streamlining of purification, and waste streams[31]. Once suitable chassis organisms have been evaluated and selected, the DBTL cycle can integrate staged co-design of the optimal process hardware (e.g. molecular biological set-ups, genetic engineering tools, bioreactors, and product post-processing systems) configuration, operating parameters, and process controllers. Aerobic organisms may be much more efficient but only viable in systems in which

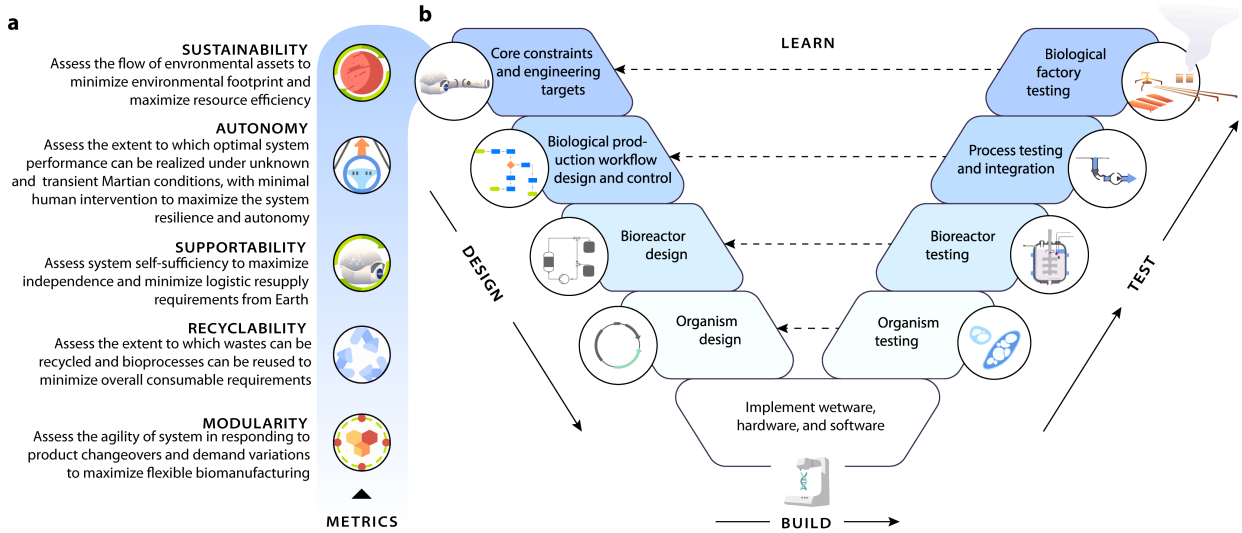

Figure 2.2: Overview of space systems bioengineering (SBE) performance metrics and the SBE-specific Design, Build, Test, Learn (DBTL) cycle. The SBE performance metrics in **(a)** are shaded to correspond to the top level core constraints and engineering targets within the **(b)** DBTL cycle.

oxygen is available and easily obtainable. This in particular provides insight into the specific questions that require further study in terms of organism engineering. The question of anaerobic versus aerobic metabolism really depends on the product and the style of process – at small scale aerobics may have an advantage in terms of yield and rate, due to more energy being derived from the transfer of reducing equivalents to cellular metabolism – while at large scale, mass-transfer limitations are dominating these parameters (yield and rate), which gives anaerobics an advantage[560]. Additionally, bioproduct isolation and purification processes need to be considered beyond the Earth-centric means of fermentation. For example, cell-free bioproduction systems may prove critical in biotransformation and point-of-care biosensing as shown in recent space pharming techoeconomic analyses[367]. Operation of the cycle over increasing scale and ever more realistic deployment environments permits controlled traversal of the technology readiness levels for each technology and mission.

Design-Build-Test-Learn

In the design phase, we argue that efforts must be made to (1) create a database of engineering targets (products, production rates, production yields, production titers, risk factors, waste/recyclability factors, material costs, operational costs, weight, power demand/generation) that set the core constraints for workflow and mission optimization; (2) leverage emerging pathway design software and knowledge bases[26] to identify the key types of biological production workflows (i.e. metabolic engineering strategies[328]) that need to be modified for different space-based scenarios; (3) identify the supporting biomanufactory design elements within which these production workflows could be implemented[80, 21, 197];

and (4) identify the chassis organisms and other biological components[489, 77, 117] that will be required to compose the complete set for downstream engineering specifications. Systems designed from a minimal set of reliable parts, standard interconnects, and common controller languages also offer the best possible chance of characterized reliability under changing environmental conditions. Therefore, control of hardware and wetware should be augmented through the design and operation of software support. We see a fundamental effort in SBE as the amalgamation of space-driven hardware, software, and wetware that follows a synthetic biology DBTL cycle[97].

The foundation of new SBE performance metrics that guide the design phase of the DBTL cycle must be augmented with additional downstream efforts in the build and test phases to (1) develop a process design framework that takes in specific production needs in amounts/time over acceptable ranges under the constraints expected across different offworld scenarios; (2) create the biological, process, and mission design software platforms to allow sophisticated DBTL, risk assessment, and mission choice support; (3) create the sensor/-controller sets that will allow real-time optimization of biological production workflows; and (4) develop the online process controller framework that coordinates reactor conditions and inter-reactor flows to optimize reliable production across all units within acceptable ranges with minimal power and risk. The realization of this SBE DBTL cycle depends on the integration of such benchmark models and modeling standards. These benchmarks describe the dynamics of all SBE processes and relate to the SBE metrics in the design phase from which optimization can be carried out in the learn phase.

DBTL cycles within the scope of SBE must prepare for both ground- and flight-based system operations. Ground-based developments must prioritize designs that meet the requirements for flight-based testing, during which system behaviors may be better characterized in unique environments such as those offered in micro- and zero-gravity. For instance, a biological nitrogen-fixing system on Earth must at least be designed to meet the mass and volumetric constraints required for validated ground-based simulators of microgravity, GCR, other physical stressors. Meeting certain requirements for time, power, and substrate usage is essential for any degree of long-term operation. This allows for the in-flight testing of bioreactors previously evaluated on Earth that can more directly measure the effects micro-gravity, radiation and other stressors on the bioprocessing system. A combination of ground- and flight- based tests are required for the development of functional and robust space biosystems.

Development of Means for SBE Flight

Deployment of SBE platforms as mission critical elements will likely be reserved for longer duration human exploration missions such as those in the Artemis or Mars programs[44]. These future programs are still in the concept and planning stage in development, but will certainly be composed of a myriad of technologies that range in degree of flight-readiness as standardized by NASA's Technology Readiness Level[339] (TRL, used to rate the maturity of a given technology during the acquisition phase of a program). Recent updates in NASA's

definitions of and best-practices for applying the TRL paradigm led to the standardization and merging of exit criteria between hardware and software systems[229]. However, the TRL concept as it relates to SBE must be further expanded to include definitions and exit criteria for 'wetware' in addition and in relationship to hardware and software elements.

Deployment of SBE is space requires a level of rigor in technology acceptance that is of a different order than most Earth-based systems because mission failures are exceptionally costly and difficult to recover from. The missions into which SBE processes will integrate are hugely complicated and as noted above will be interdependent in complex ways. Thus while

Platform	Volume	Power	Op. Lifetime	Temperature	Air Comp.
CubeSat	0.0187 m^3	20-45 W	~20 years	Requires heating unit within constraints	Self-contained
PocketQube	0.000125 m^3	Variable	~5 years		
Bioculture System	Not stated	140W	~60 days	37-45°C in main chamber, ambient to 5°C in cooling chamber	Self-contained medical grade gas
WetLab-2 (SmartCycler)	235.97 m^3	350W	Extractions <3hrs, no lifetime stated	50-95°C	
Rodent Habitat Hardware System	0.019 m^3	Not stated	~30 day experiments		
Compact Science Experiment Module	0.0015 m^3	3.2W	>1 month experiments	Ambient temp, no heating module	None, reliant on cabin air system
Vegetable Production System (Veggie)	0.48 m^3 growth area		>12 day experiments, can replace crops		
Advanced Plant Habitat (APH)	889.44 m^3 growth area	Not stated	~1 year	18-30°C	Self-contained gas supply
Spectrum	10 x 12.7 cm internal area		12 day experiments	18-37°C	None, reliant on cabin air comp
BRIC-60	11.03 m^3		>12 day experiments	Ambient temp, no heating module	60M variant can draw from an external gas tank
BRIC-100	38.78 m^3				Self-contained gas canister of designated
BRIC-100VC	16.33 m^3	Unpowered	4.5 months		Airtight, reliant on cabin air comp
KSC Fixation Tubes (KFTs)	0.2387 m^3		67 days		
miniPCR	0.00066 m^3	65W	~2 year	<120°C	
Group Activation Pack-Fluid Processing Apparatus (GAP-FPA)	Eight 6.5 cm^3 test tubes	Unpowered for manual		4-37°C	
Multi-use Variable-g Platform (MVP)	Twelve 800 cm^3 modules	Not stated	Not stated	14-40°C	Airtight, reliant on cabin air comp
MinION	0.0796 m^3	5W	~1 year	Ambient temp, no heating module	
Perseverance (MOXIE)	0.017 m^3	300W	~2 years	800°C operational -60°C ambient	CO_2 input CH_4 output
Gateway (HALO)	>125 m^3 planned internal volume	~60kW	>2 years	~18°C	Pressurized cabin air
Mars Hab (6 Crew)	300 m^3	~100kW	600 day nominal, 619 day maximum	~18°C	Pressurized cabin air

Table 2.1: Constraints on past and current experimental platforms including Small Satellites (light blue), Space Stations (medium blue), Rovers (dark blue), planned Lunar Habitation (light red), and Martian Habitation (red). The shade of color darkens with increasing complexity and cost. The specific sources can be found in the SI.

low levels TRLs can be reach through unit testing in modest formats both on Earth and in limited flight experiments, the integrated nature of the bioprocess control and engineering will require integration testing even at the TRL 4 and 5 levels[229]. To meet acceptance at TRL 6 and beyond will require long term planning realistic integration and deployment testing with actual sophisticated space missions and their logistics.

Even at low TRLs, research on the timescales needed to validate extended-use systems as would be leveraged on extended-stay forward deployment such as Martian or lunar missions are not possible given the current ISS capabilities and constraints. Constraints in astronaut time and limitations in hardware designed for shorter experiments prevent testing times comparable to long duration missions. Table 2.1 outlines a number of constraints on past and current experimental platforms and provides some basis for constraints of future systems (Fig. 2.1d). Here we note that extended multigenerational studies, especially in microbiology, can be difficult with some of the operational lifetimes. [85]. Volume is also constrained, and available space is broken up into segmented rack testbeds and independent machines, which can prevent aspects of a system from interacting with each other (Table 2.1). Much of the testing hardware on the ISS is designed for front-end processing and basic science, and many experiments in microbial observation[286, 67], hybrid life support[284], antibiotic response[28], and more all require returning samples to Earth for efficient processing, limiting the end-product downstream analysis and use as feedstocks for other integrated processes, as is needed to advance TRL beyond 6. This also cuts down on the ability to run DBTL diagnostics and SBE performance metrics on the system *in toto* as recyclability and sustainability are reliant on those end-products, and supportability if the processing is often reliant on Earth resources. Though much of the potential testing: PCR[56], imaging[311], and DNA sequencing[361, 256] is possible with current miniaturized ISS modules, it may not all be at the scale needed for future experiments, and there may be gaps in capability as the field matures. Improved *in situ* data analysis through development of new, high-throughput instruments could help close those gaps[280] and allow better metricization of whole systems under these new performance paradigms.

Lunar and Martian gravity is likely to have distinct biological effects compared to Earth gravity, resource composition, and radiation profile – and the ISS has only a limited volume in which to simulate them[583]. Additionally, both ambient environmental and target temperature windows span an extensive range across extraterrestrial environments, as do gas compositions, making representative testing more difficult in growth and testing chambers (plant, animal, and microbial) without full environmental control (Table 2.1). Environmental Control and Life Support System (ECLSS) systems for large-scale plant science requisite for advancing TRL for downstream lunar and Martian missions also require larger volume bounding boxes than is currently provided on the ISS[508]. Here we note the trade-offs with the tight volume and power stores on board. Smaller satellite modules can get technologies off the ground to advance TRL[351, 329, 469], but feature even greater size handicaps, and may prevent testing at the integrated, factory level in the DBTL cycle[124, 259]. Scientific instruments and modules on rovers have been geared primarily for exploration and observation, not technology validation. Dedicated rovers or simply landing SBE payloads

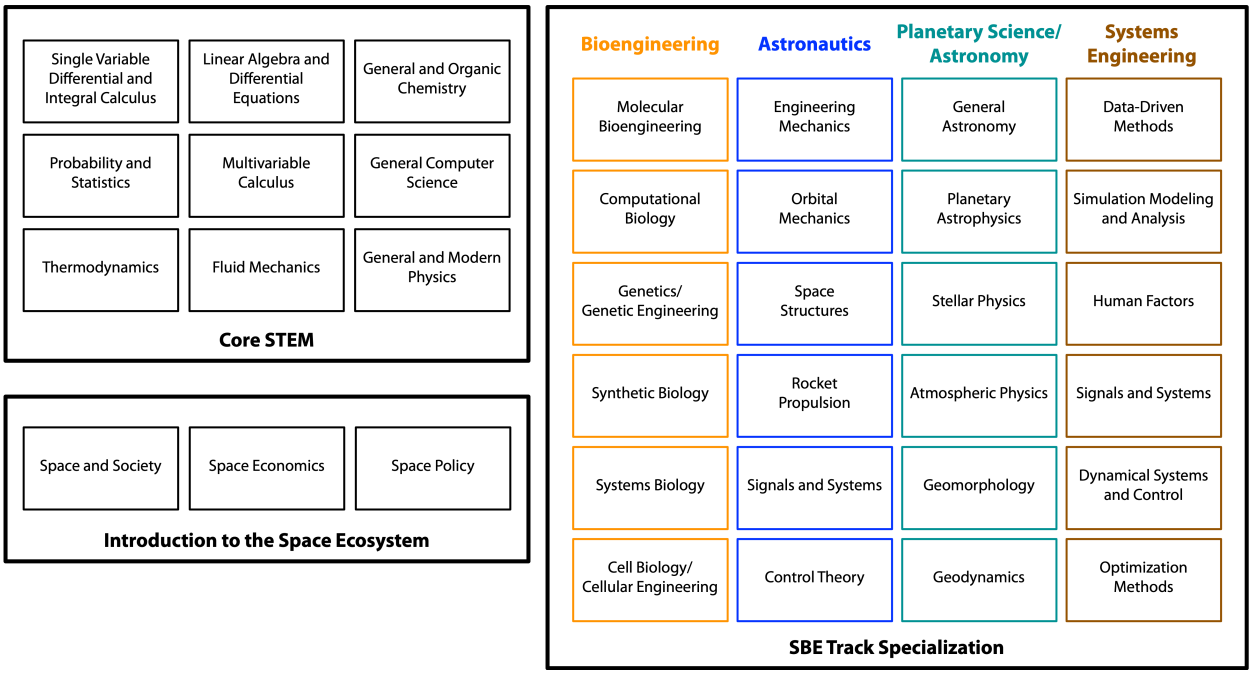

Figure 2.3: Conceptual undergraduate SBE program. The SBE program is broken in three segments: core STEM courses, introduction to space ecosystem courses, and track specialization courses for tracks in bioengineering, astronautics, planetary science & astronomy, and systems engineering.

onto extraterrestrial sites, SBE-ready orbiters, and Artemis operations as a stepping-stone to Mars can all demonstrate technology within a representative context and stand as some of the premier testbeds to "flight qualify" SBE prototypes[339]. *In situ* testing is key to the proposed SBE performance metrics: it forces technology and bioprocesses into accurate, integrated environments, and provides better confidence under radiation, microgravity, and isolation.

2.3 Training of SBE Minds

Maturation of space bioprocess engineering requires specialization of the training needed to produce the next generation of spacefaring scientists, engineers, astronauts, policy makers, and support staff[243]. Lessons learned from the Space Transportation System (STS) era led to calls for an increase in Science-Technology-Engineering-Mathematics (STEM) educational programs[170] beginning in secondary schools[162] and propagating to novel astronautics-based undergraduate[62] and graduate programs[501], and to the establishment of specialty space research centers[365] focused on technology transfer[174]. The calls for workforce development were repeated just prior to the collapse of the STS program, noting the dangers likely to arise from the lack of educational and training resources for those entering the space industry.[204]. Such a risk as described is especially poignant in the case of space-

based biotechnologies given that mature technologies are far fewer, the new applications more futuristic, and the disciplines are not well represented in the traditional physics and engineering curricula. The Universities Space Research Association (USRA) lists 114 institutions with Space Technologies/Science academic programs while recent accounting of bioastronautics programs numbers 36[579]. However, the intersection between these lists yields only 22 schools. Given that US News names 250 world schools that have tagged themselves with Space Science programs, only ∼8% of these are currently offering bioastronautics specialization – demonstrating that efforts that integrate human performance, life support and bioengineering are under-served. Furthermore, the bioastronautics programs such as those offered by schools like Harvard-MIT, University of Colorado Boulder, and Baylor University are not focused on biomanufacturing aspects that underlie SBE[289].

Academia must be prepared to capitalize on the opportunities of future SBE applications starting with either the creation of new and interdisciplinary programs or by assembling those from related disciplines (Fig. 2.1a). Because scientific and mathematical core courses are relatively standard across SBE-related disciplines, an effective foundation of technical skills could be easily constructed from the shared curriculum (Fig. 2.3). From there, specific SBE-driven training can be offered in (1) effects of space on plant and microbes; (2) process design for low gravity/high radiation; (3) management and storage of biological materials in space based operations; (4) low energy/low mass bioreactor/bioprocessor design; (5) integrated biological systems engineering; (6) biological mission planning and logistics; (7) risk and uncertainty management; (8) containment and environmental impact of biological escape, films, corrosion and cleanup; (9) policy awareness/development; and (10) ethics of cultivation and deployment. While the logistics for organizing such pathways for formal SBE training are non-trivial within the academic machine, we note that nearly all schools listed by USRA offer the component programs in bioengineering, planetary science or astronomy, and electrical or systems engineering. Since the courses for such engineering programs are standardized[120], it stands to reason that establishing focused SBE programs can begin by collecting and highlighting course combinations. As programs grow, additional faculty with SBE-driven research can be sourced. Such openings offer a much needed opportunity to address systemic issues of diversity, equity, and inclusion both within SBE-based academia and the industrial space community at large[406].

2.4 Moving Forward

Making progress on the program above requires scientists, engineers, and policy experts to work together to verify, open, and update campaign specifications. The science requires scientists from multiple disciplines spanning biological and space systems engineering that require a degree of modularity, small footprints, and robustness not found elsewhere. Additionally, bioprocess and biological engineering must be applied to the building of cross-compatible and scalable processing systems and optimized organisms within the confines of space reactor and product. Finally, coordination mission specialists are critical to deploy tests into

space during the run-up and through crewed missions. We argue that such groundwork requires multidisciplinary centers that can build long term partnerships and understanding; train the workforce in this unique application space; and perform the large-scale, long-term science necessary to succeed.

Chapter 3

Perspective: Towards a Biomanufactory on Mars

A crewed mission to and from Mars may include an exciting array of enabling biotechnologies that leverage inherent mass, power, and volume advantages over traditional abiotic approaches. In this perspective, we articulate the scientific and engineering goals and constraints, along with example systems, that guide the design of a surface biomanufactory. Extending past arguments for exploiting stand-alone elements of biology, we argue for an integrated biomanufacturing plant replete with modules for microbial *in situ* resource utilization, production, and recycling of food, pharmaceuticals, and biomaterials required for sustaining future intrepid astronauts. We also discuss aspirational technology trends in each of these target areas in the context of human and robotic exploration missions.

The following chapter can also found here: A.J. Berliner, J.M. Hilzinger, A.J. Abel, G. Makrygiorgos, N. Averesch, A. Benvenuti, D. Caddell, S. Cestellos-Blanco, A. Doloman, S. Friedline, D. Ho, W. Gu, S. Sen Gupta, A. Hill, P. Kusuma, I. Lipsky, M. McNulty, J. Meraz, V. Pane, K. Sander, F. Shi, J. Skerker, A. Styer, K. Valgardson, K. Wetmore, S. Woo, Y. Xiong, K. Yates, C. Zhang, B. Bugbee, D. Coleman-Derr, S. Nandi, R. Waymouth, P. Yang, C.S. Criddle, K.A. McDonald, L.C. Seefeldt, A. Mesbah, D.S. Clark, A.A. Menezes, A.P. Arkin. **Towards a Biomanufactory on Mars**. *Frontiers in Astronomy and Space Sciences* (2021). DOI: 10.3389/fspas.2021.711550.

3.1 Feasibility, Needs, and Mission Architecture

The standard specifications for Mars exploration from 2009[147] and 2019[319] are not designed as biomanufacturing-driven [40] due to the novelty of space bioengineering. Here, we outline biotechnological support to produce food, medicine, and specialized construction materials on a long-term mission with six crew-members and surface operations for ∼500

sols (a Martian sol is ∼40 min longer than an Earth day) flanked by two interplanetary transits of ∼210 days[376]. We further assume predeployment cargo that includes *in situ* resource utilization (ISRU) hardware for Mars-ascent propellant production[467], which is to be launched from Earth to a mission site. Additional supplies such as habitat assemblies[232, 113], photovoltaics[300, 301], experimental equipment, and other non-living consumables[38] will be included.

The proposed biomanufactory would augment processes for air generation and water and waste recycling and purification – typically associated with Environmental Control and Life Support Systems (ECLSS)[221, 194] – since its needs overlap but are broader, and drive a wider development of an array of ISRU, *in situ* manufacturing (ISM), food and pharmaceutical synthesis (FPS), and loop closure (LC) technologies (Fig. 3.1).

Food, medicine, and gas exchange to sustain humans imposes important ECLSS feasibility constraints[576, 574, 551]. These arise from a crewmember (CM) physiological profile, with an upper-bound metabolic rate of ∼11-13 MJ/CM-sol that can be satisfied through

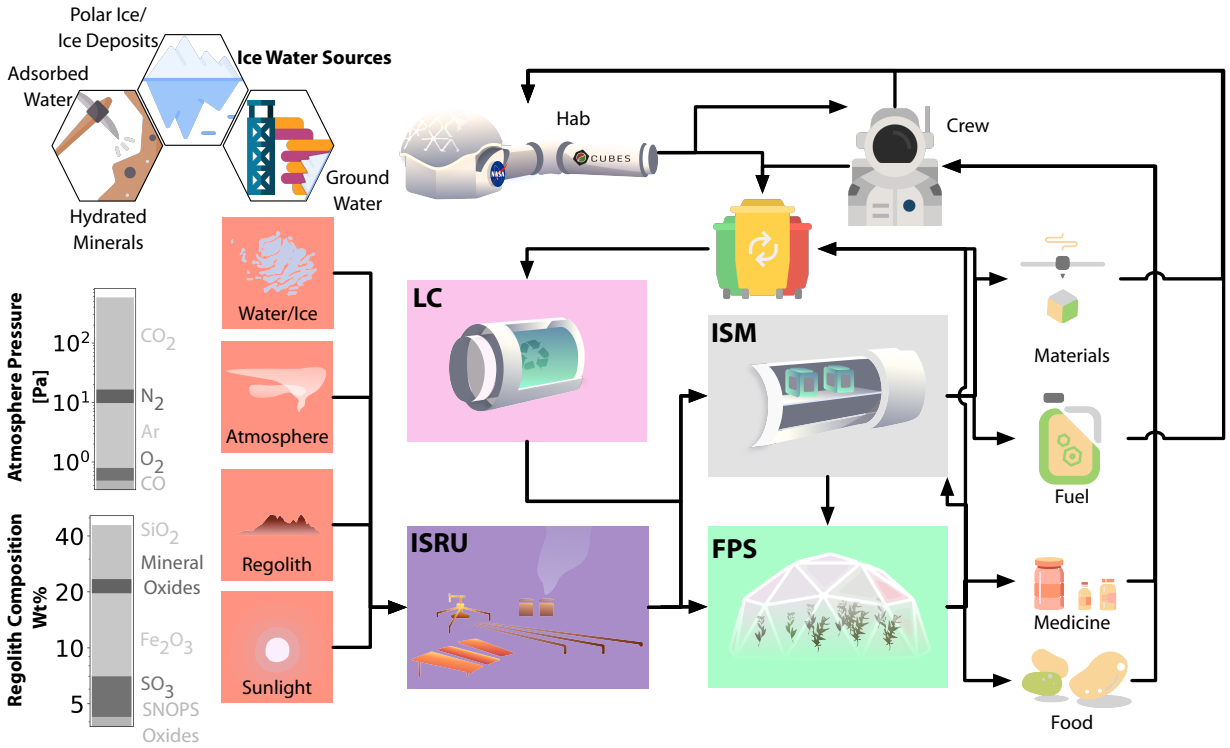

Figure 3.1: Proposed surface operations are drawn from inventories of *in situ* resources (red) such as ice, atmosphere, regolith, and sunlight. Atmospheric feedstocks of carbon and nitrogen are biologically fixed via the ISRU (*in situ* resource utilization) biomanufactory components (including abiotic processes, purple), providing the source of biopolymer manufacturing via the ISM (*in situ* manufacturing) component (grey) and food via the FPS (food and pharmaceutical synthesis) component (green), which are used for astronaut consumption and utilization during mission operations. Waste from each of these elements is collected and fed into the LC (loop closure) element (pink) to maximize efficiency and reduce the cost of supply logistics from Earth.

prepackaged meals and potable water intake of 2.5 kg/CM-sol[17, 321]. Sustaining a CM also entails providing oxygen at 0.8 kg/CM-sol and recycling the 1.04 kg/CM-sol of CO_2, 0.11 kg of fecal and urine solid, and 3.6 kg of water waste within a habitat kept at ∼294 K and ∼70 kPa. Proposed short duration missions lean heavily on chemical processes for life support with consumables sent from Earth[147]. As the length of a mission increases, demands on the quantity and quality of consumables increase dramatically. As missions become more complex with longer surface operations, biotechnology offers methods for consumable production in the form of edible crops and waste recycling through microbial digestion[221]. Advancements in biomanufacturing for deep space exploration will ensure a transition from short-term missions that are reliant on single-use-single-supply resources to long-term missions that are sustainable.

Biomanufactory Systems Engineering

Efficiency gains in a biomanufactory come in part from the interconnection (Fig. 3.1) and modularity of various unit operations (Figs. 3.2-3.5)[121]. However, different mission stage requirements for assembly, operation, timing, and productivity can lead to different optimal biomanufactory system configurations. A challenge therefore exists for technology choice and process optimization to address the high flexibility, scalability, and infrastructure minimization needs of an integrated biomanufactory. Current frameworks for biomanufacturing optimization do not dwell on these aspects. A series of new innovations in modeling processes and developing performance metrics specific to ECLSS biotechnology is called for, innovations that can suitably capture risk, modularity, autonomy, and recyclability. Concomitant invention in engineering infrastructure will also be required.

3.2 Food and Pharmaceutical Synthesis

An estimated ∼10,000 kg of food mass is required for a crew of six on a ∼900 day mission to Mars[371]. Food production for longer missions reduces this mission overhead and increases food store flexibility, bolsters astronaut mental health, revitalizes air, and recycles wastewater through transpiration and condensation capture[536, 298]. Pharmaceutical life support must overcome accelerated instability (∼75% of solid formulation pharmaceuticals are projected to expire mid-mission at 880 days[371]) and long re-supply times. Pharmaceutical production for longer missions can mitigate the impact of this anticipated instability and accelerate response time to unanticipated medical threats. In early missions, FPS may boost crew morale and supplement labile nutrients[286]. As mission scale increases, FPS may meet important food and pharmaceutical needs[76]. A biomanufactory that focuses on oxygenic photoautotrophs, namely plants, algae and cyanobacteria, enhances simplicity, versatility, and synergy with intersecting life support systems[563, 194]. While plant-based food has been the main staple considered for extended missions[147, 17, 76], the advent of cultured

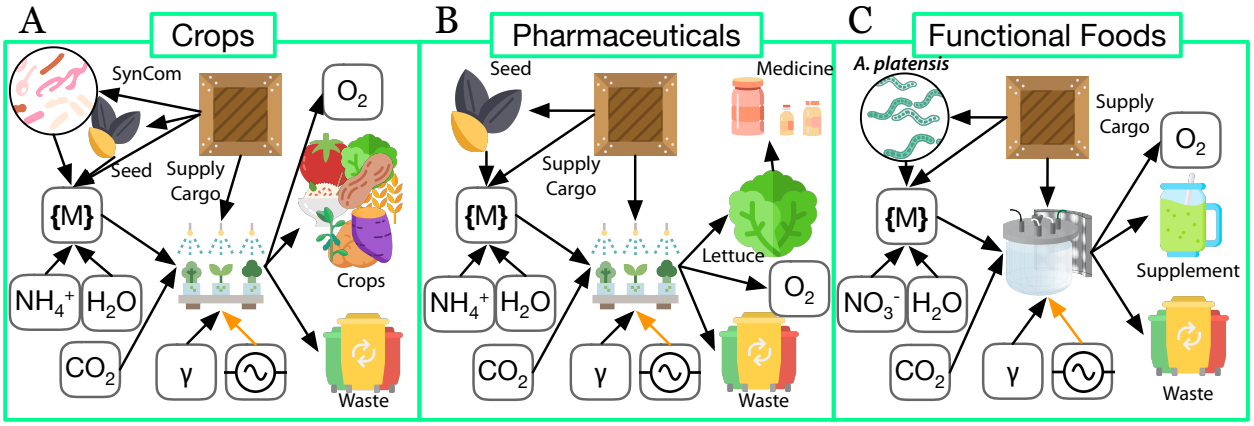

Figure 3.2: FPS (green) system breakdown for biomanufactory elements of **(A)** crops, **(B)** a biopharmaceutical, and **(C)** functional food production. In all cases, growth reactors require power (electrical current symbol) and light (γ). **(A)** Crop biomass and oxygen gas (O_2) are produced from hydroponically grown plants using seeds and media ({M}) derived from supply cargo. The reactor is also supplied with an ammonium (NH_4^+) nitrogen source and CO_2 carbon source from ISRU processes. **(B)** In a similar fashion, medicine can be produced from genetically modified crops such as lettuce. **(C)** Functional foods such as nutritional supplements are produced via autotrophic growth of *A. platensis*. In all cases, biomass is produced, collected, and inedible biomass is distributed to the LC module for recycling.

and 3D printed meat-like products from animal, plant and fungal cells may ultimately provide a scalable and efficient alternative to cropping systems[73, 420, 226].

FPS organisms for Mars use must be optimized for growth and yields of biomass, nutrient, and pharmaceutical accumulation. Providing adequate and appropriate lighting will be a challenge of photoautotrophic-centric FPS on Mars[352, 296]. Developing plants and algae with reduced chloroplast light-harvesting antenna size has the potential to improve whole-organism quantum yield by increasing light penetration deeper into the canopy, which will reduce the fraction of light that is wastefully dissipated as heat and allow higher planting density[181]. Developing FPS organisms for pharmaceutical production is especially complicated, given the breadth of production modalities and pharmaceutical need (e.g., the time window of intervention response, and molecule class)[366]. Limited-resource pharmaceutical purification is also a critically important consideration that has not been rigorously addressed. Promising biologically-derived purification technologies[334, 555] should be considered for processing drugs that require very high purity (e.g., injectables).

Developing FPS growth systems for Mars requires synergistic biotic and abiotic optimization, as indicated by lighting systems and plant microbiomes. For lighting, consider that recent advancements in LED efficiency now make LEDs optimal for crop growth in extraterrestrial systems[213]. The ideal spectra from tunable LEDs will likely be one with a high fraction of red photons for maximum production efficiency, but increasing the fraction of shorter wavelength blue photons could increase crop quality[257]. Similarly, higher photon intensities increase production rates but decrease production efficiency. Understanding the associated volume and power/cooling requirement tradeoffs will be paramount to increasing

overall system efficiency.

For microbiomes, consider that ISS open-air plant cultivation results in rapid and widespread colonization by atypicaly low-diversity bacterial and fungal microbiomes that often lead to plant disease and decreased plant productivity[286]. Synthetic microbial communities (SynComs, Fig. 3.2A) may provide stability and resilience to the plant microbiome and simultaneously improve the phenotype of host plants via the genes carried by community members. A subset of naturally occurring microbes are well known to promote growth of their plant hosts[215], accelerate wastewater remediation and nutrient recycling[411], and shield plant hosts from both abiotic and biotic stresses[72], including opportunistic pathogens[464, 49, 305]. While SynCom design is challenging, the inclusion of SynComs in life support systems represents a critical risk-mitigation strategy to protect vital food and pharma resources. The application of SynComs to Mars-based agriculture motivates additional discussions in tradeoffs between customized hydroponics versus regolith-based farming, both of which will require distinct technology platforms and applied SynComs.

FPS Integration into the Biomanufactory

Our biomanufactory FPS module has three submodules: crops, pharmaceuticals, and functional foods (Fig. 3.2). The inputs to all three submodules (Fig. 3.2) are nearly identical in needing H_2O as an electron donor, CO_2 as a carbon source, and light as an energy source, with the required nitrogen source being organism-dependent (e.g., *A. platensis* requires nitrate). H_2O, CO_2, and light are directly available from the Martian environment. Fixed nitrogen comes from the biomanufactory ISRU module. The submodules output O_2, biomass, and waste products. However, the crop submodule (Fig. 3.2A) chiefly outputs edible biomass for bulk food consumption, the pharmaceutical submodule (Fig. 3.2B) synthesizes medicines, and the functional foods submodule (Fig. 3.2C) augments the nutritional requirements of the crop submodule with microbially-produced vitamins (e.g., vitamin B_{12}). These outputs will be consumed directly by crew-members, with waste products entering the LC module for recycling.

All submodules will have increased risk, modularity, and recyclability relative to traditional technological approaches. Increased risk is associated with biomass loss due to lower-than-expected yields, contamination, and possible growth system failure. Increased modularity over shipping known pharmaceuticals to Mars derives from the programmability of biology, and the rapid response time of molecular pharming in crops for as-needed production of biologics. Increased recyclability stems from the lack of packaging required for shipping food and pharmaceuticals from Earth, as well as the ability to recycle plant waste using anaerobic digestion.

At a systems integration level, FPS organism care will increase the crew time requirements for setup, maintenance, and harvesting compared to advance food and pharmaceutical shipments. However, overall cost impacts require careful scrutiny: crop growth likely saves on shipping costs, whereas pharmaceutical or functional food production on Mars may increase costs relative to shipping drugs and vitamins from Earth.

3.3 In situ Materials Manufacturing

Maintaining FPS systems requires cultivation vessels/chambers, support structures, plumbing, and tools. Such physical objects represent elements of an inventory that, for short missions, will likely be a combination of predeployment cargo and supplies from the crewed transit vehicle[147]. As mission duration increases, so does the quantity, composition diversity, and construction complexity of these objects. The extent of ISM for initial exploration missions is not currently specified[147]. Nevertheless, recent developments[417, 418, 391] imply that ISM will be critical for the generation of commodities and consumables made of plastics[82], metals[168], composite-ceramics[279], and electronics[554] as mission objects, with uses ranging from functional tools[199] to physical components of the life-supporting habitat[418].

Plastics will make up the majority of high-turnover items with sizes on the order of small parts to bench-top equipment, and will also account for contingencies[437]. Biotechnology in combination with additive manufacturing can produce such polymeric constructs from basic feedstocks in a more compact and integrated way than chemical synthesis, because microbial bioreactors operate much closer to ambient conditions than chemical processes[336]. The versatility of microbial metabolisms allows direct use of CO_2 from Mars' atmosphere, methane (CH_4) from abiotic Sabatier processes[227], and/or biologically synthesized C_2 compounds such as acetate, as well as waste biomass.

A class of bioplastics that can be directly obtained from microorganisms[399] are polyhydroxyalkanoates (PHAs). While the dominant natural PHA is poly(3-hydroxybutyrate) (PHB), microbes can produce various co-polymers with an expansive range of physical properties[396]. This is commonly accomplished through co-feeding with fatty acids or hydroxyalkanoates, which get incorporated in the polyester. These co-substrates can be sourced from additional process inputs or generated *in situ*. For example the PHA poly-lactic acid (PLA) can be produced by engineered *E. coli*[276], albeit to much lower weight percent than is observed in organisms producing PHAs naturally. PHA composition can be modulated in other organisms[452]. The rapid development of synthetic biology tools for non-model organisms opens an opportunity to tune PHA production in high PHB producers and derive a range of high-performance materials.

Before downstream processing (melting, extrusion / molding), the intracellularly accumulating bioplastics need to be purified. The required degree of purity determines the approach and required secondary resources. Fused filament fabrication 3D-printing, which works well in microgravity[436, 437], has been applied for PLA processing and may be extendable to other bio-polyesters. Ideally, additive manufacturing will be integrated in-line with bioplastics production and filament extrusion.

ISM Integration into the Biomanufactory

Figure 3.3 depicts the use of three organism candidates (*Cupriavidus*, *Methylocystis*, *Halomonas*) that can meet bioplastic production needs requires a different set of parameters to optimize

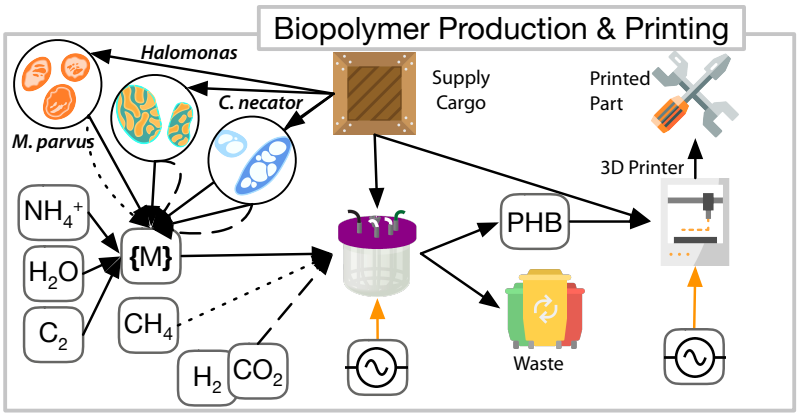

Figure 3.3: ISM systems breakdown for biomanufactory elements of biopolymer production and 3D-printing. 3D printed parts are fabricated from bioproduced plastics. Biopolyesters such as PHB, along with corresponding waste products, are formed in cargo-supplied reactors with the aid of microorganisms. A variety of available carbon feedstocks can serve as substrates for aerobic auto-, hetero-, or mixotrophic microorganisms such as *C. necator*, *Methylocystis parvus* and *Halomonadaceae*. All three microbes are capable of using C_2 feedstocks (like acetate), while *C. necator* and *Methylocystis* can also use C_1 feedstocks. The former utilizes a combination of CO_2 and H_2 (large dotted line), while only *M. parvus* can leverage CH_4 (small dotted line).

their deployment, which strongly affects reactor design and operation. These microbes are capable of using a variety of carbon sources for bioplastic production, each with a trade-off. For example, leveraging C_2 feedstocks as the primary source will allow versatility in the microbe selection, but may be less efficient and autonomous than engineering a single organism like *C. necator* to use CO_2 directly from the atmosphere. Alternatively, in the event that CH_4 is produced abiotically for ascent propellant[394], a marginal fraction of total CH_4 will be sufficient for producing enough plastic without additional hardware costs associated with ISRU C_2 production. Relying on *Halomonas* in combination with acetate as substrate may allow very rapid production of the required bioplastic, but substrate availability constraints are higher than for CH_4 or CO_2/H_2. A terminal electron acceptor is required in all cases, which will almost certainly be O_2. Supplying O_2 safely without risking explosive gas mixtures, or wasting the precious resource, is again a question of reactor design and operation. Certain purple non-sulfur alphaproteobacteria (e.g., *Rhodospirillum rubrum* and *Rhodopseudomonas palustris*) also feature remarkable substrate flexibility and can produce PHAs.

Bioplastic recovery and purification is a major challenge. To circumvent the need for halogenated organic solvents, an osmolysis process[445] may be employed with the halophile[515, 96]. As this still requires substantial amounts of water, an alternative for all three proposed organisms is to use acetate or methanol as solvents[15, 24]. These inputs can be provided from other biomanufactory modules.

The high crystallinity of pure PHB makes it brittle and causes it to have a narrow melting range, resulting in warp during extrusion and 3D-printing. Such behavior places operational constraints on processing and hampers applications to precision manufactur-

ing[342]. Workarounds may be through additives, biocomposite synthesis, and copolymerization. However, this ultimately depends on what biology can provide[392]. There is a need to advance space bio-platforms to produce more diverse PHAs through synthetic biology.

ISM of biomaterials can reduce the mission cost, increase modularity, and improve system recyclability compared to abiotic approaches. In an abiotic approach, plastics will be included in the payload, thereby penalizing up-mass at launch. As with elements of FPS and ISRU, ISM increases flexibility and can create contingencies during surface operations, therefore reducing mission risk. The high modularity of independent plastic production, filament formation, and 3D-printing allows for a versatile process, at the cost of greater resources required for systems operations. Overall, this maximizes resource use and recyclability, by utilizing mission waste streams and byproducts for circular resource management.

3.4 In situ Resource Utilization

Biomanufacturing on Mars can be supported by flexible biocatalysts that extract resources from the environment and transform them into the complex products needed to sustain human life. The Martian atmosphere contains CO_2 and N_2[371]. Water and electrolytically produced O_2 and H_2 are critical to mission elements for any Mars mission. It is very likely that the expensive and energy-intensive Sabatier plants[227, 369, 107] for CH_4 production will be available per DRA 5.0[147]. While a Haber-Bosch plant could be set up for ammonia production, this is neither part of the current DRA[147] nor exceptionally efficient (citation). Thus, For a biomanufactory, we must have carbon fixation reactors to fix CO_2 into feedstocks for non-methanotrophs, and have nitrogen fixation reactors to fix N_2 to fulfill nitrogen requirements for non-diazotrophs. Trace elements and small-usage compounds can be transported from Earth, or in some cases extracted from the Martian regolith. In the case where power is provided from photocollection or photovoliatics, light energy will vary with location and season, and may be critical to power our bioreactors.

Although photosynthetic organisms are attractive for FPS, a higher demand for carbon-rich feedstocks and other chemicals necessitates a more rapid and efficient CO_2 fixation strategy. Physicochemical conversion is inefficient due to high temperature and pressure requirements. Microbial electrosynthesis (MES), whereby reducing power is passed from abiotic electrodes to microbes to power CO_2 reduction, can offer rapid and efficient CO_2 fixation at ambient temperature and pressure[3]. MES can produce a variety of chemicals including acetate[323], isobutanol[316], PHB[324], and sucrose[402], and therefore represents a flexible and highly promising ISRU platform technology[5].

Biological N_2-fixation offers power- and resource-efficient ammonium production. Although photoautotrophic N_2 fixation with, for example, purple non-sulfur bacteria, is possible, slow growth rates due to the high energetic demand of nitrogenase limits throughput[145]. Therefore, heterotrophic production with similar bacteria using acetate or sucrose as a feedstock sourced from electromicrobial CO_2-fixation represents the most promising

production scheme, and additionally benefits from a high degree of process redundancy with heterotrophic bioplastic production.

Regolith provides a significant inventory for trace elements (Fe, K, P, S, etc.) and, when mixed with the substantial cellulosic biomass waste from FPS processes, can facilitate recycling organic matter into fertilizer to support crop growth. However, regolith use is hampered by widespread perchlorate [125, 86, 407], indicating that decontamination is necessary prior to enrichment or use. Dechlorination can be achieved via biological perchlorate reduction using one of many dissimilatory perchlorate reducing organisms[559, 132, 70, 71].

ISRU Integration into the Biomanufactory

A biomanufactory must be able to produce and utilize feedstocks along three axes as depicted in Figure 3.4: CO_2-fixation to supply a carbon and energy source for downstream heterotrophic organisms or to generate commodity chemicals directly, N_2-fixation to provide ammonium and nitrate for plants and non-diazotrophic microbes, and regolith decontamination and enrichment for soil-based agriculture and trace nutrient provision. ISRU inputs are submodule and organism dependent, with all submodules requiring water and power. For the carbon fixation submodule (Fig. 3.4A), CO_2 is supplied as the carbon source, and electrons are supplied as H_2 or directly via a cathode. Our proposed biocatalysts are the lithoautotrophic *Cupriavidus necator* for longer-chain carbon production (e.g., sucrose[402]) and the acetogen *Sporomusa ovata* for acetate production. *C. necator* is a promising chassis for metabolic engineering and scale-up[402], with *S. ovata* having one of the highest current consumptions for acetogens characterized to date[326]. The fixed-carbon outputs of this

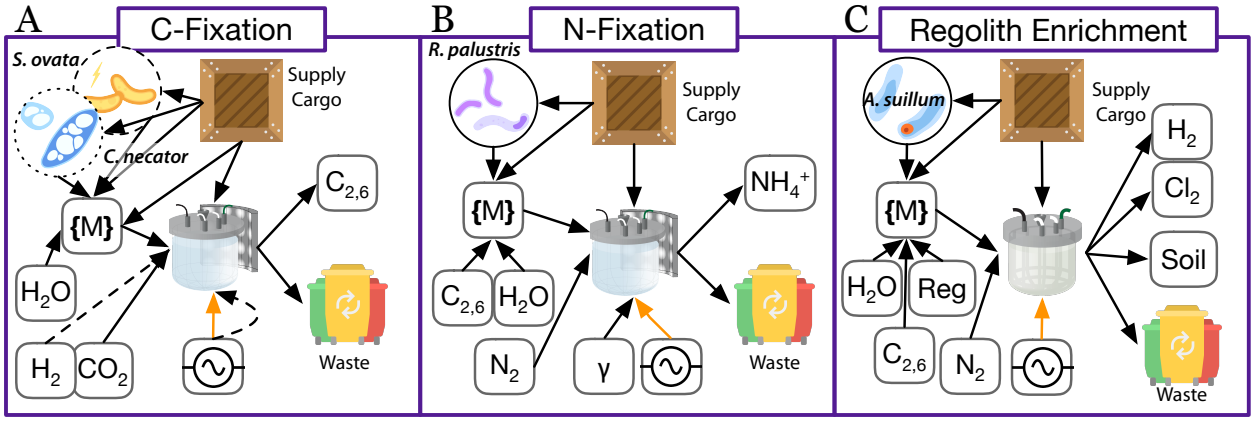

Figure 3.4: ISRU (purple in Fig. 3.1) system breakdown of biomanufactory elements. **(A)** Carbon fixation with the autotrophic bacteria *Sporomusa ovata* or *Cupriavidus necator* through electrosynthesis or lithoautotrophic fixation of C_1-carbon (cathodes or H_2 as the electron donor). **(B)** Microbial nitrogen fixation with diazotrophic bacteria like *Rhodopseudomonas palustris* growing photoheterotrophically. **(C)** Regolith (Reg) enrichment using the perchlorate-reducing microbe *Azospira suillum*. Black lines represent material and energy flows related to biological consumption and production. Orange lines indicate additional power supply to the system.

submodule are then used as inputs for the other ISRU submodules (Fig. 3.4B,C) in addition to the ISM module (Fig. 3.1). The inputs to the nitrogen fixation submodule (Fig. 3.4B) include fixed carbon feedstocks, N_2, and light. The diazotrophic purple-non sulfur bacterium *Rhodopseudomonas palustris* is the proposed biocatalyst, as this bacterium is capable of anaerobic, light-driven N_2 fixation utilizing acetate as the carbon source, and has a robust genetic system allowing for rapid manipulation[145, 5]. The output product is fixed nitrogen in the form of ammonium, which is used as a feedstock for the carbon-fixation submodule of ISRU along with the FPS and ISM modules. The inputs for the regolith enrichment submodule (Fig. 3.4C) include regolith, fixed carbon feedstocks, and N_2. *Azospira suillum* is a possible biocatalyst of choice due to its dual use in perchlorate reduction and nitrogen fixation[71]. Regolith enrichment outputs include soil for the FPS module (in the event that solid support-based agriculture is selected instead of hydroponics), H_2 that can be fed back into the carbon fixation submodule and the ISM module, chlorine gas from perchlorate reduction, and waste products.

Replicate ISRU bioreactors operating continuously in parallel with back-up operations lines can ensure a constant supply of the chemical feedstocks, commodity chemicals, and biomass for downstream processing in ISM and FPS operations. Integration of ISRU technologies with other biomanufactory elements, especially anaerobic digestion reactors, may enable (near-)complete recyclability of raw materials, minimizing resource consumption and impact on the Martian environment[431, 332].

3.5 Loop Closure and Recycling

Waste stream processing to recycle essential elements will reduce material requirements in the biomanufactory. Typical feedstocks include inedible crop mass, human excreta, and other mission wastes. Space mission waste management traditionally focuses on water recovery and efficient waste storage through warm air drying and lyophilization[576, 17]. Mission trash can be incinerated to produce CO_2, CO, and H_2O [228]. Pyrolysis, another abiotic technique, yields CO and H_2 alongside CH_4[482]. The Sabatier process converts CO_2 and CO to CH_4 by reacting with H_2. An alternate thermal degradation reactor[79], operating under varying conditions that promote pyrolysis, gasification, or incineration, yields various liquid and gaseous products. The fact remains however, that abiotic carbon recycling is inefficient with respect to desired product CH_4, and is highly energy-intensive.

Microbes that recover resources from mission wastes are a viable option to facilitate loop closure. Aerobic composting produces CO_2 and a nutrient-rich extract for plant and microbial growth[442, 443]. However, this process requires O_2, which will likely be a limited resource. Hence, anaerobic digestion, a multi-step microbial process that can produce a suite of end-products at lower temperature than abiotic techniques ($\sim$35-55°C compared to $\sim$500-600°C, an order of magnitude difference), is the most promising approach for a Mars biomanufactory[368, 506] to recycle streams for the ISM and FPS processes. Digestion products CH_4 and volatile fatty acids (VFA, such as acetic acid) can be substrates for

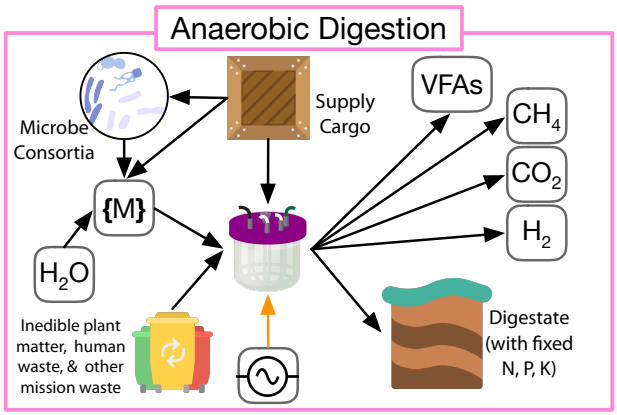

Figure 3.5: LC-based (pink) anaerobic digestion of mission waste such as inedible plant matter, microbial biomass, human, and other wastes produce methane, volatile fatty acids (VFAs), and digestate rich with key elemental nutrients (N, P, K), thereby supplementing ISRU operation.

polymer-producing microbes[397, 94]. Digestate, with nutrients of N, P, and K, can be ideal for plant and microbial growth[384], Fig. 3.5. Additionally, a CH_4 and CO_2 mixture serves as a biogas energy source, and byproduct H_2 is also an energy source[474, 285].

Because additional infrastructure and utilities are necessary for waste processing, the extent of loop closure that is obtainable from a treatment route must be analyzed to balance yield with its infrastructure and logistic costs. Anaerobic digestion performance is a function of the composition and pretreatment of input waste streams (crop residuals, feces, urine, end-of-life bioproducts), as well as reaction strategies like batch or continuous, number of stages, and operation conditions such as organic loading rate, solids retention time, operating temperature, pH, toxic levels of inhibitors (H_2S, NH_3, salt) and trace metal requirements[474, 23, 368, 506, 322, 456]. Many of these process parameters exhibit trade-offs between product yield and necessary resources. For example, a higher waste loading reduces water demand, albeit at the cost of process efficiency. There is also a potential for multiple co-benefits of anaerobic digestion within the biomanufactory. Anaerobic biodegradation of nitrogen-rich protein feedstocks, for example, releases free NH_3 by ammonification. While NH_3 is toxic to anaerobic digestion and must thus be managed[456], it reacts with carbonic acid to produce bicarbonate buffer and ammonium, decreasing CO_2 levels in the biogas and buffering against low pH. The resulting digestate ammonium can serve as a fertilizer for crops and nutrient for microbial cultures.

LC Integration into the Biomanufactory

FPS and ISM waste as well as human waste are inputs for an anaerobic digester, with output recycled products supplementing the ISRU unit. Depending on the configuration of the waste streams from the biomanufactory and other mission elements, the operating conditions of the process can be varied to alter the efficiency and output profile. Open problems

include the design and optimization of waste processing configurations and operations, and the identification of optimal end-product distributions based on a loop closure metric[39] against mission production profiles, mission horizon, biomanufacturing feedstock needs, and the possible use of leftover products by other mission elements beyond the biomanufactory. A comparison with abiotic waste treatment strategies (incineration and pyrolysis) is also needed, checking power demand, risk, autonomy, and modularity benefits.

3.6 Discussion and Roadmap

Biomanufactory development must be done in concert with planned NASA missions that can provide critical opportunities to test subsystems and models necessary to evaluate efficacy and technology readiness levels (TRLs)[339]. Figure 3.6 is our attempt to place critical elements of a biomanufactory roadmap into this context. We label critical mission stages using RMA-S and RMA-L, which refer to Mars surface missions with short (∼30 sols) and long (>500 sols) durations, respectively.

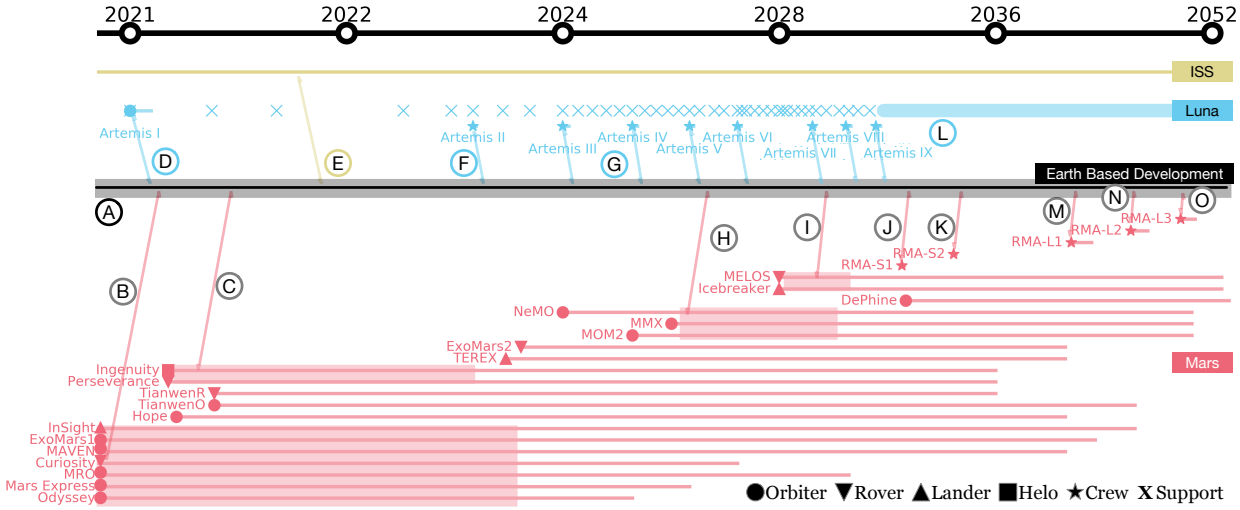

Figure 3.6: Proposed roadmap from 2021 to 2052 in $\log_2$-scale time of Earth-based developments (black) and their relationships to ISS (gold), lunar (blue), and Martian (red) missions. Missions range in status from currently operational, to enroute, planned, and proposed. Reference Mission Architecture (RMA)-S is a 30-sol mission, and RMA-L are missions with more than 500 sols of surface operations. RMA-L1 is the mission target for deployment of a biomanufactory. An arrival at target location is denoted with a symbol to indicate its type as orbiter, rover, lander, helicopter, support, or crewed operations. Circled letters are colored by location and correspond to specific milestones or opportunities for biomanufactory development.

Reliance on biotechnology can increase the risk of forward biological contamination[430]. Beyond contamination, there are ethical issues that concern both the act of colonizing a new land and justifying the cost and benefits of a mission given needs of the many here on earth. Planetary protection policies can provide answers or frameworks to address extant ethical

questions surrounding deep-space exploration, especially on Mars[516, 457]. Critically, scientists and engineers developing these technologies cannot be separate or immune to such policy development.

Autonomous Martian Surface Missions

Figure 3.6Ⓑ denotes the interconnection between current Martian mission objects[347, 349, 33, 355, 348, 345, 1] and Earth-based process development elements for a biomanufactory (Figs. 3.2-3.5). Together with *en route* autonomous surface missions[346, 344] (Fig. 3.6Ⓒ), these missions provide a roadmap for continued mission development based on landing location biosignatures[69, 532]. The biomanufactory (Figs. 3.2-3.5) will require ample water in media, atmospheric gas feedstocks, and power that can be bounded by measurements from autonomous missions. Upcoming sample return missions offer an opportunity to shape the design of ISRU processes such as regolith decontamination from perchlorate and nitrogen enrichment for crop growth. Additional orbiters[254] and lander/rover pairs (Fig. 3.6Ⓗ) have been planned and will aid in the selection of a landing site for short term Martian exploration missions (Fig. 3.6Ⓙ,Ⓚ). Such locations will be determined based on water/ice mining/availability[362] in Fig. 3.6Ⓘ. These missions can be deployed with specific payloads to experimentally validate biomanufactory elements. Low TRL biotechnologies can be flown as experimental packages on upcoming rovers and landers, offering the possibility for TRL advancement of biology-driven subsystems. Planning for such testing will require coordination with, and validation on, ISS and satellite payloads (Fig. 3.6Ⓔ), for instance, to understand the impact of Martian gravity, to contrast levels of radiation exposure, and so on.

Artemis Operations

The upcoming lunar exploration missions, Artemis[497] and Gateway[122], provide additional opportunities for integration with Earth-based biomanufactory development. Early support missions (Fig. 3.6Ⓓ,Ⓕ) will provide valuable experience in cargo predeployment for crewed operations, and is likely to help shape logistics development for short-term (Fig. 3.6Ⓙ,Ⓚ) as well as long-term Mars exploration missions (Fig. 3.6Ⓜ) when a biomanufactory can be deployed. Although ISRU technologies for the Moon and Mars will be sufficiently distinct due to different resource availabilities, crewed Artemis missions (Fig. 3.6Ⓕ,Ⓖ) provide a testing ground for crewed Mars bioprocess infrastructure. Later Artemis missions (Fig. 3.6Ⓛ) also provide a suitable environment to test modular, interlocked, scalable reactor design, as well as the design of compact molecular biology labs for DNA synthesis and transformation. Since these technologies are unlikely to be mission critical during Artemis, their TRL can be increased and their risk factors studied through in-space evaluation.

The Artemis missions also provide a testbed to evaluate the space-based evolution of microbes and alterations of seedstocks as a risk inherent to the biological component of the biomanufactory. This risk can be mitigated by incorporating backup seed and micro-

bial freezer stocks to reset the system. However, ensuring that native and/or engineered traits remain robust over time is critical to avoid the resource penalties that are inherent to such a reset. Consequently, while optimal organisms and traits can be identified and engineered prior to a mission, testing their long-term performance on future NASA missions prior to inclusion in life support systems will help to assess whether engineered traits are robust to off-planet growth, whether microbial communities are stable across crop generations, and whether the *in situ* challenges that astronauts will face when attempting to reset the biomanufacturing system are surmountable. Quantifying these uncertainties during autonomous and crewed Artemis missions will inform tradeoff and optimization studies during the design of an enhanced life support system for Martian surface bio-operations.

Human Exploration of Mars

Crewed surface operations of ∼30 sols by four to six astronauts are projected[147] to begin in 2031 (Fig. 3.6Ⓙ), with an additional mission similar in profile in 2033 (Fig. 3.6Ⓚ). Given the short duration, a mission-critical biomanufactory as described herein is unlikely to be deployed. However, these short-term, crewed missions RMA-S1,S2 provide opportunities to increase the TRL of biomanufactory elements for ∼500 sol surface missions RMA-L1 (Fig. 3.6Ⓜ) in ∼2040 and RMA-L2 (Fig. 3.6Ⓝ) in ∼2044. Building on the abiotic ISRU from early Artemis missions, we propose that RMA-S1 carry experimental systems for C-and-N-fixation processes such that a realized biomanufactory element can be properly scaled (Fig. 3.4). Since RMA-S1,S2 will be crewed, regolith process testing becomes more feasible to be tested onsite on the surface of Mars, than during a complex sample return mission. Additionally, while relying on prepacked food for consumption, astronauts in RMA-S1 will be able to advance the TRL of platform combinations of agriculture hardware, crop cultivars, and operational procedures. An example is growing crops under various conditions (Fig. 3.2A) to validate that a plant microbiome can provide a prolonged benefit in enclosed systems, and to determine resiliency in the event of pathogen invasion or a loss of microbiome function due to evolution. Additionally, the TRL for crop systems can be re-evaluated on account of partial gravity and/or microgravity.

The RMA-S1 and RMA-S2 crews will be exposed for the first time to surface conditions after interplanetary travel, allowing for an initial assessment of health effects that can be contrasted to operations on the lunar surface (Fig. 3.6Ⓕ), and that may be alleviated by potential biomanufactory pharmaceutical and functional food outputs (Fig. 3.2B,C). The RMA-S1 and RMA-S2 mission ISRU and FPS experiments will also provide insight into the input requirements for downstream biomanufactory processes. ISM technologies such as bioplastic synthesis and additive manufacture (Fig. 3.3) can be evaluated for sufficient TRL. Further, loop closure performance for several desired products can also be tested. This will help estimate the impact of waste stream characteristics changes on recycling[60].

Moving Forward

We have outlined the design and future deployment of a biomanufactory to support human surface operations during a 500 day manned Mars mission. We extended previous stand-alone biological elements with space use potential into an integrated biomanufacturing system by bringing together the important systems of ISRU, synthesis, and recycling, to yield food, pharmaceuticals, and biomaterials. We also provided an envelope of future design, testing, and biomanufactory element deployment in a roadmap that spans Earth-based system development, testing on the ISS, integration with lunar missions, and initial construction during shorter-term initial human forays on Mars. The innovations necessary to meet the challenges of low-cost, energy and mass efficient, closed-loop, and regenerable biomanufacturing for space will undoubtedly yield important contributions to forwarding sustainable biomanufacturing on Earth. We anticipate that the path towards instantiating a biomanufactory will be replete with science, engineering, and ethical challenges. But that is the excitement — part-and-parcel — of the journey to Mars.

Chapter 4

Mathematical Formulations For Mission Design, Comparison, and Optimization

NASA mission systems proposals are often compared using an equivalent system mass (ESM) framework, wherein all elements of a technology to deliver an effect – its components, operations and logistics of delivery – are converted to effective masses, which has a known cost scale in space operations. To date, ESM methods and the tools for system comparison largely fail to consider complexities stemming from multiple transit and operations stages, such as would be required to support a crewed mission to Mars, and thus do not account for different mass equivalency factors during each period and the inter-dependencies of the costs across the mission segments. Further, ESM does not account well for the differential reliabilities of the underlying technologies. The uncertainty in the performance of a technology should incur an equivalent mass penalty for technology options that might otherwise provide a mass advantage. Here we draw attention to the importance of addressing these limitations and formulate the basis of an extension of ESM that allows for a direct method for analyzing, optimizing, and comparing different mission systems. We outline a preliminary example of applying extended ESM (xESM) through a technoeconomic calculation of crop-production technologies as an illustrative case for developing offworld biomanufacturing systems.

The following chapter can also found here: D. Ho, G. Makrygiorgos, A. Hill, A.J. Berliner **Towards the Extension of Equivalent System Mass for Human Exploration Missions on Mars**. *npj Microgravity*. (2022) DOI: 10.1038/s41526-022-00214-7

4.1 Towards an Extension of Equivalent System Mass

Travel to space is limited by the expense of transporting resources beyond Earth's gravity well[556]. As a result, early metrics of usability for space systems, especially life support[270], favored mass as the primary decision factor. Following a request to "provide the designers

of future missions with mature technologies and hardware designs, as well as extensive performance data justifying confidence that highly reliable Advanced Life Support Systems (ALS) that meet mission constraints can be developed" by the 1997 NASA Research Council (NRC)[116], the scope of the Equivalent System Mass (ESM) framework was broadened to account for differences in the cost of resources[150]. The general principle behind this early metric was to calculate the mass of all of the resources required to make the system work[153]. ESM was expanded from theory[314] to the practice of accounting for processes ranging from controls[375], agriculture[416], and recycling[295, 233]. Currently, ESM remains the standard metric for evaluating ALS technology development[388, 7, 295] and systems[17, 154, 511, 473]. It has been adopted for use in trade studies[313, 176, 171], as the metric for life support sizing[574, 572, 573], and has been incorporated into several tools[129, 137, 415].

In its current form[312], the total ESM M is defined only for the operations at a specific location as the sum over the set of all systems as

$$M = L_{\text{eq}} \sum_{i=1}^{\mathcal{A}} [\underbrace{(M_i \cdot M_{\text{eq}}) + (V_i \cdot V_{\text{eq}}) + (P_i \cdot P_{\text{eq}}) + (C_i \cdot C_{\text{eq}})}_{M_{\text{NCT}}} + \underbrace{(T_i \cdot D \cdot T_{eq})}_{M_{\text{CT}}}]$$

for subsystem $i \in \mathcal{A}$ of the ESM excluding crew-time M_{NCT} and the ESM including crewtime M_{CT} where M_i, V_i, P_i, C_i are the initial mass [kg], volume [m^3], power requirement [kW$_e$], and cooling requirement [kg/kW$_{\text{th}}$], D is the duration of the mission segment [sol], T_i is the crew-time requirement based on an astronaut crew-member (CM) [CM-h/sol], M_{eq} is the stowage factor for accounting for additional structural masses for a subsystem such as shelving [kg/kg], V_{eq} is the mass equivalency factor for the pressurized volume support infrastructure [kg/m^3], P_{eq} is the mass equivalency factor for the power generation support infrastructure [kg/kW$_e$], C_{eq} is the mass equivalency factor for the cooling infrastructure [kg/kW$_{\text{th}}$], T_{eq} is the mass equivalency factor for the crew-time [kg/CM-h], and L_{eq} is the location factor for the mission segment [kg/kg] which accounts for the cost to transport mass from one location in space to another (such as Earth orbit to Martian orbit). Mass equivalency factors (V_{eq}, P_{eq}, C_{eq}, T_{eq}) are used to convert the non-mass parameters to mass. While the ESM framework[312] has been widely adopted in Environmental Control and Life Support Systems (ECLSS) analysis[165, 138, 136, 137, 126, 429], it has faced critique for the ambiguity in its application as well as its difficulty in accounting for development costs[261] and uncertainty[6]. Alternative frameworks have been proposed to replace[264] or extend ESM with additional metrics[273] that factor in complexity[272]. Given the widespread use of ESM, we believe that the framework should be improved with the addition of missing elements rather than replaced completely.

Previous efforts to quantify the cost in problems of mission-planning/space logistics have relied on metrics based solely on the Initial Mass to Low Earth Orbit (IMLEO)[231, 444] for constant commodity supply and demand[249] or on carryalong mass[143]. In such logistics frameworks like SpaceNet[307, 201, 202] and HabNet[142], cost is kept simple to allow for the analysis of complex mission architectures with multiple mission segments. Comparatively, ESM has been most fully developed for ECLSS where the costs of capital equipment, power,

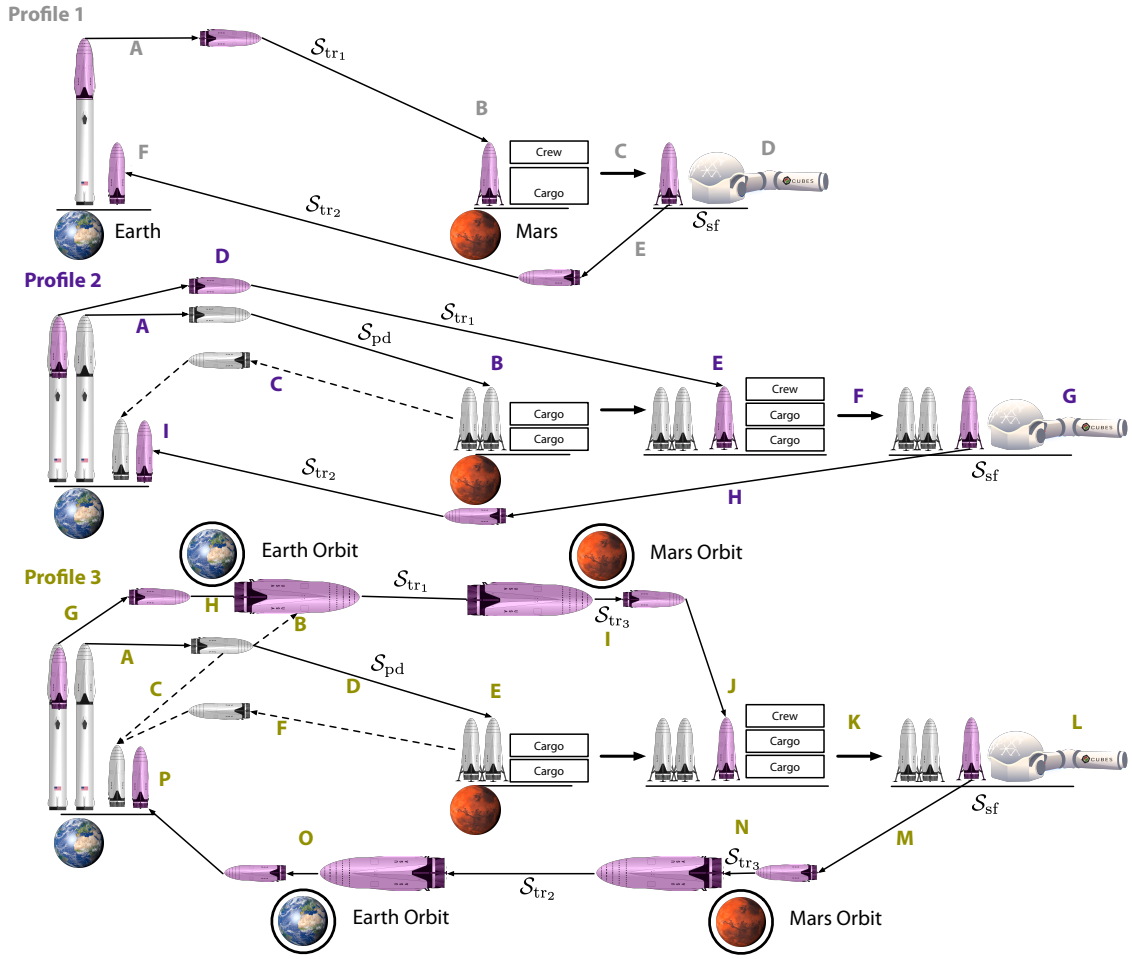

Figure 4.1: Transit Diagram of proposed Mission Architecture. In **Profile** 1(grey), **(A)** a crewed transit ship is launched directly from the surface of Earth and **(B)** lands on the surface of Mars where **(C)** the crew assembles the cargo in a habitat and carries out **(D)** surface operations until **(E)** the crew launches from their initial transit ship from the surface of Mars into space and **(F)** lands back on the surface of Earth. In **Profile** 2(purple), **(A)** cargo transit ships without crew are launched directly from the surface of Earth and **(B)** land on the surface of Mars where cargo can be unloaded. In the case of reusable rocket systems[449], **(C)** the cargo rockets can be launched from Mars and returned to Earth. Once all the cargo has been loaded onto the surface of Mars, **(D)** a crewed transit ship is launched directly from the surface of Earth and **(E)** lands on the surface of Mars where (F) the crew assembles the cargo in a habitat and carries out **(G)** surface operations until **(H)** the crew launches from their initial transit ship from the surface of Mars into space and **(I)** lands back on the surface of Earth. In **Profile** 3(green), a number of **(A)** cargo transit ships without crew are launched directly from the surface of Earth and either **(B)** supply a previously interplanetary rocket then **(C)** return to the surface of Earth or **(D)** travel to the surface of Mars where **(E)** cargo can be unloaded. In the case of reusable rocket systems, **(F)** the cargo rockets can be launched from Mars and returned to Earth. Once all the cargo has been loaded on the surface of Mars, **(G)** a crewed transit ship is launched directly from the surface of Earth to Earth Orbit **(H)** where it rendezvous with an interplanetary rocket which **(I)** travels to Martian orbit. The crew **(J)** then boards a descent vehicle and lands on the surface of Mars where **(K)** the crew assembles the cargo in a habitat and carries out **(L)** surface operations until **(M)** the crew launches from their initial transit ship from the surface of Mars into **(N)** Martian orbit where they again rendezvous with their interplanetary rocket which travels to **(O)** Earth orbit at which point they board a descent rocket in which they **(P)** finally return to the surface of Earth.

operations, transport, and other things have been captured on a common unit scale of mass. While it provides a method for summing the weighted terms of many subsystems, there is no explicit ESM equation that captures total mission costs across systems in various stages of a complex mission[261]. Thus the standard ESM approach faces limitations in that there (1) exists no explicit language for capturing the set of all segments and (2) there exists interdependent relationships between the decision variables within separate segments. Here we see a trade-off in the complexity of the cost function for the complexity of the mission architecture.

As plans for human exploration continue to be made in anticipation of returning to the moon[190, 497] and travelling to Mars[404, 44], an added emphasis will be required for optimization of mission architecture[202]. As of now, the current instance of the ESM framework does not lend itself for use as an objective function in an optimization over a mission – although this ESM has been proposed as the metric for mission optimization[267]. The result is that this standard framework remains fixed for multi-stage missions and generally (but not always[138]) faces challenges in providing design or planning information based on subsystem risk. Thus, the ESM metric is not always helpful when comparing missions with differential reliability for systems in their proper context. That is, given two possible technologies for meeting a mission objective, the one that is less likely to fail might be a better choice. To demonstrate how to formally add reliability metrics to the ESM framework, we take the case of a new technology platform, biomanufacturing[371, 401, 44], for which there are known and quantifiable reliability concerns and for which there is little *in situ* testing for space missions. In the following work, we propose an extended ESM (xESM) framework to account for the proposed multi-stage missions and critical mission features, such as reliability. As the scope of human exploration missions has expanded, the need for new technology platforms has grown, and it has been proposed that these features best capture the potential of biomanufacturing systems[44]. We do not claim a completion of xESM, but rather, we demonstrate progress along this trajectory in the form of a more generalized framework to (1) account for multi-staged mission segments (beyond simple summation); (2) account for reliability; and (3) feed into downstream optimization problems. We also note that this later progress is less developed in more in line with a discussion rather than a ready-to-use operational strategy.

4.2 Extending ESM for Long-Duration Mission Profiles

Figure 4.1 depicts three profiles with varied transit architectures. Profile 1 (grey) uses a single journey from Earth to Mars, and although it has been proposed in some forms[590], it is unlikely this architecture will be adopted due to the substantial mass demands of the transit ship and the ascent propellant required to leave Mars[61]. In the case of Profile 2 (purple), cargo can be predeployed to Mars through some number of predeployment missions. Profile 2 introduces segments to a crewed mission to Mars which are not actually crewed, but instead are either purely cargo-based in which case only the M and V terms factor into the ESM cost, or autonomous where M, V, P and C for uncrewed operations matter.

Since cargo missions do not require life support systems, the M cost is reduced greatly[17], leading to a reduction in overall mission cost, especially for missions that require a great quantity of goods that can be predeployed. In the most likely Profile 3[394, 395] (green), crew transportation can further broken down such that smaller crewed vehicles make the jump from planet to surface and vice-versa, but the interplanetary transit is made on a larger craft to reduce the mass required for egress from planetary gravity wells.

Previous ESM literature allows for varied equivalency factors based on mission staging[312], and in such cases, the ESM of distinct segments of a mission are calculated separately, then normalized through the use of location factors[172]. However, ESM M for any set of systems is calculated using a single location factor L_{eq} term as a multiplier. In this form it is assumed that each subsystem is transported in uniform fashion or that all parts of a subsystem would correspond to a single L_{eq} term. The profile expansion in Figure 4.1 shows that inventory can be transported in different segments using different crafts which change the value of L_{eq}. This is supported by non-ESM logistics methods[202]. We argue that the use of predeployment missions for transporting cargo implies that a system on one particular segment may utilize components transported from multiple segments, each with different location factors, motivating the a more generalized articulation of xESM (M_0) as

$$M_0 = \sum_{k}^{\mathcal{M}} \underbrace{L_{\text{eq},k} \sum_{i}^{\mathcal{A}_k} [(M_{k_i} \cdot M_{\text{eq},k}) + (V_{k_i} \cdot V_{\text{eq},k}) + (P_{k_i} \cdot P_{\text{eq},k}) + (C_{k_i} \cdot C_{\text{eq},k}) + (T_i \cdot D_k \cdot T_{\text{eq},k})]}_{M_{0,k}}$$
$$= M_{0,\text{pd}} + M_{0,\text{sf}} + M_{0,\text{tr}_1} + M_{0,\text{tr}_2} + M_{0,\text{tr}_3}$$

where $\mathcal{M}$ is sum of ESM for segments in a mission set with index k. Mission segment $\mathcal{S}$ can be constructed via set-builder notation as $\mathcal{S} = \{ (i, j) \mid i \in \mathcal{L}_2; j \in \mathcal{O} \}$ for specific combinations of locations and operations (see Methods for additional definitions). Essentially, we have established a graph where the locations represent nodes and the segments represent arcs, which matches previous formulations of mission logistics[202], although our set of location nodes is reduced for simplicity and does not include specific Lagrange Points[231]. The generalization enables accounting of mission segment-specific terms such as location factor L_{eq} and equivalency factors (M_{eq}, V_{eq}, P_{eq}, C_{eq}, T_{eq}). This generalization also allows for indexing of mission segment specific subsystems $\mathcal{A}$, further enabling an accounting of inventory $\mathcal{I}$ elements between mission segments $\mathcal{S}$.

Since these developments have been primarily applied to longer-duration ECLSS systems for the International Space Station (ISS) and not Mars missions, xESM does not include recent developments in resupply logistics[263] as enabled by the decreasing cost to LEO[266]. Despite a decreased cost to LEO, resupply logistics will be unlikely to impact the initial set of crewed exploration missions[61] given the difference in resupply costs between the ♁⊕ and ♁♂ systems. Although arguments have been raised against the adoption of crew-time within the ESM[271], we include these terms in our formulation as it has been the standard.

Inventories and Dependent Factors

With the addition of our method for indexing factors by their location, operation, and hardware, we are now able to address the accountancy of relationships between equivalency/location factors and the segment inventory that defines them. In essence, equivalency/location factors convert non-mass properties to mass properties by means of a ratio, but because that mass originates from some subset of inventory elements, equivalency and location factors

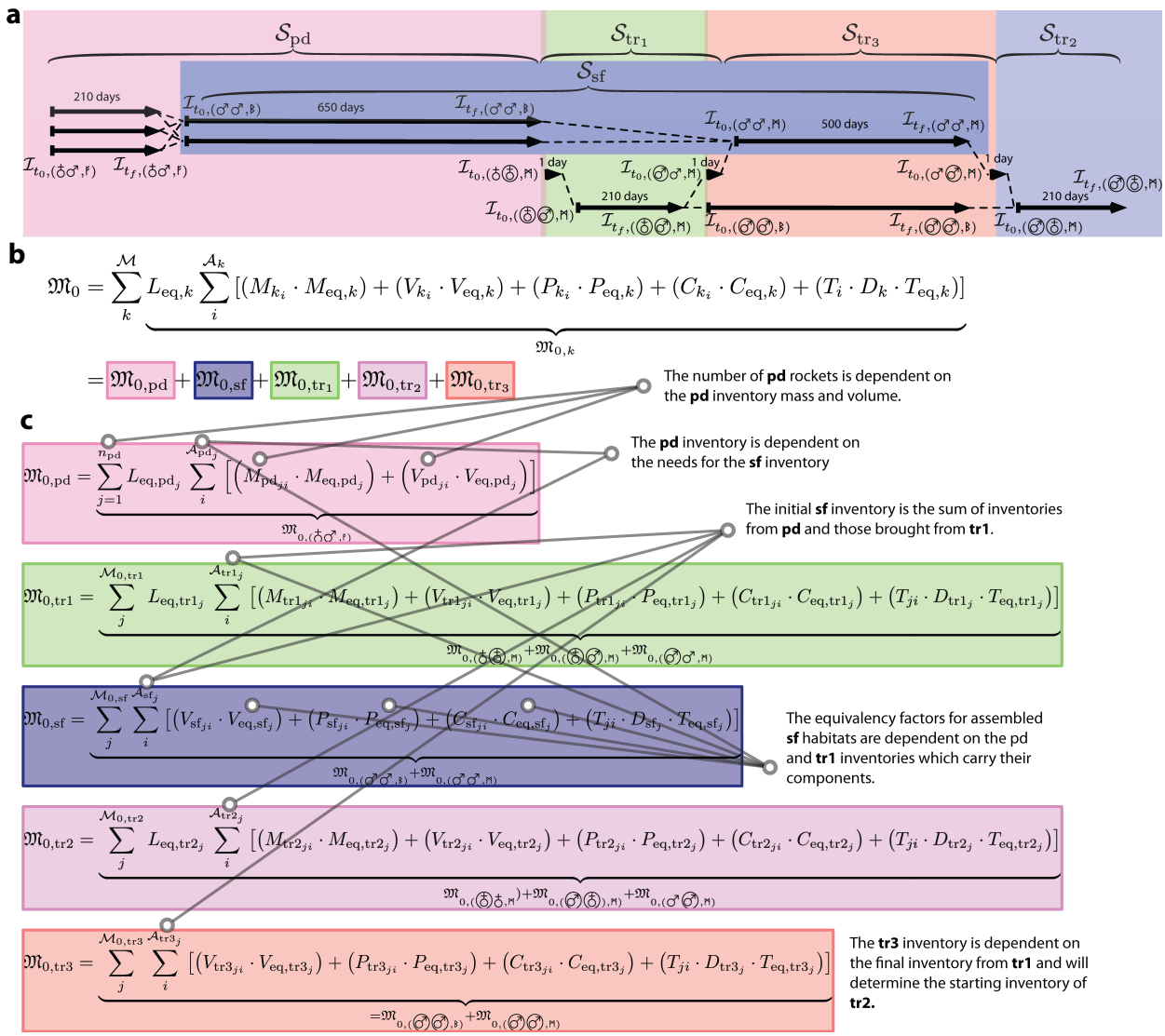

Figure 4.2: xESM equation for Profile 3 (Figure 4.1) with terms decomposed by subsystem. **(a)** Breakdown of inventory transfers across mission timeline colored by mission segment. **(b)** The generalized xESM equation colored by mission segment. **(c)** Expanded xESM equation with colored by mission segment with a non-exhaustive set of specific segment-dependent relationships elucidated.

are coupled. The exact nature of this interaction depends on the scenario and the modeling itself, and we aim to present a preliminary rendering of these relationships in Figure 4.2. In our assumptions, we say that predeployment cargo is grouped into cargo shipments in set j of $\mathcal{M}_{\mathrm{pd}_j}$ across some number of predeployments n_{pd}. We assume that this set of cargo is composed of items such as habitat assemblies, control hardware, photovoltaics & batteries, reactors, tanks refrigerators, various experimental apparatus, 3D printers, and other tools[17]. In the more expanded surface operations term, Figure 4.2 demonstrates that inventory for surface operations is composed of an assembled habitat, process and reactor assemblies, mission crew, and integrated power systems. In this scenario, a set of equivalency factors are required for each segment of the mission.

The location factor L_{eq} is the reciprocal of the payload fraction for transporting mass between two points in space and can be evaluated as the sum of across multiple orbital maneuvers with different Δv. Each element in the location mapping $\mathcal{L}_2$ has a specific required Δv. Any segment describing operations in a single location, such as Martian surface operations, has no mass transport and thus will have a $L_{\mathrm{eq}} = 1.0$. Since Δv can be related to the specific impulse I_{sp} and mass fraction m_0/m_f via the Tsiolkovsky rocket equation[556], we see how the mass of a specific segment inventory affects the location factor term. In terms of specific calculations, the mass fraction is the ratio of the of initial total rocket mass m_0 to final total mass m_f, and the payload fraction is the ratio of initial total mass m_0 to final delivered mass m_p (no propellant, tanks, etc). Meanwhile, the m_0, m_f, and m_p will be constrained by rocket technology choice. The scaling of the location factor is nonlinear in the case where some number of predeployments are each limited in payload mass. We calculate the $M_{0,\mathrm{pd}}$ as the sum over the number of total predeployments n_{pd} where a given predeployment j has a set of cargo $\mathcal{I}_{\mathrm{pd}_j}$ that doesn't require V, P, or T. The number of predeployment rockets will be parametric based on the m_p for predeployment rockets and the sum of all inventory mass to be used on the martian surface shipped by predeployment. As shown in Figure 4.2, the $L_{\mathrm{eq,pd}_j}$ in the $M_{0,\mathrm{pd}}$ term can be related to the M and V terms for the components of predeployment j, while the $L_{\mathrm{eq,tr}_1}$ and $L_{\mathrm{eq,tr}_2}$ terms are related to the M and V for all cargo transported in the complete mission.

Like L_{eq}, equivalency factors are also parametric based on certain elements of a segment inventory as showed by the cross-dependent mission-segment network (Figure 4.2c). For example, the volume equivalency V_{eq} for crewed transits in space will be based on the pressurized volume[172, 155] of the vehicle. Our notation affords the specification of equivalencies with relation to other decision variables, as opposed to the cruder method of assigning general constants. Figure 4.2 illustrate how the equivalency factors for one segment will often be parametrically related to decision variables in other segments. This realization only enforces the importance of our extension by which multiple segments are represented by a single optimization metric.

Example Calculations

To illustrate the process for calculating xESM with both the traditional approach and our

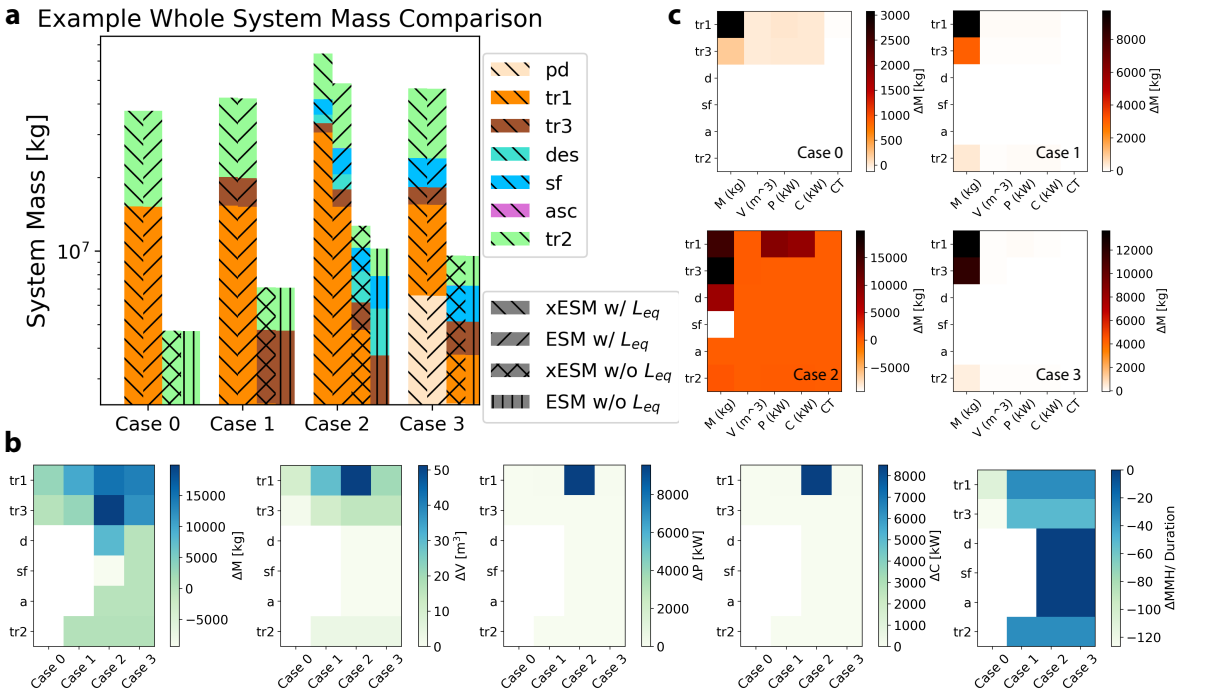

Figure 4.3: Comparison of ESM and xESM metrics for whole system mass scenarios. **(a)** Log-scale comparison of mission segment mass for increasing mission assembly. **Case 0** is a baseline inventory for the flight from Earth orbit to Mars orbit (tr_1) and back (tr_2), while life support for a 500 day Mars orbit (tr_3) is added in **Case 1**. The mission in **Case 2** includes descent (des), Mars surface operations (sf), and ascent (asc). All inventory for sf is predeployed (pd) in **Case 3**. As the mission grows, both the mass required and the difference between xESM and ESM increases. The final case shows falling xESM with the removal of sf inventory from tr_1 and des. **(b)** Inventory difference between xESM and ESM in raw mass, volume, power, cooling, and crewtime across each mission segment, before the application of location and equivalency factors. **(c)** Raw inventory difference between xESM and ESM displayed across the four cases.

proposed method, we provide the following example problems. The first explores a calculation across all inventory systems of a mission (Figure 4.3) and the second that has been scoped to the food production (Figure 4.4) using Controlled Ecological Life Support Systems (CELSS)[561, 32], which we feel serves as an established and graspable biomanufacturing-based technology[44] for comparison against "bring-everything" or physical/chemical life support systems[260].

The first example is offered to demonstrate a broad comparison between ESM/xESM, and in Case 0, we represent a base mission with the corresponding inventory required to fly from Earth orbit to Mars orbit ($\mathcal{S}_{\mathrm{tr}_1}$: 210d, 6CM) and back ($\mathcal{S}_{\mathrm{tr}_2}$: 210d, 6CM), and we assume the orbital mechanics allow for this transit. In Case 0, the inventory elements in a craft are scaled for their entire duration of use (420d), and consumables (food, waste collection, water) are used or discarded as time passes. In Case 1, we build on the base case by including the segment in which the crew would orbit Mars ($\mathcal{S}_{\mathrm{tr}_3}$: 210d, 6CM); and like in the previous case, items in a craft are scaled for their entire duration of use (920d). In Case 2, we continue to

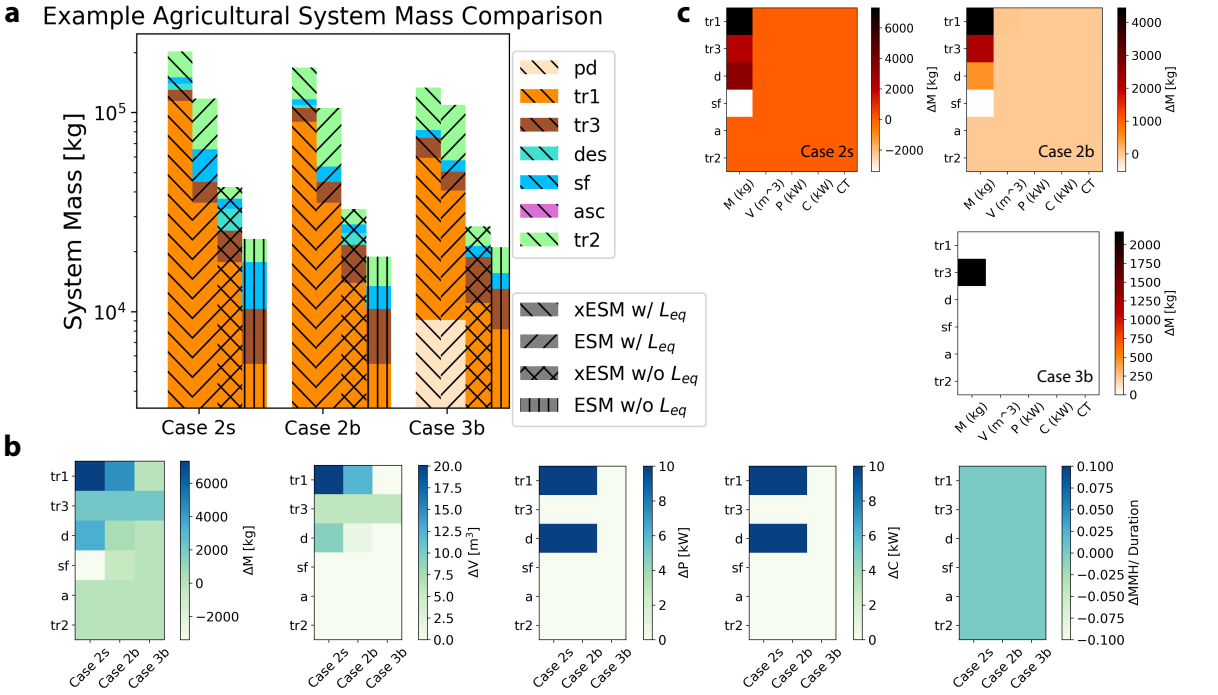

Figure 4.4: Comparison of ESM and xESM metrics focused on the stored food cost. **(a)** Log-scale comparison of mission segment mass for different food strategies. **Case 2s** is the food cost of Case 2 in Figure 4.3. **Case 2b** reduces the amount of stored food for sf from 500 days to 70 days, assuming a hypothetical future agriculture system could grow the difference. In **Case 3b**, the sf inventory is predeployed, and grown food also sustains the majority of sf. The ESM differences between 2s and 2b and between 2s and 3b show the rough mass requirement for the design and development of such an agricultural system. **(b)** Raw inventory difference between xESM and ESM mass, volume, power, cooling, and crewtime across each mission segment, before the application of location and equivalency factors. **(c)** Raw inventory difference between xESM and ESM displayed across the three cases.

build on the previous case by including descent ($\mathcal{S}_{\text{dec}}$: 500d, 4CM), surface operations ($\mathcal{S}_{\text{sf}}$: 500d, 4CM), and ascent ($\mathcal{S}_{\text{asc}}$: 1d, 4CM). Here the M, V, P, C inventory terms needed for $\mathcal{S}_{\text{sf}}$ are carried in $\mathcal{S}_{\text{tr}_1}$ and $\mathcal{S}_{\text{dec}}$ (with crewtime requirements for these items not accounted for). Here, 4 crew-members are left in orbit on $\mathcal{S}_{\text{tr}_3}$. In calculating xESM, the M term for $\mathcal{I}_{\text{sf}}$ is ignored during $\mathcal{S}_{\text{sf}}$, as no mass is "moved" during this segment as it was previously transported to the surface via $\mathcal{S}_{\text{tr}_2}$ and $\mathcal{S}_{\text{dec}}$; additionally, $\mathcal{S}_{\text{asc}}$ is assumed only to transport crew-members back to orbit. In Case 3, we achieve the proposed Profile 3 architecture from Figure 4.1 where the surface mission inventory is supplied via predeployment ($\mathcal{S}_{\text{pd}}$) rather than the initial transit and decent. Calculations of system mass (ESM and xESM) in Figure 4.3 show the expected increase in cost moving from Case 0 to Case 2 in which the size of the inventory grows in relation to the complexity of the situation (see SI for details). Also as expected, the use of predeployments in Case 3 deduces the xESM cost by ∼26% while only reducing ESM cost by ∼2.5% (Figure 4.3a). As the mission scope grows, both the mass required and the difference between xESM and ESM increases as outlined by Figure 4.3b,c.

The three Cases in Figure 4.4 consider the food system and the potential impact of

agricultural biotechnology to supply astronauts with their caloric and nutritional needs. We assume that each of 6 CMs has a daily dry mass food requirement of 0.617kg/CM-d[17]. We use this requirement to calculate the prepackaged food requirements of the two transit legs of each mission scenario, as well as the extra 70 or 500 days of food for surface operations in Cases 2s and 2b respectively. Given the recently updated infrastructure costs[17] associated with a Mars Surface Habitat Vehicle[574], we calculate ESM through consideration of the food subsystem including food, packaging, refrigeration[574, 17], and processing. In Case 2s, we consider only the stored food requirements from Case 2 from Figure 4.3. In Case 2b, we consider the stored food requirements during surface operations decreased from 500d to 70d and the remaining food was produced via agriculture. In a long-duration mission scenario in which food is grown during surface operations, and where literature suggests that a sizable initial hardware set would be required[17]. This set could include hydroponic growth chambers, water filtration, refrigeration, etc. along with additional support hardware like pumps, filters, etc[17]. In Case 3, we consider the transportation of the biomanufacturing system during predeployment rather than with the crew. During initial transit as well as the return transit, the crew relies on prepackaged food – crop growth begins on the first day of surface operations, necessitating another ∼70 days of predeployed food while the surface hardware grows the first crop[17]. Variation in crop selection and growth conditions during surface operations have been proposed, but this bounding assumption is consistent with crops such as lettuce and wheat[17, 561, 542].

Like Cases 0-4, xESM costs for Cases 2s, 2b, and 3b are larger than their ESM alternative, however, in Case 2s (w/o biomanufacturing, only 'bring everything') and Case 2b (w/ biomanufacturing), the xESM option is significantly larger than the ESM option for calculation. The difference between the xESM and ESM calculation results is an increased mass on the transit to Mars and reduced mass for surface operations and return transit. The primary trade-off here is that xESM provides a higher fidelity model for multi-segmented missions given that it includes the costs for all mission segments where an item is carried, while the ALSSAT's ESM calculation method does not include preceding mission segments ALSSAT[574]. This result is especially important considering downstream biomanufacturing options which show a reduced xESM metric in scenarios where predeployment is leveraged to reduce the cost associated with the transit. Additionally, our "bring everything" mission which does not rely on biomanufacturing yields larger costs overall from increased stored food. All three scenarios have equivalent Tr_2 ESM and xESM; this shows that in the last leg of the journey, or in a segment that is not influenced by future operations, ESM equals xESM. While simplified, this captures many of the critical features necessary to demonstrate the need for ESM extension. In cases where inventory from one segment can be used to satisfy constraints in another segment, the ESM summation of separately optimized mission segments can be less optimal than an ESM optimized with an objective function that accounts for both segments and constraint functions containing both terms from both segments. Given that system mass analyses are often used in the preliminary evaluation of technologies, it becomes more important for when considering biomanufacturing platforms to leverage the xESM formulation to provide a higher fidelity and more favourable metric. However, we

also must clarify that the aim in exploring this example is not to make claims about specific technology, but rather to provide an example for differentiating ESM and xESM.

4.3 Towards xESM Analysis and Optimization Under Uncertainty

So far, we have looked at the xESM framework for calculating segmented costs. Based on the scenario chosen, the xESM metric is ultimately determined based on some set of specific technologies that are used. Simpler cases, as the ones given in the examples assume that (1) the behavior of a particular system is fully known on Mars and (2) the operation of the systems is undisturbed by external factors. Although several systems can reliably be considered as deterministic in this scope, effects such as micro-gravity might affect the dynamics of specific processes in a biomanufacturing context. Moreover, each process possesses a set of faulty states, i.e., technical issues may cause a system to under-perform significantly. Detailed analysis of novel systems, e.g., in the biomanufacturing case, requires the description of the operation of systems using mathematical models. To this end, the xESM framework can be used both to analyze the cost of individual processes as well as the cost of integrated processes in any desired segment, as they operate in time. A simulation-based analysis, either some cost analysis of specific elements or some end-to-end optimization procedure, makes use of models to simulate the systems, the environment and associated costs for achieving the mission objectives. As a remark, we should note that the sophistication of the simulated case study can vary. For instance, higher-level decisions can be optimized for without the need of detailed models for individual components, while exact scheduling [47] and operational decision making should involve dynamical models for the various subsystems [383]. This principle has been widely adopted in manufacturing settings for design and control. Parts of the costs not commonly accounted for in cost calculations for space missions like ESM are uncertainty and risk. The latter are important factors during the design phase as we need to ensure safety in a robust, worst-case setting[398].

Uncertainty can be broken down categorically into two groups: aleatory[20] and epistemic[139]. Aleatory uncertainties are random and stochastic in nature and, although they can be examined via systematic testing, they cannot be reduced below some threshold. On the other hand, epistemic uncertainties can be reduced through applying additional knowledge and testing much more effectively. Moreover, uncertainties can be categorized and modeled as time-varying and time-invariant. In our case, there are several components, both explicitly and implicitly appearing in the xESM framework, that can be considered as uncertain. Let $\theta \in \Theta \subset \mathbb{R}^n_\theta$ denote a vector of uncertainties (both time-varying and invariant). Epistemic uncertainties include time-varying variables such as unmodeled dynamics (e.g., states of the system not taken into account) or time-invariant variables, for example, physical parameters of systems (e.g., kinetic parameters) or operational factors (e.g., efficiency of lights). Aleatory uncertainties can include purely stochastic dynamics

of systems and are typically time-varying, while including operational uncertainties related to equipment switching to a faulty state. In our context, note that the multi-segment approach allows for considering segment-specific uncertainties, for example, $\theta_{pd} \subset \Theta$ are the predeployment-specific uncertainties and $\theta_{sf} \subset \Theta$ are the uncertainties directly related to the surface operations.

Before formally defining an optimization problem, we should mention that the cost is generally a function of decision variables which reflect design choices regarding the specific utilization of available technology. Let us now focus on a particular segment, i.e., the surface operations and let $u_{sf} \in \mathbb{R}^n$ denote a set of decision variables for the surface operations. (e.g., amount of crop biomass that should be grown over some production cycle or the allocated area for plant growth). The mass-equivalent cost for the surface operations in this case is a function in the form $M_{0,sf}(u_{sf}; \theta_{sf})$. The decision variables can be fixed *a priori* or, more realistically, should be determined upon the solution of an optimization problem that seeks to minimize $M_{0,sf}$ in while accounting for uncertainties. The latter implies that typically we are interested in some expected value of the cost, i.e., $\mathbb{E}_{\Theta}\left[M_{0,sf}(u_{sf}; \theta_{sf})\right]$. In a more general sense, each segment j induces an expected cost $\mathbb{E}_{\Theta}\left[M_{0,j}(u_j, \theta_j)\right]$. Thus, reliability and uncertainty metrics also should be considered in an optimization setting. [441].

As the entire mission is broken down into segments and sub-segments, we can define task-specific performance level requirements which, when not fulfilled at several points in time, the mission can be considered to be failing. In other words, when simulating some part of the mission, uncertainty can lead to a sequence of faults manifesting themselves (either due to uncertainty in the system dynamics or due external disturbances and equipment faults) until the mission has to be abandoned. This is a useful definition for incorporating risk into the mission design given the dynamic nature of operations and the breakdown of mission stages that was introduced earlier. Using the notion of segments, we can define as $\pi_{t,j}(\boldsymbol{\theta_j}; u_j)$ the probability density function of segment j failing the earliest at time t, under some decision variable vector u_j. Subsequently, we can rely on sample-based methods to calculate the aforementioned probability, e.g., Monte Carlo sampling. Subsequently, we can define the expected failure time of segment j under the set of decisions u_j as $\hat{t}_f(u_j) = \mathbb{E}_{\Theta}\left[\pi_{t,j}(\boldsymbol{\theta_j}; u_j)\right]$, which also reflects the reliability of the design u_j. Note that faults and failure are connected but not identical [535]. We define as faults the sequence of events that need to occur such that their accumulation over time (in terms of number and magnitude) lead to an overall failure condition. Therefore, all uncertainties can be propagated into a single indicator which is the time of mission failure, which can be used for further analysis.

We can now shift our attention towards a stochastic optimal decision making for u_j, discussing the elements that would construct a proper stochastic optimization problem [373, 374] . The main element is the objective function. In a naive approach, we would seek the design u_j such that the expected segment cost is minimized. Nevertheless, this is not the best approach because we need to account for the confidence in the value of the expected cost. Therefore, the objective should include the variance of the segment cost due to uncertainty, i.e., $\mathbb{V}\left[M_{0,j}(u_j, \theta_j)\right]$. Last, but not least, a design that causes the segment to fail at a particular day should be incur a penalty to the objective, related to the probability of failure

as opposed to the probability of a loss of crew (Pr(LOC))[140]. We can define a scale of that penalty as $s(u_j)$, which can assume many forms, with the requirement that a mission that lasts longer is penalized less.

Under the simple assumptions that (1) the goal of human exploration missions is to carry out science experiments[61] and that (2) experiments are carried out each day, a worst case scenario is a complete mission scrub in which all science objectives planned beyond the day of mission failure cannot be completed. Overall, the main idea is that if the mission is to fail on the very first days, then it would need to be redone on a following mission. The assumption being made by this simple penalty is that if a mission were to fail early, the ESM cost of that mission left incomplete would be partially added onto next one. We argue that this is a valid initial construction of a penalty term based on assumption that incomplete work during a mission is required. This statement is especially valid for early human exploration missions where experimental use of new equipment is important in validating its use or raising technology readiness level to acceptable values for future missions. While we recognize that the standard recommendation in Decision Theory is to ignore sunk costs, we argue that the in our paradigm, this added penalty is not such a sunk cost. In classical decision analysis, a sunk cost is a sum paid in the past that is no longer relevant to decisions in the future[244] and thus should be ignored when making decisions. We argue that in our paradigm, we are analyzing the impact on a mission of some choice in technology that has some defined uncertainty, and thus no cost has been sunk. In the parlance of decision analysis, this is an example of a prospective cost, and is not to be ignored.

The objective for an optimization problem on a segment can now be written as

$$f(u_j) = \mathbb{E}\left[M_{0,j}(u_j, \theta_j)\right] + w_v \mathbb{V}\left[M_{0,j}(u_j, \theta_j)\right] + w_p s(u_j)$$

where w_v is a weight that assesses the importance of variance of the cost in the objective and w_p is a cost, in system mass units, which, as discussed, attains values approximately equal to a nominal ESM cost for the segment. Moreover, depending on the nature of the problem, the optimization is complemented with various robust constraints. The latter ensure the safe operation of the systems, such as achieving several thresholds of productivity. A detailed optimal decision making problem formulation is heavily case-dependent and a complex issue to address, however, we envision that the objective function would generally attain this particular in most cases. Last, but not least, the optimization can be extended to a mission-wide horizon by replacing the segment-specific cost with the total cost.

4.4 Future Work

The use of the xESM framework helps guide the development and implementation of software for a reference mission architecture for long-duration human exploration of Mars. We recognize that this extension of ESM as a metric for mission scenario comparison is preliminary and not exhaustive in its scope. We also note that no single analytical result such as ESM or xESM will be the sole factor the technology specification or platform decision-making. The

differences presented are important but modest and are in scale with the uncertainty of the quantities used as the inputs. In addition to incorporation of mission parameters, specific constants and terms in our formulation are required, such as a more precise calculation of equivalency factors for cooling, power, volume, and crew-time and distillation of the specifics for risk fractions. Future endeavors include a comprehensive optimization problem formulation and solution based on the xESM framework both for biologically and non-biologically driven missions. Moving forward, we hope that our extension of ESM provides the basis for continued systems engineering and analysis research for a more quantitative and inclusive design and optimization of long-term human exploration missions.

4.5 Methods

Mathematics

Let $\mathcal{L}$ be a set of locations composed by $\mathcal{L} = \{ \text{♁}, \text{⊕}, \text{♂}, \text{⊕♂} \}$ where ♁ is Earth surface, ⊕ is low Earth orbit, ♂ is Martian Surface, and ⊕♂ is low Martian orbit. Let $\mathcal{L}_2$ be the set of pairs in $\mathcal{L}$ which describe from starting to ending location. Let $\mathcal{O}$ be the set of operations composed by $\mathcal{O} = \{ \text{ᚠ}, \text{ᛒ}, \text{ᛗ} \}$ where ᚠ[1] is cargo, ᛒ[2] is robotic, and ᛗ[3] is crewed. Let $\Lambda(i, j)$ be the mapping from some pair of $i \in \mathcal{L}_2$,$j \in \mathcal{O}$ to the set $\mathcal{R}$ of rockets, vehicles, and habitats. A mission segment $\mathcal{S}$ can be constructed via set-builder notation as $\mathcal{S} = \{ (i, j) \mid i \in \mathcal{L}_2; j \in \mathcal{O} \}$ for specific combinations of locations and operations as

$$
\begin{aligned}
\mathcal{S} &= \{ (i, j) \mid i \in \mathcal{L}_2; j \in \mathcal{O} \} \\
\mathcal{S}_{\text{pd}} &= \{ (i, j) \mid i \in \{ \text{♁⊕}, \text{⊕⊕♂}, \text{⊕♂♂} \} ; j = \text{ᚠ} \} \\
&= \{ (\text{♁⊕}, \text{ᚠ}) + (\text{⊕⊕♂}, \text{ᚠ}) + (\text{⊕♂♂}, \text{ᚠ}) \} \\
\mathcal{S}_{\text{sf}} &= \{ (i, j) \mid i = \text{♂♂}; j \neq \text{ᚠ} \} \\
&= \{ (\text{♂♂}, \text{ᛒ}) + (\text{♂♂}, \text{ᛗ}) \} \\
\mathcal{S}_{\text{tr}_1} &= \{ (i, j) \mid i \in \{ \text{♁⊕}, \text{⊕⊕♂}, \text{⊕♂♂} \} ; j = \text{ᛗ}; k \in \Lambda(i, \text{ᛗ}) \} \\
&= \{ (\text{♁⊕}, \text{ᛗ}) + (\text{⊕⊕♂}, \text{ᛗ}) + (\text{⊕♂♂}, \text{ᛗ}) \} \\
\mathcal{S}_{\text{tr}_2} &= \{ (i, j) \mid i \in \{ \text{⊕⊕♁}, \text{⊕♂⊕}, \text{♂♂⊕} \} ; j = \text{ᛗ} \} \\
&= \{ (\text{⊕⊕♁}, \text{ᛗ} + (\text{⊕♂⊕}, \text{ᛗ}) + (\text{♂♂⊕}, \text{ᛗ}) \} \\
\mathcal{S}_{\text{tr}_3} &= \{ (i, j) \mid i \in \{ \text{⊕♂♂} \} ; j \neq \text{ᚠ} \} \\
&= \{ (\text{⊕♂♂}, \text{ᛒ}) + (\text{⊕♂♂}, \text{ᛗ}) \}
\end{aligned}
$$

for the abstract segments of predeployment (pd), crewed transit from Earth to Mars (tr_1), Martian surface operations (sf), crewed transit back from Mars to Earth (tr_2), and either autonomous or crewed operations aboard the interplanetary vehicle in Martian orbit (tr_3).

[1] Elder Furthark[519] rune ᚠ *fehu meaning "cattle", used here to imply "cargo"

[2] Elder Furthark rune ᛒ *berkanan meaning "tree", used here to imply "autonomy"

[3] Elder Furthark rune ᛗ *mannaz meaning "man", used here to imply "crewed"

The complete mission object $\mathcal{M}$ is therefore constructed as the collection of these abstract segments in conjunction with the selection of a specific technology in $\mathcal{R}$ as

$$\mathcal{M} = \{ (k, \ell) \mid k = (i, j) \forall \{ \mathcal{S}_{\text{pd}}, \mathcal{S}_{\text{sf}}, \mathcal{S}_{\text{tr}_1}, \mathcal{S}_{\text{tr}_2}, \mathcal{S}_{\text{tr}_3} \} ; \ell = \Lambda(i, j) \}$$

and can be used in the construction of a generalized total mission ESM M_0 as

$$M_0 = \sum_k^{\mathcal{M}} \underbrace{L_{\text{eq},k} \sum_i^{\mathcal{A}_k} [(M_{k_i} \cdot M_{\text{eq},k}) + (V_{k_i} \cdot V_{\text{eq},k}) + (P_{k_i} \cdot P_{\text{eq},k}) + (C_{k_i} \cdot C_{\text{eq},k}) + (T_i \cdot D_k \cdot T_{\text{eq},k})]}_{M_{0,k}}$$
$$= M_{0,\text{pd}} + M_{0,\text{sf}} + M_{0,\text{tr}_1} + M_{0,\text{tr}_2} + M_{0,\text{tr}_3}$$

as the sum of ESM for segments in a mission set $\mathcal{M}$. Essentially, we have established a graph where the locations represent nodes and the segments represent arcs, which matches previous formulations of mission logistics[202], although our set of location nodes is reduced for simplicity and does not include specific Lagrange Points[231]. The generalization enables accounting of mission segment-specific terms such as location factor L_{eq} and equivalency factors (M_{eq}, V_{eq}, P_{eq}, C_{eq}, T_{eq}). This generalization also allows for indexing of mission segment specific subsystems $\mathcal{A}$, further enabling an accounting of inventory elements between mission segments.

Example Problem Calculations

Inventories for the whole system mass in Figure 4.3 and the agricultural system mass in Figure 4.4 are rendered from ALSSAT[574] calculation outputs for a Closed Loop (Air and Water subsystems) mission. The segment parameters for a full transit are as follows; tr1: 6 crew, 210 days, tr2: 6 crew, 210 days, tr3: 2 crew, 500 days, sf: 4 crew, 500 days, asc: 4 crew, 1 day, desc: 4 crew, 1 day. All other configurations are set to their default value. Note that to calculate xESM inventories, technologies that remain on the same craft were scaled to their upper bound of usage. For example, the air processing equipment for the craft throughout tr1, tr2, and tr3 were scaled for 920 days of operation. Consumables (such as stored food) were initially be scaled for 920 days and decreased accordingly as they were used.

Penalty for Mission Failure

The penalty associated with the mission failure can be defined in various ways. For example, we can define the following relationship between the penalty cost and the duration of the mission

$$s(u_j) = \left(1 - \frac{\hat{t}_f(u_j)}{t_{tot}}\right),$$

which expresses a linear decrease of the penalization with the number of days.

Chapter 5

Computational Methods and Construction of echusOverlook Software

Design practices and tools for human exploration missions have evolved in concert with mission complexity over the past half century of the space age. As collective thought turns toward the exploration of Mars and of the Moon, including the Artemis Program, technologies new and old have been proposed to address challenges in astronautics. However, the coordination of these challenges has lagged behind the advances of technologies themselves. This drives our development of echusOverlook (eO), an open-source Python library that captures the explorable mission design space, standardizes the definition of mission components, and democratizes the process of distilling technologies to sustain human exploration. No existing mission design software allows users to build and simulate technologies of their own design, because they are limited to the space of hard coded options. The open and modular framework of eO attempts to reflect and integrate the collaborative contributions of the community. For a given configuration, eO calculates the exchange of resources between system components using a crewmember model and mass balancing logic. This mission representation is a precursor to computations including inventory generation, techno-economic analysis, and performance assessment of simulated discrete and stochastic behavior. Calculations are benchmarked against and on par with the ALSSAT for inventory generation, and with HabNet for mission simulation. eO supports both private, local data and the publishing of mission designs to a central public server, where they can be extended by the global community. We reproduce the ALSSAT model of a closed-loop mission with a biomass system, and extend it in eO with the modular addition of a novel bioprocess that produces parathyroid hormone for skeletal anabolism. The expansion of mission technologies beyond abiotic hardware to biotic design is a key motivator for eO's accessibility, which attempts to meet NASA's Space Technology Grand Challenges by bridging the space sciences and biological engineering communities. Our software, data, and models will be released and maintained on GitHub.

The following chapter is under development for publication as A.J. Berliner, D. Ho, K. Yates, G. Makrygiorgos, A. Mesbah, S. Nandi, K. McDonald, A.P. Arkin. **echusOverlook: In silico Knowledge-base and Simulation Framework for Human Exploration Operations of Mars**. (In preparation, expected submission Fall 2022).

5.1 Introduction to Mission Design Software

Design practices and tools for human exploration missions have existed since the earliest of the Mercury program[87] and have evolved in concert with mission complexity over the past half century of the space age[304]. As the collective thought across multiple space agencies turns to the exploration of Mars[546, 503], technology platforms – new and old, incremental, and novel – have been proposed to address a wide array of challenges across nearly all aspects of astronautics[147, 385]. However, the coordination of such challenges has lagged behind specific advances of the technologies themselves – motivating a need for systems engineering frameworks capable of exploring the interplay between platforms and solutions[377]. Such a design space must be subtended in order to distill an optimal set of technologies and operational strategies for sustaining a long-duration human exploration mission on Mars.

Among the many newly-proposed technologies that have been shown as critical in enabling human exploration on Mars, biological technologies have been identified as critical in sustaining astronauts and reducing mission cost[371, 372]. The optimal set of technologies and operational strategies for sustaining a long-duration human exploration mission on Mars is driven by the design, optimization, deployment, and management of a surface biomanufactory[44]. Recently the components of Space Bioprocess Engineering (SBE)[43] have been codified to include (1) *in situ* microbial media production, which harnesses Mars atmospheric and regolith resources for downstream biological use; (2) *in situ* manufacture of mission products, which creates outputs like propellants and building materials that are fundamental enablers of any long-duration space mission; and (3) *in situ* food and pharmaceutical synthesis, which enables manned long-term space missions and the use of plants and microbes for food, nutrients and medicine to astronauts[44]. The realization of these systems into a technology platform for future work by NASA requires both the biological engineering required to achieve technology milestones as described above, and the systems engineering needed to analyze, test, improve, and integrate the many processes into a single biomanufacturing system. Here we present the design and construction of the echusOverlook (eO) software as a means and method for evaluating mission architecture across a myriad of metrics common to Environmental Control and Life Support System (ECLSS)[429]. Such metrics may include equivalent system mass (ESM)[314, 314, 152], reliability, and cost-benefit trade-offs.

Mission 'planners' have requirements for basal support of the crew for particular[17, 230]. These requirements are staged out from prelaunch through the return in multiple stages – each with different requirements to be met that may include preparation for the next stage and operation within a stage[147]. A fraction of these can be provided by systems that

incorporate biological components beyond the crew themselves- plants and microbes most probably[42]. These systems each have their own costs and benefits that accrue in both their independent operation and their connections to other mission systems and operations across stages[41]. Costs include material costs, power costs, weight, operational costs in labor and risks of failure, etc. Benefits include the production of required functions and possible side-benefits to other mission operations (e.g. waste recycling or air filtration). There may be more than one possible system available to fulfill a given requirement. Thus, selection of a set of biotechnologies to fulfill a set high level mission requirements, calls for selecting a set of operationally compatible biotechnological systems optimized within and across the mission elements and mission stages so that the most optimal system configuration can be chosen.

Various aspects of mission design have been explored across a number of software artifacts as shown in Table 5.1. Beginning with the Microsoft Excel-based Advanced Life Support Sizing Analysis Tool (ALSSAT)[573] in 1998, the complexity of such software has grown through the establishment of dynamic modeling methods. Likewise, the fidelity of models has increased with moderate tradeoffs in convergence time. Table 5.1 also shows that software has been developed in parallel by both NASA and ESA which underscores a lack

Modeling Tool	Year of Initial Release	Year of Last Update	Summary	SS/D/S	Fidelity	Speed	Availability	Programming Language
ALSSAT[573, 572, 574]	1998[360]	2012[575]	NASA's Advanced Life Support Sizing Analysis Tool was developed for use in the sizing and analysis of Environmental Control and Life Support Systems (ECLSS) for spacecraft and habitats. The purpose of this tool is to perform life support system trade studies and analysis.	SS	L	O(s)	Lengthy application through NASA's Software Portal. Under export control	Microsoft Excel and Visual Basic Macros
ELISSA[138, 136]	1999[360]	2018[137]	The Environment for Life-Support Systems Simulation and Analysis (ELISSA) tool has been developed at the Institute of Space Systems (IRS), University of Stuttgart since the mid-90s and allows the analysis and validation of new ECLSS designs, as well as system optimization	SS/D	M	O(m)	Unavailable	MATLAB
EcoSim[428]	1999[534]	2021[149]	ESA's Standard Software based on a simulation tool developed by Empresarios Agrupados for modelling physical processes that can be expressed in terms of Differential algebraic equations or Ordinary differential equations and Discrete event simulation.	D/S	M	O(w)	Commercial Payware	Standalone Tool in Visual Basic and C++
BioSim	2003[293]	2015[292]	Intended for detailed ECLSS controls and operations analysis. Developed by TracLabs (NASA JSC Contractor) exclusively for integrated ECLSS controls research	D/S	H	O(s)	Available. GPL v3	Java
V-Hab[476, 130]	2009[128]	2019[440]	Developed by TU-Munich dynamically simulates life support systems and their subsystems, as well as their interactions with a modeled crew metabolism. the goal of V-HAB is to create a holistic tool that can be used during the complete life cycle of an ECLSS, from the initial feasibility studies, through requirements definition to subsystem and system design and even utilization and operation of the system.	D/S	H	O(m)	Private. Accessible by request.	MATLAB
SCALISS /ALiSSE	2010[63]	2017[57]	A European Tool for Automated Scaling of Life Support Systems. The aim of the SCALISS study was to understand and investigate in ECLSS functionality, technologies and scalabilities in order to produce a robust initial design starting point for future Phase-A studies with an automated tool.	SS	M	O(m)	Unavailable	Standalone Tool, Java
HabNet	2015[142]	2019[58]	Developed by MIT as an integrated habitation and supportability architecting and analysis package. Tool quantitatively evaluates various technology options for a proposed mission architecture in terms of their functional performance, their failure modes, their supportability requirements, and ultimately their initial deployment and lifecycle operational costs.	D	H	O(m)	Partially accessible.	MATLAB
eO	2021	–	Tool for designing, exploring, and optimizing a biologically-driven reference mission architecture for human exploration of Mars	D/S	H	O(m)	Available and Open Source	Python

Table 5.1: Comparison of Life Support Systems Software Packages

of standardization between space agencies. Moreover, the development of recent tools has been outsourced either by private industries in the case of EcoSimPro[428] or by academic institution via V-Hab[128] or HabNet[142]. The result of such outsourcing has led to two primary issues with the life support systems software: tools (1) operate on poorly-standardized mission architectures, methods, and data (2) are predominately either protected for reasons of academic priority or private financial concerns. Propagation of such issues has led to barriers in both the free discussion of methods and the agency for new players to contribute – in many forms ranging from mission elements to performance metrics to general biological ideas – to the grander mission of human exploration.

As outlined in Table 5.1, the echusOverlook software has been designed to maximize availability to the space mission design community while also meeting the fidelity and convergence time of previously developed tools. What cannot be captured by these criteria, however, is that eO is a dynamic, living software framework. There are no predetermined and immutable data types, calculations, metrics, or simulations. At this level of abstraction, eO fully supports the design of non-biological missions while being extensible enough to accurately describe and model complex bioengineering systems. *Any* mission to Mars with any reference mission architecture, any set of processes, and any inventory can be described and modeled inside eO. This allows eO to address both the ECLSS-based goals of SBE[372] and meet NASA's Space Technology Grand Challenges[514] by bridging the space sciences and biological engineering communities[43]. eO fosters both Standardization of mission elements and operations by the space science and engineering community and Democratization of novel biological system elements by the biological science and engineering community to meet the needs and requirements of both user-groups.

5.2 Preliminary eO Software Design and Overview

Initial feedback in regards to eO gathered from NASA stakeholders at the CUBES Y4 Spring Review stressed the importance of not developing the software in a vacuum – and encouraged our team to renew our efforts to establish communication with NASA's mission design specialists. After much assistance from our NASA point-of-contact, Dr. John Hogan, we were able to schedule an initial meeting to

1. Form a community of mission planners, life support systems designers, espace scientists, and bioengineers;

2. Review what is known about possible mission specification or modeling that has been done for chemical and biotechnologies that support food, pharmaceutical and material production in space; and

3. Explore current Bioregenerative LSS and ECLSS and determine what elements have been missing from mission design.

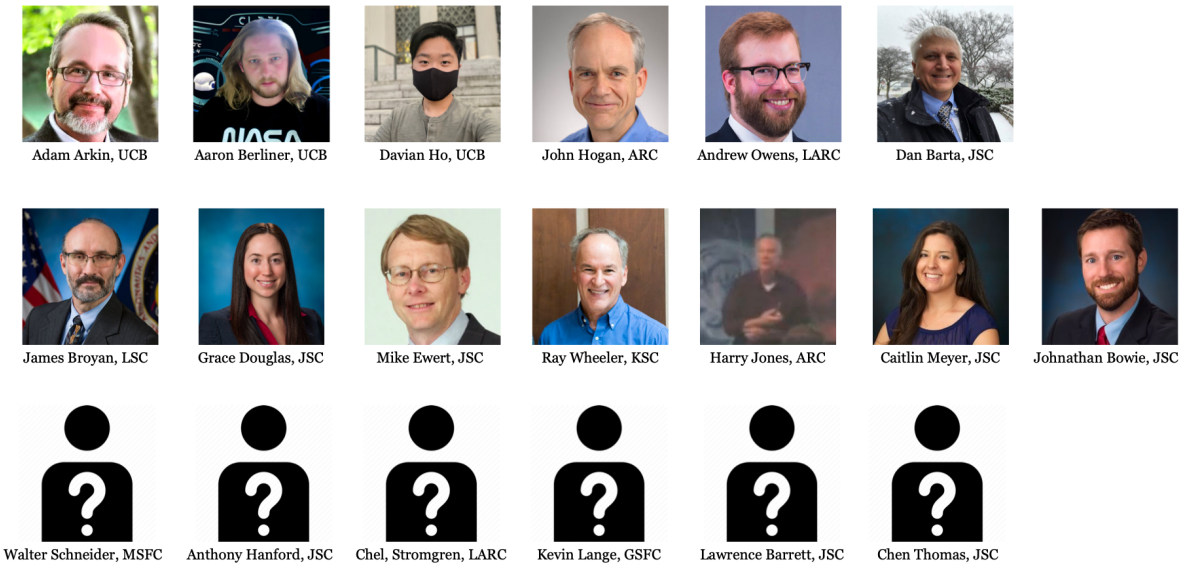

Figure 5.1: eO Meeting Attendees

Prior to the meeting with the attendees outlined in Figure 5.1, we solicited feedback to a set of questions designed to gauge the interest for the echusOverlook software for human exploration mission design and optimization (emphasizing biomanufactory-driven RMAs and technologies). We collected the responses and presented them back to the attendees at the meeting which was designed to explain our preliminary efforts, discuss struggles, collect needs, and learn of others we might need to interview. The responses are presented in Figure 5.2.

We presented eO with a preliminary user story in which a user would want

1. to specify mission goals formally,
2. to be prompted towards inclusion of mission elements/processes to support those goals,
3. be able to efficiently populate those processes with possible inventories to support those processes and models of their operation, and
4. given these constraints to select from possible mission architectures that can support lift of these proceses to their sites of action.

Given these sets of possible alternatives to process, inventory and mission architecture, we proposed that the user would wish to be able to create more or less optimal scenario composed of these and compare them for trade-offs against different mission metrics including standard mass, power requirements; modularity/ interoperability requirements, minimum waste and maximum recycling requirements, etc. The user story provided a preliminary design pathway in which the proposed story would be supported through:

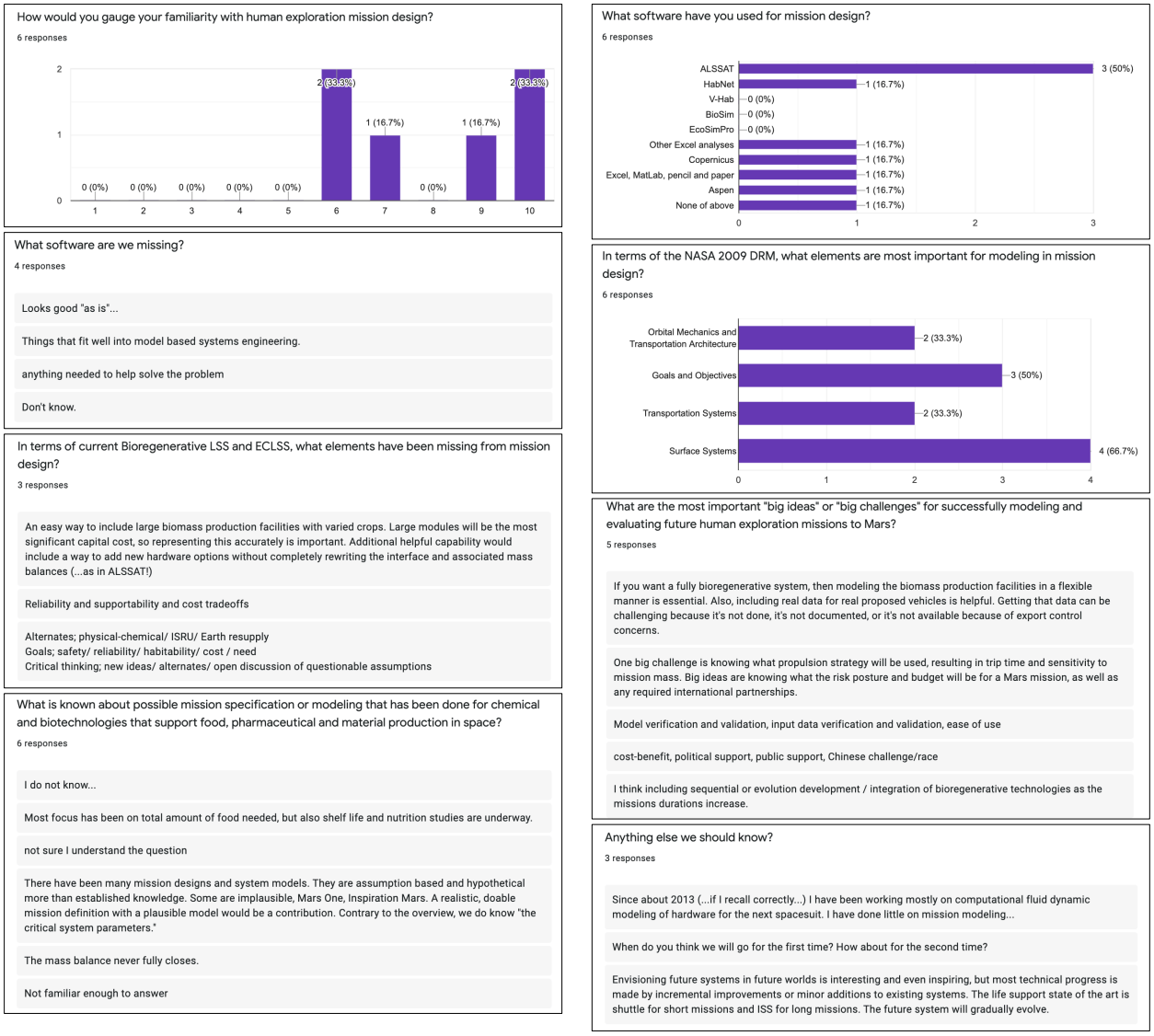

Figure 5.2: Feedback from a form distributed to stakeholders to gauge the interest for in eO.

1. Creation of a databases of processed, models, inventory elements, mission architectures that can be extended, and used together to create models of different mission scenarios

2. Allow building of multiple and community extension of models of mission elements ranging from very top level ESM like models of their costs to detailed dynamical models of their operation

3. Allow model optimization, sensitivity/uncertainty analysis, and cross-model comparison for decision support.

4. Allow open, transparent, FAIR sharing of data, models and analysis among diverse communities to support effective comparison, incremental development, and ease of checking/rechecking results.

Following the preliminary meeting, we established a set of future goals:

1. Collecting and collating all known information about the physical specifications and form factors for operation of technological elements (life support, biomanufacturing, etc.) on-board transit craft, space-stations and surface elements.

2. Collecting and collated all known information about costs/models for operations of these platforms that affect the costs and operations of the tech support elements (how different rockets, etc. effect the cost of operations in 1.)

3. Collecting and collating all known actual and possible mission architectures for planned missions over the next 30 years to serve as templates for the RMA structures in echusOverlook

4. Collecting, improving, and testing different models of critical technological elements in the LSS, ECLSS, biomanufacturing space or other biologically-linked operations for test bedding the systsem and supporting the evolution of this community for driving innovation in these elements over the next decades.

5. Developing a community to ensure we are building a usable, accelerating software framework for the larger community even beyond space bioengineering;

6. Developing a clear communication and alliance with other mission planning and tech development groups so we remain relevant.

5.3 Software Overview

eO models the parametric constraints on and tradeoffs among bioprocesses such that they meet or exceed mission need and are engineered to minimize the risk of failure under different orbital, crew, and landing site scenarios. Through the integration of both a knowledge-base and simulations, eO is designed to elucidate the critical system parameters for demonstrating the feasibility and advantages of biological engineering on a human exploration mission to Mars. The echusOverlook repository is available for download (https://github.com/cubes-space/echusOverlook) and can be accessed via command line, Jupyter notebook, or text editor.

User Story

The user story diagram (Figure 5.3a) describes how a user starts with the setup of "campaign" and proceeds through from design to the technoeconomic calculation through simulation

and ends with either the submission of results back to the eO database or an adjusting of parameters for additional calculation and/or simulation. Users begin by creating a space logistics network (SLN) by selecting the data elements for use from existing data in eO which can then be modified. eO is initially seeded with a library of common ontologies, datasets, and operations, and the user community is encouraged to upload new components and their results. Each SLN is used to determine mission needs and constraints and is

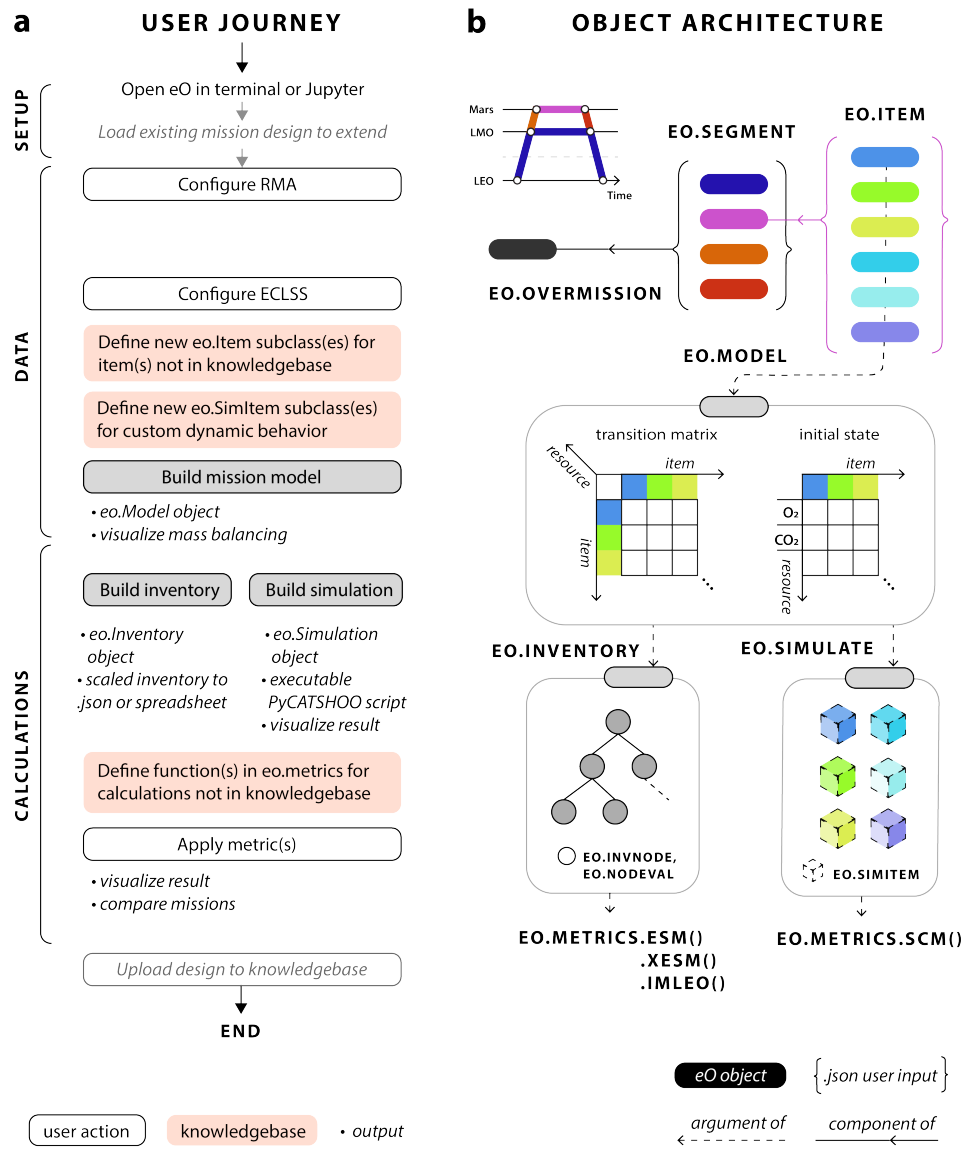

Figure 5.3: Overview or echusOverlook software. Design of eO **(a)** user journey/story with **(b)** system architecture.

composed of operations across a series of mission segment with locations such as Earth, Low Earth Orbit (LEO), Cis-lunar Space, Luna, Interplanetary Space, Martian Orbit, Mars, etc. Default mission data packages are available as a starting point for users to not only decrease the barrier of entry to space mission design, but also to standardize the use of eO across multiple instances. The user can easily create additional ontologies, variables, and models by uploading new types of information, allowing for the freedom to construct a mission component using any data type necessary to describe it. Once a SLN has been validated, the user can perform downstream a variety technoeconomic analyses and/or initiate a simulation for exploring the dynamics of their system.

Systems Architecture

The eO data module acts as a knowledgebase to describe the mission parameters – both user-defined and calculated – and can be considered as the set of instructions from which simulations are first constructed, parametrized, and run – and later as the container in which simulation results are added. The interactions of these components (Figure 5.3b) are governed by a number of modules including `OrbitalMechanics`, `MartianEnviornment`, `Processes`, `Inventory`, and `Crew`. A number of "start-up" examples are provided in the knowledgebase and include complete reference mission architectures and other case studies such as inventory constructs from NASA's ALSSAT[575] and BVAD[16] and sortie and outpost surface missions described in HabNet[142].

Mission architectures are assembled from disparate data types, from graphs[231] to inventories[16] to simulated processes[128]. Currently, data and their associated context are siloed in spreadsheets, on pencil and paper, and in publications. Not only is there no initiative for communicating and sharing this data, but this also slows the process of making global updates across the field based on new information. To address these issues, we use CORAL: a backend framework for creating FAIR data—findable, accessible, interoperable, and reusable—among a community of researchers[91]. CORAL supports dynamic creation of FAIR data types for data kept in spreadsheets, translating information stored locally into objects that can be found and used by others. All data uploaded to the eO database through CORAL is validated by eO ontologies and accompanied by context, such as units, sources, and references to other modules.

Through CORAL, spreadsheet uploads to describe components of the mission, including the inventory, processes, and reference mission architecture, allow users of eO to build and simulate missions of their own design. Default and user-defined information that has been uploaded through CORAL resides in an ArangoDB database instance on the local machine.

5.4 Results

The following results are presented for three distinct case studies that validate eO against alternative frameworks for TEA calculations and process simulation while also demonstrating

the extensibility of eO for the creation and analysis of novel SSB technologies in a mission context.

Case Study 1: Technoeconomic Analysis and Validation of "Bring Everything" Scenario

eO was designed to be competitive with previously created software such as the ALSSAT[575] and thus requires methods for carrying out technoeconomic analysis (TEA) in the form of sizing and trade studies – and thus eO's TEA methods require the inclusion of mission design metrics. The history of space mission design is replete with a number of such metrics that range in scope and complexity (Table 5.2). ECLSS technology selection was initially carried out by assigning a Technology Readiness Level (TRL)[339] value and has evolved to account for Integration and Systems Readiness (IRL, SRL)[470, 471, 472, 473]. However, despite the standardization of TRL criteria[179, 229], such "mangagement" metrics are often considered lacking in objectivity[269] and do not readily lend themselves to optimization.

The impact of specific technology choices are usually evaluated through the more quantifiable metric of the equivalent system mass (ESM)[312] which provides a method for distilling the mass of all of the resources of a larger system. Despite its status as the gold standard, ESM has been criticized for a number of short-comings such as ambiguity of application and non-accounting of development costs[261] and uncertainty[6]. Efforts to address these challenges metric have been proposed in the form of (extended ESM) which addresses unresolved complexities stemming from multiple transit and operations stages, such as would be required to support a crewed mission to Mars and also provides an accountancy for the uncertainties inherent in mission planning[41]. Additionally, a number of alternative metrics have been proposed to surplant[264, 273] ESM that consider complexity[272]. Most recently, the Life Support Multi-Dimensional Assessment Criteria (LSMAC) metric has been proposed to incorporate a myriad influences of influences including maintainability, risk Analysis, TRL, radiation impacts, manufacturing costs, reliability, human factors, and autonomous operation[6]. Such a multitude of metrics underlying TEA has led to a difficulty in comparing the technologies that have been evaluated differently – compounding complexity to the previously described differences in technology specifications from across multiple data-sets and literature sources. The initial release of eO addresses these challenges through the inclusion of all frameworks in Table 5.2 – enabling multi-metric TEA. Additionally, the extensibility of eO provides for creation of new metrics which can be uploaded and shared similarly to specific technology objects – further standardizing and democratizing mission design.

Preliminary RMAs propose 30 sols of surface operations driven by an opposition-class transit by a small crew of 4-6 astronauts[147]. Such short-term missions do not led themselves construction and operation of biomanufactory-based set of technologies and instead opt for a "bring everything" (BE) scenario in which the majority of consumables such as food, tools, and medicine are packaged turn-key and transported via predeployment or as cargo on the primary mission vehicle[44, 42]. Given that the BE scenario serves as a standard

Metric	Description	Formulation
Technology-Integration-Systems Readiness Level (T/I/S-RL)[339, 473]	A series of methods for estimating the maturity, interoperability, usability of technologies on a scale from 1-9 during the acquisition phase of a program	$T, I \in [1, 9]$, $S = \sum_{j=1}^{n} \sum_{i=1}^{n} \frac{I_{ij} T_j}{m_j}$
Equivalent System Mass (ESM)[314, 312]	A method to evaluate a system or technology based upon its mass, volume, power, cooling and manpower requirements by relating all parameters to mass equivalency.	$M = L_{\text{eq}} \sum_{i=1}^{\mathcal{A}} [(M_i \cdot M_{\text{eq}}) + (V_i \cdot V_{\text{eq}}) + (P_i \cdot P_{\text{eq}}) + (C_i \cdot C_{\text{eq}}) + (T_i \cdot D \cdot T_{eq})]$
Extended Equivalent System Mass (xESM)[41, 367]	A method for extending ESM to account for multi-staged missions and reliability and feed into downstream optimization problems.	$M = \sum_{k}^{\mathcal{M}} L_{\text{eq},k} \sum_{i}^{\mathcal{A}_k} [(M_{k_i} \cdot M_{\text{eq},k}) + (V_{k_i} \cdot V_{\text{eq},k}) + (P_{k_i} \cdot P_{\text{eq},k}) + (C_{k_i} \cdot C_{\text{eq},k}) + (T_i \cdot D_k \cdot T_{\text{eq},k})]$
Initial Mass to Low Earth Orbit (IMLEO)[444, 231]	A method for calculating the total mass of a system from to LEO for downstream relationship to the gear ratio.	$M = \sum_{k}^{\mathcal{M}} \sum_{i}^{\mathcal{A}_k} M_{k_i}$
Systems Complexity Metric (SCM)[272]	A method for evaluating the complexity of an integrated system in terms of the interactions and interoperability between subsystems.	$C = (L-1)S^2 + \frac{N^2}{S^{L-1}}$

Table 5.2: Mission desgin metrics. **For T/I/S-RL:** T and I are the TRL and IRL values in range $[1, 9]$, n is the number of subsystems, m is the mass of the subsystem, and S is the SRL value. **For ESM, xESM:** M is the calculated mass, $\mathcal{A}$ is the set of subsystems, $\mathcal{M}$ is the set of mission segments, M_i, V_i, P_i, C_i are the initial mass [kg], volume [m^3], power requirement [kW$_e$], and cooling requirement [kg/kW$_{\text{th}}$], D is the duration of the mission segment [sol], T_i is the crew-time requirement based on an astronaut crew-member (CM) [CM-h/sol], M_{eq} is the stowage factor for accounting for additional structural masses for a subsystem such as shelving [kg/kg], V_{eq} is the mass equivalency factor for the pressurized volume support infrastructure [kg/m^3], P_{eq} is the mass equivalency factor for the power generation support infrastructure [kg/kW$_e$], C_{eq} is the mass equivalency factor for the cooling infrastructure [kg/kW$_{\text{th}}$], T_{eq} is the mass equivalency factor for the crew-time [kg/CM-h], and L_{eq} is the location factor for the mission segment [kg/kg] which accounts for the cost to transport mass from one location in space to another. Mass equivalency factors (V_{eq}, P_{eq}, C_{eq}, T_{eq}) are used to convert the non-mass parameters to mass. **For IMLEO:**, $\mathcal{M}$ is the set of mission segments to LEO. **For SCM:** C is the systems complexity value, L is the level number, N is the number of nodes, and S is the number of subsystems.

for RMA design, we leverage the existing literature for programmatic representation of a 500 sol surface mission with an initial inventory population to demonstrate the validation of eO's TEA module. Validations of the eO TEA capabilities are presented in Figure 5.4 as a comparison across a myriad mission architectures using the metrics presented in Table 5.2. Each RMA was constructed by assigning standard mission variables such as crew-number and mission duration, a "scenario" such as open loop (OL) or closed-loop (CL), and technology choices the corresponding variable specification for air, food, thermal and waste subsystems. The comparison of eO's calculated ESM values against those from the ALSSAT validate our agency in constructing the distribution of BE scenarios.

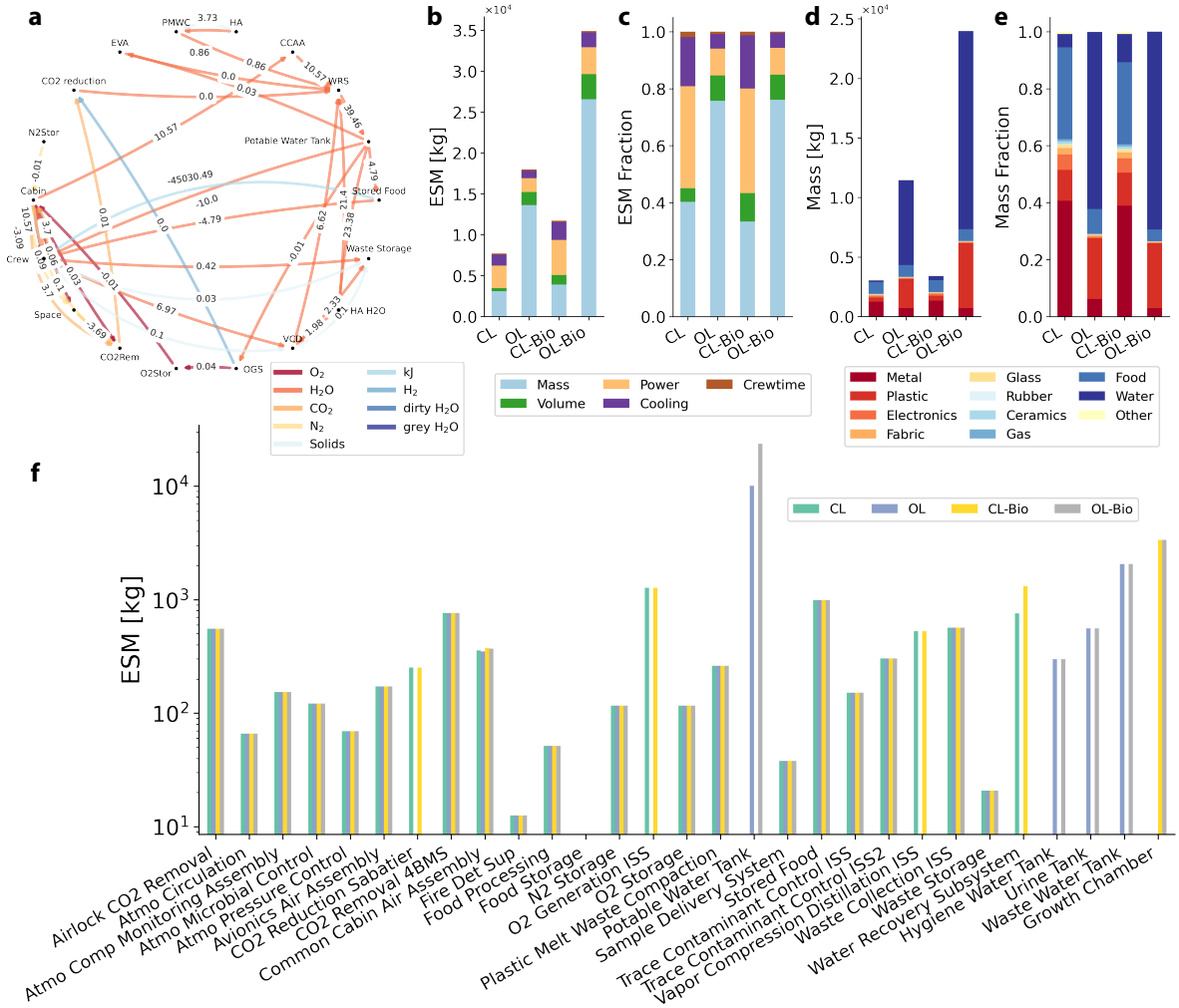

Figure 5.4: Technoeconomic Validation of eO against the NASA ALSSAT. **(a)** Visual depiction of transition matrix for closed loop "bring everything" scearnio. **(b)** Bar chart demonstrating eO calculation and comparison of 4 scenarios in terms of the standard ESM metric using a breakdown of ESM by components such as Mass, Volume, Power, Cooling, and Crew Time. **(c)** Bar chart with same comparisons as (b) using ESM fraction. **(d)** Bar chart demonstrating eO calculation and comparison of 4 scenarios in terms of the standard ESM metric using a breakdown of ESM by material composition in terms of metal, plastic electronics, water, etc. **(e)** Bar chart with same comparisons as (d) using ESM fraction. (f) Bar chart comparison of subsystems for each scenario.

The basic schema for carrying out ESM-based TEA in eO is shown in Figure 5.3 in which resources such as O_2 are used to populate stocks of transition matrices given some initial states. The transition matrices (Figure 5.4a) serve as the starting point for all TEA calculations. Transition matrices can be visualized in eO as a combined directed graphic showing the transfer of resources. Here we show an example transition matrix for a closed loop (CL) BE scenario with resources of O_2, H_2O, CO_2, N_2, solids (define), and energy in [kJ]. In Figure 5.4b we demonstrate eO's agency in calculating and comparing 4 scenarios in

terms of the standard ESM metric, and we further compare each scenario using a breakdown of ESM by components such as Mass, Volume, Power, Cooling, and Crew Time. In Figure 5.4c we breakdown the same elements from 5.4b using ESM fraction rather than pure ESM which allows for a more in depth comparison of ESM components on a standardized scale. In Figures 5.4d,e we further compare each scenario using a breakdown of Mass and Mass Fraction (respectively) by element such as structural metal, plastic, water, biomass, electronics, etc. This demonstrates eO's extensibility beyond the standard ALSSAT. In Figure 5.4f we further expand the subsystem hardware to compare each scenario.

Case Study 2: Dynamic Simulation

The nature of manned missions and their components can be modeled by hybrid systems that mix two kinds of behaviours: (1) the discrete and stochastic behaviour which is in general due to failures and repairs of the system's constituents and (2) the continuous and deterministic physical phenomena which evolve inside the system. eO was designed to be competitive with previously created software such as the HabNet[142] and thus requires methods for defining and running simulations of both individual systems for exploring the deep subsystem-specific parameters and their local optima and entire campaigns composed of many systems in order to understand their dynamics and interoperabilities globally.

Simulations in eO are carried out using the PyCATSHOO framework[103, 102, 135] for Piecewise Deterministic Markov Processes (PDMPs)[183]. PyCATSHOO is a modeling tool for distributed hybrid stochastic automata. eO endeavors to simulate the failures and repairs of Inventory objects and the continuous products of chemical and physical reactions carried out during surface operations. The relationships between and within the Environment, Inventory, Habitat, Processes, and Crew classes are expressed through PyCATSHOO. Mission reliability is calculated by PyCATSHOO as the expected duration of time that mission parameters are within safety margins. Cases resulting in mission failure as described by Do *et al.* in HabNet[142] included the following: crew starvation, crew dehydration, crew hypoxia, crew hyperoxia, crew CO_2 poisoning, cabin pressure, high fire risk, and crop death. Therefore, while simulating a mission, PyCATSHOO tracks and plots CO_2 levels, O_2 levels, pressure, and amount of food over time.

While inventory models in the previous case explored the technology choice landscape problem[106], the assumptions necessary to static mission design tools limit their ability to describe and compare real missions. Dynamic simulations are required to articulate and asses system behaviors like processing cycles, processor scheduling, supply and demand variations, transients, interruptions, and failures – all of which can determine the cost and success of a proposed mission architecture[265].

The first step towards dynamic models is to raise abstraction barriers between items; for example, through the object-oriented frameworks in tools like Biosim and HabNet [142]. This enables the definition of objects that store attributes about themselves, while responding to incoming information from other objects. Past tools store this mission information in Excel formulas or MATLAB/Java code. However, accessibility and standardized definitions are

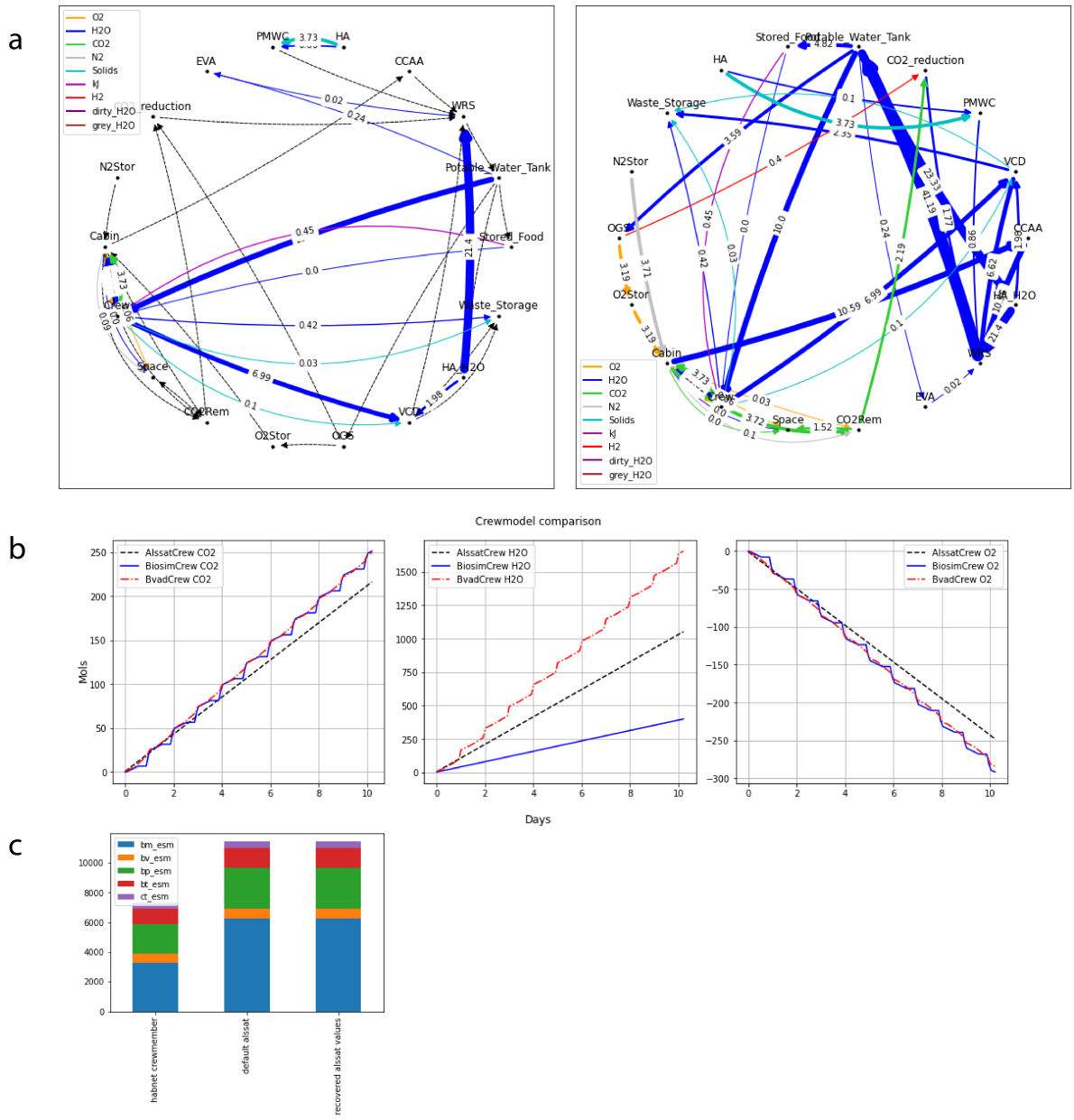

Figure 5.5: Process simulation in terms of **(a)** representation of systems & states, **(b)** dynamics, and a preliminary (**c** technoeconomic analysis.

related: even if an object was dynamic, users would be limited to a static set of said objects if they could not create new items of their own. In eO, we formalize the definition of objects and their interactions. We chose PyCATSHOO for its ability to describe an object's dynamic variables; the conditional update of those values; an object's automata; the conditional transitions between those states; and the importing and exporting of values without prior

knowledge of who to receive resources from, or distribute resources to. Furthermore, the transition rate matrices in eO exposes these innards of a mission, displaying every string in the network that can be pulled, and summarizing them at a glance.

In 5.5, the static mission configuration from the previous section is extended to a duration of 500 days and converted to a dynamic model. The usage requirements of a technology (by which it is scaled) often originate from information that originates from the crewmembers, not the machine itself, so such edges that were once assigned a float value were now defined by a method that is evaluated at each simulation timestep. As a benchmark, these values were recovered after simulation, and their averages were found to be nearly identical to the original static float. The graph on the right was repopulated with simulation results.

Given how mission architectures spring from crew needs, we next benchmarked eO's simulation module on different metabolic models, from HabNet and the BVAD, that capture hourly fluctuations in resource needs based on the daily schedule. Because eO objects are modular, we also used eO to scale the same inventory configuration as before, except with dynamic simulation that allows for fluctuation in crew need, and then calculated ESM. While there was negligible difference between the dynamic model of the static original, using the same mission design with a different crew metabolic models caused great differences in the resulting ESM, showing the need for such a modular framework that allows benchmarking across multiple versions of the same object, and the standardization of which models to use.

Chapter 6

Case Study 1: Photovoltaics-Driven Power Production on Mars

A central question surrounding possible human exploration of Mars is whether crewed missions can be supported by available technologies using *in situ* resources. Here, we show that photovoltaics-based power systems would be adequate and practical to sustain a crewed outpost for an extended period over a large fraction of the planet's surface. Climate data were integrated into a radiative transfer model to predict spectrally-resolved solar flux across the Martian surface. This informed detailed balance calculations for solar cell devices that identified optimal bandgap combinations for maximizing production capacity over a Martian year. We then quantified power systems, manufacturing, and agricultural demands for a six-person mission, which revealed that photovoltaics-based power generation would require <10 t of carry-along mass, outperforming alternatives over ∼50% of Mars' surface.

The following chapter can also found here: A.J. Berliner, A.J. Abel, M. Mirkovic, W. Collins, A.P. Arkin, D. Clark. **Photovoltaic and Photoelectrochemical Production Capacity can Support Human Exploration on Mars**. *Frontiers in Astronomy and Space Sciences* (2022). DOI: 10.3389/fspas.2022.868519.

6.1 Power Production on Mars

Long-duration space missions or continuously-occupied extraterrestrial outposts require Earth-independent power and chemical supply. Mars has an abundance of *in situ* resources, including (sub)surface water ice[567] and carbon and nitrogen in atmospheric CO_2 and N_2[552]. Efficient conversion of these resources to reduced forms of hydrogen, nitrogen, and carbon would represent an enabling step towards sustaining a permanent human presence in space. In analogy to the proposed terrestrial "Hydrogen Economy", molecular hydrogen (H_2) can be used as a platform molecule for energy storage, on-demand power supply, and as a reactant

driving CO_2 and N_2 (bio)chemical reduction on Mars[341, 44, 95].

Water electrolysis with selective catalysts can drive water reduction to H_2 on cathode surfaces. This technology is attractive for space manufacturing applications since reactions can proceed at high rates at room temperature, enabling the use of low-weight, 3D-printable plastic reactors[44]. Commercial electrolyzers can evolve H_2 from water with up to ∼80% energy efficiency[531]. Directly solar-powered (i.e., photoelectrochemical (PEC)) devices have also received significant attention, with solar-to-chemical efficiencies reaching blue>19% for H_2 production[98]. Once generated, H_2 can drive N_2 reduction to ammonia via the Haber-Bosch process for crop fertilizer[44], CO_2 reduction to CH_4 via the Sabatier process or methanogenesis for ascent propellant generation[371], and CO_2 reduction to bioplastics

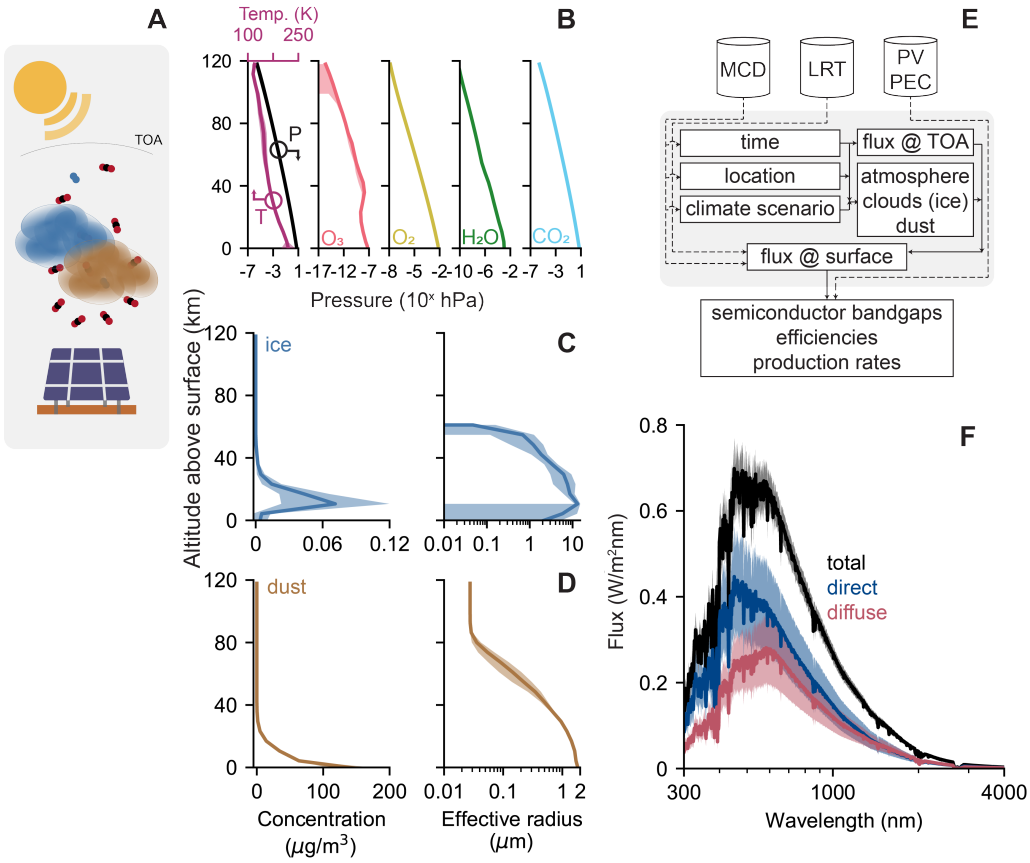

Figure 6.1: Overview and calculation of spectral flux using atmospheric data. (A) Sunlight incident on the solar cells is mediated by orbital geometry and local atmospheric composition of gases, ice, and dust. **(B, C, and D)** Temperature, partial pressure of atmospheric gases and concentration and effective radii of ice and dust particles as a function of altitude above the surface. **(E)** Information flow in the calculation scheme. Dotted lines represent functions used for calculations; solid lines represent data used as parameters. MCD, Mars Climate Database; LRT, LibRadtran. **(F)** Total (black), direct (blue), and diffuse (red) solar flux at Jezero Crater at solar noon averaged over the course of a typical Martian year. In **(B)**, **(C)**, **(D)**, and **(F)**, solid lines represent yearly averages and shaded regions represent the standard deviation due to seasonal variation.

following a variety of metabolic processes for habitat and spare parts manufacturing[44, 401].

The primary alternatives for powering life support systems and chemical production facilities on Mars are miniaturized nuclear fission reactors[147] and photovoltaic (PV) arrays. While fission reactors are expected to behave similarly regardless of their location, the productivity limits of PV and photoelectrochemical devices are not well-characterized for the Martian surface mainly due to differences in the surface temperature and solar intensity and spectrum from typical conditions on Earth or in space.

In an effort to determine the potential of PV and PEC devices to support a crewed mission to Mars, we integrated relevant climate data from the Mars Climate Database[448] into a radiative transfer model, libRadtran[358], to predict spectrally-resolved solar flux across the Martian surface over the course of a year. The modeling overview and sample calculations for Jezero Crater are provided in Fig. 6.1. Sunlight incident on the surface originating from the top of the atmosphere (TOA) is mediated by orbital geometry and local atmospheric composition of gases, ice, and dust for a given location (Fig. 6.1A). We determined the partial pressures of constituent gases (Fig. 6.1B) and the concentrations and effective radii of ice (Fig. 6.1C) and dust (Fig. 6.1D) particles as a function of altitude above the surface and provided these data as inputs to a downstream radiative transfer model (diagrammed in Fig. 6.1E). We then calculated the spectrally-resolved solar flux (Fig. 6.1F). At short wavelengths (<400 nm), light transmission through the atmosphere is limited by molecular scattering (primarily by CO_2) and scattering from dust particles[539]. Scattering and absorption by gas molecules is significant at wavelengths below 300 nm, but this region is not considered here because it represents a very small fraction of the available solar flux (<0.5%). Above 400 nm, most transmission loss is due to scattering from dust particles. This is markedly different from the case on Earth, where significant molecular absorption by water molecules limits the transmission of near-infrared light.

6.2 Results

The modeling results were used to inform efficiency calculations for PV and PEC devices producing electricity and H_2. Detailed balance calculations (section 4 in the Supplementary Information)[146, 211] revealed ideal current-voltage characteristics for optically-thick devices consisting of 1-, 2-, and 3- junction PV and 1- and 2-junction PEC absorbers dependent on the bandgaps associated with each absorber (Fig. 6.2). Absorber numbers were selected to represent historical choices for PV devices on Martian rovers[505, 299] and state-of-the-art PEC devices[98, 578, 255]. For PEC devices, we assumed an electrical load consisting of the thermodynamic redox potential and a variable overvoltage term that incorporates loss mechanisms inevitable to a practical PEC device beyond radiative recombination already considered in the detailed balance[146, 211].

m

The maximum efficiency for PV devices increases from 31.4% (1-junction; E_g=1.23 eV) to 51.3% (3-junction; $Eg, 1 = 1.77$ eV, $E_{g,2} = 1.16$ eV, $E_{g,3} = 0.72$ eV) with judicious

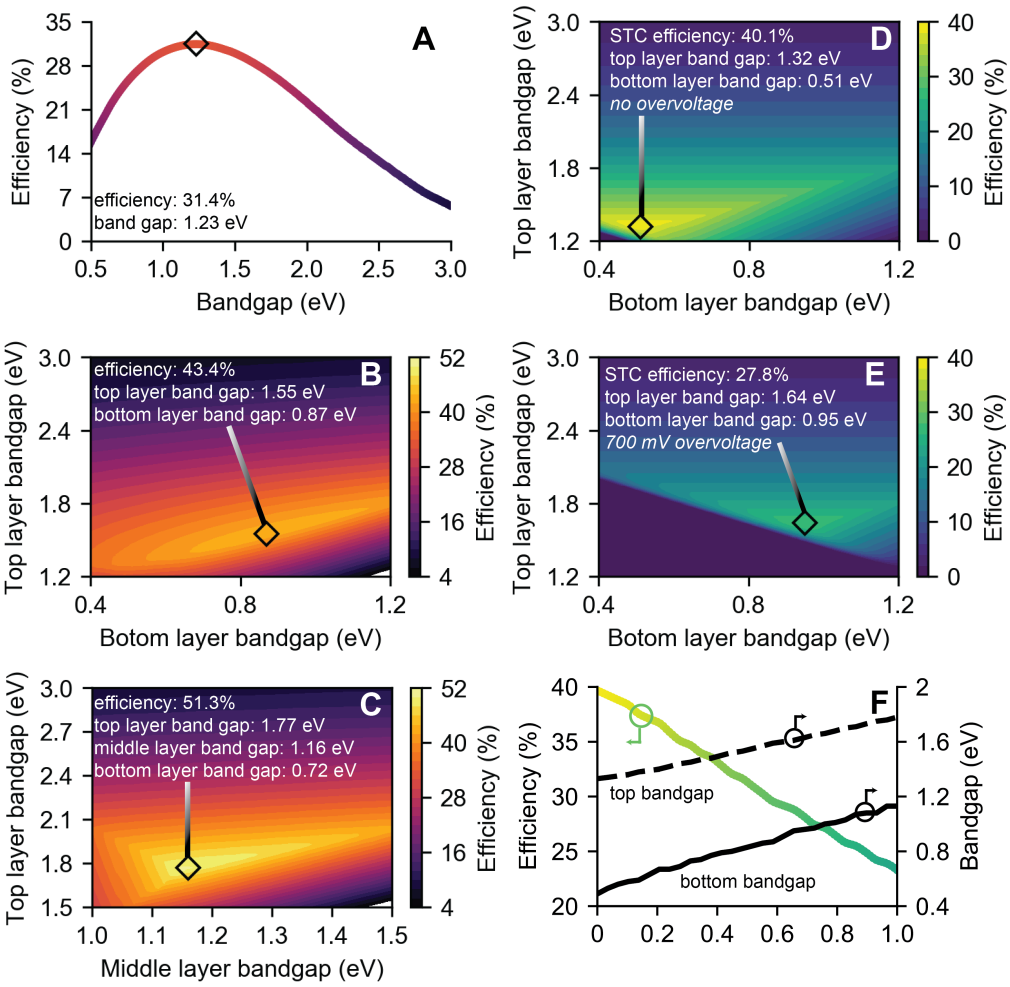

Figure 6.2: Theoretical efficiencies of PV and PEC devices. Detailed-balance efficiency limits as a function of bandgap energies for **(A)** single-junction, **(B)** two-junction, **(C)** three-junction photovoltaic devices. **(D, and E)** Solar-to-chemical (STC) efficiency for two-junction water splitting PEC devices producing molecular hydrogen with 0 mV (D) and 700 mV (E) overvoltage. **(F)** STC efficiency and optimal bandgaps for two-junction H_2-generating PEC devices as a function of overvoltage. Coloring in **(A)** and **(F)** correspond to contour coloring in **(B, C)** and **(D, E)** respectively. Average flux at solar noon at Jezero Crater is used as the reference solar spectrum.

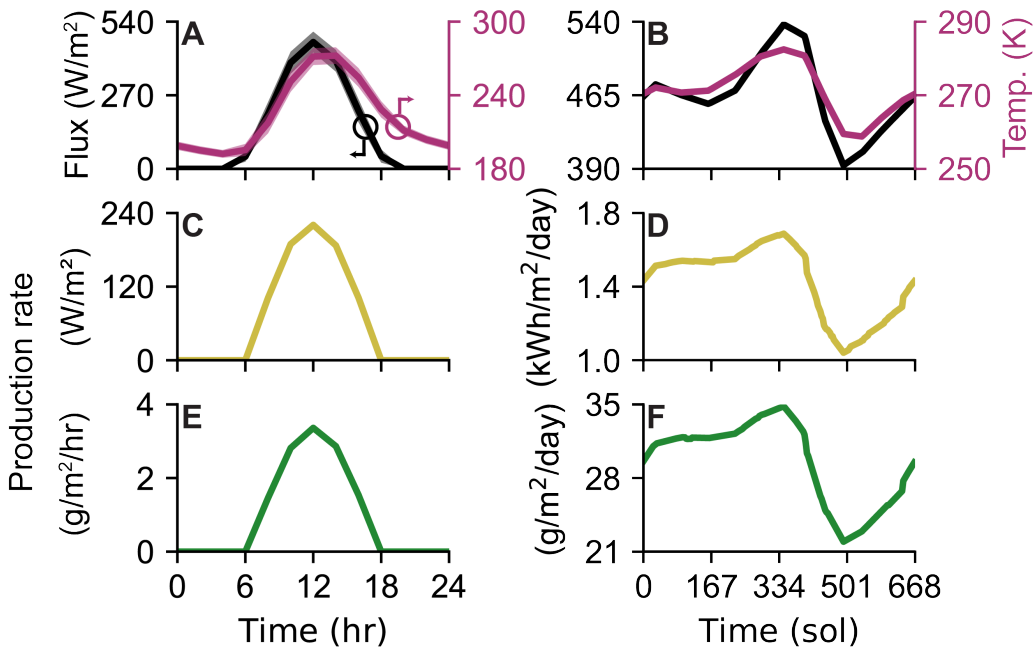

Figure 6.3: PV and PEC production rates. (A) Average and **(B)** daily maximum solar flux (black, left axis) and surface temperature (purple, right axis) as function of **(A)** time of day and **(B)** time of year. **(C, E)** average and **(D, F)** daily maximum production capacity of power **(C, D)** and H_2 **(E, F)** using 3-junction PV and 2-junction PEC cells as described in the main text. Solid lines in **(A, C, E)** correspond to averages; shaded areas represent the standard deviation due to seasonal variation. Jezero Crater is used as the location for plots.

choice of bandgaps (Fig. 6.2A-C). For PEC devices, optimal bandgap choice and efficiency are strongly dependent on system losses (Fig. 6.2D-F), reflecting the importance of careful device construction and catalyst selection[239]. For a realistic overvoltage loss of 700 mV[211, 146, 239], a maximum solar-to-chemical blueconversion (SCC) efficiency of 27.8% is feasible for H_2 production.

To evaluate the potential for solar cells to supply power and commodity chemicals, we determined the maximum practical production capacity for 3-junction PV (operating at 80% of the detailed balance limit) and 2-junction PEC devices (with a 700-mV overvoltage) over the course of a Martian year (Fig. 6.3). Daily and seasonal variation in solar flux and temperature (Fig. 6.3A, B) cause substantial (∼27% deviation from the yearly average) changes in production rates (Fig. 6.3C, D). We defined solar day (sol) 0 at a solar longitude (Ls) of 0° (vernal equinox) and assumed the solar cell operating temperature was equal to the surface temperature at all points. Dust storm season begins at sol ∼372 (Ls∼180°) and is primarily responsible for the drop in production capacity from a peak of blue∼1.7 kWh/m^2/day at Jezero Crater to a minimum of blue∼1.0 kWh/m^2/day at the height of dust storm intensity around the winter solstice (Ls ∼270°, sol ∼514).

Bandgap combinations that maximize production over the course of a year are 5-15%

different from those that optimize efficiency at solar noon (Table S8). For both PV and PEC devices, the top junction bandgap shifted up (for H_2-generating PEC devices, from 1.64 eV to 1.77 eV), while the bottom junction bandgap shifted down (from 0.95 eV to 0.83 eV). Hence, the photon absorption window for the bottom junction is broadened (by ∼35% for the PEC device). This likely works to maximize productivity during the less dusty season (higher solar flux, Fig. 6.3B) by accounting for the relative blue-shift of surface-incident light (Fig. 6.1F) due to reduced scattering.

6.3 Discussion

Production capacity of power and commodity chemicals must compare favorably to the demand necessary to sustain a Martian habitat and depends on the outpost location on the planet surface (Fig. 6.4A). Moreover, energy storage capacity is crucial for solar-powered production systems because the sun sets daily. We therefore developed a detailed process model to account for power systems demands, including habitat maintenance (for example, habitat temperature control and pressurization), fertilizer production for agriculture, methane production for ascent propellant, and bioplastics production for spare parts manufacturing (Fig. S12). We considered four different power generation scenarios: (1) nuclear power generation with the miniaturized nuclear fission Kilopower system; (2) PV power generation with battery energy storage (PV+B); (3) PV power generation with compressed H_2 energy storage produced via electrolysis (PV+E); and (4) PEC H_2 generation with compressed H_2 energy storage (PEC). In our calculations, we assumed a capacity factor of 75% to account for the solar flux deviation throughout the Martian year (Fig. 6.3) and sized energy storage systems (batteries or compressed H_2) to enable 1 full day of operations from reserve power. We then calculated the carry-along mass requirements for each of the power generation systems considered.

Of the three solar-driven power generation options, only the PV+E system outcompetes the nuclear system based on carry-along mass (Fig. 6.4B, C; supplementary Fig. S13). For the PV+E system, the total carry-along mass increases from ∼8.3 t near the equator to ∼22.4 t near the South Pole (Fig. 6.4B), corresponding to the reduced average daily power generation of the PV array as the latitude is adjusted away from 0° (Fig. 6.4A). The nuclear power system is predicted to require ∼9.5 t; hence, the PV+E system out-performs this option across ∼50% of the planet's surface (Fig. 6.4B).

In addition to predicting production capacity and carry-along mass, our model provides design rules for optimal solar cell design. Optimal absorber bandgaps for the PV array are strongly dependent on the location on the surface of Mars blue(Fig. 6.4D-F). Several factors cause this variation: the total depth of the air column above a given location (i.e., the difference between the height of the atmosphere and the altitude), gradients in dust and ice concentrations and particle radii, and orbital geometry effects that cause different effective air column thicknesses for locations near the poles. Lower elevations, higher dust and/or ice concentrations, and increasing distance away from the equator (near-polar latitudes)

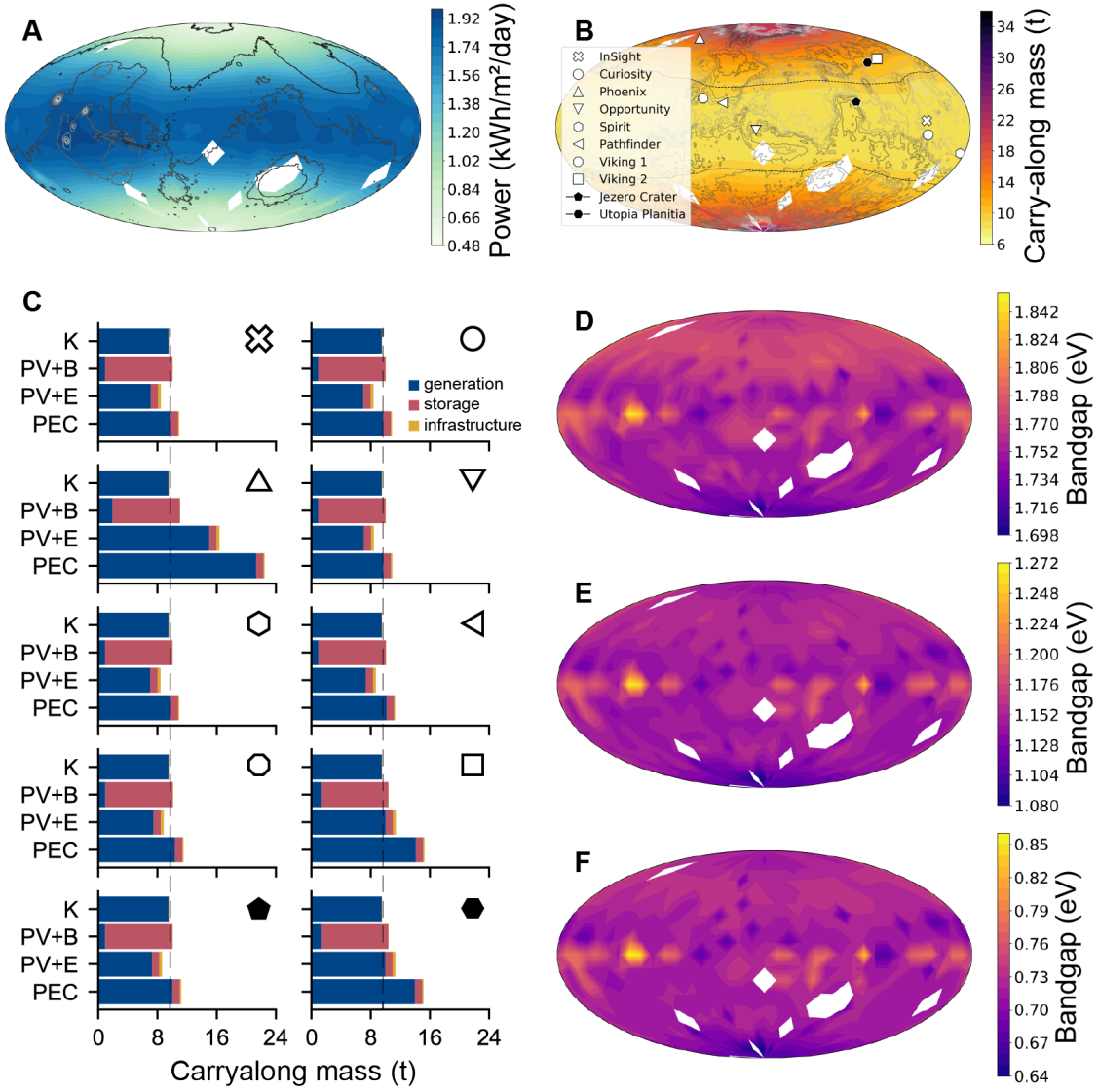

Figure 6.4: Solar productivity across the Martian surface. (A) Average daily solar power production capacity across the Martian surface. **(B)** Total carry-along mass required for power production using the PV+E generation system. Black dashed line corresponds to breakeven location with nuclear power generation. **(C)** Carry-along mass breakdown for locations in **(B)** for each power generation option. Black dashed line corresponds to breakeven with nuclear power generation. Optimal **(D)** top, **(E)** middle, **(F)** bottom bandgaps for the 3-junction PV array.

all cause an increase in the optical depth of the air column, which enhances the fraction of light that is scattered. Because the spectrum of scattered light is slightly red-shifted with respect to direct light (Fig. 6.1F), optimal bandgaps decrease to capture more lower-energy photons (Fig. 6.4D-F) in regions where the optical depth is higher. For example, at equivalent latitudes, the optimal bandgaps are wider for regions with higher elevations than for those with lower elevations because the fraction of light that gets scattered is lower.

Regional differences in atmospheric conditions can drive countervailing effects; because the Northern Hemisphere experiences generally lower dust concentrations than the Southern Hemisphere, the lower elevation in the Northern Hemisphere does not result in (on average) narrower optimal bandgaps. Instead, the reduced dust concentration (relative to that of the Southern Hemisphere) results in a reduced optical depth, resulting in wider optimal bandgap combinations (Fig. 6.4D-F). blueIn sum, optimal bandgaps for the top absorber range from ∼1.7 eV to ∼1.84 eV (Fig. 6.4D), from ∼1.08 eV to ∼1.27 eV for the middle absorber (Fig. 6.4E), and from ∼0.64 eV to ∼0.85 eV for the bottom absorber (Fig. 6.4F). Optimized triple-junction solar cells could be fabricated from, for example, GaInAsP alloys on Ge substrates with minimal lattice mismatch (<∼1%)[578] or by utilizing compositionally graded buffer layers to minimize threading dislocations[287]. These strategies have been deployed previously with success in high-efficiency triple junction device architectures[186].

In conclusion, solar cell arrays with careful attention to semiconductor choice and device construction represent a promising technology for sustaining an Earth-independent crewed habitat on Mars. Our analysis provides design rules for solar cells on the Martian surface and shows that solar cells can offer substantial reduction in carry-along mass requirements compared to alternative technology over a large fraction of the planet's surface.

Chapter 7

Case Study 2: Nitrogen Accountancy in Space Agriculture

Food production and pharmaceutical synthesis are critical biotechnologies to enable human exploration of Mars because they reduce mass and volume requirements through scalable and modular agriculture in closed-loop systems. The NASA-sponsored modified energy cascade (MEC) model used to evaluate crop growth is insufficient as a tool to support exploration missions in its monocrop architecture, incomplete material balances on key crop cultivation and life support resources like nitrogen, and lack of the rigorous physical inventory accounting that is required to evaluate mission costs. We expand the MEC model to account for nitrogen dependence across an array of crops and validate our model with experimental fitting of parameters. By adding nitrogen limitations, the extended MEC model accounts for potential interruptions in feedstock supply. Furthermore, we use sensitivity analysis to distil key consequential parameters that may be the focus of future experimental efforts. Finally, the integration of physical system inventories enables comparisons in the choice of architecture and technology.

The following chapter is under development for publication as A.J. Berliner, K. Yates, M. McNulty, P. Kusuma, S. Zhen, S. Sen Gupta, G. Makrygiorgos, A.A. Menezes, B. Bugbee, A. Mesbah, A.P. Arkin, S. Nandi, K. McDonald. **Nitrogen Accountancy in Space Agriculture**. (In preparation, expected submission Summer 2022).

Martian-based agriculture (Fig 7.1A) has been shown to be a feasible[17, 564] alternative to prepackaged meals, but caloric intake alone does not fully describe the requirements for astronaut sustainability; pharmaceutical needs must also be met to ensure crew health. Additionally, the space environment imposes further risk of compromised food consumables necessitates additional reserves of elemental carbon, nitrogen, and phosphorus[366, 253]. While some physico-chemical means exist for recycling a subset of these elements, they are usually mass and energy intensive[356], and generally require additional downstream

processing[173]. Given that the demand for consumable food mass scales nearly linearly with the increasing mission duration/crew size and that storage of larger quantities of food necessitates additional costs in refrigeration, storage, and power, crop cultivation provides a means for cost reduction[581, 41]. Furthermore, consumables must be maintained longer in harsher environments, increasing both financial and mass costs.

Martian-based agriculture (Fig 7.1a) has been shown to be a feasible[17, 564] alternative to prepackaged meals, but caloric intake alone does not fully describe the requirements for astronaut sustainability; pharmaceutical needs must also be met to ensure crew health. Additionally, the space environment imposes further risk of compromised food consumables necessitates additional reserves of elemental carbon, nitrogen, and phosphorus[366, 253].

Variable	**Description**	**Unit**	**Former Variable**[17]
a	Empirical exponent	-	n
c_{CO2}	Concentration of CO_2, molar	$\mu\mathrm{mol}_{\mathrm{CO2}}\,\mathrm{mol}_{\mathrm{air}}^{-1}$	$[CO_2]$
f_{E}	Fraction of edible biomass after t_{E}	-	XFRT
g_{atm}	Atmospheric aerodynamic conductance	$\mathrm{mol}_{\mathrm{water}}\,\mathrm{s}^{-1}\,\mathrm{m}^{-2}$	g_{A}
g_{sfc}	Canopy surface conductance	$\mathrm{mol}_{\mathrm{water}}\,\mathrm{s}^{-1}\,\mathrm{m}^{-2}$	g_{C}
g_{sto}	Canopy stomatal conductance	$\mathrm{mol}_{\mathrm{water}}\,\mathrm{s}^{-1}\,\mathrm{m}^{-2}$	g_{S}
h_{R}	Relative humidity	-	RH
$\hat{\dot{m}}_B$	Biomass per time, areal	$\mathrm{g}\,\mathrm{d}^{-1}\,\mathrm{m}^{-2}$	CGR
$\hat{m}_{\mathrm{E}}$	Biomass, areal, edible	$\mathrm{g}\,\mathrm{m}^{-2}$	TEB
$\hat{m}_{\mathrm{T}}$	Biomass, areal, total	$\mathrm{g}\,\mathrm{m}^{-2}$	TCB
$\check{m}$	Mass, molar	$\mathrm{g}\,\mathrm{mol}^{-1}$	MW
$\hat{\dot{n}}$	Moles per time, areal	$\mathrm{mol}\,\mathrm{d}^{-1}\,\mathrm{m}^{-2}$	DCG, DOP
$\hat{\dot{n}}_{\mathrm{ps,gross}}$	Gross canopy photosynthesis	$\mu\mathrm{mol}_{\mathrm{C}}\,\mathrm{s}^{-1}\,\mathrm{m}^{-2}$	P_{GROSS}
$\hat{\dot{n}}_{\mathrm{ps,net}}$	Net canopy photosynthesis	$\mu\mathrm{mol}_{\mathrm{C}}\,\mathrm{s}^{-1}\,\mathrm{m}^{-2}$	P_{NET}
P_{atm}	Total atmospheric pressure	kPa	P_{ATM}
p_{S}	Saturated vapour pressure	kPa	VP_{SAT}
T_{D}	Temperature, dark cycle	°C	T_{DARK}
T_{L}	Temperature, light cycle	°C	T_{LIGHT}
t_{sol}	Length of local sol	$\mathrm{h}\,\mathrm{d}^{-1}$	D_{PG}
$\hat{\dot{V}}_{\mathrm{trs}}$	Daily transpiration rate	$\mathrm{L}\,\mathrm{d}^{-1}\,\mathrm{m}^{-2}$	DTR
w_{C}	Biomass carbon fraction	-	BCF
Y_{O2}	Oxygen production factor	$\mathrm{mol}_{\mathrm{O2}}\,\mathrm{mol}_{\mathrm{C}}^{-1}$	OPF
Y_{Q}	Canopy quantum yield	$\frac{\mathrm{mol}_{\mathrm{C,fixed}}}{\mathrm{mol}_{\gamma,\mathrm{absorbed}}}$	CQY
Δp	Vapour pressure deficit	kPa	VPD
η_{C}	Carbon use efficiency, 24 hr	$\frac{\mathrm{mol}_{\mathrm{C,biomass}}}{\mathrm{mol}_{\mathrm{C,fixed}}}$	CUE_{24}
σ	Density, areal, mass	$\mathrm{kg}\,\mathrm{m}^{-2}$	-
σ_N	Density, areal, numeric	m^{-2}	-
Φ_{γ}	Photosynthetic photon flux	$\mu\mathrm{mol}_{\gamma}\,\mathrm{m}^{-2}\,\mathrm{s}^{-1}$	PPF
$\Phi_{\gamma,\mathrm{E}}$	Photosynthetic photon flux, effective	$\mu\mathrm{mol}_{\gamma}\,\mathrm{m}^{-2}\,\mathrm{s}^{-1}$	PPF_{E}

While some physico-chemical means exist for recycling a subset of these elements, they are usually mass and energy intensive[356], and generally require additional downstream processing[173]. Given that the demand for consumable food mass scales nearly linearly with the increasing mission duration/crew size and that storage of larger quantities of food necessitates additional costs in refrigeration, storage, and power, crop cultivation provides a means for cost reduction[581, 41]. Furthermore, consumables must be maintained longer in harsher environments, increasing both financial and mass costs.

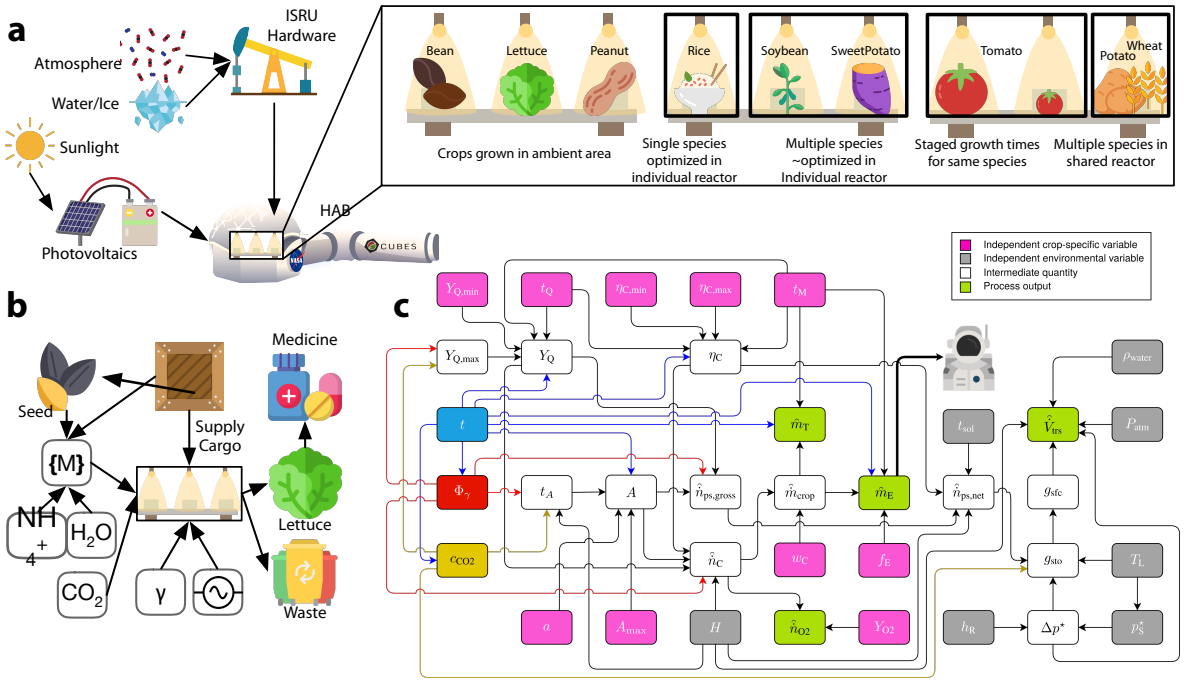

Figure 7.1: Mars-based Agriculture Overview. **(a)** Scheme for deploying agriculture systems on Mars using ISRU with an expansion of potential crops within habitat and their index within extended MEC model. The expansion of crop systems includes example groupings of crops with hydroponic reactor logistics. **(b)** Systems diagram for crop growth reactor taking in media ($\{M\}$), ammonium (NH_4^+), water (H_2O), carbon dioxide (CO_2), light (γ), and power ($\sim$) to produce some crop (in this case lettuce), pharmaceuticals, and biowaste. **(c)** Graphical breakdown of and interaction between MEC Lettuce model variables. **D.** Total crop biomass $\hat{m}_{\mathrm{T}}$ (blue) and crop growth rate $\hat{\dot{m}}_B$ (gold) for Dry Bean, Lettuce, Peanut, Rice, Soybean, Sweet Potato, Tomato, Wheat, White Potato at $\Phi_\gamma = 500$ [$\mu\mathrm{mol}_\gamma\,\mathrm{m}^{-2}\,\mathrm{s}^{-1}$], $c_{\mathrm{CO2}} = 1200$ [$\mu\mathrm{mol}_{\mathrm{CO2}}\,\mathrm{mol}_{\mathrm{air}}^{-1}$]. **E.** Contours of biomass accumulation for each crop terminating at each crop's harvest time t_{M} across Φ_γ and c_{CO2}.

A primary advantage of a synthetic biology in space is the interconnectivity and recyclability of diverse capability elements. Thus far, crop cultivation has been studied and characterized in many configurations (Fig 7.1a) as an isolated system, with the exception of some studies on air revitalization[158, 194]. Correspondingly, the established crop cultivation mathematics[17] of NASA's modified energy cascade (MEC) model[268] are designed to model crop cultivation behavior of a single crop type in isolation (Fig 7.1b,c), focusing on providing information relevant to traditional crop cultivation outcomes (e.g. food, environ-

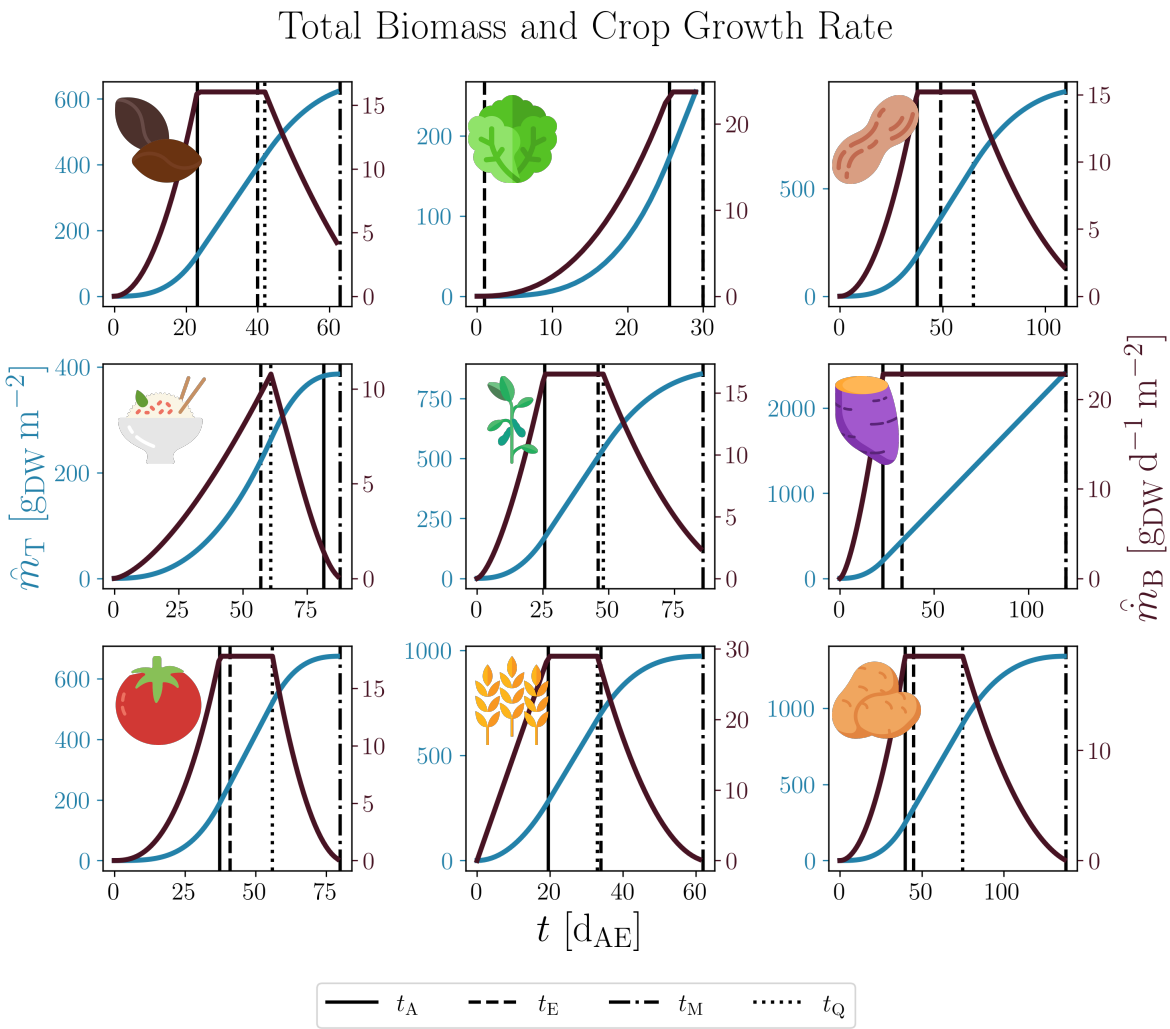

Figure 7.2: Total crop biomass $\hat{m}_{\mathrm{T}}$ (blue) and crop growth rate $\hat{\dot{m}}_B$ (gold) for Dry Bean, Lettuce, Peanut, Rice, Soybean, Sweet Potato, Tomato, Wheat, White Potato at $\Phi_\gamma = 500$ [$\mu\mathrm{mol}_\gamma\,\mathrm{m}^{-2}\,\mathrm{s}^{-1}$], $c_{\mathrm{CO2}} = 1200$ [$\mu\mathrm{mol}_{\mathrm{CO2}}\,\mathrm{mol}_{\mathrm{air}}^{-1}$].

mental revitalization). In the MEC, biomass per unit area in a single reactor of some crop i is denoted as $\hat{m}_{B,i}$ and formulated as a continuous differential equation by

$$\frac{d\hat{m}_{B,i}}{dt} = \hat{\dot{m}}_{B,i} = \frac{\check{m}_{\mathrm{C}}}{w_{\mathrm{C},i}} \hat{\dot{n}}_{\mathrm{C},i} \tag{7.1}$$

$$= 0.0036 \cdot \frac{\check{m}_{\mathrm{C}}}{w_{\mathrm{C},i}} \left(H_i \cdot \eta_{\mathrm{C},i} \cdot A_i \cdot Y_{\mathrm{Q},i} \cdot \Phi_{\gamma,i} \right) \tag{7.2}$$

where $\hat{\dot{m}}_B$ is areal crop biomass growth rate on a dry weight basis in [$\mathrm{g\,m^{-2}\,d^{-1}}$], t is time in [$\mathrm{d_{AE}}$] (days after emergence of the cotyledon), $\check{m}_{\mathrm{C}}$ is the molar mass of carbon in [$\mathrm{g\,mol^{-1}}$],

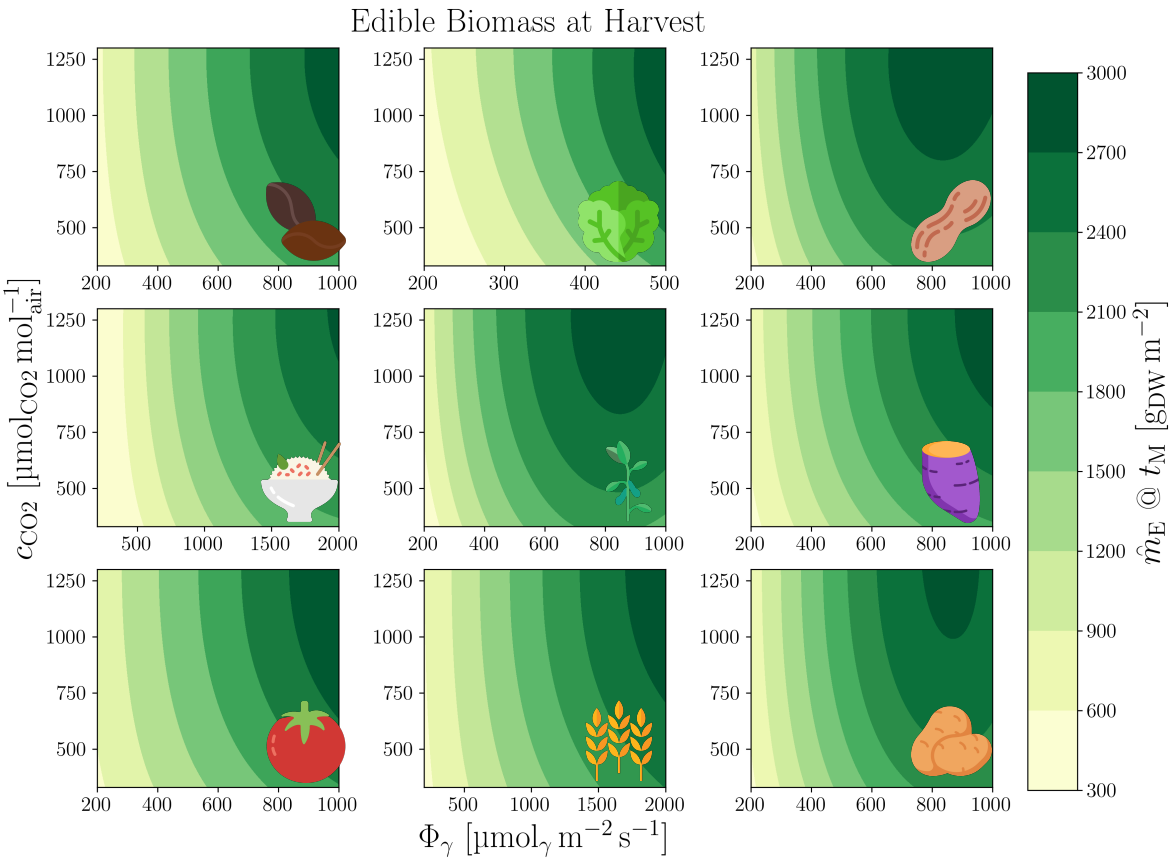

Figure 7.3: Contours of biomass accumulation for each crop terminating at each crop's harvest time t_{M} across Φ_γ and c_{CO2}.

w_{C} is the unitless biomass carbon fraction, and $\hat{\dot{n}}_{\mathrm{C}}$ is the daily carbon gain in $[\mathrm{mol_C\,m^{-2}\,d^{-1}}]$. The $\hat{\dot{n}}_{\mathrm{C}}$ term can be represented as the product of photoperiod H in $[\mathrm{h\,d^{-1}}]$, 24-hour carbon use efficiency η_{C} in $[\mathrm{mol_{C,biomass}\,mol_{C,fixed}^{-1}}]$, the unitless fraction of photosynthetic photon flux absorbed by the plant canopy A, canopy quantum yield Y_{Q} in $[\mathrm{mol_{C,fixed}\,mol_{\gamma\ absorbed}^{-1}}]$, photosynthetic photon flux density Φ_γ in $[\mathrm{\mu mol_\gamma\,m^{-2}\,s^{-1}}]$. We find the total areal biomass $\hat{m}_{\mathrm{T},i}$ in $[\mathrm{g\,m^{-2}}]$ and the edible areal biomass $\hat{m}_{\mathrm{E},i}$ in $[\mathrm{g\,m^{-2}}]$ for some crop i by

$$\hat{m}_{\mathrm{T},i} = \int_0^{t_{\mathrm{M},i}} \hat{\dot{m}}_{B,i}\ dt \tag{7.3}$$

$$\hat{m}_{\mathrm{E},i} = f_{\mathrm{E},i} \int_{t_{\mathrm{E},i}}^{t_{\mathrm{M},i}} \hat{\dot{m}}_{B,i}\ dt \tag{7.4}$$

where $f_{\mathrm{E},i}$ is the unitless, crop-specific fraction of daily carbon gain allocated to edible biomass after $t_{\mathrm{E},i}$, which is the crop-specific time at onset of organ formation in $[\mathrm{d_{AE}}]$ (Figs. 7.2,7.3).

Like most of the traditional life support elements, crop cultivation, and the supporting mathematics, require re-packing and updating to meet the demands of long-duration missions, including aspects of synthetic biology. The following characteristics lacking from the current crop cultivation mathematics are critical for a model in a long-duration space exploration mission architecture: (1) systems design – the ability to fit within a larger systems framework and interconnect with upstream and downstream operations; (2) compatibility with equivalent system mass (ESM) based decision making and optimization; (3) well understood parameter sensitivity and robustness. In this work, we aim to adapt the existing MEC model for crop cultivation to improve its readiness for systems integration and next-generation space exploration analysis. We implement model improvements in each of the three aforementioned critical characteristics. The MEC model is re-worked for systems design – mathematics are converted into differential equations, communicated in terms of mass and energy balances, generalized for multiple crops and multiple reactors, and written in code compatible with systems integration. Additionally, the model is improved through the inclusion of nitrogen-based limitations. This enables a more robust scenario and systems analysis that may be particularly important for synthetic biological approaches to life support. More robust ESM integration is added, using preliminary and pre-optimized values. Finally, the crop cultivation model mathematics are characterized in further depth through sensitivity analysis.

Nitrogen Productivity Model

Nitrogen is an essential plant nutrient central to the synthesis of photosynthetic proteins and pigments. The availability of nitrogen in the rootzone is therefore a decisive factor for plant photosynthetic capacity, growth, and yield [216, 167]. Modeling the effect of nitrogen on plant growth conditions becomes of paramount importance within the scope of biologically-driven mission planning since nitrogen is a limited resource that needs to be optimally allocated to ensure proper food and pharmaceuticals production and subsequently safety of the crew members. A Martian mission design is a non-trivial problem and since the decision making is partially driven by models, any uncertainty regarding their predictive capability should be taken into account. Thus, working toward a validated model that forecasts the success of crop growth given the availability of nitrogen, as well as a description of confidence in this prediction, is of great importance towards our goal.

Nitrogen productivity theory (NPT) is a model of plant growth rate as a linear function of plant nitrogen content[13]. NPT is applicable when nitrogen is the limiting factor for biomass growth. The equation which describes growth has the form:

$$\frac{\mathrm{d}m_B}{\mathrm{d}t} = \dot{Y}_{\mathrm{N}}(m_B, m_{\mathrm{N}})m_{\mathrm{N}} \tag{7.5}$$

where m_B is total plant biomass on a dry weight basis in [$\mathrm{g_{DW}}$], t is time in [d], and m_{N} is total amount of nitrogen in the plant in [$\mathrm{g_N}$]. $\dot{Y}_{\mathrm{N}}$ is nitrogen productivity, the biomass produced

per amount of nitrogen in the plant per day, a function of m_B and m_{N}, in $[\mathrm{g_{DW}\,g_N^{-1}\,d^{-1}}]$. Rearranging, nitrogen productivity is defined in quantities that can be experimentally measured (Equation 7.6).

$$\dot{Y}_{\mathrm{N}} = \frac{1}{m_{\mathrm{N}}} \frac{\mathrm{d}m_B}{\mathrm{d}t} \tag{7.6}$$

Results and Discussion

An experiment was designed to characterize the effect of nitrogen concentration in the nutrient support solution (NSS) of a hydroponic system on biomass generation in *Lactuca sativa* cv. "Waldmann's Green", a loose leaf lettuce. Nitrate (NO_3^-) was given in equal concentration for all N conditions, while ammonia (NH_3) concentration varied. Three nitrogen concentrations were chosen: deficient (1.0 mM nitrate, 1.5 mM ammonia), normal (1.0 mM nitrate, 6.5 mM ammonia), and excess (1.0 mM nitrate, 11.5 mM ammonia). Environmental set points were bounded as follows: photosynthetic photon flux density, Φ_γ: $225 \pm 25\,\mu\mathrm{mol}\gamma\,\mathrm{m}^{-2}\,s^{-1}$; atmospheric concentration of carbon dioxide, c_{CO2}: 525 ± 125 ppm; air temperature, T: $22 \pm 2\,°\mathrm{C}$; relative humidity, h_{R}: $50 \pm 10\,\%$; pH: 6.0 ± 1.0; photoperiod, H: $16\,\mathrm{h\,d^{-1}}$. Biomass and nitrogen measurements were taken at 11, 20, 25, 30, 35, and 40 $\mathrm{d_{AE}}$.

The biomass data were compared to the output of the MEC model in Equation 7.1 using the average values of Φ_γ and c_{CO2} logged in the hydroponic system (Fig. 7.4a). The planting density, σ_N, was normalized to $19.2\,\mathrm{m}^{-2}$, and the fresh weight water fraction was assumed to be 0.95, both per their NASA reference values[17].

The excess nitrogen condition resulted in the lowest average biomass at harvest time ([range-units = single]3035AE), while the normal condition resulted in the highest. The MEC prediction of biomass followed the normal nitrogen condition closely over the time period shown. Its predicted values were similar to the deficient condition measurements until day 30, and its predictions were consistently higher than the measured biomass in the excess condition. This demonstrates that the MEC needs to be extended to account for nitrogen availability whether in deficit or excess.

Over time, the plants under all conditions contained an increasing average quantity of nitrogen (Fig. 7.4b), but the average weight percentage of N decreased. Toward t_{M}, the average percentage of N in plants in the normal condition was less than that of the plants in the excess condition, but the plants in the normal condition achieved the greatest average biomass, indicating that excess nitrogen condition may result in growth-inhibiting stresses. In the deficient condition, the average plant N content was lower than in the other conditions, but the average biomass was higher than the plants in the excess condition and was similar to that of the plants in the normal condition up to $30\,\mathrm{d_{AE}}$. This indicates that the plants in deficient conditions may have used N for growth more efficiently than plants in the other conditions at the expense of their average biomass at t_{M}.

Nitrogen productivity was calculated from biomass and nitrogen content data. The values are plotted in Figure (Fig. 7.4c). The overall average nitrogen productivity under the

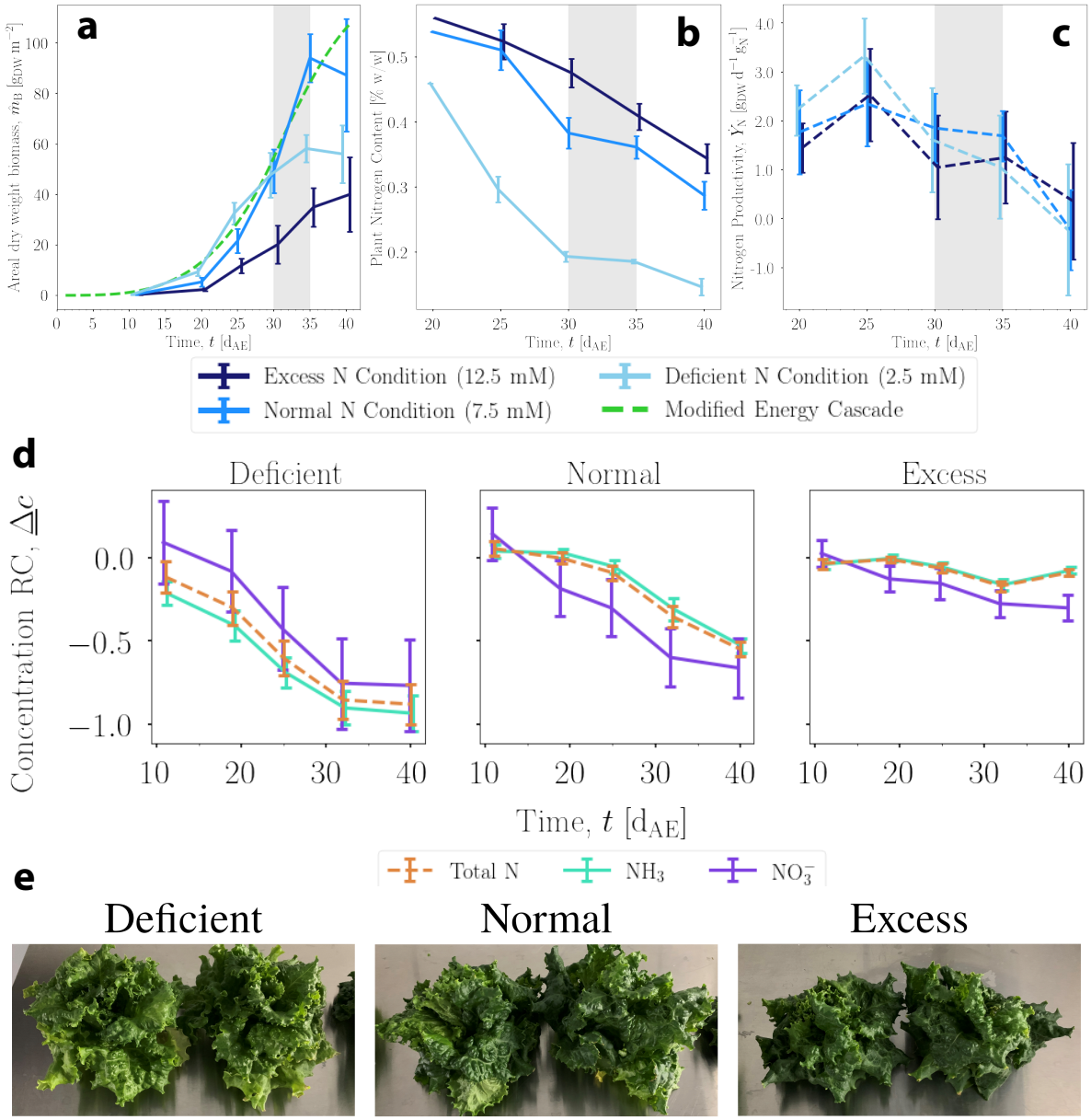

Figure 7.4: **(a)** Measured areal ("per area") biomass and MEC model prediction. The MEC output was calculated with Φ_γ of $225\,\mathrm{mol}\gamma\,\mathrm{m}^{-2}\,s^{-1}$ and c_{CO2} of 525 ppm. **(b)** Measured percentage of total nitrogen by weight in plants over time. Only one measurement could be performed at $20\,\mathrm{d_{AE}}$. **(c)** Nitrogen productivity calculated from two measured quantities, biomass and nitrogen content. Error bars represent propagated error. **(d)** Relative change (RC, $\underline{\Delta}c$), of measured molar concentration, $c(t)$, of ammonia and nitrate, and their calculated sum, to initially charged concentration, $c(t_0)$, in NSS reservoirs over time for each N condition, where $\underline{\Delta}c \equiv [c(t) - c(t_0)]/c(t_0)$. Error bars represent 1 SD. $N = 3$ for each data point. **(e)** Lettuce in different conditions at $27\,\mathrm{d_{AE}}$. The range marked in grey is the specified harvest time, t_M, [range-units = single]3035AE [17]. Error bars represent 1 SD. $N = [5, 10]$ for each data point. Solid lines represent measurements; dotted lines are derived/calculated values

normal N condition was $1.33 \pm 0.79\,\mathrm{g_{DW}\,g_N^{-1}\,d^{-1}}$; under the deficient and excess conditions, it was 1.49 ± 0.99 and 1.90 ± 1.32, respectively. The average of $\dot{Y}_\mathrm{N}$ across all conditions is 1.47 ± 0.99. Empirical values in literature for $\dot{Y}_\mathrm{N}$ in other plants are on the order of 10^{-1} to 10^{0}, though it should be noted that these mostly describe woody plants [13]. $\dot{Y}_\mathrm{N}$ appears to decrease near the end of the exponential phase of growth.

The levels of nitrate and ammonia in the NSS reservoirs were measured from [range-units = single]240AE to determine uptake behavior. The relative change of the concentrations from the initial value is shown in Figure 7.4. Relative to the initial concentration, nitrate was depleted more quickly than ammonia in the excess and normal N conditions, while in the deficient condition it was depleted similarly to the ammonia. The depletion of nitrogen continued even as a number of plants were harvested and removed from the system every 5 days. By $32\,\mathrm{d_{AE}}$, the plants in the deficient condition had depleted almost all available nitrogen. Nonetheless, plants are able to effectively take up nitrogen even when its concentration is near zero [414].

Plant growth and development and depends largely on the available concentration of nitrogen in growth conditions, whether in soil or in soil-less hydroponic systems. The mineral nutrients are absorbed by plant roots and therefore their availability in the soil or hydroponic medium is critical for its absorption to maintain normal physiological processes[447].

Nitrogen plays an essential role in the structure of amino acids and N-bases; therefore its depletion in the growth medium may halt important physiological processes crucial for plant growth[10]. In general, a plant in N stress conditions exhibits symptoms such as stunted growth, yellowing of the leaves, leaf death, and reduction in chlorophyll production, and therefore ultimately contributes heavily to the reduction of overall crop yield[386]. Alternatively, an excess of N availability can also negatively affect plant growth parameters such as root and shoot biomass[447]. In lettuce, nitrogen stress conditions result in a slower growth rate and reduction in water content[480].

Recently, as an alternative to conventional soil production, growing lettuce hydroponically is a popular approach, especially in urban settings, uncultivated lands, and other constrained environments. Comparing key parameters in lettuce plants grown in the same nitrogen and environmental conditions in soil and hydroponics revealed no significant differences in morphological features except enhanced root growth in hydroponics[310]. Therefore, lettuce plants may exhibit comparable morphological features or biomass production in both soil and hydroponics given equal concentration of N, and the results presented here are expected to be applicable across different biomass production systems.

While the value of $\dot{Y}_\mathrm{N}$ was calculated from measured data and could simply be assumed to be a species-specific constant, a deterministic approach should be pursued. Ågren assumes its form is

$$\dot{Y}_\mathrm{N} = \alpha - \beta \frac{m_B}{m_\mathrm{N}} \tag{7.7}$$

where α is the leading term in $[\mathrm{g_{DW}\,d^{-1}\,g_N^{-1}}]$ and β is a correction term in $[\mathrm{d^{-1}}]$. Combining Equations 7.5 and 7.7:

$$\frac{1}{m_B}\frac{\mathrm{d}m_B}{\mathrm{d}t} = \alpha\frac{m_\mathrm{N}}{m_B} - \beta \tag{7.8}$$

we define in terms of the two parameters the relative growth rate (left hand side), which is the change in plant biomass per change in time, $\mathrm{d}m_B/\mathrm{d}t$ $[\mathrm{g_{FW}\,d^{-1}}]$, per plant biomass, m_B $[\mathrm{g_{FW}}]$, in units of $[\mathrm{d^{-1}}]$. Both parameters could be fitted to the empirical data, but a biochemical interpretation is preferred. Ågren presented one such quantity: the amount of nitrogen in the plant allocated for non-growth purposes, which may be described by $\beta m_B/\alpha$ (from Equation 7.8 rearranged)[13]. Building on NPT, Verkroost & Wassen described α as the product of the efficiency of formation of photosynthetic nitrogen from total plant nitrogen [unitless] and efficiency of biomass formation from photosynthetic nitrogen $[\mathrm{g_{DW}\,d^{-1}\,g_N^{-1}}]$ and β as the degradation rate of photosynthetic nitrogen $[\mathrm{d^{-1}}]$ [537]. Photosynthetic nitrogen refers to biologically active nitrogen in photosynthesis-involved enzymes. A fully deterministic model would also require modeling the nitrogen uptake rate of the plant, which is complicated by the plant's growth and dynamic response to the nature of its nitrogen supply in terms of quantities and molecular forms[247].

Methods

Nomenclature reformation considered chemical engineering conventions, IUPAC[220] and IUPAP documentation, and intuitive understanding. Variables and subscripts which refer to quantities are typeset in *italic*, while non-quantitative subscripts are in roman. Accent marks above variables are used to denote per time ($\dot{\square}$), per area ($\hat{\square}$), and per volume ($\breve{\square}$). Mnemonically, one might think of the breve above volumetric variables as a vessel to be filled, while the inverted breve above areal variables implies relation to the breve while perhaps reminding one of a surface.

The lettuce plants were grown in an environmentally controlled chamber with their roots immersed in the NSS liquid. The chamber is designed to produce consistent results. Whole plants were harvested and weighed, pooled by nitrogen condition, then frozen to −80 °C, followed by measurement of the nitrogen content via the Dumas method (AOAC 992.15)[https://www.medallionlabs.com/tests/protein-dumas/]. Nitrate concentration in the NSS was measured using a sensor (Horiba Scientific LAQUAtwin NO3-11). Ammonia concentration was determined by a spectrophotometric method adapted from Kempers & Kok[283].

Chapter 8

Case Study 3: Evaluating the cost of pharmaceutical purification in space

There are medical treatment vulnerabilities in longer-duration space missions present in the current International Space Station crew health care system with risks, arising from spaceflight-accelerated pharmaceutical degradation and resupply lag times. Bioregenerative life support systems may be a way to close this risk gap by leveraging *in situ* resource utilization (ISRU) to perform pharmaceutical synthesis and purification. Recent literature has begun to consider biological ISRU using microbes and plants as the basis for pharmaceutical life support technologies. However, there has not yet been a rigorous analysis of the processing and quality systems required to implement biologically produced pharmaceuticals for human medical treatment. In this work, we use the equivalent system mass (ESM) metric to evaluate pharmaceutical purification processing strategies for longer-duration space exploration missions. Monoclonal antibodies, representing a diverse therapeutic platform capable of treating multiple space-relevant disease states, were selected as the target products for this analysis. We investigate the ESM resource costs (mass, volume, power, cooling, and crew time) of an affinity-based capture step for monoclonal antibody purification as a test case within a manned Mars mission architecture. We compare six technologies (three biotic capture methods and three abiotic capture methods), optimize scheduling to minimize ESM for each technology, and perform scenario analysis to consider a range of input stream compositions and pharmaceutical demand. We also compare the base case ESM to scenarios of alternative mission configuration, equipment models, and technology reusability. Throughout the analyses, we identify key areas for development of pharmaceutical life support technology and improvement of the ESM framework for assessment of bioregenerative life support technologies.

The following chapter can also found here: M.J. McNulty, A.J. Berliner, P. Negulescu, L. McKee, O. Hart, K. Yates, A.P. Arkin, S. Nandi, and K.A. McDonald. **Evaluating the cost of pharmaceutical purification for a long-duration space exploration medical foundry**. *Frontiers in Microbiology.* (2021).
DOI: 10.3389/fmicb.2021.700863.

8.1 The need for a pharmaceutical foundry in space

Surveying missions to Mars, like the InSight lander (Overview | Mission – NASA's InSight Mars Lander) launched in 2018 and Perseverance rover in 2020, directly support the objectives of NASA's long-term Mars Exploration Program: an effort to explore the potential for life on Mars and prepare for human exploration of Mars. The maturation of the program requires redefining the risks to human health as mission architectures transition from the current 'Earth Reliant' paradigm used on the International Space Station (ISS) to the cislunar space 'Proving Grounds' and finally to deep-space 'Earth Independent' mission architectures, as defined in NASA's report titled, "Journey to Mars: Pioneering Next Steps in Space Exploration".

Human missions to Mars will be "Earth Independent", meaning there will be very limited emergency evacuation and re-supply capabilities along with substantially delayed communications with the Earth-based mission team. The NASA Human Research Roadmap currently rates most human health risks, which include 'risk of adverse health outcomes & decrements in performance due to inflight medical conditions' and 'risk of ineffective or toxic medications during long-duration exploration spaceflight', as either medium or high risk for a Mars planetary visit/habitat mission. Risk ratings are based on failure mode and effects analysis and on hazard analysis using dimensions of severity, occurrence, and detectability. A recent review highlights the current understanding of the primary hazards and health risks posed by deep space exploration as well as the six types of countermeasures: protective shielding, biological and environmental temporal monitoring, specialized workout equipment, cognition and psychological evaluations, autonomous health support, and personalized medicine[11].

Of these countermeasures, it could be argued that medicine is the most crucial and least advanced towards mitigating space health hazards. There is very limited information on, and few direct studies of, pharmaceutical usage, stability, and therapeutic efficacy (i.e., pharmacokinetics, pharmacodynamics) in spaceflight or in a Mars surface environment[53]. Furthermore, flown stores of pharmaceuticals face two additional barriers: (1) radiation-accelerated degradation[156], and (2) addressing a myriad of low occurrence and high impact health hazards without the ability to fly and maintain potency of therapeutics for all of them. In these circumstances, it is often more beneficial to build robustness to these low occurrence health hazards rather than to try to predict them. It is therefore imperative that on-planet and/or in-flight pharmaceutical production be developed to bridge this risk gap. These pharmaceutical foundry technologies will supplement, not replace, the flown pharmaceutical formulary designed to treat anticipated medical threats during space missions.

8.2 The bottleneck of space foundries: purification

Biopharmaceuticals must be purified after accumulation with the biological host organism, or cell-free transcription-translation reaction, in order to meet requirements for drug delivery and therapeutic effect[214]. The majority of commercial biopharmaceutical products are administered via intravenous and subcutaneous injection[493]. Biopharmaceutical formulations for injection requires high purity (>95%) product, as impurities introduced directly into the bloodstream can trigger significant immune responses and reduce efficacy[208].

Downstream processing of biopharmaceuticals is therefore usually a resource-intensive section of overall processing, being cited as high as 80% of production costs (and contributions of input mass) for monoclonal antibody (mAb) therapeutics produced using mammalian cell cultures[446, 64]. In addition to the processing burden for biopharmaceutical injectables, there are also often substantial storage costs involving complex supply chain and storage management with stability requirements for factors including temperature, time, humidity, light, and vibration[512]. There are several approaches being pursued to overcome the challenges and costs associated with downstream processing and formulation.

First are the tremendous efforts in process intensification[507]. While the highly sensitive nature of biopharmaceuticals to minor process changes has introduced barriers and complexities to innovation through process intensification that have not been realized in non-healthcare biotechnological industries, there have been significant strides made in the past decade in the areas of process integration[504], automation[433], and miniaturization[9, 121].

Another route that researchers are pursuing to reduce downstream processing costs and resources is a biological solution to processing technology. In the same vein that the biopharmaceutical industry sprung out of researchers leveraging the power of biology to produce therapeutically relevant molecules that were inaccessible or excessively costly by means of chemical synthesis, researchers are now also trying to apply that same principle to purifying therapeutically relevant molecules. The simplicity of production, reagents that can be produced using self-replicating organisms, and potential recyclability of spent consumables are significant advantages of biological purification technology for space or other limited resource applications. Examples of primary biological technologies include fusion tags[36, 36], stimuli-responsive biopolymers[488], hydrophobic nanoparticles[275], and plant virus nanoparticles[555, 528].

Lastly, there are vast efforts to establish alternative drug delivery modalities[18]. Other modalities that do not require injection and which might be more compatible to administration in limited resource environments, such as oral consumption, nasal spray, inhalation, and topical application, have long presented challenges in biopharmaceutical stability (e.g., denaturation in stomach acid) and delivery to the active site (e.g., passing the gut-blood barrier) that minimize product efficacy and necessitate costly advanced formulations and chemistries[381].

A particularly promising drug delivery technique to circumvent downstream processing burdens is to sequester the active pharmaceutical ingredient in the host cells of the upstream

production system as a protective encapsulation in order to facilitate bioavailability through oral delivery[297]. It represents an opportunity to greatly lower the cost of *in situ* production of human medicine for a space mission. This technique presumes that the host system is safe for human consumption, and so naturally lends itself to utility in systems such as yeast and plant production hosts. Oral delivery via host cell encapsulation has been recently established as commercial drug delivery modality with the US Food and Drug Administration approval of Palforzia as an oral peanut-protein immunotherapy[540]. However, this solution is not necessarily amenable to the diversity of pharmaceutical countermeasures that may be required, especially for unanticipated needs in which the product may not have been evaluated for oral bioavailability.

8.3 Space economics

In 2011, the space shuttle program was retired due to increasing costs, demonstrating that reduction of economic cost is critical for sustaining any campaign of human exploration[549]. Although recent efforts in reducing the launch cost to low earth orbit by commercial space companies have aided in the redefinition of the space economy[188], the barrier to longer term missions, such as a journey to Mars, is still limited by the extreme financial cost in transporting resources. Additionally, it has been shown that as the mission duration and complexity increases – as expected for a human mission to Mars – the quantity of supplies required to maintain crew health also increases[17]. In the case of meeting the demand for medication, biopharmaceutical synthesis has been proposed as an alternative to packaging a growing number of different medications[371, 367]. Assuming that both technologies can meet mission demand, selection of the production-based biotechnology platform will be dependent on its cost impact. It is therefore critical that the cost model of biopharmaceutical synthesis accounts for and minimizes the cost of any and all subprocesses, including those for purification.

The current terrestrial biopharmaceutical synthesis cost model does not align with the needs for space exploration environments. For example, the literature highlights the high cost of Protein A affinity chromatography resin ($8,000 – $15,000/L) and the need to reduce the price[357]. However, the purchase cost of chromatography resin is not nearly as critical in space environment applications where the major costs are more closely tied to the physical properties of the object (mass, volume, refrigeration requirements, etc.), as a result of fuel and payload limitations and the crew time required for operation[271]. The distinct cost models of space and terrestrial biopharmaceutical production may increase the burden of identifying space-relevant processing technologies and may also limit direct transferability of terrestrial technologies without attention given to these areas.

On the other hand, changing incentives structures relating to sustainability and the advent of new platform technologies are rapidly increasing alignment and the potential for technology crossover. For example, companies like On Demand Pharmaceuticals (ondemand-pharma.com), EQRx (eqrx.com), and the kenUP Foundation (kenup.eu), initiatives leading

to industry adoption of environmental footprint metrics such as E-factor[487]and Process Mass Intensity (PMI)[64], and diffusion from the adjacencies of green and white biotechnology[527] all promote development of accessible and sustainable technologies. As these trends pertain to space-relevant processes, these examples can also be viewed as driving more closed loop systems composed of simpler components.

Reference mission architecture

The evaluation of biopharmaceutical system cost for space applications requires the establishment of a reference mission architecture (RMA) as a means for describing the envelope of the mission scenario and distilling initial technology specifications which relate to the proposed subsystem in question[61]. This RMA can be used to orient and define the specific mission elements that meet the mission requirements and factor into the calculations of cost for deploying biopharmaceutical technologies. Ultimately, the RMA provides the means to determine and compare cost given specification of mission scenarios that utilize the technology in question. We envision developing and integrating biotechnological capabilities back-ended by purification and quality systems into standard methods composed of a series of unit procedures that maintain astronaut health via the Environmental Control and Life Support Systems (ECLSS)[221]. In this study, we begin to build towards this vision by proposing a high-level RMA that specifies a biopharmaceutical demand partially fulfilled through biomanufacturing over the course of a defined production window.

In planning for future human exploration missions, technology choices and life-support systems specifications are often evaluated through the metric of the equivalent system mass (ESM)[312]. Driven by the economic factor of cost in dollars required to transport mass into orbit, the ESM framework accounts for non-mass factors such as power, volume, and crew-time by relating them to mass through predetermined equivalency factors. ESM has been used to evaluate the mass of all of the resources of a larger system including water, shielding materials, agriculture and recycle loop closure. Currently, ESM remains the standard metric for evaluating advanced life support technology platforms[233, 581]. In the Space Systems Bioengineering context of realizing a biomanufactory on the surface of Mars[44], recent advances in extending this metric have been proposed in the form of extended equivalent system mass which attempts to address complexities stemming from multiple transit and operations stages, as would be required to support a crewed mission to Mars[41]. It also accounts for uncertainties inherent in mission planning such as technology failures and their downstream effects as propagated through a mission such as refrigeration failures in systems housing medicine that requires specific cooling. Such advances in the ESM framework aid in the assessment of biopharmaceutical technologies as elements in the context of proposed ECLSS given the inherent stochastic nature of human health, especially in a space environment[52]. Here, we calculate ESM at multiple mission segments across which biopharmaceutical purification is deployed.

8.4 Materials & Methods

Unit procedure selection

The medical significance of mAb therapies and the highly developed and specialized purification technology provide a fertile ground for techno-economic feasibility analysis of an ISRU-based pharmaceutical foundry for space. The first reason is that there are mAb therapies commercially approved or in development for multiple important disease states of spaceflight including osteoporosis[169], migraines/headaches[477], seizure[587], pneumonia[241], ocular herpes[294], otitis media[246], various oncological indications[582], and fungal infections[529]. A second reason is that degradation products of mAb therapies are known to result in, not just reduced efficacy, but also deleterious effects (e.g., harmful immune reactions in patients) that further compound concerns of pharmaceutical stability over a long-duration mission[303]. Thirdly is that a common manufacturing system can be used to produce treatments for a variety of indications which is highly advantageous in mass and volume savings for spaceflight. And fourthly, the economic incentive of research into mAb purification technology has resulted in a plethora of technologies, enabling this analysis to include head-to-head comparisons between multiple mAb capture steps of different origins

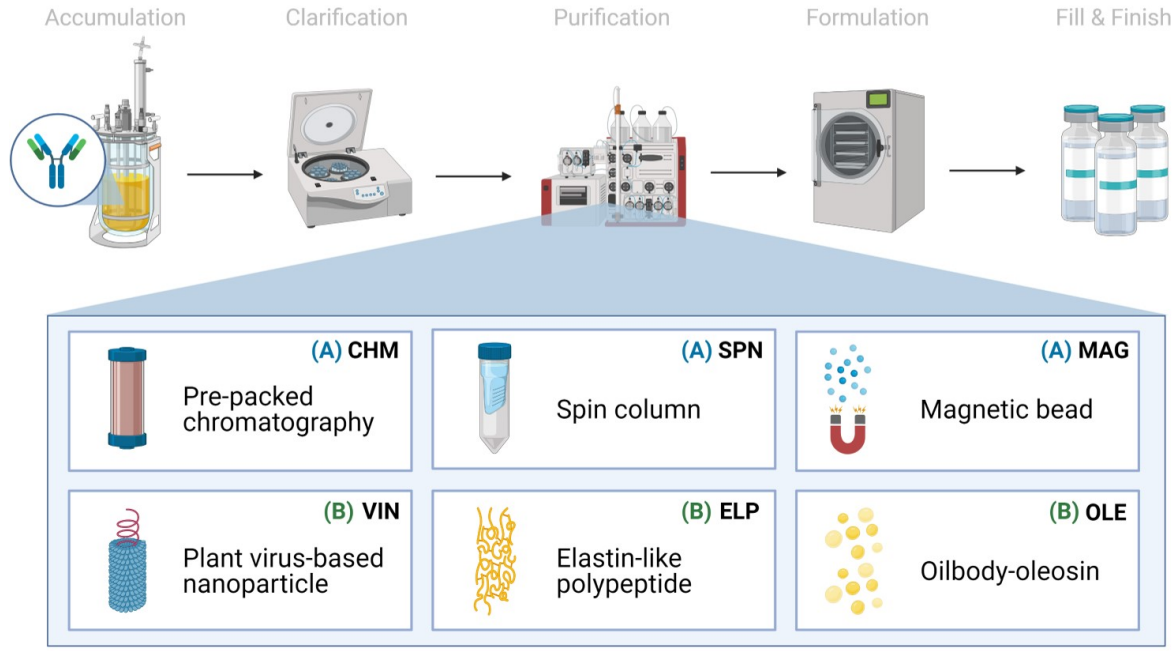

Figure 8.1: Monoclonal antibody production consists generically of product accumulation, clarification, initial purification, formulation, and fill & finish. Here we investigate six technologies for the capture step within the first purification step in a space mission context using extended equivalent system mass. The manufacturing origin of the capture reagent is denoted as either **(A)** abiotic or **(B)** biotic.

(e.g., biotic, abiotic) and different processing mechanisms (e.g., bind-and-elute mode liquid chromatography, precipitation). It is in comparing the differences between these technologies that we can uncover general insights into the desired components of a pharmaceutical foundry for space.

Monoclonal antibody therapy is a platform technology that supports human health across a diversity of medical indications with a generally maintained molecular structure, in large part due to the coupling of high target selectivity in the two small and highly variable complementarity-determining regions located in the antigen-binding fragments[195] and control of the biological action on that target (i.e., effector function) through the generally conserved fragment crystallizable (Fc) region[277]. This otherwise high structural fidelity conserved across mAb therapy products (which are primarily of the immunoglobulin G class) spans a wide variety of therapeutic indications and creates an opportunity for generic mAb production process flows, which include technologies devised specifically for mAb production[499]. This specialized manufacturing, which is most notable in the use of the affinity capture step targeting the Fc region of an antibody with the use of the protein-based ligands derived from the Staphylococcus aureus Protein A molecule, can be tuned for highly efficient purification of mAb and antibody-derived (e.g., Fc-fusion protein) class molecules[357]. Therefore, we have decided to investigate the Protein A-based affinity capture step in isolation as a starting point for understanding the costs of a potential pharmaceutical foundry in space.

It is worth noting that other similar protein ligands, such as Protein G and Protein L, are also widely used for their ability to capture different types of immunoglobulin classes and subclasses more efficiently[99].

We chose to analyze six Protein A-based capture step procedures: three commercially available abiotic technologies (pre-packed chromatography (CHM), spin column (SPN), magnetic bead (MAG)) and three development-stage biotic technologies (plant virus-based nanoparticle (VIN), elastin-like polypeptide (ELP), and oilbody-oleosin (OLE)) (Fig. 8.1). Commercial technology procedures are based on product handbooks while the procedures of developing technologies, which we would classify as Technology Readiness Level 2 per NASA's guidelines, are based on reports in literature. This set of procedures was selected to survey a wide range of operational modalities, technological chassis, and perceived advantages and disadvantages (Table 8.1).

All six of the unit procedures are operated in bind-and-elute mode, in which a clarified mAb-containing liquid stream is fed into a capture step containing Protein A-based ligand, which selectively binds the mAb and separates the mAb from the bulk feed stream. The mAb is eluted from the Protein A-based ligand and recovered using a low pH buffer to dissociate the mAb from the ligand. Finally, the low pH environment of the recovered mAb is pH neutralized for future processing or storage. The analysis does not consider differences in mAb processing upstream or downstream of the affinity capture step that may arise from differences in the unit procedure operations.

CHM is a chromatography system consisting of a liquid sample mobile phase which is pumped through a pre-packed bed of Protein A-fused resin beads housed in a column. SPN is

a similar system, in which a Protein A-fused resin bead bed has been pre-packed into a plastic tube housing and the mobile phase flow is controlled via centrifugation of the plastic tube. MAG is a slurry-based magnetic separation system that uses superparamagnetic particles coated with Protein A-fused resin mixed as a slurry with the feed mAb stream for capture and elution of the mAb by magnet. VIN is a sedimentation-based system that uses plant virion-based chassis fused with Protein A-based ligands in suspension for capture of the mAb and centrifugation, assisted by the sedimentation velocity contribution of the chassis, to isolate and elute the mAb. ELP is a precipitation-based system that uses stimuli-responsive biopolymers fused with Protein A-based ligands in suspension for capture of the mAb and external stimuli (e.g., temperature, salt) to precipitate the bound complex and elute the mAb. OLE is a liquid-liquid partitioning system that uses oil phase segregating oleosin proteins fused with Protein A-based ligands to capture mAb in the oil phase and then elute the mAb into a clean aqueous phase.

Techno-economic evaluation

Techno-economic evaluations are performed using the recently proposed equations for ESM that include calculation of costs at each mission segment[41]. Equivalent system mass (ESM)

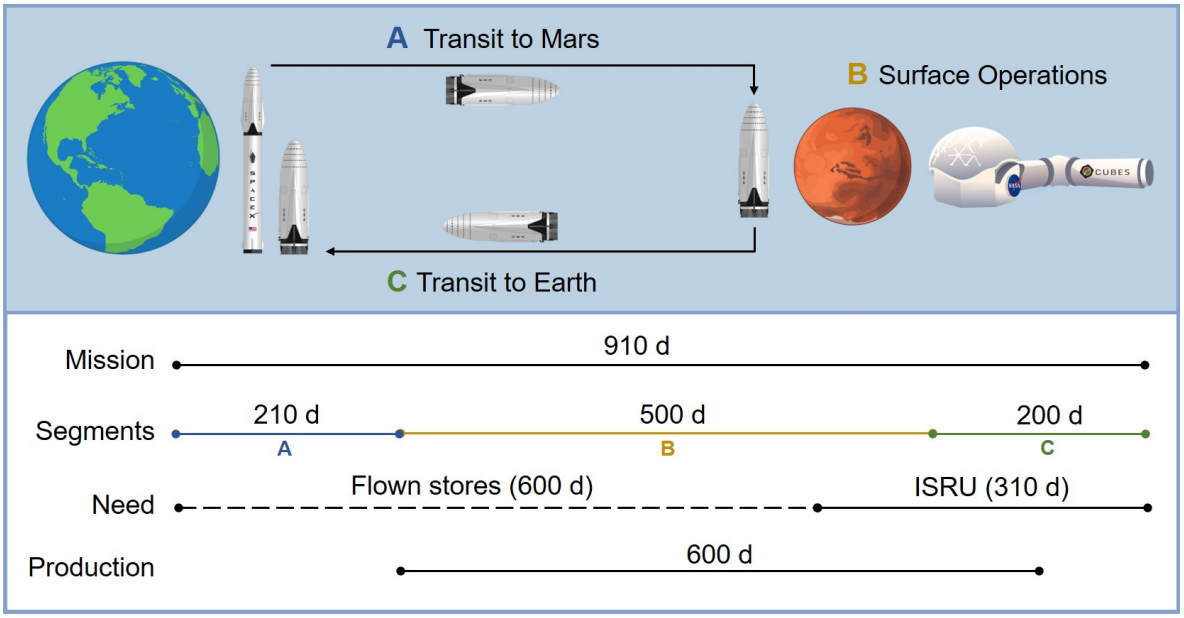

Figure 8.2: An illustration of the reference mission architecture in which **(A)** a crewed ship is launched from the surface of Earth and lands on Mars and **(B)** assembles a pre-deployed habitat on the Martian surface to perform operations before **(C)** a return transit to Earth on the same ship. Pharmaceutical needs are supported by flown stores until partway through surface operations, at which point needs are met by pharmaceuticals produced using *in situ* resource utilization. Production is initiated prior to the need window to ensure adequate stocks are generated by the time it is needed. Rocket artwork adapted from Musk, 2017[394]. Habitat artwork by Davian Ho.

for the mission M_0 is defined as

ENTER LATER

The mission timeline depicted in Figure 8.2 provides insight into the proposed RMA and downstream crew needs and mAb production horizon. Here we assume a total mission duration of 910 days. First, a crew of 6 will travel from Earth to low Earth orbit, then board an interplanetary craft for a 210-day journey to Martian orbit, where the crew will descend to the surface in a separate craft, allowing the large transit vehicle to remain in orbit. Once on Mars, the crew will perform surface operations for 600 days. Following surface operations, the crew will leave Mars in a fueled ascent craft, board the interplanetary vehicle, and return to Earth orbit in 200 days. The mission timeline, crew size, and ESM equivalency factors are consistent with the recent RMA presented for inclusion of biomanufacturing elements[44].

The mission demand for mAb therapies is assumed to be 30,000 mg over the entirety of the mission (supporting logic detailed in Supplementary Information, Table S10). Pharmaceutical stores and production resources are assumed to be flown with the crew transit (no pre-deployment in order to maximize shelf-life). We assume that the production resources are stable throughout the mission duration. We conservatively assume (in the face of insufficient spaceflight stability data for biologics for a more refined estimate) that the first 600 days of pharmaceutical demand will be met through flown stores (20,000 mg), at which point pharmaceutical ISRU manufacturing is needed (10,000 mg) to alleviate the impact of accelerated pharmaceutical degradation and provide supplementary medication. The pharmaceutical production window opens prior to the ISRU demand timeframe and persists through a portion of the return transit (up to mission day 810) to reflect the expected life support advantage of maintaining capabilities to counter unanticipated needs or threats. We assume that the Protein A-based unit procedures consistently yield 98% recovery of mAb from the input stream.

Unit Procedure Selection

Deterministic models for each unit procedure were developed in Microsoft Excel using reference protocols cited in Table 8.1 as a series of executable operations, each containing a set of inputs defined by cost categories (labor, equipment, raw materials, consumables) that are correspondingly populated with characteristic ESM constituent (mass, volume, power, cooling, labor time) values (model composition illustrated in Supplementary Information, Figure S14). Unit procedures have been defined as the smallest single execution (i.e., unit) of the secondary purification capture step procedure according to the reference protocol. We define the unit capacity by volume according to the equipment and consumables used (e.g., 2 mL maximum working volume in a 2 mL tube) and by mAb quantity according to the binding capacity for the given method (e.g., 1 mg mAb/mL resin) (Supplementary Information, Table S11). Unit procedures with no explicit working volume constraints (i.e., the liquid solution volume for biotic technologies) have been defined with a maximum unit volume of 2 mL. ESM-relevant characteristics of individual inputs (e.g., equilibration buffer,

2 mL tube) are defined based on publicly available values, direct measurements taken, and assumptions (which are explicitly identified in the spreadsheet).

Unit Procedure ID	Method	Technology Used	Reference
Pre-packed chromatography[A]	Liquid chromatography	Pre-packed HiTrap MabSelect SuRe column of novel alkali-tolerant recombinant Protein A-based ligand coupled with an agarose matrix	Vendor handbooks
Spin column[A]	Centrifuge-assisted liquid chromatography	Pre-packed Protein A HP SpinTrap spin column containing Protein A Sepharose High Performance	
Magnetic bead[A]	Magnetic separation	Protein A Mag Sepharose superparamagnetic beads coupled with native Protein A ligands	
Plant virus-based nanoparticle[B]	Sedimentation complex	Plant virion, Turnip vein clearing virus, presenting a C-terminal coat protein fusion display of Protein A (domains D & E)	Werner *et al.* 2006[555]
Elastin-like polypeptide[B]	Inverse transition cycle	Elastin-like polypeptides (78 pentapeptide (VPGVG) repeats) fused with Z domain, an engineered B domain of Protein A	Sheth *et al.* 2014[488]
Oilbody-oleosin[B]	Liquid-liquid partition	*Arabidopsis oleosin* fused at the N-terminal with an engineered Protein A(5)	McLean *et al.* 2012[363]

Table 8.1: List of Protein A-based monoclonal antibody capture step unit procedures included for analysis. [A] abiotic technology; [B] biotic technology

There are several model features that we have considered and decided not to include within the scope of analysis. Packing and containers for the inputs are not included for three reasons: 1) the contributions of the container are considered negligible as compared to the input itself (e.g., container holding 1 L buffer as compared to the 1 L of liquid buffer); 2) materials flown to space are often re-packaged with special considerations (Wotring, 2018); and 3) the selection of optimal container size is non-trivial and may risk obscuring more relevant ESM findings if not chosen carefully. We do not consider buffer preparation and assume the use of flown ready-to-use buffers and solutions. Furthermore, refrigeration costs of the input materials and costs that may be associated with establishing and maintaining a sterile operating environment (e.g., biosafety cabinet, 70% ethanol in spray bottles) are expected to be comparable between unit procedures and not considered. Impacts of microgravity on unit procedure execution are not considered for the return transit production. Refrigeration costs associated with low temperature equipment operation (e.g., centrifugation at 4°C) are included in the equipment power costs.

Inputs common across unit procedures are standardized (Supplementary Information, Table S11). One operational standardization is the inclusion of pH neutralization of the product stream following the low pH elution mechanism, which was explicitly stated in some procedures while not in others. Input quantities are scaled from a single unit to determine the

number of units required to meet the reference mission architecture specifications. The ESM constituent inputs (mass, volume, power, cooling, labor time) are converted into equivalent mass values using RMA equivalency factors (Supplementary Information, Table S13).

8.5 Results & Discussion

Standardization of manufacturing efficiency

Given the limited granularity of the presented reference mission architecture, which was scoped as such to reflect the lack of literature presenting an overarching and validated Concept of Operations for a Transit to Mars[19], we do not define strict manufacturing scheduling criteria for pharmaceutical production. Construction of a detailed pharmaceutical production RMA is hindered by uncertainty in the number and identity of mAb therapy products that would be included within mission scope, the decay rate of mAb therapy stores in the mission environments, and a reasonable basis for building robustness to unanticipated disease states. Rather, we choose to establish an objective comparison between unit procedures by normalizing for scheduling-associated manufacturing efficiencies. We accomplish this by first identifying the number of batches per mission (and thus batch size) needed to meet the mAb demand (base case of 10,204 mg mAb feed assuming 98% recovery) that minimizes the ESM output for a given unit procedure, and then running the simulation of pharmaceutical production at that number of mission batches, as shown in Figure 8.3a and tabulated in Supplementary Information, Table S14.

In Figure 8.3b – e, we visualize a deconstruction of ESM output, using the VIN unit procedure as an example, by key performance metrics that vary with a scheduling dependence in order to illustrate the significance of batch optimization in unit procedure comparison. The processing of a given batch volume and mAb quantity is allocated into a number of units, as determined by the volume and mAb quantity constraints of a given unit procedure, and a number of use cycles per batch, as determined by the capacity of the equipment specified in the given unit procedure. We show how the variation in ESM output over the number of mission batches maps to extent of unit vacancy or underutilization (Figure 8.3b), extent of operational equipment (e.g., centrifuge) vacancy or underutilization (Figure 8.3c), and number of required use cycles (Figure 8.3d). We also show an oscillatory behavior in the scheduling (i.e., total mAb purified per mission, % purified at surface operations) that quickly dampens as number of mission batches increases (Figure 8.3e). This behavior is a result of the assumption that the mAb feed stream is coming from a discrete upstream production batch (e.g., batch-mode bioreactor) that does not output partial batch quantities, as opposed to a continuous upstream production for which there are no defined batches. Accordingly, partial batch needs are met by the processing of a full batch.

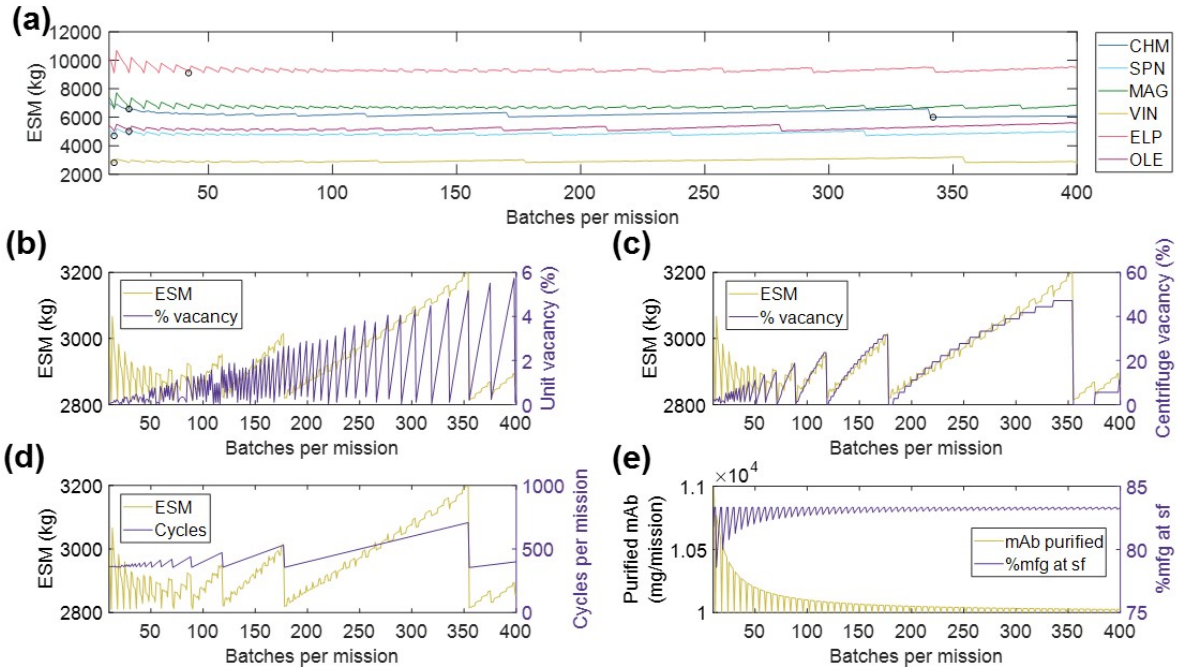

Figure 8.3: **(A)** Scheduling optimization for the establishment of base case scenarios for each unit procedure. The value for number of batches corresponding to the minimum equivalent system mass for each unit procedure, as indicated by black circle markers. Key operational parameters impacted by mission scheduling (shown using the VIN procedure) include **(B)** unit underutilization or vacancy, **(C)** equipment underutilization or vacancy, in this case represented by the centrifuge as the bottleneck, **(D)** the number of use cycles, and **(E)** the total quantity of monoclonal antibody (mAb) per mission and per surface operation (sf). CHM, pre-packed chromatography; SPN, spin column; MAG, magnetic bead; VIN, plant virus-based nanoparticle; ELP, elastin-like polypeptide; OLE, oilbody-oleosin.

Base case scenario

The ESM and output metrics of the base case scenario (10,000 mg mAb demand, 1 mg mAb/mL feed concentration, 98% recovery) for each of the six unit procedures are shown in Figure 8.4a-f. From this viewpoint of an ESM output for an isolated unit procedure outside the context of a full purification scheme, the ESM ranked from lowest to highest are VIN < SPN < OLE < CHM < MAG < OLE. However, we reason that it is more important to understand the model inputs that influence the ESM output rankings than to use the rankings in this isolated subsystem analysis to make technology selection choices, which requires the context of a full pharmaceutical foundry and of linkages to other mission elements.

We observe that mass costs are generally the primary contributor to ESM output, except for the MAG and ELP procedures in which labor time costs are larger. The mass costs are not closely associated to any given cost category across unit procedures, but rather the breakdown of mass costs varies widely by unit procedure.

Power costs (kW) are disproportionately high given that the static nature of ESM assumes constant usage, and thus energy (kWh) in this context (i.e., the power supply to the

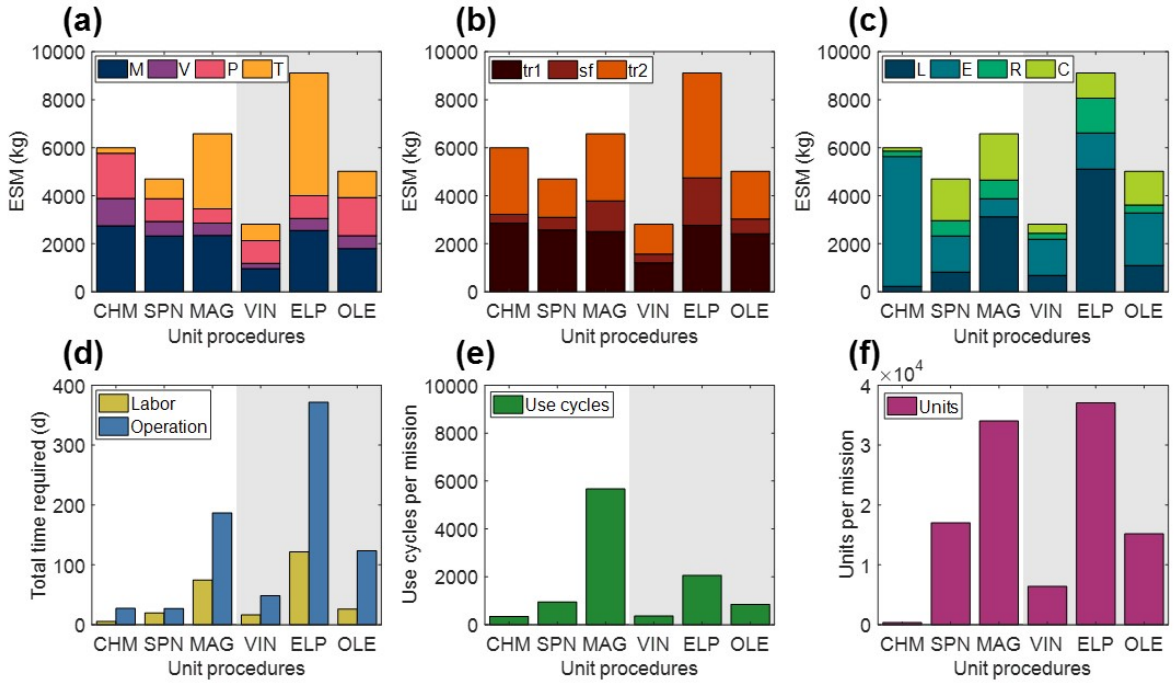

Figure 8.4: Base case equivalent system mass results broken down by **(A)** mass (M), volume (V), power (P), and labor time (T) constituents, **(B)** transit to Mars (tr_1), surface operations (sf), and return transit (tr2) mission segments, and **(C)** labor (L), equipment (E), raw materials (R), and consumables (C) cost category for the six tested Protein A-based monoclonal antibody affinity capture step unit procedures segregated by abiotic (white background) and biotic (grey background) technologies. Also shown are the **(D)** labor and operation times, **(E)** number of use cycles, and **(F)** number of units required for each unit procedure to meet the reference mission demand. CHM, pre-packed chromatography; SPN, spin column; MAG, magnetic bead; VIN, plant virus-based nanoparticle; ELP, elastin-like polypeptide; OLE, oilbody-oleosin.

equipment is not turned off in this analysis). These costs represent an upper bound assuming that the power supply system capacity is sized to support a maximal power consumption in which all power-drawing elements are simultaneously in operation. Time of power usage as a fraction of duration are as follows: CHM (99%) > MAG (78%) > ELP (48%) > SPN (45%) > OLE (42%) > VIN (30%). The lower use fraction unit procedures are therefore paying a relatively higher cost per unit power demand in this current method. The electrical needs of the equipment used by the unit procedures are within NASA-proposed Mars mission RMA bounds, with energy use across all unit procedures would peak at ∼1% of a proposed Mars transfer vehicle electric capacity (50 kWe) or ∼5% of the habitat capacity (12 kWe) of a reference stationary surface nuclear fission power reactor[147].

The mission segment breakdown of ESM illustrates the relatively high costs of pharmaceutical manufacturing capabilities for transit, even for the transit to Mars (tr_1) in which there is no actual production taking place. There is a strong economic incentive to limit the amount of supplies flown on tr_1. Alternatives such as the pre-deployment of reagents and consumables and limiting of production to surface operations on Mars (which has lower

RMA equivalency factors for mass and volume than transit operations) must be balanced against the risk to human health posed by removing pharmaceutical production capabilities from a mission segment and potentially exposing the supplies to longer storage times that could challenge shelf lives.

Labor and operation times are important parameters in the broader mission and pharmaceutical foundry context. These unit procedures represent a single step of pharmaceutical production, which if realized in a space mission context, would, in turn, need to be a small portion of a crew member's time allocation. Assuming 40-hour work weeks for crew members, the labor time spans a range of ∼1% (CHM) to ∼14% (ELP) of the available crew time over the 600-day production window. It is not feasible to operationalize with such high labor and operation times at this scale of production, particularly as they stand for MAG and ELP. While strategies such as batch staggering and concurrency can be used to reduce durations, advanced automation will almost certainly need to be built into the core of a pharmaceutical foundry.

A prevailing trend throughout the unit procedures is that the number of unit executions and use cycles required by a given unit procedure are positive correlated with the ESM output value, except for the equipment cost-dominant and higher unit capacity CHM procedure. The equipment modeled in the analysis for CHM and the other unit procedures are almost certainly not space-ready and could be further designed to reduce mass and volume and increase automation to reduce crew labor time. The increased equipment costs in the CHM procedure are primarily due to automation and monitoring hardware for running liquid chromatography, which is reflected in the minimal labor costs of the CHM procedure. Miniaturization efforts, such as those focusing on microfluidic systems [Millet et al., 2015; Rodríguez-Ruiz et al., 2018; Murphy et al., 2019], are emerging as a potential path towards mitigating the high equipment costs associated with highly automated and tightly controlled manufacturing, which are crucial for freeing up valuable crew time.

The number of unit executions is determined by the binding capacity of the technology and the nominal unit size. This indicates that the unit capacity for purification is an important consideration and influential factor. Unit sizing is an important consideration that is valuable to assess more holistically within the broader pharmaceutical production and mission context.

The number of use cycles is determined by the number of unit executions required and by the maximal unit capacity of the equipment items (e.g., if you presume that an 18-slot centrifuge is the equipment bottleneck then the effective number of batches is the number of units required divided by 18). Therefore, it can be understood that the equipment unit capacity is a critical parameter in tuning the number of use cycles and, by extension, the labor costs. For processes with lower labor costs, due to the intrinsic nature of the procedure or through automation of labor, equipment unit capacity will still influence the total duration and production throughout. The MAG and ELP procedures yield both high labor and duration times and are thus particularly sensitive to the equipment capacity.

Contextualizing ESM with supporting evaluations

Having acknowledged shortcomings of ESM as a decision-making tool for comparison of alternative approaches in isolated subsystems, we propose that supplementary evaluations can assist in contextualization. A primary gap of an isolated subsystem ESM analysis is a lack of information on the holistic usefulness or cost of a given employed resource, which could include its synergy with other mission subsystems and its extent of recyclability, or waste loop closure, within the mission context. For example, the isolated subsystem analysis does not capture information on the broad applicability that a centrifuge might have for use in other scientific endeavors, nor do the ESM outputs reflect the > 93% recyclability of water achieved by the recycler on the ISS (Steven Siceloff, 2008) that may be generalizable to future missions.

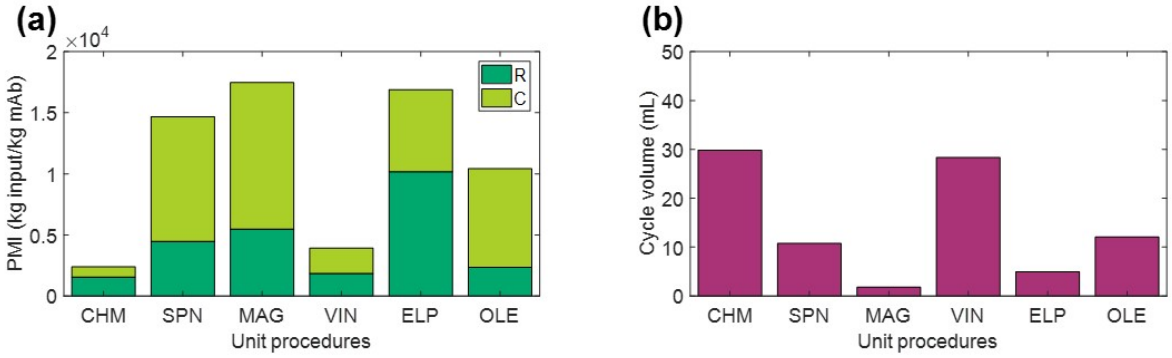

Figure 8.5: **(A)** Process mass intensity (PMI) evaluation of the unit procedures broken down by raw materials (R) and consumables (C) contributions. **(B)** Cycle volume for each unit procedure. CHM, pre-packed chromatography; SPN, spin column; MAG, magnetic bead; VIN, plant virus-based nanoparticle; ELP, elastin-like polypeptide; OLE, oilbody-oleosin.

The use of environmental footprint metrics, such as PMI, may be one valuable step towards capturing missed information on recyclability. PMI is a simple metric of material efficiency defined as the mass of raw materials and consumables required to produce 1 kg of active pharmaceutical ingredient. The study by Budzinski *et al.* introducing PMI for biopharmaceuticals presents data from 6 firms using small-scale (2,000 - 5,000 L reactor) and large-scale (12,000 - 20,000 L reactor) mAb manufacturing operations, finding an average 7,700 kg of input is required to produce 1 kg of mAb[64]. Figure 8.5a presents PMI evaluation for the six capture steps included in analysis, which result in PMI outputs as low as 2,390 kg of input (CHM) and as high as 17,450 kg of input (MAG) per 1 kg of mAb. A comparison of these outputs to those of Budzinski *et al.* indicates that we may be observing roughly similar values after accounting for the high cost of initial purification in the study, representing ∼60% of the total PMI reported, the elevated feed mAb concentration (i.e., cell culture titer) of $1 - 5.5$ g mAb/L, and adjustments for economies of scale when operating at such low cycle volumes (Figure 8.5b). Consumable costs appear to be the most sensitive to scale, which represents ∼1% total PMI on average in the values reported by Budzinski *et al.* and ranges

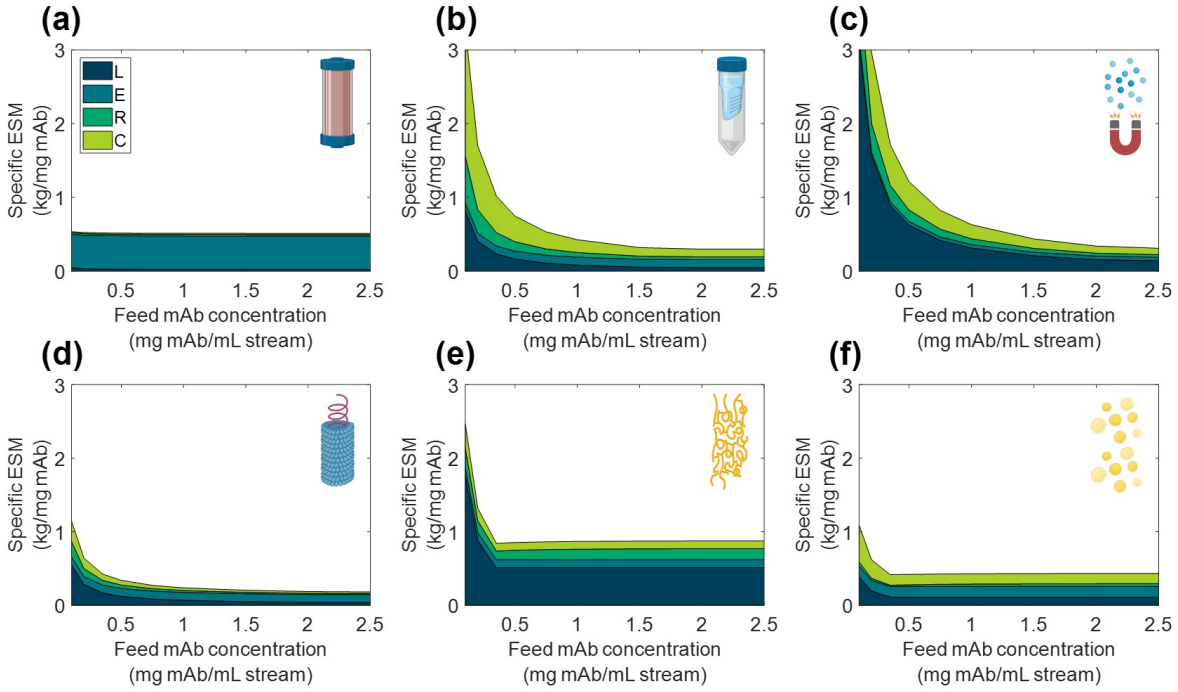

Figure 8.6: Specific equivalent system mass (per unit mass monoclonal antibody produced) broken down by labor (L), equipment (E), raw materials (R), and consumables (C) cost categories as a function of feed monoclonal antibody (mAb) concentration for **(A)** CHM, **(B)** SPN, **(C)** MAG, **(D)** VIN, **(E)** ELP, and **(F)** OLE. CHM, pre-packed chromatography; SPN, spin column; MAG, magnetic bead; VIN, plant virus-based nanoparticle; ELP, elastin-like polypeptide; OLE, oilbody-oleosin.

from 35% (CHM) to 77% (OLE) here. Budzinski *et al.* also go one step further to distinguish water as a separate category from raw materials and report that >90% of the mass is due to water use. Here we assume pre-made buffers and do not directly add water in this study, so we refrain from a similar calculation, but it is worth noting that the extent of water use may also serve as a reasonable starting surrogate for extent of achievable recyclability in a space mission context.

Scenario analysis

We analyzed the specific ESM output broken down by cost category for the six unit procedures over a range of input stream mAb concentrations (Figure 8.6) and mission demand for mAb (Figure 8.7). Specific ESM, termed cost of goods sold in traditional manufacturing analyses, is the ESM output required to produce 1 mg mAb. This is used in the scenario analyses to normalize ESM output across variation in mission demand for mAb. The optimal number of batches per mission was found and used for each unit procedure and scenario tested (Supplementary Information, Tables S16 – S17).

We observe the general and expected trends that specific ESM decreases with an in-

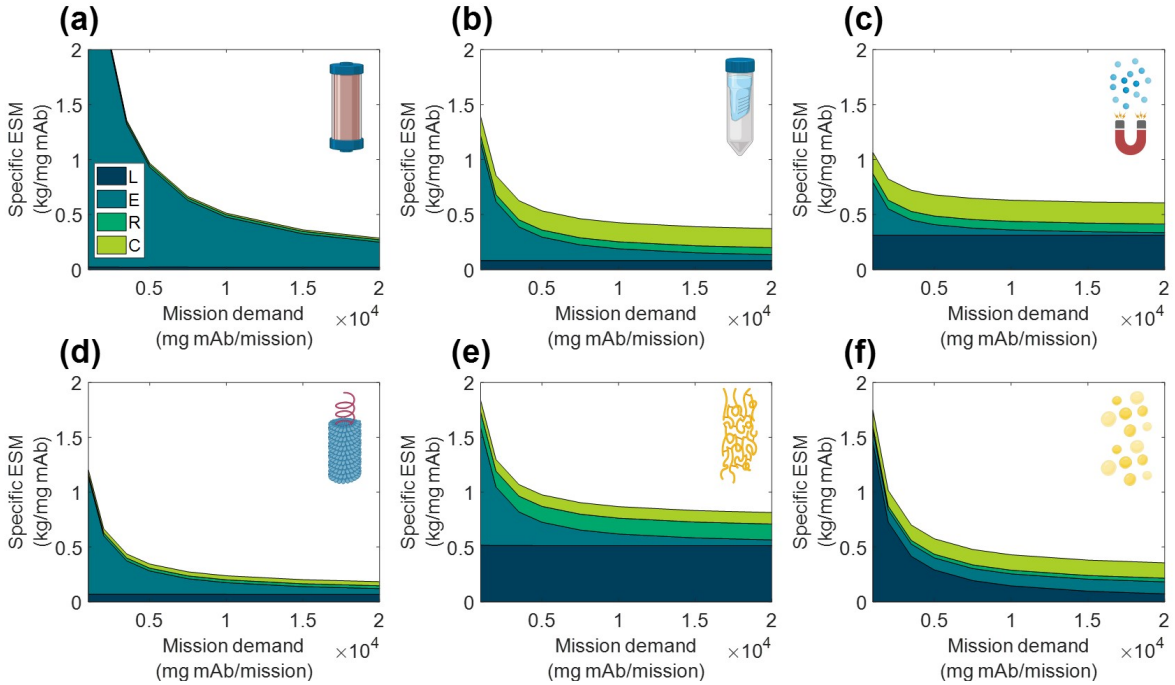

Figure 8.7: Specific equivalent system mass (per unit mass monoclonal antibody produced) broken down by labor (L), equipment (E), raw materials (R), and consumables (C) cost categories as a function of mission production demand for monoclonal antibody for **(A)** CHM, **(B)** SPN, **(C)** MAG, **(D)** VIN, **(E)** ELP, and **(F)** OLE. CHM, pre-packed chromatography; SPN, spin column; MAG, magnetic bead; VIN, plant virus-based nanoparticle; ELP, elastin-like polypeptide; OLE, oilbody-oleosin.

creasing feed stream mAb concentration and mission demand. The CHM procedure exhibits notably limited sensitivity to feed stream mAb concentration, which can be attributed to the equipment-dominated cost profile, fixed column size, and nature of the governing reference protocol that does not specify restrictions on sample load volume. Depending on the pre-treatment of the feed stream, it may be more reasonable to impose constraints on the sample load volume. In contrast, the specific ESM output of the CHM procedure is the most sensitive to mission mAb demand with higher demand increasingly offsetting the fixed capital costs. The CHM procedure is also the largest capacity unit modeled in the analysis (i.e., CHM capacity is 30 mg mAb/unit as compared to 2.7 mg mAb/unit for MAG, the next highest capacity unit) and is accordingly expected to scale well with demand.

The SPN, ELP, OLE procedures exhibit behaviors in which the specific ESM output abruptly plateaus with an increasing feed stream mAb concentration. This observation can be attributed to the unit procedure operating in a mAb binding capacity-limited regime (as opposed to volume-limited for more dilute feeds) which also then controls and maintains unit procedure throughput (e.g., the ELP number of units, 37,044, and use cycles per mission, 2,058, is constant at and above 0.35 mg mAb/mL input stream concentration). This can be de-bottlenecked via technology (e.g., improved chemistry of the capture step unit leading to

higher binding capacity) or methodology (e.g., increased concentration of the capture step unit leading to higher binding capacity) improvements.

Low demand scenarios are particularly relevant for examination in a space health context, as small capacity redundant and emergency utility is a likely proving ground for inclusion of a space pharmaceutical foundry. At the lower boundary of the tested range (1,000 mg mAb/mission), we see the ESM outputs from lowest to highest are re-ordered as MAG < VIN < SPN < OLE < ELP < CHM. Minimization of equipment costs are particularly important in this regime, and it is observed that, indeed, the ESM output near completely aligned with the ranking of equipment cost (MAG < VIN < SPN < ELP < OLE < CHM). It is likely that other non-ESM factors such as integration with other flown elements will understandably influence the design and composition of early and low capacity flown pharmaceutical foundries.

Alternate scenarios and mission configurations

We explored variations to the base case RMA for all six unit procedures including scenarios in which the pharmaceutical manufacturing resources are shipped prior to the crew in pre-deployment, (+)pd, the production window has been truncated to close with the end of surface operations, (-)tr_2, and a combination of the two prior modifications, (+)pd (-)tr_2 (Figure 8.8). Costs of pre-deployment are included in the analyses and mission demand is kept constant regardless of the production window.

In all cases the ESM totals were reduced from the base case. Additionally, the general trend held that (-)tr2 scenario resulted in lower ESM totals than (+)pd scenario except for SPN, in which the increased raw material and consumable costs of (-)tr2 were sufficiently large to outweigh the reduction in equipment and labor costs of (+)pd. The combination (+)pd (-)tr2 scenario resulted in the lowest ESM totals at a fraction of the base case (as high as 39% reduction in SPN and as low as 21% reduction in ELP).

Equipment & unit throughput

Acknowledging the significance of the equipment capacity on ESM output, we further explored this contribution by comparing the base case ESM output of the centrifuge-utilizing procedures (SPN, VIN, ELP, OLE) to that resulting from the use of alternative centrifuge models (Supplementary Information, Table S18). This effectively results in a trade of equipment costs and batch throughput. The optimal number of batches per mission was found and used for each unit procedure and interval tested (Supplementary Information, Table S19).

We observe in Figure 8.9 that the ESM values increased with the size of the centrifuge model, 12-slot < 18-slot (base) < 48-slot. The labor and consumables savings of higher batch throughput were outweighed by the higher equipment costs (including higher power costs). Operation duration is an important metric relevant to a pharmaceutical foundry that is not well reflected in ESM that is also impacted by this alternative scenario. The exception to

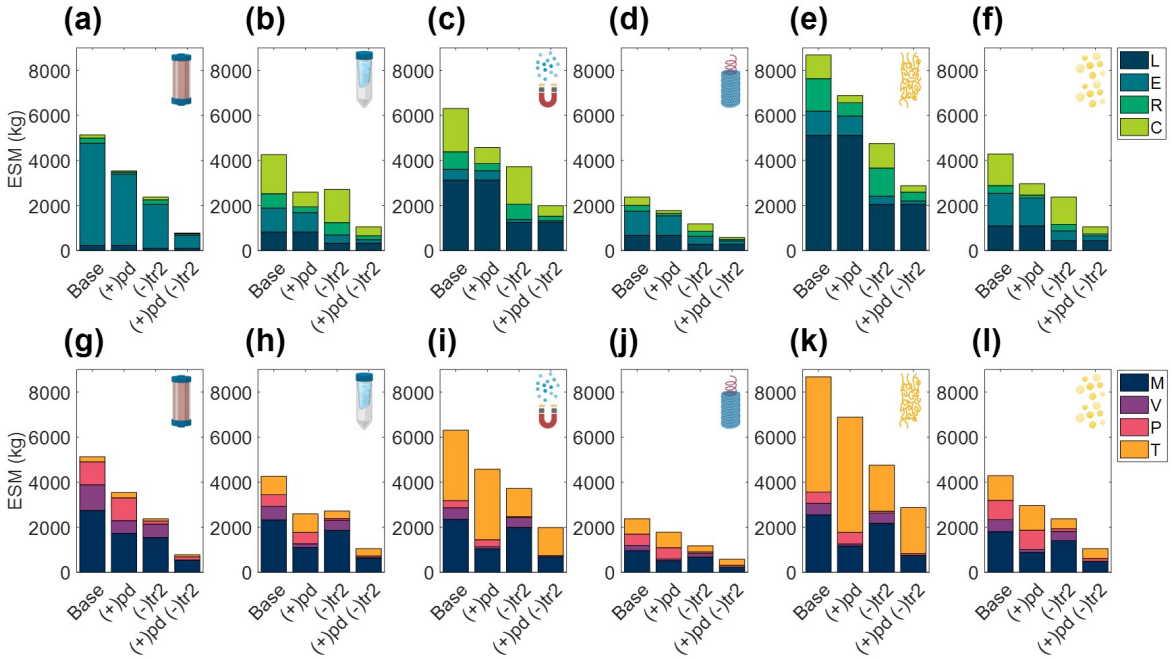

Figure 8.8: Evaluation of extended equivalent system mass values in various mission configurations broken down by labor (L), equipment (E), raw materials (R), and consumables (C) cost categories cost category and mass (M), volume (V), power (P), and labor time (T) constituents for CHM, **(A, G)**, SPN, **(B, H)**, MAG, **(C, I)**, VIN, **(D, J)**, ELP **(E, K)**, and OLE, **(F, L)**. Configurations include the base case scenario of manufacturing resources flown with the crew for pharmaceutical production on the surface and return transit (Base), and alternatives in which the manufacturing resources are flown prior to the crew in pre-deployment, (+)pd, the production window is limited to surface operations, (-)tr_2, and a combination of the two previously stated alternatives, (+)pd (-)tr_2. CHM, pre-packed chromatography; SPN, spin column; MAG, magnetic bead; VIN, plant virus-based nanoparticle; ELP, elastin-like polypeptide; OLE, oilbody-oleosin.

this trend is the 48-slot condition for the ELP procedure, in which a lower consumable cost related to the number of use cycles per mission (i.e., pipette tips, tubes, gloves) sufficiently lowered the total ESM below the 18-slot condition.

Technology reusability

The number of use cycles for liquid chromatography resins is an important economic parameter in commercial pharmaceutical manufacturing[425]. Here we explore the impact of use cycles on the CHM and ELP procedures in a space mission context, looking at no reuse nor regeneration operation of the purification technology, (-)Reuse, and at an increased number of use cycles, (+)Reuse (Figure 8.10).

We observe that the terrestrial importance of use cycles does not prevail in this isolated ESM evaluation in a space context. The high purchase costs of resin are not considered in ESM and the impact of the reuse cycles is reduced to the mass and volume savings of the pre-packed column consumable. There is a minor decrease in ESM of the (+)Reuse

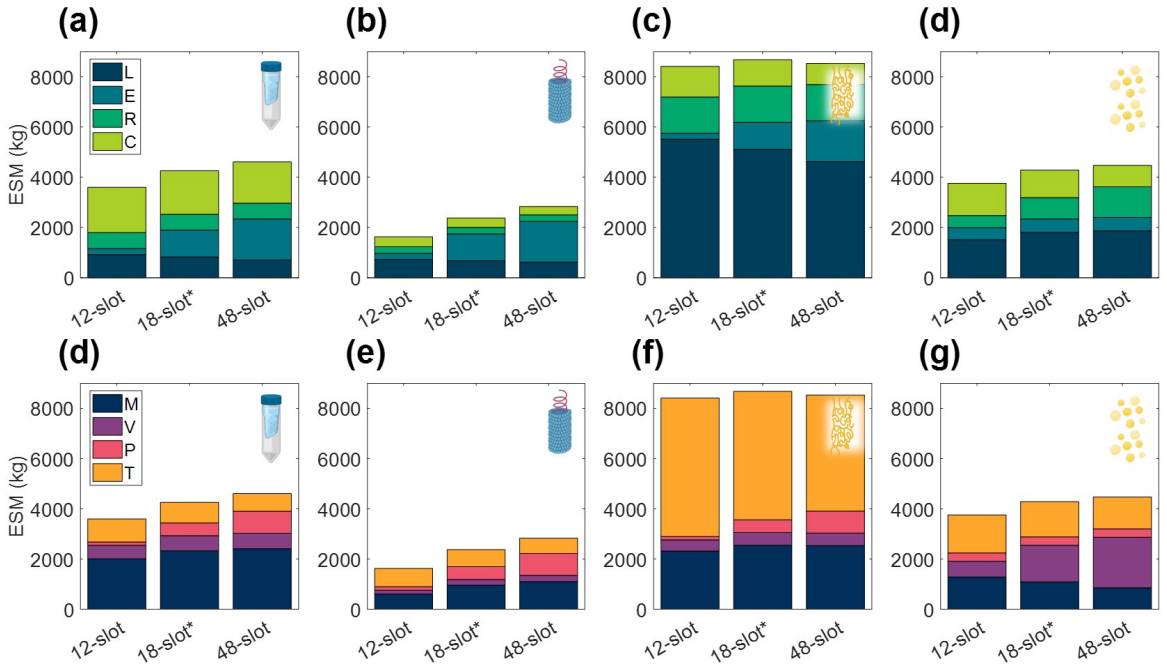

Figure 8.9: Changes in extended equivalent system mass values with different capacity centrifuge models broken down by labor (L), equipment (E), raw materials (R), and consumables (C) cost categories and mass (M), volume (V), power (P), and labor time (T) constituents for SPN **(A, E)**, VIN **(B, F)**, ELP **(C, G)**, and OLE **(D, H)**. SPN, spin column; VIN, plant virus-based nanoparticle; ELP, elastin-like polypeptide; OLE, oilbody-oleosin.

over the base case scenario, but both of these result in substantially higher ESM than the (-)Reuse scenario, particularly for the ELP procedure, in which the regeneration operation has been removed in addition to the reusability of the technology. These results echo the trend of single-use technology in commercial biotechnology in which manufacturers look to disposable plastic bioreactor and buffer bags as a means to reduce cleaning and validation costs (Shukla and Gottschalk, 2013). It would be valuable to further consider the utilization of single-use technology in a space pharmaceutical foundry, and in other space systems bioengineering applications, but it is important to point out the limited scope of this ESM analysis. Here we reiterate that the single unit procedure scope establishes a modular basis for pharmaceutical foundry ESM evaluation but does not realize the true circular economy advantages of reuse, which may be considerable for the regeneration step, and of biological systems for production of the purification reagent in general.

Conclusion & Future Directions

In this study, we have introduced and applied the ESM framework to biopharmaceutical processing as a first step towards modeling and understanding the costs of Space Systems Bioengineering and, more specifically, of a long-duration space exploration medical foundry,

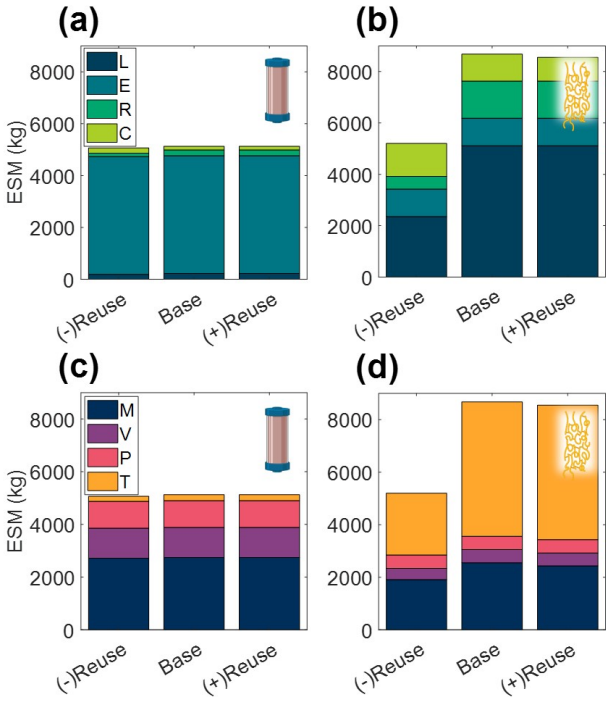

Figure 8.10: Changes in extended equivalent system mass values with reusability of purification technology broken down by labor (L), equipment (E), raw materials (R), and consumables (C) cost categories and mass (M), volume (V), power (P), and labor time (T) constituents for CHM **(A, C)**, and ELP **(B, D)**. (-)Reuse considers the technology as single-use and accordingly discards the unit procedure cleaning operations; (+) Reuse considers additional reuse cycles of the technology. CHM, pre-packed chromatography; ELP, elastin-like polypeptide.

which we believe may one day constitute a critical bioregenerative component of ECLSS for humans to be able to explore the surface of Mars. We have observed that the static behavior of ESM, while certainly maintaining usefulness in early-stage analyses, may stymie later-stage analyses of bioregenerative life support technologies, which tend to behavior more dynamically than traditional abiotic counterparts. In the future, higher fidelity analyses may be performed using tools such as HabNet[142], although the use of such dynamic mission design and modeling tools will require additional software engineering efforts. As it stands now, our techno-economic calculations both satisfy the three fundamental aspects for life support modeling[263, 267] and provide helpful directions for future efforts to incorporate purification processes in space systems bioengineering.

The mAb affinity capture step represented an ideal starting point for biopharmaceutical purification cost analysis given the breadth of the mAb treatments for space-important health indications, the fact that mAb purification is considered a platform technology, and the diversity of affinity capture technologies. However, there are additional processing categories, such as size exclusion, ion exchange, and hydrophobic interaction unit procedures, which could be similarly studied in isolation for their general relevance in biopharmaceutical manufacturing. Establishing a unit procedure knowledge base for space-relevant economics

of biopharmaceutical purification would provide additional benefit to the community.

We acknowledge that the ESM analysis performed in this study utilizes current Earth-based technologies, not Mars-designed processes, and that as technologies evolve and expand the analysis will need to be updated. The need to revisit and update ESM analyses periodically as technology develops is standard practice. This is well illustrated in a recent ESM analysis of plant lighting systems that compares solar fiber optics to photovoltaic-powered light emitting diode hybrid systems[213]. The study results reversed decade-old trade study outcomes in which solar fiber optics scored more favorably, citing rapid advances in solar photovoltaics and light emitting diode technologies.

Furthermore, the analysis presented does not encapsulate potentially significant characteristics of the unit procedures at the interfaces of the upstream and downstream biomanufacturing elements. For example, at the upstream interface the biotic unit procedures (VIN, ELP, OLE) have been reported in literature to be effective capture mechanisms in "dirtier" feed solutions, perhaps absolving the need for more complex pre-capture clarification steps by virtue of process integration. At the downstream end, the eluate of the CHM unit procedure can be directly fed to the subsequent processing step, which would be particularly amenable for other column-based unit procedures, resulting in lower labor time and manufacturing duration. We also do not account for the uncertainty in performance associated with the developmental state of the technology. There have been substantially lower research and development investments in the biotic technologies than in the commercially available abiotic technologies; one may reasonably assume that there is more potential for improvements through biotic unit procedure optimization, while also considering that a larger driving force in abiotic unit procedure optimization for commercial terrestrial operations may balance or outweigh this. Forecasting on the technology development dynamics in the context of these, and other, forces could provide significant additional insights.

Several overarching lessons on the development required for deployment of pharmaceutical purification technology to support human health in space can be gleaned from the cost breakdown of the ESM framework employed in this study. The high mass costs for the mAb capture technologies investigated suggest strong incentives to pursue efforts in miniaturization to reduce not only equipment mass, but also reagent mass, as preparation for pharmaceutical foundries in space. The high labor costs and duration of some of the technologies studied likewise suggests that automatization of biopharmaceutical purification would be impactful. Automatization could also conceivably be valuable in reducing mass costs associated with manual manipulation, such as pipette tips and gloves, and those associated with ensuring sterile operation. We also underline the importance of scheduling and equipment sizing optimization; for example, the ESM penalty for capturing the mission demand of mAb with the VIN unit procedure yielded up to 40% higher total ESM for non-optimal scheduled manufacturing batches. Given the advantage of *in situ* manufacturing to respond to uncertainty in mission medicine demand, further research to explore scheduling and equipment sizing under uncertainty would provide valuable insight.

There are a series of challenges facing pharmaceutical foundries in space beyond processing. Perhaps the most daunting of these is the incompatibility of existing pharmaceutical reg-

ulatory compliance frameworks with the design constraints of *in situ* manufacturing. There are currently dozens to hundreds of analytical tests required to confirm process and product quality prior to release of the pharmaceutical for administration to human patients[389], which translates into a highly burdensome cost for *in situ* manufacturing of pharmaceuticals in space. Fortunately, there is a strong and parallel terrestrial need to reduce the burden of regulatory compliance while maintaining standards of quality assurance and control for personalized medicine, an individualized and patient-specific approach to medical care with widespread support. As mentioned earlier, trends of distributed and sustainable biomanufacturing on Earth provide additional support for reducing ESM-relevant costs.

The analyses presented in this study motivate future investigation into the ESM output of a complete pharmaceutical foundry for a more complete comparison to other ECLSS needs and subsequent formal evaluations of medical risk (i.e., loss of crew life, medical evacuation, crew health index, risk of radiation exposure-induced death from cancer) mitigation as a balance to the ESM costs. The Integrated Scalable Cyto-Technology system[121], reported in literature as capable of "end-to-end production of hundreds to thousands of doses of clinical-quality protein biologics in about 3 d[ays]," is an automated and multiproduct pharmaceutical manufacturing system that may serve well as a starting point for a complete pharmaceutical foundry evaluation. While downstream costs are typically a large proportion of terrestrial biopharmaceutical production costs, they may represent an even higher proportion of the overall ESM costs. ESM is more closely aligned to PMI as a metric than to cost of goods sold in dollars, suggesting that downstream contributions to ESM may similarly dominate. Budzinski and team found that downstream operations contributed 82% of the total PMI for commercial mAb production[64].

Assembly of a complete pharmaceutical foundry ESM model would also enable investigation of more nuanced RMA design considerations, such as those relating to the influence of a fixed set, or anticipated probability distribution, of pharmaceutical product diversity and batch size on optimal system composition to meet given medical risk thresholds. As stated in the original presentation of ESM theory and application, comparison of multiple approaches for a given subsystem with ESM, such as we are studying with the capture step of a mAb pharmaceutical foundry, should satisfy the same product quantity, product quality, reliability, and safety requirements[314]. Of these assumptions, the product quality and safety requirements prove challenging for implementation in pharmaceutical foundry comparisons. It is worth noting that reliability is not considered in the scope of this preliminary study, given the varying technology readiness levels of the unit procedures, but that it should be included in future analyses of full purification schemes. By extension, the impact of microgravity and reduced gravity on reliability and unit operation performance, while not investigated in this study, is an important and complex consideration, that requires significant research to address. Similarly, stability of the production resources over the course of a mission duration should be further considered in future works. High product sensitivity to process changes, and the large battery of testing sometimes required to observe them (the extent of which will also change with the processes employed), creates a situation where ESM comparisons of pharmaceutical foundries that serve as technology decision making tools will

absolutely need to meet this requirement, albeit at a considerable cost and/or complexity of execution.

The assessment of equivalent safety requirements, to the best of the knowledge of the authors, has been approached thus far in an ad hoc and qualitative manner, relying on extensive subject manner expertise and working process knowledge. One promising route to strengthening these critically important safety assessments would be to implement a formal assessment framework based on the environmental, health, and safety (EHS) assessment proposed by Biwer and Heinzle[51] , in which process inputs/outputs are ranked based on a series of hazard impact categories (e.g., acute toxicity, raw material availability, global warming potential) and impact groups (e.g., resources, organism). The key to a systematic space health-centric safety assessment like this is to establish space-relevant EHS impact categories (e.g., planetary protection, crew and ship safety). An improvement of the EHS underpinnings has the potential to provide significant benefits to future ESM analyses in the increasingly complex mission architecture of longer-duration missions.

Chapter 9

Futures: Biomanufacturing for Space Exploration - What to Take, When to Make, How to Break Even

As renewed interest in human space-exploration intensifies, a coherent and modernized strategy for mission-design and planning has become increasingly crucial. Biotechnology has emerged as a promising approach to increase mission resilience, flexibility, and efficiency by virtue of its ability to efficiently utilize in situ resources and reclaim resources from waste streams. Since its infancy during the Apollo years, biotechnology, and specifically biomanufacturing, have witnessed significant expansions of scope and scale. Here we outline four primary mission classes, on Luna and Mars, that drive a staged and accretive biomanufacturing strategy. Each class requires a unique approach to integrate biomanufacturing into the existing mission architecture and so faces unique challenges in technology development.These challenges stem directly from the resources available in a given mission class—the degree to which feedstocks are derived from cargo and *in situ* resources—and the degree to which loop-closure is necessary. We see that as mission duration and distance from Earth increase, the benefits of specialized sustainable biomanufacturing processes increases. Here we present a strategic approach, guided by technoeconomics, to development, testing, and deployment of these technologies serves to nucleate the larger effort of supporting a sustained human presence in space. The processes needed for each scenario spans the technical breadth of synthetic biology to design engineering, from sophisticated genetic tailoring of chassis-organisms to building scalable, automated, easily operable bioreactors and processing systems. As space-related technology development often does, these advancements are likely to have profound implications for the creation of a stable, resilient bioeconomy on Earth.

The following chapter is under development for publication as A.J. Berliner, N.J.H. Averesch, S.N. Nangle, S. Zezulka, G.L. Vengerova, D. Ho, C.A. Casale, B.A.E. Lehner, J.E. Snyder, K.B. Clark, L.R. Dartnell, C.S. Criddle, A.P. Arkin. **Biomanufacturing for Space Exploration – What to Take and When to Make**. (In review, *Nature Communications*, Preprint: 10.20944/preprints202207.0329.v1).

With reinvigorated curiosity and enthusiasm for space-exploration and increasingly complex campaigns, humanity prepares to return to the Moon en route to Mars[497, 175, 119]. Efforts to modernize mission architectures[394]—combinations of inter-linked system elements that synergize to realize mission goals[557]—will need to leverage an array of enabling technologies including biomanufacturing towards the realization of such grand visions[385, 401, 17, 380]. Microbial biomanufacturing has the potential to provide integrated solutions for remote or austere locations, especially where supply chains for consumable and durable goods cannot operate reliably[44, 110]. Complementary to, but distinguished from merely remediative and extractive microbial functions, such as biomining[205, 468], off-world biomanufacturing corresponds to any deployable system that leverages biology as the primary driver in generating mission-critical inventory items of increased complexity, i.e., the *de novo* synthesis of components for the formulation of food, pharmaceuticals, and materials [375, 538, 164, 258, 219, 340, 453]. When integrated effectively into mission architectures, bio-based processes will significantly de-risk crewed operations through increased autonomy, sustainability, and resilience, freeing up valuable payload capacity[43].

Key to the efficacy of biotechnology as a support of human space-exploration is its efficiency in using *in situ* resources (*in situ* resource utilization, ISRU) and the ability to utilize waste streams from other mission elements and recycle its own products (loop-closure LC)[391, 320, 198]. As missions expand, progressive advancement and wider implementation of *in situ* (bio)manufacturing (ISM/bio-ISM) will lead to greater independence, enabling more complex mission-designs with extended goals, and may eventually enable a self-sufficient human presence across the solar system. Biomanufacturing is appropriate for that purpose, because high-volume resources, like fixed carbon and nitrogen (as well as as well as low-volume, but critical resources such as minerals) can be produced and recovered in compact autonomous systems that are analogous to Earth's biogeochemical cycles[375, 538, 164, 258, 219, 340, 453, 160]. Biochemistry also provides access to a plethora of organic compounds, often at unrivaled purity and selectivity, many of which are not accessible by other means [309, 12].

Biologically-driven ISM in support of space-exploration becomes more significant the deeper humans venture into space: As the support of supply chains becomes increasingly challenging the further humans travel, ISM is most feasible in locations where resources are available, accessible and abundant, such as the Moon but even more so Mars (Figure 9.1). The advantages and drawbacks of biotic and abiotic approaches for ISM, in particular for life-support but also auxiliary functions for extended human operations beyond Earth-orbit, have previously been discussed at length[371, 372, 401, 44] (qualitatively summarized in Table S4), but an actionable roadmap for deploying biomanufacturing-based systems within upcoming

campaigns has yet to be formulated. Here, we discuss the applicability of biologically driven ISRU and LC in different off-world cases and present a qualitative techno-economic analysis (TEA) to assess different space-travel scenarios. Pursuant, we lay out paths for readying bio-based technologies for inclusion into mission-design and deployment, to enable the next phase of roadmapping for crewed missions into deep-space.

9.1 Off-world Biomanufacturing Approaches

Concepts-of-Operations: Differentiating ISM-Modes

Given that biomanufacturing is uniquely suited to play significant roles in the specific realms of food, materials, and therapeutics, a key challenge in realizing its potential rests in the availability and abundance of feedstocks that are mobilizable by microbes—provided through logistic resupply (directly or from re- and up-cycling of mission products) or obtained from *in situ* resources. This abundance depends on the destination and mission class and leads to a qualitative discrimination of cases as shown in Figure 9.1a. The *in situ* resources that may provide useful feedstocks to drive biomanufacturing processes on the Moon and Mars are broken down in Figure 9.1b, which aids in comparing mission profiles. For each case, different concepts-of-operations (CONOPS) are applicable—these CONOPS conform to specific inventory needs as they relate to mission- and crew-requirements and depend on the resources availability for ISM. The environmental context informs the specification of feedstocks and processing pipelines (LC or ISRU), as shown in Figure 9.1c.

Each case comprises a unique set of inventory elements; such elements may include infrastructure components (e.g., habitat assemblies and furnishing, functional hardware/appliances as well as scientific equipment and tools), transported as either pre-deployment cargo or with the crew. These elements are used to assemble the larger integrated habitation and life-support systems as well as (bio-)ISM-based LC or ISRU systems and infrastructure related to mission-objectives[218]. While all such cases are distinct in terms of operations[147], they serve as exemplars to better understand biomanufacturing strategies in relationship to mission elements that might provide resources, crew count/needs, and logistical constraints.

Implementation of Bio-ISM Dependent on Off-World Case

Case 1 (Moon, stable logistics) considers Artemis-like Lunar operations[497], specifically short stay missions for small numbers of astronauts carrying out tight scientific and technical explorations and tests. Because of the short times and logistic accessibility, crew-needs for food, medicine and materials can be provided through carry-along and resupply from Earth[492, 250], rather than relying on the more complex, risky and time-intensive technologies of biomanufacturing. Also, due to the dearth of *in situ* resources on the Moon (Figure 9.1b)[118], the scale of biomanufacturing will be constrained by the supply chain and capability for recycling these elements[191]. However, because of the well-supported environment,

it is an ideal location to prove and improve technologies for biomanufacturing in space by testing automated and scaling operation of critical bioreactor systems for different bioprocess types (e.g., electro- and photo-autotrophic (gas) bioreactors for lithoautotrophic and/or saprotrophic fermentation of macronutrients[31]), all of which are likely to have physiological and operational challenges in a low-gravity, resource-poor environment[290, 242, 481]. To this end, systems that have achieved a Technology Readiness Level[339, 179] (TRL) of 5 are well suited to be implemented and evaluated. While these systems currently exist in isolation or partially integrated in laboratory and industrial contexts, building automated end-to-end, compact systems (advancement past TRL 7) will be a key requirement for case 1, so as to meaningfully scale to future, more constrained mission architectures.

Case 2 (Moon, disrupted logistics) considers advanced Lunar operation capabilities when

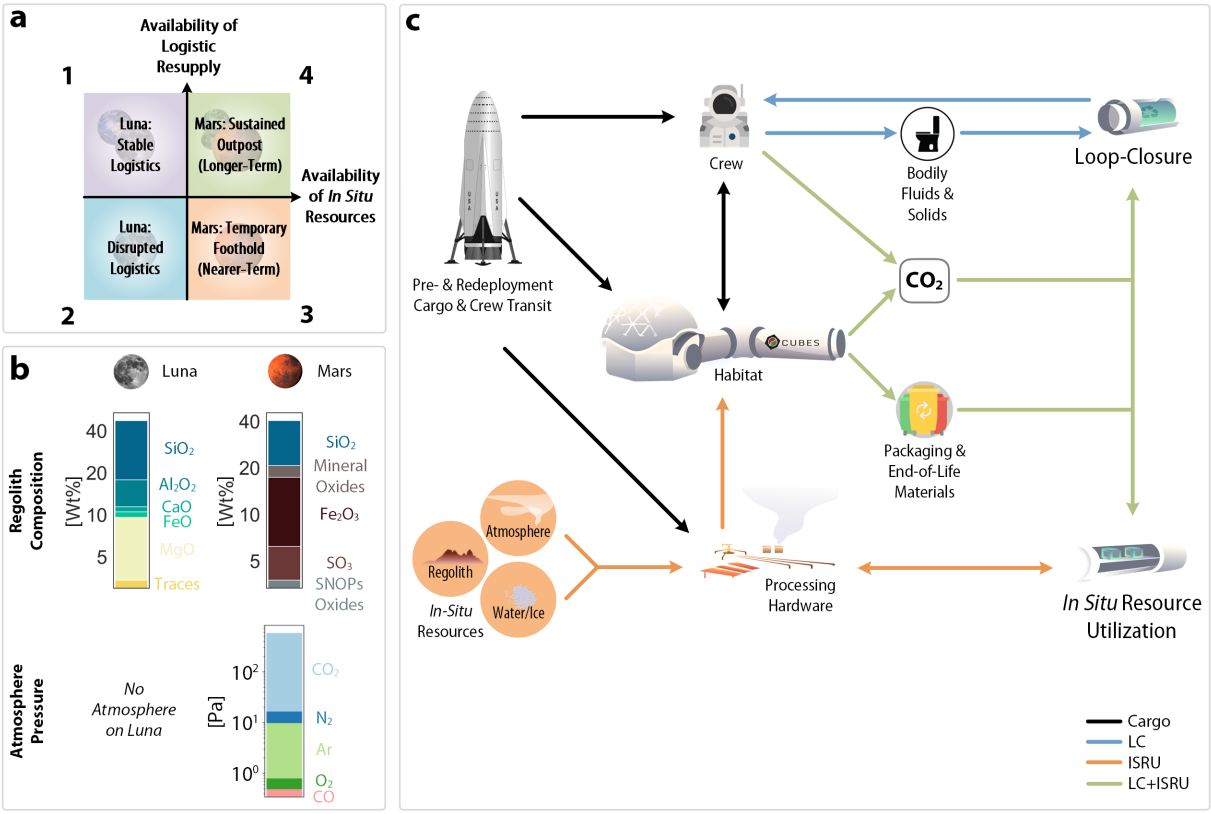

Figure 9.1: Approaches to in situ biomanufacturing dependent on off-world cases. The context-specific off-world cases 1-4 are defined in **a**, mapped as quadrants on qualitative spectra for the availability of *in situ* resources and logistic resupply. The surface-accessible *in situ* resources for the Moon and Mars are compared in **b** in form of gases and solids, broken down into elemental compositions (SNOPs: sulfur, nitrogen, oxygen, phosphorus). Biomanufacturing concepts-of-operations (CONOPS), outlined in **c**, are color-coded for the operational mode: outgoing from initial cargo (black lines), CONOPS can rely on either loop-closure (LC, blue lines), *in situ* resource utilization (ISRU, orange lines), or both (LC+ISRU, green lines).

extensive infrastructure has been deployed on the Moon. To increase the time for operations between resupply (and defending against unexpected resupply disruption), storage facilities will be increased and biomanufacturing become more attractive. Given the paucity of feedstock raw materials on the Moon, which do not provide the central resources necessary for bio-ISM (Figure 9.1b)[118], hyper-efficient use of stored supplies and efficient use of other available mission products and waste-streams via LC must be engineered. Derivatization of packaging materials, such as biodegradable plastics, and minimal processing systems for black and grey water could provide significant augmentations to expected feedstock and extend the operational times of biomanufacturing systems in the event of scheduled or unplanned disruption of the supply chain[17]. Under extreme conditions, being able to switch biomanufacturing operations from, for example, complex vegetable foods to faster and less resource-intense production of simple cellular foods becomes paramount to defray risk. These challenges require innovations in new alternative feedstock engineering in organisms; co-design of mission materials for biological consumption; development of basic waste-processing systems; and flexible re-configurable infrastructures for production to respond to changing resource conditions. Applicable technologies comprise systems that have been tested in the relevant environments and brought to TRL over 7 within operations of Case 1, and are ready for implementation into mission architecture.

Case 3 (Mars, rudimentary logistics) considers basic biomanufacturing systems deployed on Mars with poor logistic resupply due to increased interplanetary distance but with greater availability of *in situ* resources compared to the Moon. While mission-design is still characterized by small crews on round-trips, resource constraints carry different weight. Given the extent and degree of the unknowns involved, these missions are ideally designed to maximize safety and stability by preparing for diverse contingencies. Providing those redundancies is exceedingly challenging due to the remoteness of Mars[147]. Hence, meaningful bio-ISM is necessary—with substantial scaling of the systems brought to TRL 8 to 9 in cases 1 and 2. While a portion of the food, therapeutics and materials will still derive from cargo, significant ISRU of regolith, water, and atmosphere must be implemented in addition to LC, to ensure mission flexibility and resilience. For food, nutritional completeness and palatability, together with customization of texture, flavor, and format will be of central importance. To further safeguard crew-health, essential therapeutics that cannot be included in cargo due to restrictions such as shelf-life, are within scope. For maximum fidelity of mission operations, a range of multi-purpose (thermoplastic) materials is useful for additive manufacturing—demand scales in correlation with mission duration with a greater factor than for food or pharmaceuticals. Enabling technologies include: modular fermentations and bioprocesses at scale, optimized genetically engineered microbial strains to efficiently produce intermediates (i.e., ingredients, agents, crude polymer), and formulation/processing systems to assemble the final products (i.e., meals, drugs, manufactured items)[44].

Case 4 (Mars, developed logistics) envisages a fully developed and integrated biomanufactory where essential logistic resupply is enabled by interplanetary networks and deep-space outposts[331, 84, 25], combined with extensive ISRU and LC. Specifically, this case would entail sustained human operations on Mars on the verge of permanent settlement. The

extensive infrastructure that must be deployed for this kind of mission-design enables production of complete and diverse foods with a spectrum of forms and nutrition, a holistic range of therapeutics, and different bulk as well as specialty materials (plastics, metals, composites) that allow not only the maintenance but also expansion of infrastructure, semi- or fully autonomously. Biomanufacturing technologies and auxiliary infrastructure need to be fully developed and matured to readily deploy tailored microbial cell factories that can potentially be engineered on-demand as the need arises. To this end, even the accommodation of a "space biofoundry" (i.e., automated infrastructure for engineering and analytics of biological systems[234]) in the mission architecture is within scope. Eventually, this will also entail the ISM of specialty chemicals and reagents like e.g., phosphoramidites for DNA synthesis, supporting on-site bioengineering[466], in addition to the total inventories of foods, therapeutics and materials.

Off-World Mission-Scenarios and Bio-Available Inventories

CONOPS for ISM—the flow of resources and integration of LC with ISRU—not only differ for the four considered off-world cases, but are dependent on and influenced by mission-design scenario. To assess the potential impact that biomanufacturing can have on mission-design more quantitatively, five distinct but comparable scenarios were established as per Figure S15a. The outlined scenarios were designed with the objective of greatest comparability among destinations (Moon or Mars), and are agnostic of the cases previously described in Figure 9.1 (which served to aide in grouping mission architectures by location and biomanufacturing strategies). Scenarios 'A' and 'B' correspond to single sorties to the Moon and Mars, respectively, using standard surface operation duration[17]. Meanwhile, scenarios 'C' to 'E' consider 5,400 days of surface operations either as multi-sortie campaigns (scenarios 'C' and 'D') or in a single sortie (scenario 'E'). Using NASA's 'Advanced Life Support Sizing Analysis Tool' (ALSSAT)[317], an analysis of cargo inventory broken down for each scenario and compared by means of Equivalent Systems Mass (ESM, see BOX)[314] was conducted (see SI for details on data aggregation). The bar-charts in Figure S15 decompose the scenario-cost by means of ESM, differentiated by components (mass, power, cooling, volume, crew-time; S15b), system elements (waste, food, water, air, thermal; S15c) and material composition (structural metal, plastic, water, biomass, electronics, etc; S15d), serving as *prima facie* estimates for mission-expense.

This preliminary TEA provides a primary step towards drawing a relationship from the availability of cargo resources to potential inventory elements that lend themselves to biomanufacturing. Apart from highlighting that longer duration Mars journeys have the highest ESM effort, the analysis also provides insight into inventory differences, which has implications for applicability of ISM among the scenarios. Figure S15b shows that across all scenarios the primary cost in terms of ESM will be mass itself, followed by volume. The biomanufactory schema breakdown in Figure 9.1 is supported by the data in Figure S15c, which shows that ESM for scenarios 'A' and 'C' (Moon) are dominated by air systems (∼30% and 26%, respectively) while scenarios 'B' ,'D' and 'E' (Mars) are dominated by

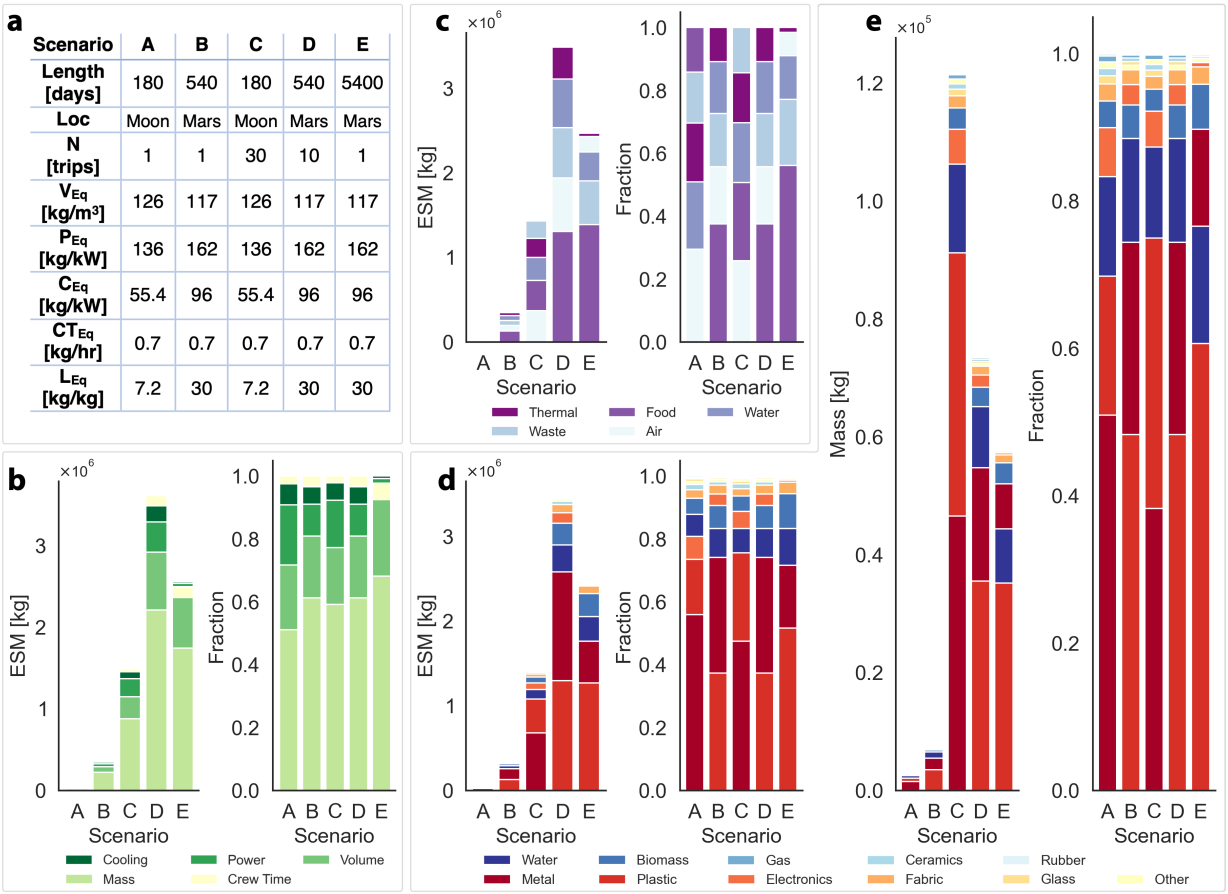

Figure 9.2: Breakdown of inventory elements dependent on mission scenario. Panel **a** provides an overview of parameters for exemplar mission-design scenarios: 'A' and 'B' correspond to single sorties (N) to the Moon and Mars respectively using standard surface operation duration[17], while 'C' and 'D' correspond to multi-sortie campaigns with the same 5,400 days of total surface operation as in 'E'. These parameters can be used to calculate the ESM cost and include equivalency factors for Volume (V_{eq}), Power (P_{eq}), Cooling (C_{eq}), Crew-Time (CT_{eq}), and Location (L_{eq}). Panels **b** – **e** visualize the inventory breakdown by component (**b**), system element (**c**), and material composition (**d** & **e**), respectively: the bar-charts in panels **b** – **d** show the breakdown in ESM units (on the left, in mass [kg]), and the fractional breakdown of each scenario (on the right, unit-less). The bar-charts in panel **e** visualize the absolute (left, in mass [kg]) and fractional (right, unit-less) inventory breakdown of material composition. ESM = Equivalent Systems Mass[314] – for more information see the BOX, as well as the SI.

food systems (∼38%, 38% and 59%, respectively). Given the resources associated with each location, more air system supplies are required on the Moon, which does not lend itself to carbon dioxide fixation technologies as on Mars. In all scenarios the primary costs will be structural metals, plastics, water, and biomass. Most notably, Figure S15c shows that both, the mass and ESM for each scenario, is dominated by cargo composed of metal and plastics. Unfortunately, structural metal is likely to remain unsuitable for biomanufacturing for the foreseeable future. While biomanufacturing is usually conceived towards food production or therapeutics for sustaining astronauts, we note that plastic represents ∼17% of mass in

BOX: Assessment of Economics, Feasibility and Risk of Mission-Architecture
In-space biomanufacturing systems will need to demonstrate superiority over traditional systems in supporting crewed space-missions. To this end, traditional mission-designs must be directly comparable to those augmented with biomanufacturing. One of the more widely used metric to quantify specific attributes of life-support systems is Equivalent Systems Mass (ESM)[314]. In brief, ESM allows mass, volume, power and crew-time to be converted into a single metric in kilograms-equivalent to predict the up-mass requirement[312]. ESM has become a standard metric also for comparing biomanufacturing systems[148, 39], however, it cannot account for aspects such as risk, sustainability, recyclability, complexity, modularity, reliability, robustness, resilience, readiness, scalability, or safety.
As a complement to ESM, the concept of payback time (PBT)[541] has been developed to assess some of these criteria – PBT reflects cost, recyclability, and economic sustainability. Specifically, the PBT is useful in assessing ISRU options, as it allows comparison of the cost to launch and deploy (bio)manufacturing capabilities with the cost of a continuous resupply from Earth over time. Adding statistical risk assessments to the PBT can also help to quantify risk, safeguarding robust and reliable systems. For example, the concept could determine the statistical risk of landing on Mars, with the risk reduction of reduced number of landings on one side but a loss of the payloads carrying ISM hardware being more critical than failure of resupplying missions on the other side. The statistical value of those risk-factors must be carefully assessed based on previous missions, the general technology development roadmap, and the expected learning rates on those factors. Through reliable and generalizable analyses like these, the biomanufacturing approaches which are most vital can be meaningfully assessed.

shorter duration scenarios 'A' and 'B' and from ∼36% up to 60% in longer duration scenarios 'C', 'D' and 'E'. This supports the emphasis on ISM of these materials with increasing mission-duration. Further, with an estimated ∼12% to 16% of the total cargo-mass being water, the associated systems contribute ∼15% to 20% of total ESM (Figure S15c). Because the mass contribution from water is higher for scenarios 'A' and 'B', any biomanufacturing strategy employed should be geared towards water recovery and reuse.

9.2 Integrating Biomanufacturing with Mission-Architecture

Rational Coupling of Biological Systems and Resources

Selection of the specific feedstocks utilizable for different ISM purposes must be guided by critical consideration for recycling of resources at molecular and elemental level—any dead-end, non-recyclable stream will eventually require a resupply from Earth. For auxiliary

functions (e.g., materials for additive manufacturing), production volume is more important than continuity and response time (as is critical in case of food and therapeutics), therefore requiring the adaptation of widely available resources (carbon dioxide and derivable single-carbon compounds or crude biomass), either directly (where available), or through (physico)chemical means (e.g., as secondary beneficiary of propellant production from *in situ* resources)[486]. Hence, the collective approach to more deeply developing synthetic biological tools for bio-ISM must begin with the feedstocks—sugars or other purified multi-carbon compounds (e.g., higher alcohols and fatty acids) will likely not be the prime substrates of biomanufacturing in space, but rather the products/intermediates in a manufacturing chain or loop that serves life-support (within LC elements such as regeneration of oxygen and waste reclamation)[479]. Critically, because in space savings on payload supersedes commercial relevance, adaptation of non-model microbes that save mass is much more valuable. The range of microbial taxa being proposed and investigated for in space-applications is, however, still narrow and often limited to the few model organisms (e.g., *E. coli* and *S. cerevisiae*) whose popularity in Earth-based applications is mostly rooted in legacy. Although a great deal of progress has been made to adapt these organisms to utilization of single-carbon feedstocks[192, 184], they are still outclassed by organisms naturally capable of these functions[427, 465]. Therefore, species with nutritional modes and metabolism uniquely suited to leverage resources available through LC and ISRU must be considered for development of ISM systems, basing their selection on application (feedstock/product pairing, scale, continuity, and responsiveness of the respective process) and scenario-specific criteria (environmental parameters)[31, 419]. Specifically, organisms with the ability to assimilate single-carbon compounds alongside organics (mixotrophy) are most suitable. For this purpose, expansion of metabolic engineering efforts to create (synthetic) pathways that increase the carbon-efficiency of metabolism and/or allow the catabolism and subsequent up-cycling of non-natural feedstocks, like e.g., synthetic plastics, is also sensible[522, 115]. To illustrate these considerations, a qualitative breakdown of possible production routes/flow of carbon through different biomanufacturing approaches for inventory items from case-dependent *in situ* resources is established in Figure 9.3.

Production of Materials for Manufacturing

For off-world ISM of materials and fabrication of mission objects a multitude of different approaches exist, many of which are still inhibited by the extent of initially required critical infrastructure[203, 104]. Biomanufacturing has the potential to surmount this limitation, by supporting the fabrication of consumable and durable goods made of plastics[29, 340, 282], metals[168, 554], and ceramics[279] (∼18% to 60%, ∼13% to 50%, and ∼1% of total mission ESM respectively, Figure S15d) with uses and sizes ranging from small replacement parts and functional tools to physical components of the life-supporting habitat[418, 335].

In combination with additive manufacturing[589], bioplastics could make up the majority of high-turnover items with regular demand, while also providing for contingencies, i.e., non-anticipated servicing and repairs of incidental nature. Such polymeric constructs can be

derived from basic (carbon) feedstocks in a more compact and integrated way in a one-step bioprocess than by chemical synthesis, especially in the case of comparatively (to Earth-based manufacturing industry) low-throughput products[44, 401]. Furthermore, especially high-performance polymer-fibers such as for example aramids and arylates have a range of applications in space technology, including ballistic protection. The building blocks for these, or even final polymeric materials of equivalence, can be obtained through biomanufacturing[29, 30]. Technologies for production of biomaterials, in particular bioplastics, from *in situ* resources like carbon dioxide are also immediately relevant to providing solutions for the most pressing challenges of humanity on Earth. This includes mitigation of greenhouse gas emissions through carbon-capture and carbon-neutrality (i.e., LC), as well as reduction of environmental pollution by non-biodegradable materials. Biomaterials production from inorganic carbon is therefore an enabling technology for the evolution of a circular economy and sustainable (bio)chemical industry on Earth[461].

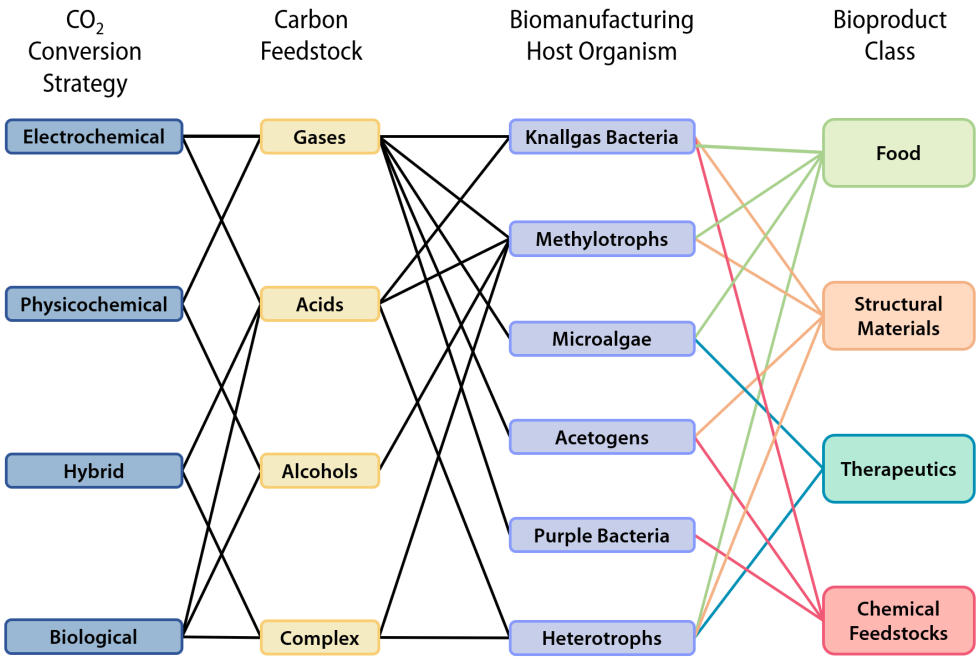

Figure 9.3: Breakdown of available routes for bioproduction of inventory elements from carbon dioxide—either as in situ or recovered resource. Connecting lines represent possible paths for carbon-compound conversion of intermediates to products. Usability of different feedstocks is tied to nutritional mode of the microbial host organism (more than one nutritional mode is possible for certain organisms). Classes of products are assigned to respective microbes in respect of their metabolism as well as not represented 'shadow-characteristics' of the chassis (e.g., aerobic/anaerobic, prokaryotic/eukaryotic, metabolic rate, robustness, etc.), rather than ability to (naturally) derive the respective compounds. While metabolic engineering theoretically allows almost any bio-available compound to be produced in any organism, the effort required for realization can be excessive. For example, oxygen-dependent pathways will hardly be functional in obligate anaerobes without extensive modifications. Likewise, correct folding of proteins with high post-translational modifications in prokaryotes is unlikely. Products may or may not comprise some of the initial feedstocks, hence consecutive runs through this chart to up-cycle carbon are conceivable.

Use of soil and rock (Figure 9.1b), while likely large by volume for surface operations as components of buildings and structures, has a limited number of applications due to the poor mechanical properties of regolith (e.g. low flexibility and plasticity)[396, 585, 100]. Nevertheless, autonomous 3D-printing of infrastructure relying on regolith and composites thereof with (thermoplastic) binding resins has been proposed and prototyped (also see SI)[517, 248]. This requires significant up-mass of auxiliary equipment to allow for e.g., stripping and processing of topsoil, as well as the raw material for the binding resin. If, however, the binding agents (such as polyesters like polylactic acid) could also be derived or produced on-site from *in situ* resources, an additive manufacturing method may become immediately more feasible[315, 251].

Another possibility to overcome the low versatility of raw regolith and leverage it as an *in situ* resource is to extract certain elements of interest for further processing and application. Performed with microorganisms, this process, known as bioleaching, is already being applied on Earth (e.g., for 20% to 30% of global copper production[577]). For space applications, three classes of resources are distinguished: (1) metals and minerals like iron and sulfur oxides[83, 343], or silicates[109], all of which are common in various regolith types and can be extracted for construction purposes and other bulk applications[468]; (2) rare earth elements like lanthanides, scandium and yttrium, which can be extracted from specific regolith types[364]; (3) noble metals found in components of electronics brought from Earth (e.g., copper), which could be reused for new circuitry. While (1) and (2) are part of ISRU and (3) contributes to LC, all of these extraction processes can be combined and coupled with additive manufacturing for perpetual or on-demand ISM. For Earth, these technologies would further contribute to advancement of remediation techniques, contributing to the move towards a more sustainable and circular economy.

9.3 Paths to Realization of Emerging Technologies

Readying Microbial Production Systems for off-world Bio-ISM

While having gained significant traction over the last decade, the study of space biomanufacturing is still limited to small-scale microgravity experiments[523, 558, 237] (e.g., BioRock[111] or Rhodium Inflight Biomanufacturing[166]). More extensive R&D will be required to ready bio-ISM technologies for implementation in mission architectures, especially to scale and adapt synthetic biology and bioprocess engineering to the relevant (off-world) environments (specifically Moon and Mars)[43, 485]. To this end, the development of microbial cell factories must go hand-in-hand with the development of appropriate hardware for in-space bio-ISM. Specifically, standardized but versatile bioreactor systems that are scalable, automatable and capable of providing the environmental conditions for handling and cultivation of microbes in different off-world scenarios are required, combined with autonomous data acquisition for process and hardware performance characterization to monitor production outcomes (scalable yield, titer, and rate, as well as controlled quality).

Integration of Research and Development with Public and Private Sectors

To evolve the technological readiness in the described areas requires scientists and engineers from various fields spanning biology, chemistry, physics, and engineering to work together to advance microbial cell factories and build cross-compatible and scalable processing systems within the confines and stressors of space[43]. Biomolecular, bioprocess, and biosystems engineering must be integrated with pre-processing of resources and downstream processing of products, and tied in with mission-support infrastructure and logistics. Coordination mission specialists are critical to deploy tests in space under different constraints (scenarios) and build long-term partnerships and understanding between the public and private sectors. Such groundwork requires long-lived multidisciplinary centers that are secure from volatility of markets and swings of political agendas to perform the large-scale, long-term science necessary to succeed. A dedicated space-based R&D Hub as an associated 'field-station' could greatly streamline and facilitate the advancement of fundamental technology that increases TRLs. Service providers would dedicate and manage resources both on the ISS (near-term) and next-generation space station(s) (mid-term). This pipeline would ensure testing, prototyping, and maturation of technologies in space with assigned, predictable launches, hardware and support.

9.4 Outlook

The strategic application of biomanufacturing will de-risk and expand crewed space-exploration capabilities. The farther from Earth the more mission-critical biomanufacturing becomes – Lunar missions may be not sustained only supplemented with LC, recycling and repurposing of waste-streams, Mars missions will require ISRU. To take full advantage of mission supplies and *in situ* resources, advanced biomanufacturing technologies must be developed – given the austerity of the Moon and Mars, research efforts must be geared towards the most abundant resources to benefit future deep-space missions. Near-term Lunar missions will serve to build-out and stress-test LC technologies that will inform long-term ISM processes on Mars. Techno-economic analyses of mission scenarios direct the strategic development of hardware and can, as opposed to hardware, be readily implemented at trivial capital cost. Biomanufacturing technologies for both, LC as well as ISRU, have promise for dual-use applications on Earth for a circular-economy and in extreme or inaccessible environments.

Chapter 10

Futures: Space Bioprocess Engineering Drives Sustainability On- and Off-World

Although *raison d'etre* of Space Bioprocess Engineering is the design, realization, and management of biologically-driven technologies for supporting offworld human exploration, it has the potential to offer transformative solutions to the global community in pursuit of the United Nations Sustainable Development Goals. Here we address the growing sentiment that investment in spacefaring enterprises should be redirected towards sustainability programs. In outlining the Earth-benefits of dual-use Space Bioprocess Engineering technologies, we both show that continued investment is justified and offer insight into specific R&D strategies.

The following chapter is under development for publication as A.J. Berliner, I. Lipsky, G.L. Vengerova, A.P. Arkin. **Space Bioprocess Engineering Drives Sustainability On- and Off-World**. (In preparation, expected submission Summer 2022).

Less than a year after the triumph of NASA's 1969 Apollo moon landing, Gil Scott-Heron's spoken-word poem, *Whitey on the Moon*, struck a resounding chord amongst the American populace by calling out social and economic disparities in the allocation of public funds[478]. Now more than 50 years after the debut of *Small Talk at 125 and Lenox* – and with NASA preparing to revisit Luna via the Artemis Program[497], many have echoed Scott-Heron's concerns that the costs associated with spacefaring could better spent by addressing problems on Earth[333, 327]. With the latest Artemis launch system projected to cost $4.1 billion/launch[177] and estimates of a human exploration campaign to Mars ranging from $150 billion to $1 trillion[54, 262, 217] (representing ∼5% of the U.S. GDP) – the need for equitable allocation and efficient management of taxpayer money is critical. Because this money could alternately be used to address political and sustainability challenges on Earth, minimizing the financial cost of the mission and maximizing societal benefit is necessary. Towards this end, space technologies developed via taxpayer dollars should offer both cross-cutting cost solutions and dual-use applications towards addressing Earth-based sus-

tainability. From among the myriad of engineering platforms, bioengineering[401, 372, 371] and integrated biomanufacturing[44] technology paradigms have been shown to support human health, reduce costs, and increase operational resilience. Only recently codified, Space Bioprocess Engineering (SBE)[43] presents exciting possibilities for the future of climate change and sustainable development – with an emphasis on SBE innovations that potentiate solutions to planetside problems, education and workforce training towards sustainable and equitable economic futures, and the academic and economic co-benefits of a new promising field of study.

"Sen' these doctor bills – Airmail special."

SBE is the multi-disciplinary approach to design, realize, and manage a biologically-driven space mission as it relates to addressing the NASA's grand challenges for advancing technologies to support the nutritional, medical, and incidental material requirements that will sustain astronauts against the harsh conditions of interplanetary transit and habitation off-world[43]. SBE combines synthetic biology and bioprocess engineering under extreme conditions to enable and sustain a biological presence in space. In 2010, NASA's Space Technology Mission Directorate (STMD) released the Space Technology Grand Challenges, 13 calls for new technologies to address need-gaps across human presence, management of space resources, and scientific progress and exploration[514]. SBE grew in part from those needs, and its main components have sought to address the challenges of space health and medicine[189, 439, 105], settlement[75, 510], and a space way station[236, 55, 553, 455] with SBE thrusts towards biological *in situ* resource utilization (ISRU) and in-space manufacturing, food and pharmaceutical synthesis, and loop closure all as measures to increase settlement health and self-sufficiency[371, 44, 43]. But beyond space, NASA technologies have often found terrestrial applications[400, 491, 278], and SBE principles of sustainability make for direct extensibility towards climate and environmental challenges too[133]. The STMD exists as a framework to precipitate, vet, and fund promising technologies, and its technology transfer program works to secure funding for dual-use industry applications of promising technologies[157]. Engineered exoelectrogens for CH_4 generation and wastewater treatment[66], yeast that can turn CH_4 into usable biomass for in-space manufacturing (ISM)[182], fungal bioremediation for targeted metal recapture[530], and more STMD biotechnologies have recently found homes outside of human spaceflight[325]. Minimum viability for integrated space biomanufacturing systems requires a degree of autonomy and adaptability that might offer applications towards climate change adaptation and natural disaster response. A modular biomanufactory on Earth could stay more independent from resource lines in case of disaster — drought resistant crops in optimal controlled-growth environments could sustain better against typical agricultural hazards, or molecular pharming, which allows astronauts[366] and terrestrial citizens[393] to quickly respond to sudden changes in medical needs. SBE as a field works to address end product recycling, loop closure, maximal utilization of available resources, and optimization for mission sustainability and long-term settlement, traits that will continue to dovetail well with environmental challenges. Technological maturation or ef-

ficiency breakthroughs in bio-additive manufacturing[90, 189], engineered high-performance crops[390], nutritional victuals[410], medicines[366], biological air purification[548], fuel manufacturing[288, 123, 412], and electrical generation[4] may offer new dual-use futures for Earthbound sustainability targets.

"No hot water, no toilets, no lights."

In 2015, the same year the Paris Agreement on Climate Change was signed, all 193 members of the United Nations adopted the Sustainable Development Goals (Fig. 10.1): 17 challenges across human, economic, and natural systems for the modern era[114, 306]. Within this framework, both the technological deliverables and the ideas explored by SBE might offer new avenues towards sustainable development. Preliminary NASA STMD technologies

NASA Space Technology Grand Challenges / United Nation Sustainability Development Goals	EXPAND HUMAN PRESENCE IN SPACE	MANAGE IN-SPACE RESOURCES	ENABLE TRANSFORMATIONAL SPACE EXPLORATION AND SCIENTIFIC DISCOVERY
2 ZERO HUNGER; 3 GOOD HEALTH AND WELL-BEING	Molecular pharming views plants as chemical factories, efficiently synthesizing desirable compounds with minimal inputs. In space as terrestrially, it would allow people to quickly respond to unanticipated disease states.	Space agriculture has led to advances in the practice of vertical farming, which minimizes the amount of inputs needed to grow crops. Vertical farming also allows crops to be grown anywhere a controlled environment can be established, including in densely populated urban areas.	The Photobioreactor on the ISS cultivates microalgae to create hybrid life support systems which can grow nutrient-rich microalga. Advances in the chamber have made it feasible for use in advanced wastewater treatment and cultivation of nutrient-laden biomass over marine water.
6 CLEAN WATER AND SANITATION	The Microbial Check Valve developed for the Space Shuttle passively kills viable microorganisms within water to prevent cross-contamination. Water tanks using this technology have been installed in cities with a scarcity of clean water.	Projections of a hypothetical urine-diversion system show that communities could lower their greenhouse gas emissions, energy consumption, and freshwater usage. On the ISS, a Urine Processor Assembly collects urine and processes it to potable standards while the remaining brine can be used as fertilizer, and in Europe, urine recovery systems are being implemented throughout wastewater systems.	Aquaporin-based filtration, inspired by aquaporins found across organisms, is highly efficient and specific to filtering out water, and is included in the Extravehicular Mobility Unit space suit design. As clean freshwater resources are increasingly strained, aquaporins are eyed for their ability to filter water through non-energy intensive means.
7 AFFORDABLE AND CLEAN ENERGY	The Urea Biochemical Reactor unit (UBR) is being studied as a way to combine wastewater treatment to separate urea from urine and convert it into energy. The UBR would work in any wastewater treatment containing urine and/or ammonia, providing a non-energy or -resource intensive method for producing energy on and off Earth.	The algae studied in NASA's OMEGA project cleaned wastewater and produced biomass that could be used as fuel. Coupled with advances made in using urine as a wastewater source for algae, this could provide a way for astronauts to produce in situ fuel. The project developed protocols for harvesting algae and demonstrated that NASA has the motivation and resources to study technology applicable both to rocketry and the search for renewable energy.	Advances in bio-crude oil manufacturing by pre-treating microalgae with NaOH and urea would mean that astronauts on the ISS would be able to conserve the amount of propellant brought and resupplied. As the environment is destroyed to mine natural oil, this technology presents an alternative way to manufacture crude oil and make it closer to becoming a renewable resource.
8 DECENT WORK AND ECONOMIC GROWTH; 9 INDUSTRY, INNOVATION AND INFRASTRUCTURE	NASA has studied closed-system applications of phytoremediation (i.e. the use of plants for remediation of contaminants) to create a healthy environment for astronauts off-world. This knowledge has been used to develop living walls, which have natural insulation and promote social and physical health using minimal inputs.	Long-term human settlement on Mars or the Moon will necessitate large amounts of concrete, but shipping tons of it is not feasible, and traditional methods of production are energy-intensive. To solve this, environmental engineers developed a method to harvest the binder needed for concrete from organisms that could be shipped to other planets relatively cheaply and used in place of boiled limestone on Earth, lowering carbon emissions from concrete production.	The original purpose of Biosphere 2 (B2), a miniaturized version of Earth's ecological environments, was to establish a baseline for structures for long-term human habituation in space. The B2 experiment informed other initiatives to simulate what life on the Moon and Mars could look like. Today, experiments in B2 focus on improving ecology and eco-technology on Earth.
11 SUSTAINABLE CITIES AND COMMUNITIES; 12 RESPONSIBLE CONSUMPTION AND PRODUCTION	One goal of MELiSSA is to create a closed-loop system in deep space which supplies astronauts with fresh air, water, and food using microbial recycling of human waste, and it offers a blueprint for human-centered and sustainability-minded cities.	Polyhydroxyalkanoate (PHA) polymers produced by microorganisms can be used as biodegradable plastics and have been tapped by NASA for long-term extraterrestrial missions because they make production of materials possible in space. Because the requirements for production in space include producing minimal waste and meeting the high standards of a top-of-the-line lab, perfecting the technology for NASA would mean that terrestrially, citizens would have access to plastics that are degradable but still safe for use in laboratory or medical environments.	NASA has funded experiments which showed that houseplants in conjunction with activated charcoal efficiently clean indoor air pollutants, and this research may be used to design space stations and terrestrial buildings which are conducive to the good health of their occupants.
13 CLIMATE ACTION	NASA has developed enzyme structures which could facilitate access to biomass and biofuels from cellulose, and on Earth, researchers are studying potentially carbon-negative biofuel production utilizing cellulosic feedstocks which could benefit from these enzymes.	The Haber-Bosch process which produces ammonia requires large energy inputs and releases carbon dioxide. Alternatives such as bacterial nitrogen fixation and urine ammonia extraction have been studied for use as low-energy in situ methods for ammonia production, and these provide industrial chemical synthesizers strategies for ammonia production with a much smaller carbon footprint.	Microalgae can grow in extreme environments to produce essential consumables and biofuels, and can be used for efficient CO2 scrubbing. NASA's Surface Adhering BioReactor provides a method for cultivating microalgae with low energy and water inputs on- and off-world.

Figure 10.1: Space Bioprocess Engineering technologies in the context of NASA's Space Technology Grand Challenges (STGCs) and United Nations Sustainability Development Goals (SDGs). Specific exemplar technologies developed in service to the STGCs (shades of grey) are described in relationship to corresponding SDGs (shades of pink). More more information and references, see Table S1 in the SI.

towards bioremediation and filtration could ameliorate water and air quality, helping towards sustainable cities and communities (SDG 11), health and well-being (SDG 3), and clean water and sanitation (SDG 6). Successful bio-additive manufacturing and bioprocesses to reduce material footprints in the name of a sustainable mission would also be levers towards decent work and economic growth (SDG 8), industry innovation and infrastructure (SDG 9), and responsible consumption and production (SDG 12), as would bio-recapture of waste products and loop closure. Space research and development has consistently generated returns, and SBE is still fledgling as a body of research. Tight mission constraints and the push for optimization and metrification in space architecture can establish more about key mechanisms, best practices, and new concepts entirely. SBE developments in crop LED lighting[502, 65, 426], acetate production for bioplastics[88, 323, 89, 90], biomining and bioremediation[111, 468], all have potential to optimize existing processes and reduce reliance on fossil fuels. Synthetic biology breakthroughs that have been democratized in the public forum through the literature could breed other breakthroughs in environmental bioprocess engineering[178]. And because bioengineering and synthetic biology represent such a huge promise to the problem of climate change[133]: crop modification for sequestration[252], rumen engineering[235], RuBisCO modification for CO_2 fixation[81, 318], bio-geoengineering[498], and much more – the greater we understand the solution sphere, the better we can meet our goals for sustainable development (SDG 13)[498, 513].

"Was all that money I made las' year?"

Totaling $5.8 trillion, the recently released U.S. 2023 Fiscal Budget by the Biden White House allocates $44.9 billion (0.7%) in discretionary budget authority to address the climate crisis[46]. Despite this increase of $16.7 billion (59%) from 2022, some worry that this is just not enough[454]. The Intergovernmental Panel on Climate Change (IPCC) has reported that global model pathways limiting global warming to 1.5°C are projected to require an investment in just energy sustainability amounting to $2.4 trillion between 2016 and 2035 – representing ∼2.5% of the world GDP[524]. In the U.S. this would amount to an additional $101 billion and some have argued that meeting this financial target can be reach in part by raiding the $26 billion slated for NASA. With only an 8% yearly increase in its budget from 2022, 2023 NASA has directed primarily to-

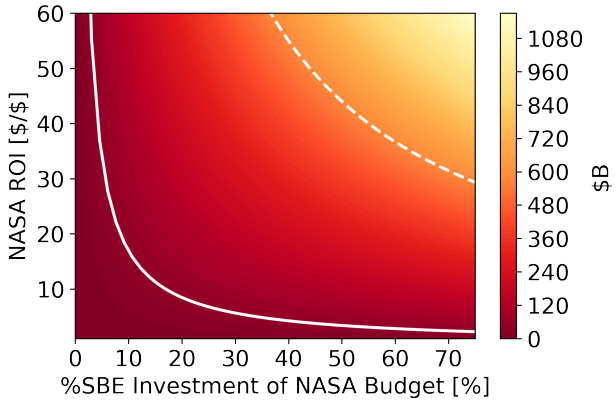

Figure 10.2: NASA-funded SBE Technology Return on Investment. A contour plot is provided showing the financial return on investment (ROI) in $Billions as a function of the NASA ROI $:$ and the SBE fraction of the NASA budget of current $26B. The solid white line corresponds sustainability budget of $44B and the dashed white line corresponds the the ROI of sustainability investments at 13:1 [$:$].

wards enabling missions on and around the Moon through Artemis while preparing for Mars exploration to the tune of $7.6 billion for deep space exploration and $4.7 billion for Common Exploration Systems Development to support lunar missions includes funding for the Orion spacecraft and Space Launch System (SLS) – compared to the $2.4 billion for Earth-observing satellites and related research will enhance NASA's ability to improve our understanding of climate change. NASA has recently allocated anywhere from ∼0.5-2.5% of their yearly budget towards SBE and SBE-adjacent programs: $115.0 million to its Human Research Program, $79.1 million towards biological and physical sciences, and a fraction of the $145 million for early stage innovation and partnerships and $287 million for small business innovation research and technology transfer[46]. If SBE technologies are considered as sustainability technologies, then we can consider the return-on-investment (ROI) on NASA-funded SBE as a contribution to the gap in funding towards sustainability. With estimates of NASA ROIs ranging from 7-21:1[200, 223] (and in some cases 40:1[193]) $/$ compared to the DOE's ROI of 13:1 for something like its Clean Coal Technology Program $/$[134], we estimate the total possible financial contribution to sustainability from NASA investment in SBE as arbitrage between the SBE fraction of the NASA budget and the ROI (Fig. 10.2).

"How come there ain't no money here?"

The primary factors predicted to govern the success of biomanufacturing are the availability of *in situ* resources and the availability of logistic resupply of cargo in the form of feedstocks. NASA's Artemis mission aims to land the first woman and person of color on the lunar surface, deepen the scientific understanding of the Moon, and test technologies that will prepare for human exploration of Mars. Due to the lack of carbon (C) and nitrogen (N) on Luna[118], the scale of any biomanufacturing-driven product will be constrained by cargo deployed from Earth and the ability to recycle these elements at each phase in their life-cycle[191]. A critical source of C and N on Luna will be waste-stream recycling. This process will leverage biological wastes produced by crews and the waste products of biomanufacturing itself are recaptured and utilized in successive rounds of biomanufacturing. Reuse of waste streams will thereby increase the sustainability of lunar missions and decrease the need for new raw materials to be shipped from Earth. In the context of Artemis, specific SBE technologies that contribute to recycling and reusing scarce cargo materials also serve as Earth-based sustainability platforms which contribute to STG 6. For instance, aquaporin-based filtration and NASA's Microbial Check Valve have been integrated in space missions already and provide passive, efficient water filtration methods for use on Earth[224] (Fig. 10.1). More broadly, closed-loop life support systems, like the Environmental Control and Life Support System (ECLSS) and Micro-Ecological Life Support System Alternative (MELiSSA) provide a blueprint for sustainably designed environments on Earth (Fig. 10.1).

As with Artemis, the specific technologies deployed as mission cargo are still the subject of much speculation and scrutiny[147]. Recent studies in mission architectures with surface operations longer than 500 days have shown that biotechnology offers mass, power, and volume advantages over traditional abiotic approaches – and the amalgamation of SBE

BOX 1: "Hm! Whitey's on the moon"

The technology for human colonization of space must operate so well that crews can survive their missions safely both mentally and physically, and quickly recover from unanticipated emergencies. The standards for astronaut life are high[460], but the same has not been always true of the standards for ordinary civilians on Earth. A history of scientific racism has led to mistrust of science and engineering within marginalized communities[238, 354, 35, 22]. Meanwhile, climate change has been shown to impact those same communities earlier and more seriously than in others[475]. While technology is likely the path to mitigating climate change, it is important that that technology is both effective and thoughtfully distributed, so it is able to reach those most impacted by climate change. Focusing on sustainability in the context of space exploration forces new technology to first be proven safe and effective for astronauts, then used terrestrially. This change may begin repairing the divide between experts and laypersons, increasing public support of and allowing technology to be adopted more broadly, as well as provide useful tools in the battle of climate change. These factors combined would pave the way for effectively minimizing the damage climate change will otherwise cause, in the communities it affects the most.

elements in the form of an integration Martian biomanufactory has been proposed[44]. Unlike Artemis, human exploration on Mars will be governed by poor logistic resupply and more availability of useful *in situ* resources. As a result, biomanufacturing strategies will be driven by more by ISRU and ISM – in particular, C and N fixation. Although the average surface pressure on Mars is <1% compared to Earth, there exists sufficient CO_2 (∼95%) and N_2(∼3%) to entertain a number of C and N fixation strategies. With many mission architectures calling for *in situ* production of ascent propellant, the abiotic conversion of CO_2 to CH_4 via the Sabatier reaction has been proposed and is being tested on board the International Space Station. Requiring extreme pressure and heat, this process is energy intensive. SBE alternatives such as cellulosic biofuel production[288], the Urea Biochemical Reactor unit[409], or bio-crude oil harvested from pre-treated microalgae[245] require less energy compared to traditional methods for propellant production and are potential dual-use technologies for addressing climate action (STG 13) via greenhouse sequestration. The ample CO_2 inventory of Mars also serves as the primary feedstock for agriculture. SBE-driven platforms for hydroponic crop cultivation have been shown to reduce mission costs for sustaining astronauts. Advances in space agriculture have already led to advances in terrestrial agriculture (SDG 2), and advances in creatively using wastewater (e.g. efficient ammonia extraction from urine) provide a means for safely supplying crops with needed nutrients by recycling waste (Fig.10.1). The Urine Processor Assembly on the ISS collects urine and processes it to potable standards[543], recovering much of the water available. However, urine can theoretically supply over 60% of the crew's water demand and the brine can be used

as fertilizer, so researchers continue to study how this system can be improved[543]. Urine recovery systems are being implemented throughout wastewater systems in Europe. Projections of a hypothetical urine-diversion system show that communities could lower their greenhouse gas emissions by up to 47%, energy consumption by up to 41%, and approximately halve their freshwater usage[225]. The Haber-Bosch process produces ammonia for use in fertilizers and pharmaceuticals but requires large energy inputs[78] and releases 1.2% of global anthropogenic carbon emissions. Low-energy ammonia production or extraction processes are being developed for use in space, and these alternatives (Fig. 10.1) provide chemical synthesizers strategies for producing ammonia with a smaller carbon footprint.

"The man jus' upped my rent las' night."

Beyond mission savings, SBE as a venture may offer co-benefits towards education, diversity and a more inclusive economy. The United Nations identified science and technology as a key lever in their 2019 Global Sustainable Development Report, and SBE could contribute to that public sector research push with sustainable technology investment[588]. NASA, and the burgeoning SBE field, train and employ high-skilled workers to stable civil servant, engineering, and scientific careers[222]: over 312,000 strong. NASA induces $19.3 billion in contracting activity[584]. To its workforce, space technology relies on significant outreach, academic partnerships, and on-the-job training that both fill the ranks of the next generation and lower barriers to entry. SBE could enable more women, cultural minorities, and the economically disadvantaged to enter the space sciences. SBE's multi-disciplinary approach could help bridge the gap between the scant 14.6% of aerospace engineering graduates that are women and the 50.6%, 42.1%, and 35.4% of women graduating towards environmental, biological and agricultural, and chemical engineering, respectively[463]. NASA's $127.0 million STEM engagement fund and a unified call for SBE workers would promote engagement across cultural and scholarly backgrounds[46]. A young field with foundational work still to be done offers early career scientists and engineers facing down other entrenched industries a new set of opportunities. Across Space Technology Research Institutes (STRIs), individual Early Stage Innovation (ESI) projects, NASA Innovative Advanced Concepts (NIAC), and all of its solicitations, the STMD boasts more than 800 active projects — all containing the necessary agency framework to promote the participation of women and underserved communities and businesses, and of historically black colleges and minority serving institutions[518]. In fact, effectively prioritizing sustainability in space exploration necessitates involving and uplifting marginalized communities. The most immediate and devastating impacts of climate change will be felt primarily by marginalized communities[37, 330], so input from underserved demographics will be crucial to fighting the looming ecological crisis, including in space exploration efforts. Furthermore, NASA partners are beholden to the extensive agency standards of diversity, equity, and workforce inclusion, which would push the lever towards gender equality and quality education (SDGs 4 and 5).

"Ten years from now I'll be payin' still."

In our pursuit of a spacefaring future, we must also give pause and remember the words of Scott-Heron. If "ten years from now I'll be payin' still," we must ensure that the investment offworld offers benefits on Earth. A central tenet of a more sustainable world is a sustainable economy. Space Bioprocess Engineering promises the powerful returns of NASA work and fundamental research as a whole, but also its own slew of sustainable development prospects. Both as a field and an economic venture, SBE grapples with a crystallized set of the same challenges that face most sustainable development. Returns are not immediate, upfront investment is hefty and comes often from the taxpayer, and SBE is uniquely positioned to meet them.

Chapter 11

Appendix

11.1 SI: xESM

Case 0

xESM	M (kg)	V (m^3)	P (kW)	C (kW)	T (MMH/ Duration)
Transit to Mars	8616.32	28.23	9483.77	8440.16	143.92
Return Transit	5741.17	19.16	9476.05	8432.44	126.66
Total	14357.49	47.39	18959.82	16872.59	270.58
ESM	**M (kg)**	**V (m^3)**	**P (kW)**	**C (kW)**	**T (MMH/ Duration)**
Transit to Mars	5538.48	17.99	9458.54	8417.79	253.27
Return Transit	5538.48	17.99	9458.54	8417.79	253.27
Total	11076.96	35.97	18917.09	16835.59	506.53

Case 1

xESM	M (kg)	V (m^3)	P (kW)	C (kW)	T (MMH/ Duration)
Transit to Mars	15290.76	47.14	9515.68	8472.30	220.76
Mars Orbit	12415.60	42.03	9488.40	8445.03	551.54
Return Transit	5918.73	21.35	9489.58	8446.20	220.76
Total	28092.95	89.55	19018.57	16931.82	772.30
ESM	**M (kg)**	**V (m^3)**	**P (kW)**	**C (kW)**	**T (MMH/ Duration)**
Transit to Mars	5538.48	17.99	9458.54	8417.79	253.27
Mars Orbit	9370.25	31.09	9490.69	8446.62	603.02
Return Transit	5538.48	17.99	9458.54	8417.79	253.27
Total	15295.32	49.45	18963.73	16878.90	856.28

Case 2

xESM	M (kg)	V (m^3)	P (kW)	C (kW)	T (MMH/ Duration)
Transit to Mars	17898.72	60.15	16942.22	15198.38	220.76
Mars Orbit	8318.85	29.07	5454.67	5097.82	551.54
Descent	22884.79	22.66	7426.54	6726.08	0.00
Surface Ops	0.00	22.66	7426.54	6726.08	603.02
Acsent	8000.00	0.00	0.00	0.00	0.00
Return Transit	5918.73	21.35	9489.58	8446.20	220.76
Total	63021.09	155.89	46739.56	42194.54	1596.08
ESM	**M (kg)**	**V (m^3)**	**P (kW)**	**C (kW)**	**T (MMH/ Duration)**
Transit to Mars	5538.48	17.99	9458.54	8417.79	253.27
Mars Orbit	4402.39	14.23	5454.67	5097.82	603.02
Descent	8000.00	0.00	0.00	0.00	0.00
Surface Ops	6884.79	22.66	7426.54	6726.08	603.02
Ascent	8000.00	0.00	0.00	0.00	0.00
Return Transit	5538.48	17.99	9458.54	8417.79	253.27
Total	38364.14	72.86	31798.31	28659.48	1712.57

			Case 3		
xESM	**M (kg)**	**V (m^3)**	**P (kW)**	**C (kW)**	**T (MMH/ Duration)**
Predeployment	14884.79	22.66	7426.54	6726.08	0.00
Transit to Mars	19194.01	38.13	9515.68	8472.30	220.76
Mars Orbit	8318.85	29.07	5454.67	5097.82	551.54
Descent	8000.00	0.00	0.00	0.00	0.00
Surface Ops	0.00	22.66	7426.54	6726.08	603.02
Ascent	8000.00	0.00	0.00	0.00	0.00
Return Transit	5918.73	21.35	9489.58	8446.20	220.76
Total	48316.37	133.87	39313.01	35468.47	1596.08
ESM	**M (kg)**	**V (m^3)**	**P (kW)**	**C (kW)**	**T (MMH/ Duration)**
Predeployment	6884.79	22.66	7426.542163	6726.076876	0
Transit to Mars	5538.48	17.99	9458.54	8417.79	253.27
Mars Orbit	4402.39	14.23	5454.67	5097.82	603.02
Descent	8000.00	0.00	0.00	0.00	0.00
Surface Ops	0.00	22.66	7426.54	6726.08	603.02
Ascent	8000.00	0.00	0.00	0.00	0.00
Return Transit	5538.48	17.99	9458.54	8417.79	253.27
Total	22364.14	95.51	39224.85	35385.56	1712.57

Table S1: xESM Parameters

11.2 SI: Case Study 1

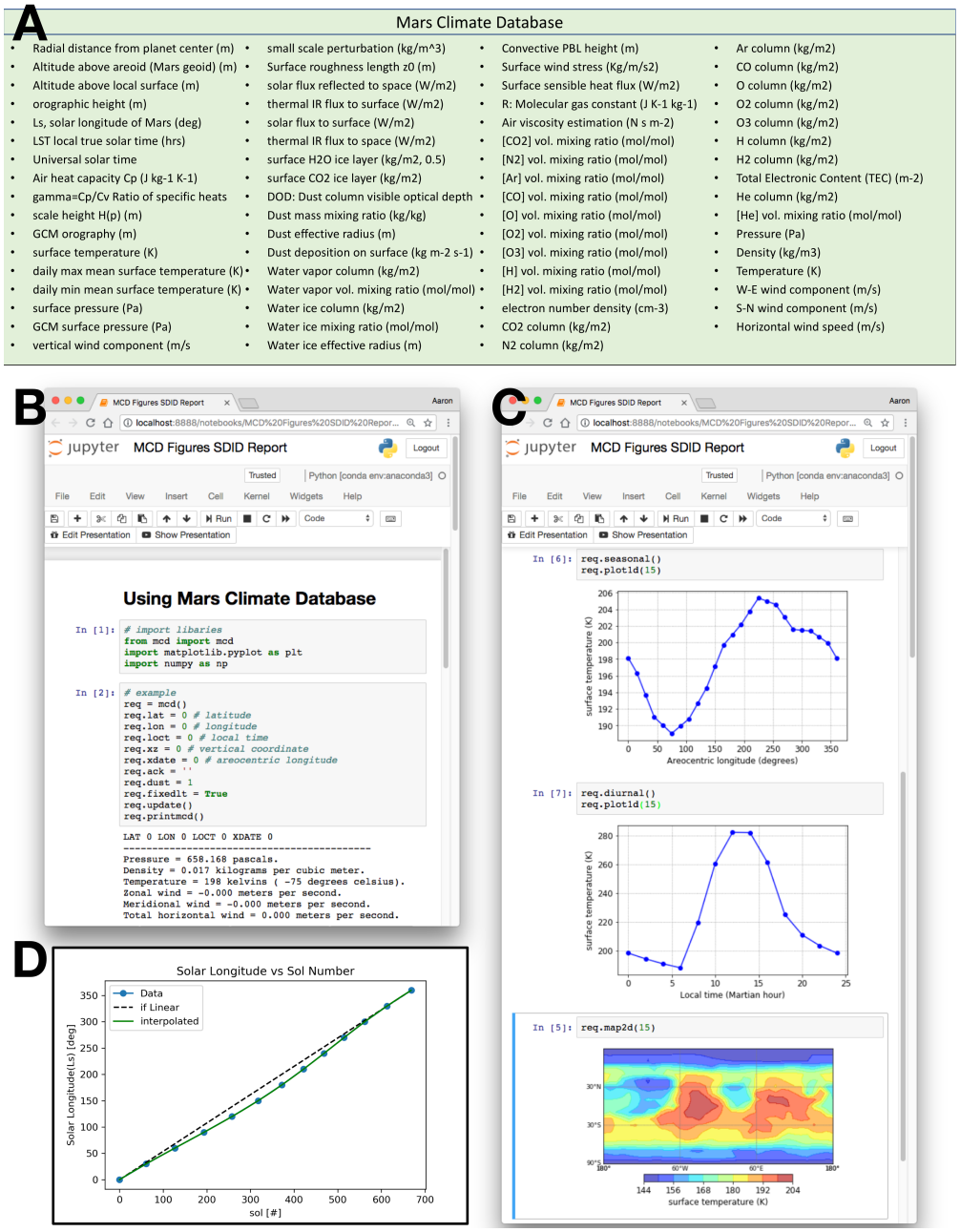

Figure S1: **(A)** all parameters available for query in the MCD; **(B.)** example query to MCD; **(C.)** i. plot of surface temperature vs areocentric longitude for local time t = 9:00; ii. plot of surface temperature vs local time for LATITUDE = LONGITUDE = 0; iii. cylindrical projection of surface temperature; **(D.)** Plot of solar longitude vs sol number, demonstrating the eccentricity of Mars's orbit and the approximate season, with northern summer solstice occurring when Ls = 90 and northern winter solstice when Ls = 270.

A central question surrounding possible settlement of Mars is whether human life can be supported by available technologies using *in situ* resources. Here we present a detailed analysis showing that photovoltaic and photoelectrochemical devices would be adequate and practical to sustain a crewed outpost for an extended period over a large fraction of the planet's surface. Climate data were integrated with a radiative transfer model to predict spectrally-resolved solar flux across the Martian surface, which informed detailed balance calculations for solar cell devices supporting power systems, agriculture, and manufacturing. Optimal design and the corresponding production capacity over a Martian year revealed the size and mass of a solar cell array required to support a six-person mission, which represents less than 10% of the anticipated payload.

The following SI describes the `redSun` software created as an integration of available software and custom code written in Python 3.6 with UNIX and Fortran backends. It can be found at https://github.com/cubes-space/redSun.

Environmental Data Aggregation

Mars Climate Database

Downstream radiative transfer calculations require a number of input streams describing the Martian environment. We make use of the Mars Climate Database (MCD) [48] developed by Le Laboratoire de Meteorologie Dynamique (LMD) in Paris, queried via the mcd-python package, to model most climate and environmental constraints, including photon flux and power spectra over time and location. The software engineering processes for building and using MCD somewhat efficiently are illustrated in Figure S1, along with input parameter profiles and sample output plots.

Initial Geotemporalspatial Grid

We began by first initializing the geotemporalspatial grid from which all downstream radiative transfer and PV/PEC calculations would be based. The grid was composed as a `.netCDF` file with dimensions of 19 points of 10° latitude × 37 points of 10° longitude × 25 points of 15° areocentric longitude × 13 points of 2 (Martian) hours. Additionally, we included the dimension of altitude above the Martian datum in 20 points ranging from 0 to 120 km. The dimensions for the initial grid are shown in Table S2.

Atmospheric Variables

Through a combination of custom code in redSun and modifications to the Python-based extension of MCD, we then looped through Lat, Lon, Hr, and Ls dimensions to initialize the data variables in Table S3.

Dimension	Units	Initial	Final	Step	Number
Latitude	degrees north	-90	90	15	19
Longitude	degrees east	-180	180	15	37
Wavelength	nm	300.5	4000	N/A	1340
Level	km	0	120	6.32	20
Aerocentric Longitude	deg	0	360	15	25
Hour	hr	0	24	2	13

Table S2: Initial grid dimensions.

Variable	Units	Dimensions	Dimension Number
Air Density	cm^{-3}	lat,lon,level,ls,hr	5
Datum Altitude	km	lat,lon,level	3
CO_2 Partial Pressure	cm^{-3}	lat,lon,level,ls,hr	5
H_2O Partial Pressure	cm^{-3}	lat,lon,level,ls,hr	5
O_2 Partial Pressure	cm^{-3}	lat,lon,level,ls,hr	5
O_3 Partial Pressure	cm^{-3}	lat,lon,level,ls,hr	5
NO_2 Partial Pressure	cm^{-3}	lat,lon,level,ls,hr	5
Pressure	hPa	lat,lon,level,ls,hr	5
Temperature	K	lat,lon,level,ls,hr	5
Ice Content	g/m^3	lat,lon,level,ls,hr	5
Ice Effective Radius	um	lat,lon,level,ls,hr	5
Dust Content	g/m^3	lat,lon,level,ls,hr	5
Dust Effective Radius	μm	lat,lon,level,ls,hr	5
Long Wave Downward Flux	W/m^2	lat,lon,ls,hr	4
Short Wave Downward Flux	W/m^2	lat,lon,ls,hr	4
Long Wave Upward Flux	W/m^2	lat,lon,ls,hr	4
Short Wave Upward Flux	W/m^2	lat,lon,ls,hr	4
Top of Atmosphere Irradiance	$W/(nm.m^2)$	lat,ls,hr,wl	5

Table S3: Initial atmospheric grid variables sourced from MCD.

i

Planetary Variables

While most of the required environmental variables could be sourced from MCD, additional efforts were made to add data on the planetary albedo and zMOL as shown in Figure S2 and in Table S4.

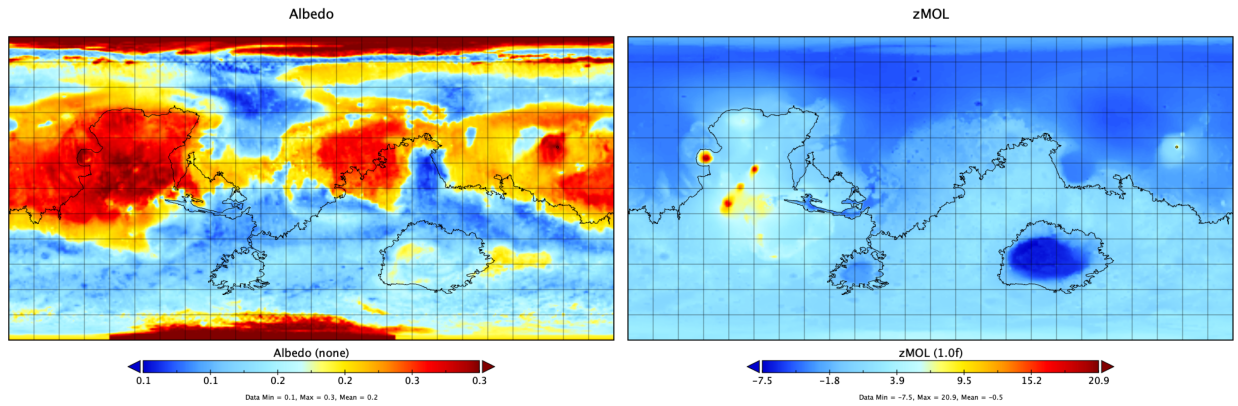

Figure S2: Albedo and zMOL (height above the Martian datum) maps.

Variable	Units	Dimensions	Dimension Number
Albedo	None	lat,lon	2
zMOL	None	lat,lon	2

Table S4: Initial planetary grid variables sourced from MCD.

Solar Variables

In addition to atmospheric and planetary variables, our initial environmental data for downstream radioactive transfer required that we calculate the solar flux at the top of the atmosphere (TOA). Downstream radiative transfer calculations required as input the spectral flux in W/(m^2·nm) whereas MCD only provided an integrated solar flux in W/(m^2). For a given Lat, Lon, Hr, and Ls, we were able to calculate the spectral flux F_0 via[424]

$$F_0 = \mu F_{1.52} \left(\frac{d^2}{r^2} \right) \tag{11.1}$$

$$F_0 = F_{1.52} \left(\sin\theta \sin\epsilon \sin L_s + \cos\theta \cos\left(\frac{2\pi t}{P} \right) \left(1 - \sin^2\epsilon \sin^2 L_s \right)^{1/2} \right) \left(\frac{1 + e\cos(L_s - L_{s,p})}{1 - e^2} \right)^2 \tag{11.2}$$

where r is the Sun-Mars distance along its orbit, d is the mean Sun-Mars distance of 1.52 AU, μ is the cosine of the solar zenith angle z, e is the Martian eccentricity ($e = 0.0934$), L_s is the aerocentric longitude, $L_{s,p}$ is the aerocentric longitude of perihelion (250°), θ is the latitude, ϵ is the Martian obliquity (25.2°), P is the duration of the Martian solar day (88775 s), t is any time measured from local noon, and $F_{1.52}$ is the flux at the average Sun-Mars distance[**Vicente-Retortillo2015ASurface**].

While the separation of the aerocentric longitude and hourly time dimensions was helpful in indexing our grid, these two dimensions are related. For any aerocentric longitude index, there are 13 time points, and as these times correspond to movement of Mars around the sun, so does the aerocentric longitude. Therefore, when computing the TOA flux F_0, we updated L_s to correspond to the change in time t using the build in functions `Ls2Sol` and `Sol2Ls` from the `MCD` package. These functions relate L_s and t through Kepler's Problem via

$$L_s = \left(\nu \frac{180}{\pi} + L_{s,p}\right)(mod 360) \tag{11.3}$$

$$\nu = 2\arctan\left[\sqrt{\frac{1+e}{1-e}}\tan\left(\frac{E}{2}\right)\right] \tag{11.4}$$

$$M = E - e\sin E = 2\pi\frac{D_s - t_p}{N_s} \tag{11.5}$$

where D_s is the sol number, t_{peri} is the time at perihelion, N_s is the number of sols in a Martian year, ν is the true anomaly, E is the eccentric anomaly, M is the mean anomaly, and N_s is the number of sols in a Martian year.

The data variables shown in Figure S3 were then added to the grid for downstream use as shown in Table S5.

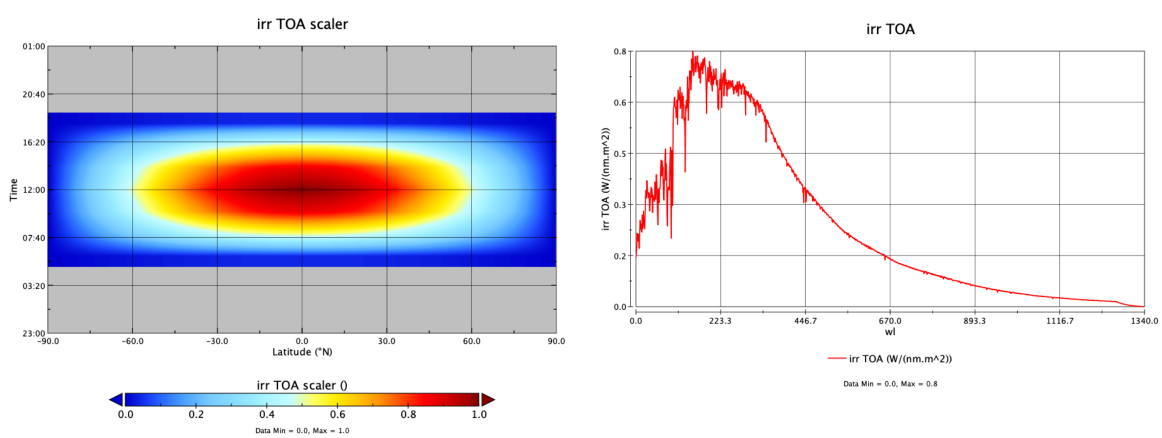

Figure S3: Left shows the calculated mu parameter as a scalar across geospace for $L_s = 0$. Right shows the spectral flux for lat=0, t=12 noon, and $L_s = 0$.

As a sanity check, we calculated the integrated standard solar flux at TOA at 1.52 AU (average Sun-Mars distance) at 576.92 W/m^2. Given a solar constant for Mars is 490 W/m^2, the equatorial annual-mean flux at the top of the atmosphere (TOA) should be ∼156 W/m^2. Our calculated equatorial annual-mean TOA flux was found to be 159.43 W/m^2 which differs by ∼1.5% from the theoretical value. We extended this calculation across all latitudes as shown in Figure S4 to confirm our methods.

Variable	Units	Dimensions	Dimension Number
Solar Zenith Angle	deg	lat,ls,hr	3
Solar Correction	None	lat,ls,hr	3
Top of Atmosphere Irradiance	W/(nm.m^2)	lat,ls,hr,wl	5

Table S5: Initial solar grid variables.

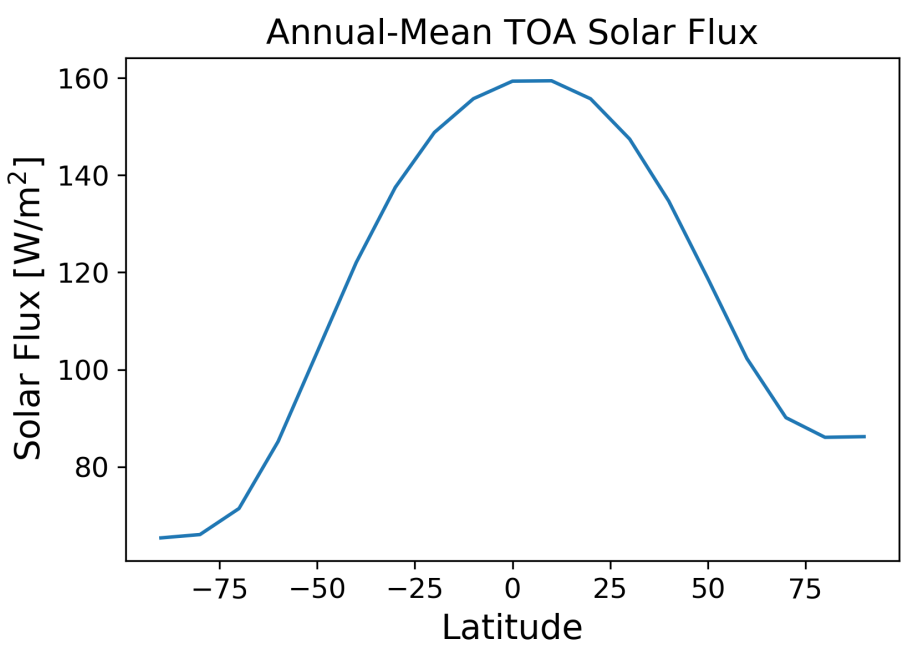

Figure S4: Calculated Annual-Mean TOA Solar Flux distributed across Latitude

Radiative Transfer Calculations

libRadtran

The radiative transfer calculations were carried out using the libRadtran library (version 2.0.4)[358, 161]. libRadtran is a collection of C and Fortran functions and programs for calculation of solar and thermal radiation in the Earth's atmosphere and is freely available under the GNU General Public License at http://www.libradtran.org/doku.php.

Mie Scattering Calculations

The presence of dust and cloud particles in the Martian atmosphere affect the propagation of sunlight. The size of such dust and cloud particles falls within the Mie scattering range.

The libRadtran package was used for Mie scattering calculations of the scattering phase matrices and corresponding Legendre polynomials[568]. Input files for both dust and ice were constructed (Listing 11.1) and fed to the `MIEV0` tool.

```
mie_program MIEV0 # Select Mie code by Wiscombe
basename cloud.
refrac file MieCloudRefrac.DAT# Use refractive index file
r_eff 0.00322766 100.1 10.0  # Specify effective radius grid
distribution lognormal 1.8903 # Specify lognormal size distribution
nstokes 1 # Calculate all phase matrix elements
nmom 6000 # Number of Legendre terms to be computed
nthetamax 2000 # Maximum number of scattering angles to be
output_user netcdf # Write output to netcdf file
verbose # Print verbose output
```

Listing 11.1: Input file for Mie calculations of cloud aerosols

Refractive indices for dust and ice were sourced from NASA Ames Legacy Mars Global Climate Model[207] (available at https://github.com/nasa/legacy-mars-global-climate-model) and fed as input (Figure S5).

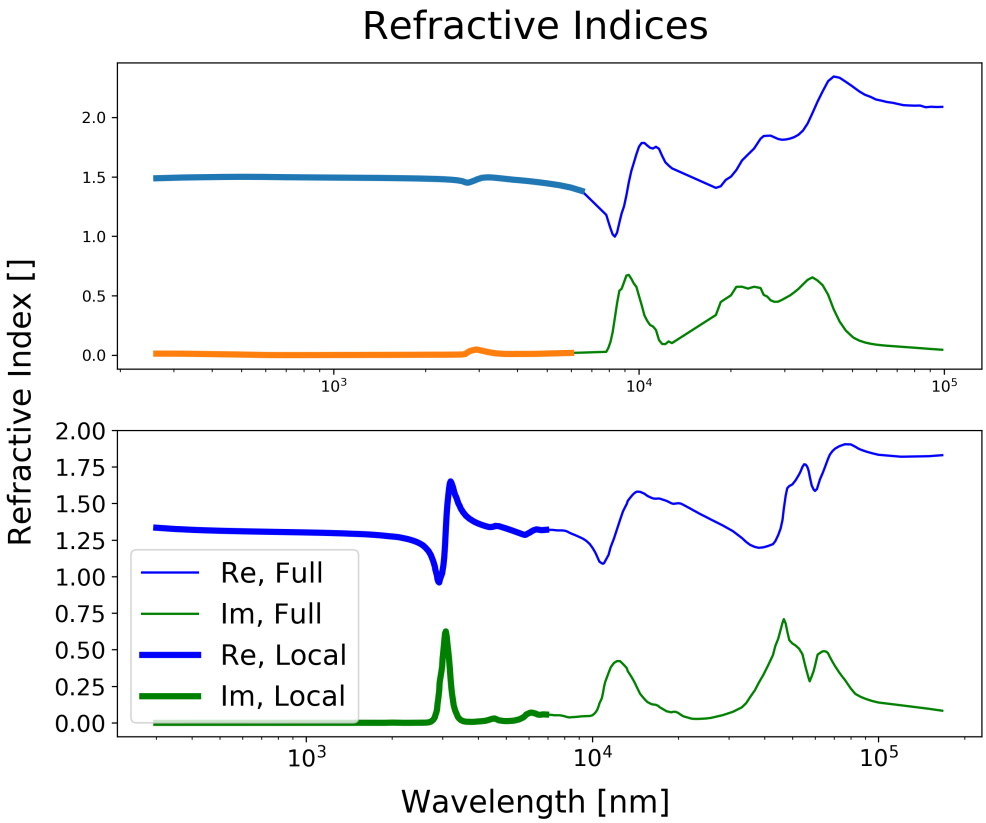

Figure S5: Refractive Indices for Dust (top) and Clouds (Bottom).

For clouds, an effective radius r_{eff} grid was set between 0.00322766 and 100.1 μm in steps of 10 μm and with a lognormal distribution with standard deviation $\sigma = 1.8903$ described as

$$n(r) = \frac{a}{r} \exp\left(-\frac{1}{2}\left(\frac{\ln(r)\ln(r_0)}{\ln\sigma}\right)^2\right) \tag{11.6}$$

where r_0 is the logarithmic mode of the distribution, calculated from r_{eff}. Through a series of trial-and-error attempts, we specified additional parameters for clouds such as the number of phase matrix elements set at 1, the number of Legendre terms to be computed set at 6000, the maximum number of scattering angles set to 2000. The resulting output from `MIEV0` was a `.netCDF` file of ∼100 MB.

For dust, an effective radius r_{eff} grid was set between 0.00310352 and 10.1 μm in steps of 1.0 μm and with a lognormal distribution with standard deviation $\sigma = 1.3616$. Again, through a series of trial-and-error attempts, we specified additional parameters for dust such as the number of phase matrix elements set at 1, the number of Legendre terms to be computed set at 2500, the maximum number of scattering angles set to 2000. The dust calculations provided more computationally expensive than those for clouds due to the smaller r_{eff} grid size. The resulting output from `MIEV0` was a `.netCDF` file of ∼10 MB.

The output `.netCDF` files include the dimensions and variables in Table S6 and a sample of the output variables are shown in Figure S6.

uvspec

The `uvspec` program was designed to calculate the radiation field of the atmosphere for Earth. Modifications were carried out such that `uvspec` could be leveraged for similar calculations of the Martian radiative transfer. Input to the model are the constituents of the atmosphere including various molecules, aerosols and clouds. The absorption and scattering properties of these constituents were calculated via the `MIEV0` tool. Boundary conditions are the solar spectrum at the top of the atmosphere and the reflecting surface at the bottom[359]. The `uvspec` program was called for each point in the geotemporalspatial grid and provided with a custom, programmatically generated input file – an example of which is shown in Listing 11.2.

```
# libRadtran Calc test
wavelength 300.5 4000 # choose wavelength range for computation
atmosphere_file __2WKSII17KGatmos.DAT # load atmosphere profile
mixing_ratio CH4 0.0 # update null mixing ratios
mixing_ratio N2O 0.0
mixing_ratio F11 0.0
mixing_ratio F12 0.0
mixing_ratio F22 0.0
altitude -0.48425 # specify altitude above datum
source solar __2WKSII17KGflux.DAT # load solar profile
# corrected for Sun-Mars Distance
```

Name	Description	Dim/Var	Unit
nlam	Wavelength Number	Dim	-
nmommax	Legendre Polynomial Number	Dim	-
nphamat	Phase Matrix Element Number	Dim	-
nreff	Refractive Index Number	Dim	-
nthetamax	Theta Max Number	Dim	-
nrho	Density Number	Dim	-
wavelen	Wavelength	Var	micrometer
reff	Effective radius	Var	micrometer
ntheta	Number of scattering angles	Var	-
theta	Theta Max Number	Var	degrees
phase	phase	Var	-
nmom	number of Legendre polynomials	Var	-
pmom	Legendre polynomials	Var	including factor 2*l+1
ext	extinction coefficient	Var	km^-1/(g/m^3)
ssa	single scattering albedo	Var	-
gg	Asymmetry factor	Var	-
refre	refractive index (real)	Var	-
refim	refractive index (imaginary)	Var	-
rho	density of medium	Var	g/cm^3

Table S6: Dimensions and variables in `.netCDF` Mie output file.

```
# corrected for geometry
ic_file 1D __2WKSII17KGcloud.DAT # setup cloud profile (assuming water/ice clouds)
ic_properties MieCalc/cloud.mie.cdf interpolate
profile_file dust 1D __2WKSII17KGdust.DAT # setup dust profile (using aerosol type)
profile_properties dust MieCalc/dust.mie.cdf interpolate
earth_radius 3389.5 # reset earth_radius to Martian radius in [km]
rte_solver disort pseudospherical # choose radiative transfer solver
pseudospherical
number_of_streams 6 # choose number of streams
output_user lambda edir eglo edn eup enet esum # define output
albedo 0.3073502629995346 # choose albedo
```

Listing 11.2: Sample input file for uvspec calculation

Due to the peculiar way `uvspec` must be called, input for atmosphere, solar flux, dust conditions, and cloud conditions are required in the form of text-based `.DAT` files. Because multiple `uvspec` calls were carried out in parallel, a random string was generated ("2WKSII17KG" in the case of Listing 11.2) and used to identify specific `.DAT` files. For each point of the grid, an

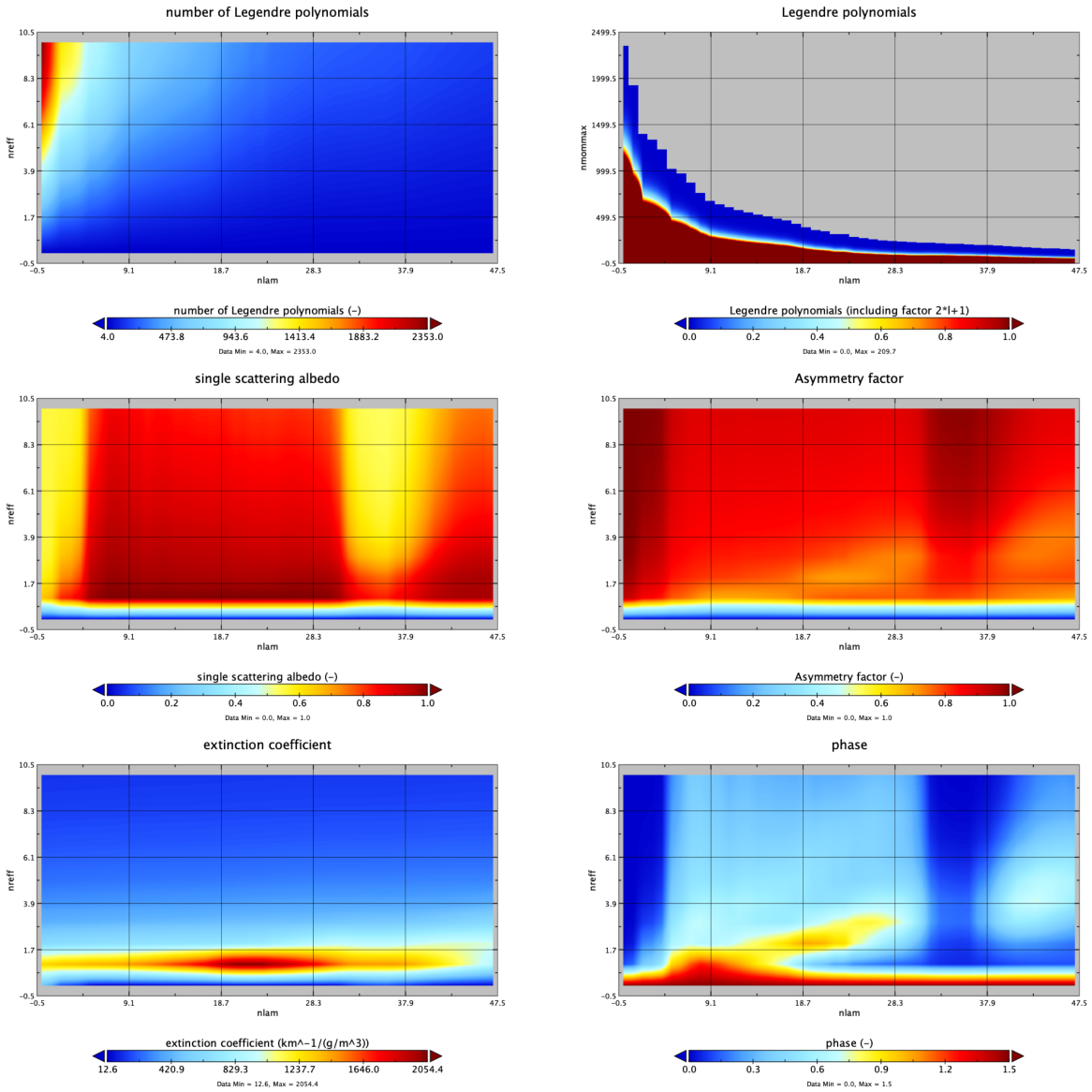

Figure S6: Sample Visualization of variables in `.netCDF` Mie output file for dust.

input `.INP` file was created along with correspond `.DAT` files for atmosphere, solar flux, dust conditions, and cloud conditions. The atmosphere file contained the altitude above sea level in km, pressure in hPa, temperature in K, air density in cm^{-3}, ozone density in cm^{-3}, Oxygen density in cm^{-3}, water vapor density in cm^{-3}, CO_2 density in cm^{-3}, and NO_2 density in cm^{-3}. The dust and cloud aerosol files contained altitude above sea level in km, dust/cloud content in kg/kg, and effective radius in μm. The solar flux file contains the wavelength in nm and the spectral flux for that wavelength in mW/(m^2nm). Data for each of these files

was sourced from the MCD data organized in the `Stupidgrid.nc` file and converted to the appropriate units using functions in the `redSun` codebase.

The wavelength range was set from 300.5 to 4000 nm. This range was selected to match available data for solar flux and significance to downstream photovoltaic calculations. Wavelengths outside these bounds were found to have negligible impact on bandgap calculations or to require substantial computational efforts, and were thus ignored. The mixing ratios for atmospheric CH_4, N_2O, and greenhouse gases (GHG) F11, F12, and F22 were set to 0.0 to reflect the change from Earth to Mars conditions. The altitude for the location was also programmatically added to the input file to specify the exact position of the surface in relationship to the Martian datum. The filenames from the Mie scattering calculations for dust and cloud aerosols were passed as well. The radius of the planet was changed to the Martian value of 3389.5 km. The albedo of the grid-point was also provided programmatically.

We selected the DIScrete ORdinate Radiative Transfer solvers (`pseudospherical disort`) radiative transfer solver for our calculations using 6 streams. The discrete ordinate method was first developed in 1960 with significant updates in 1988 and 2000 and offer 1D calculations of radiance, irradiance, and actinic flux. We opted for pseudo-spherical methods to offset any spherical effects associated with using the smaller Martian geometry. In pseudo-spherical calculations, the monochromatic radiative transfer equation in 1D can be formulated as

$$\mu \frac{dI(\tau,\mu,\phi)}{\beta^{\text{ext}} d\tau} = I(\tau,\mu,\phi) - \frac{\omega(r)}{4\pi}\int_0^{2\pi} d\phi' \int_{-1}^{1} d\mu' p(\tau,\mu,\phi;\mu',\phi') I(\tau,\mu',\phi') - (1-\omega(r))B[T(r)] - \frac{\omega(\tau)I^0}{4\pi} p(\tau \tag{11.7}$$

where $B[T(r)]$ is the Planck function, β is an extinction coefficient, μ_0 is the solar zenith angle, ϕ_0 is the azimuth angle, p is the phase function, and the single scattering albedo $\omega(r)$ is

$$\omega(r) = \omega(r,\nu) = \frac{\beta^{\text{sca}}(r,\nu)}{\beta^{\text{ext}}(r,\nu)} \tag{11.8}$$

Additionally, f_{ch} is the Chapman function[451, 131] for describing the extinction path in a spherical atmosphere and is formulated as

$$f_{ch}(r_0,\mu_0) = \int_{r_0}^{\infty} \frac{\beta^{\text{ext}}(r,\nu)dr}{\sqrt{1-\left(\frac{R+r_0}{R+r}\right)^2(1-\mu_0^2)}} \tag{11.9}$$

where R is the planet radius and r_0 is the distance above the atmosphere.

The output of each `uvspec` call was a text-like file that was indexed with a matching random string identifier. Each file consisted of the direct, global, diffuse downward, diffuse upward, net and sum irradiance in mW/(m^{2}nm) for each nm in the input flux file. The output file was then read back with additional functions from `redSun` for use in downstream calculations.

Photovoltaic Power and Photoelectrochemical Commodity Calculations

We use the detailed balance model to calculate the energy efficiency of one-, two-, and three-bandgap photovoltaic solar cells and one- and two-bandgap photoelectrochemical devices. This model has been used to calculate the limiting efficiency of ideal photovoltaic and photoelectrochemical devices for single and multiple bandgap architectures previously[211, 146, 239].

The current density (J)-voltage (V) dependence $J\left(V, E_g\right)$ for a single bandgap is given by

$$J\left(V, E_g\right) = J_G(E_g) + J_R(V, E_g) \tag{11.10}$$

where J_G is the photogeneration current, J_R is the recombination current due to radiative recombination, and E_g is the bandgap of the absorber material. The generation current J_G is calculated according to

$$J_G(E_g) = q \int_{E_g}^{E_{\max}} \Gamma(E) dE \tag{11.11}$$

where q is the electronic charge, $\Gamma(E)$ is the photon flux at a given photon energy E, and $E_{\max}$ is maximum photon energy in the solar spectrum. We used a minimum wavelength of 300 nm in our calculations, corresponding to a maximum photon energy of ∼4.14 eV because photons above 4 eV contribute negligibly to the photon flux[211]. The recombination current density J_R is calculated according to

$$J_R(V, E_g) = \frac{2\pi q}{c^2 h^3} \int_{E_g}^{\infty} \frac{E^2}{\exp\left(\frac{E-qV}{kT}\right) - 1} dE \tag{11.12}$$

where c is the speed of light in vacuum, h is Planck's constant, k is Boltzmann's constant, and T is the temperature of the device (we assume the local surface temperature in these calculations).

The photovoltaic energy efficiency η_{PV} at a given operating voltage is written as

$$\eta_{\mathrm{PV}}(V, E_g) = \frac{V}{F} J(V, E_g) \tag{11.13}$$

where F is the calculated total power flux at the Martian surface. The operating voltage can then be selected to maximize the efficiency for a given bandgap. In technoeconomic calculations (see below), we assume the device efficiency is 80% of the calculated detailed balance limit to account for absorber material and device inefficiencies (i.e., nonradiative recombination losses not captured by the detailed balance limit).

The photoelectrochemical device energy efficiency η_{PEC} is given by

$$\eta_{\mathrm{PEC}}(V, E_g) = \frac{E^0}{F} J(V, E_g) \tag{11.14}$$

where E^0 is the minimum thermodynamic potential required to drive the electrochemical reaction (1.23 V for H_2 generation from water splitting). In practical devices, the operating voltage of the photoelectrochemical device will be larger than E^0 to account for anode and cathode overpotentials and resistive potential drop in the electrolyte and electrodes. Hence, for these devices the operating voltage is

$$V = E^0 + V_o \tag{11.15}$$

where V_o is the overpotential associated with the above-mentioned losses. In all technoeconomic calculations (see below) we assume the overvoltage is 700 mV, corresponding to a practical minimum that also accounts for absorber material inefficiencies (*i.e.*, nonradiative recombination losses not captured by the detailed balance limit)[146].

For two- and three-bandgap tandem devices, we assume the absorber layers are connected optically and electronically in series. Generation and recombination currents are calculated as described above, with the modification that $E_{\max}$ is substituted with $E_{g,n-1}$ for absorber n (counted sequentially starting with the top absorber) to reflect the assumption that each absorber layer is optically thick (i.e, absorbs all the above-bandgap light incident on its surface). In tandem devices, the total current density must be equal in each absorber layer, while the total operating voltage is given by the sum of the voltages developed across each cell. For example, for a three-absorber photovoltaic device

$$J(V) = J_1(V_1, E_{g,1}) = J_2(V_2, E_{g,2}) = J_3(V_3, E_{g,3}) \tag{11.16}$$

$$V = V_1 + V_2 + V_3 \tag{11.17}$$

For tandem devices, the efficiency is calculated analogously to the single-junction devices but as a function of each absorber bandgap.

Grid Calculations via Parallel Computing

SinglePoint Calculation

The calculation of a single gridpoint's spectral flux (via `libRadtran`) and the corresponding photovoltaic and photoelectrochemical production quantities ran for ∼5 minutes. Given the grid of 228475 geotemporalspatial points composed of 19 points of 10° latitude × 37 points of 10° longitude × 25 points of 15° areocentric longitude × 13 points of 2 (Martian) hours, a serial calculation would require 2.17 years. Wanting to avoid that lengthy calculation, we opted for an "embarrassingly parallel" computing method shown in Figure S7. Since our computations require some initial or final communication (generally in the distribution and collection of data, then we call it nearly embarrassingly parallel. In parallel computing, an embarrassingly parallel workload or problem is one where little or no effort is needed to separate the problem into a number of parallel tasks. This is often the case where there is little or no dependency or need for communication between those parallel tasks, or for results between them. In the ideal case, all the sub-problems or tasks are defined before

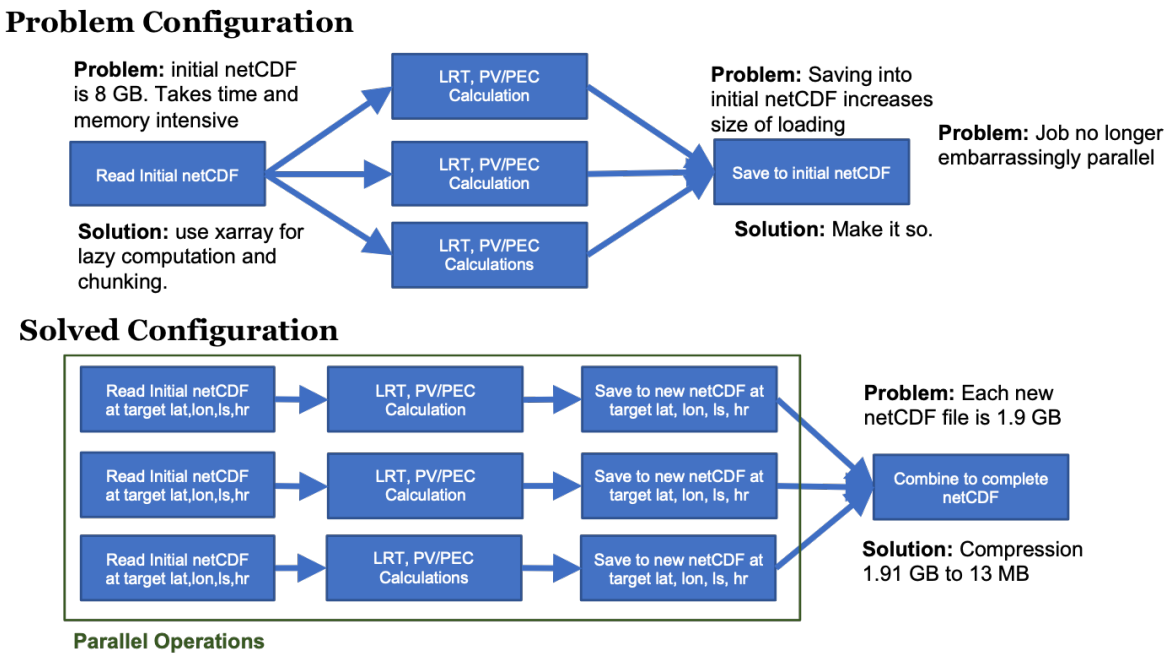

Figure S7: Initial (problem) and final (solution) configurations for the RedSun software on the UC Berkeley cluster.

the computations begin and all the sub-solutions are stored in independent memory locations (variables, array elements). Thus, the computation of the sub-solutions is completely independent[1].

Files were not constructed for grid-points that did not receive sunlight, and so the result was the storage of ∼150k `.netCDF` files, each with a size of ∼4-5 MB.

Stitching

The ∼150k singlepoint `.netCDF` files were initially stitched across time dimensions of hours and areocentric longitude to produce ∼700 time series `.netCDF` files, each for a different pair of latitudes and longitudes using the `tcsh` scripts provided in Listing 11.3 and 11.4.

```
#!/bin/tcsh -f
if ($#argv != 1) then
   echo "--> usage: csh " $0 " netcdf_file"
   exit
endif
set link = `ncdump -v ls,hr,lat,lon $argv[1] | sed -n '/^data:/,$p' | sort
    | paste -s -d" " - | awk '{printf("%s%03d%02d%s%02d%s%02d%s\n","
   ttlrecall_",$15,$3,"_",$11,"_",$7,".nc");}'`
ln -sv $argv[1] $link
```

Listing 11.3: Stitching Algorithm Part 1: Create Dynamic Links

[1] https://www.cs.iusb.edu/~danav/teach/b424/b424_23_embpar.html

```
#!/bin/tcsh -f
set lat = minimum_lat_value
set lon = minimum_lon_value
while ($lat <= maximum_lat_value)
    set latv = `echo $lat | awk '{printf("%02d\n",$1)}'`
    while ($lon <= maximum_lon_value)
           set lonv = `echo $lon | awk '{printf("%02d\n",$1)}'`
           ncecat ttlrecall_*_{$lonv}_{$latv}.nc redsun_timeseries_{$lonv}
   _{$latv}.nc
           echo "Done: " $lonv $latv
@ lon++
     end
@ lat++
end
```

Listing 11.4: Stitching Algorithm Part 2: Assemble into Time Series

Production Mapping

The resultant timeseries `.netCDF` files were then used for constructing the final maps of PV and PEC production. For each time series `.netCDF` file, we began by calculating PV power P and PEC production rate $\dot{m}$ via

$$P = \Gamma \eta_{\text{pv}} \tag{11.18}$$

$$\dot{m}_c = \epsilon_c \Gamma \eta_{\text{pec}} = \frac{Z_c}{n_c V_c F} \Gamma \eta_{\text{pec}} \tag{11.19}$$

where Γ is the solar flux in W/m^2 sourced from the `MCD` data in `StupidGrid.nc`, ϵ is the electrochemical equivalency factor, η is the calculated PV/PEC efficiency, Z is the molar mass, n is the number of moles of electrons required to make one mole of the product, F is the Faraday constant, and V is the voltage. The c term corresponds to the chemical of interest in the set of H_2, NH_3, and AA. The values used to produce the ϵ for each chemical is given in Table S7.

Chemical	n	Z	V
H_2	2	2.016	1.23
NH_3	6	17.031	1.17
AA	8	60.052	1.09

Table S7: Electrochemical equivalency factor parameters.

We calculated the optimal sol-averaged 3-junction PV P_{opt} and 2-junction PEC $\dot{m}_{\text{copt}}$

across all bandgap combinations given the form

$$P_{\text{opt}} = \max\left(\frac{1}{N}\int_{t_2}\int_{t_1} P_{ijk}dt_1dt_2 : \forall i,j,k \in B_1, B_2, B_3\right) \tag{11.20}$$

$$\dot{m}_{c,opt} = \max\left(\frac{1}{N}\int_{t_2}\int_{t_1} \dot{m}_{c,ij}dt_1dt_2 : \forall i,j \in B_1, B_2\right) \tag{11.21}$$

where i, j, k are indices of bandgaps B_1, B_2, B_3, t_1 is the time variable across a sol (∼24.616 hrs/sol), and t_2 is the time variable across a Martian year given as $N = 688$ sols/year.

Computationally, we began by converting our L_s values to the sol number using an inverted Kepler problem with a function `ls2sol` shown in Listing 11.5.

```
def ls2sol(ls):
    N_s = 668.6
    ls_peri = 250.99
    t_peri = 485.35
    a = 1.52368
    e = 0.09340
    epsilon = 25.1919
    if (ls == 0).any():
        ls = .01
    nu = np.radians(ls) + 1.90258
    E = np.arctan((np.tan(nu/2))/(np.sqrt((1+e)/(1-e))))*2
    M = E - e*np.sin(E)
    Ds = (M/(2*np.pi))*N_s + t_peri
    if (Ds < 0).any():
        Ds = Ds + N_s
    if (Ds > N_s).any():
        Ds = Ds - N_s
    return(Ds)
```

Listing 11.5: Function for converting L_s to sol number

The computational instance of calculations for 2J H_2 production is provided in Listing 11.6.

```
def point_loop(file):
    sg = xr.open_dataset('StupidGridFull.nc', group='flux')
    ds = xr.open_dataset(file)
    lat = ds['lat'][0]
    lon = ds['lon'][0]
    G = np.zeros(len(ds['lon']))
    for ri in range(0,len(ds['lon'])):
        ls = ds['ls'][ri]
        hr = ds['hr'][ri]
        G[ri] = sg['flux_dw_sw'][lat,lon,ls,hr]
    lss = np.unique(ds['ls'])
    Z = 2.016
    n = 2
    F = 96485.33212
```

```
    V = 1.23
    sg = 0
    sols = np.zeros(len(lss))
    for i in range(0,len(lss)):
        sols[i] = ls2sol(lss[i]*15)
    hrs = np.arange(0,25,2)
    vals = np.zeros(13)
    try:
        P = G[:, np.newaxis, np.newaxis] * ds['j2_etaPEC_H2_2bg'] * 0.01 *
    Z/(n*F*V)
        zz = np.zeros((len(lss),len(ds['j2-bg1']),len(ds['j2-bg2'])))
        for i in range(0,len(lss)):
            hr_int = np.where(ds['ls']==lss[i])
            inds = np.array(ds['hr'][hr_int])
            for j in range(0,len(ds['j2-bg1'])):
                for k in range(0,len(ds['j2-bg2'])):
                    y = P[:,j,k][hr_int]
                    for m in range(0,len(inds)):
                        vals[inds[m]] = y[m]
                    z = np.trapz(vals*60*60,x=hrs*1.02569)
                    zz[i,j,k] = z
        z = np.zeros((len(ds['j2-bg1']),len(ds['j2-bg2'])))
        for j in range(0,len(ds['j2-bg1'])):
            for k in range(0,len(ds['j2-bg2'])):
                y = zz[:,j,k]
                z[j,k] = np.trapz(y,x=sols)
        j2h2 = np.max(z)
        j2h2i = np.unravel_index(np.argmax(z),np.shape(z), order='C')
        h2 = j2h2 * (1/688)
        bg1 = ds['j2-bg1'][j2h2i[0]]
        bg2 = ds['j2-bg2'][j2h2i[1]]
        return([[lat,lon,0],[h2,bg1,bg2]])
```

Listing 11.6: Function for calculating the optimal H_2 production rate

The results from the calculation of the optimal sol-averaged 3-junction PV P_{opt} and 2-junction PEC $\dot{m}_{\text{copt}}$ and their corresponding bandgap combination were again saved as `.netCDF` files with dimensions of latitude and longitude.

The resulting PV power and PEC production for H_2 is provided in Figure S8-S10 with the corresponding Bandgaps distributions over the Martian grid. The distribution of bandgaps are provided in Figure S11.

Missing Location Values

We were able to complete the calculations for ∼97% of the 228475 geospatial points across the Martian grid. We found that ∼6000 of these points could not be completed due to a number of issues our method of using libRadtran for Mars-based calculations. Upon inspection, we found that the missing values were generally concentrated in areas with very low elevation below the Martian datum. Further inspection confirmed that the issues in

Commodity	**Best efficiency at averaged solar noon**	**Best production over a year**
Power (PV, 3-junction)	Top: 1.77 eV	Top: 1.83 eV
	Middle: 1.16 eV	Middle: 1.16 eV
	Bottom: 0.72 eV	Bottom: 0. 67 eV
H_2 (PEC, 2-junction)	Top: 1.64 eV	Top: 1.77 eV
	Bottom: 0.95 eV	Bottom: 0.83 eV

Table S8: Comparison of optimal bandgaps for different optimization strategies

resolving the radiative transfer were caused by errors in interpolation by the solver for the gas concentrations below the datum. However, these ∼2% of missing values do not prevent us from offering a meaningful analysis.

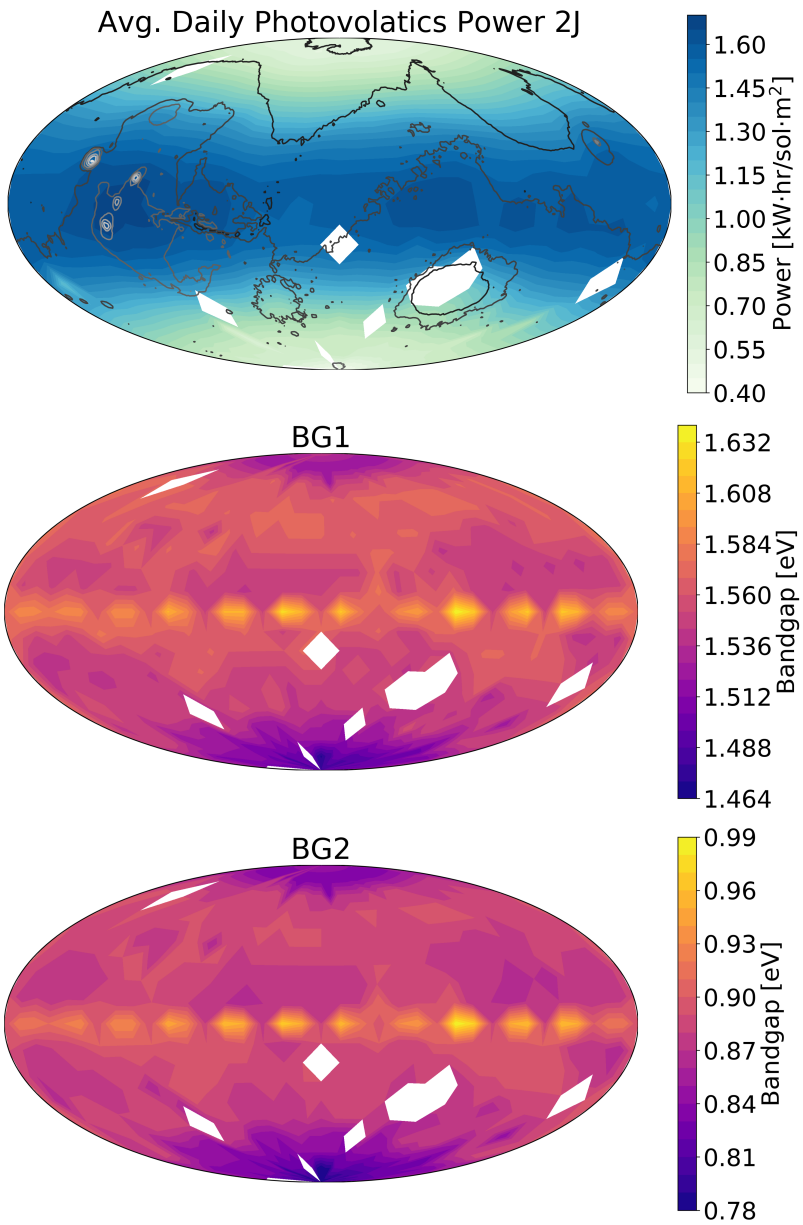

Figure S8: Two Junction Photovoltaic Power Production and Optimal Bandgaps distributed over the Martian Grid

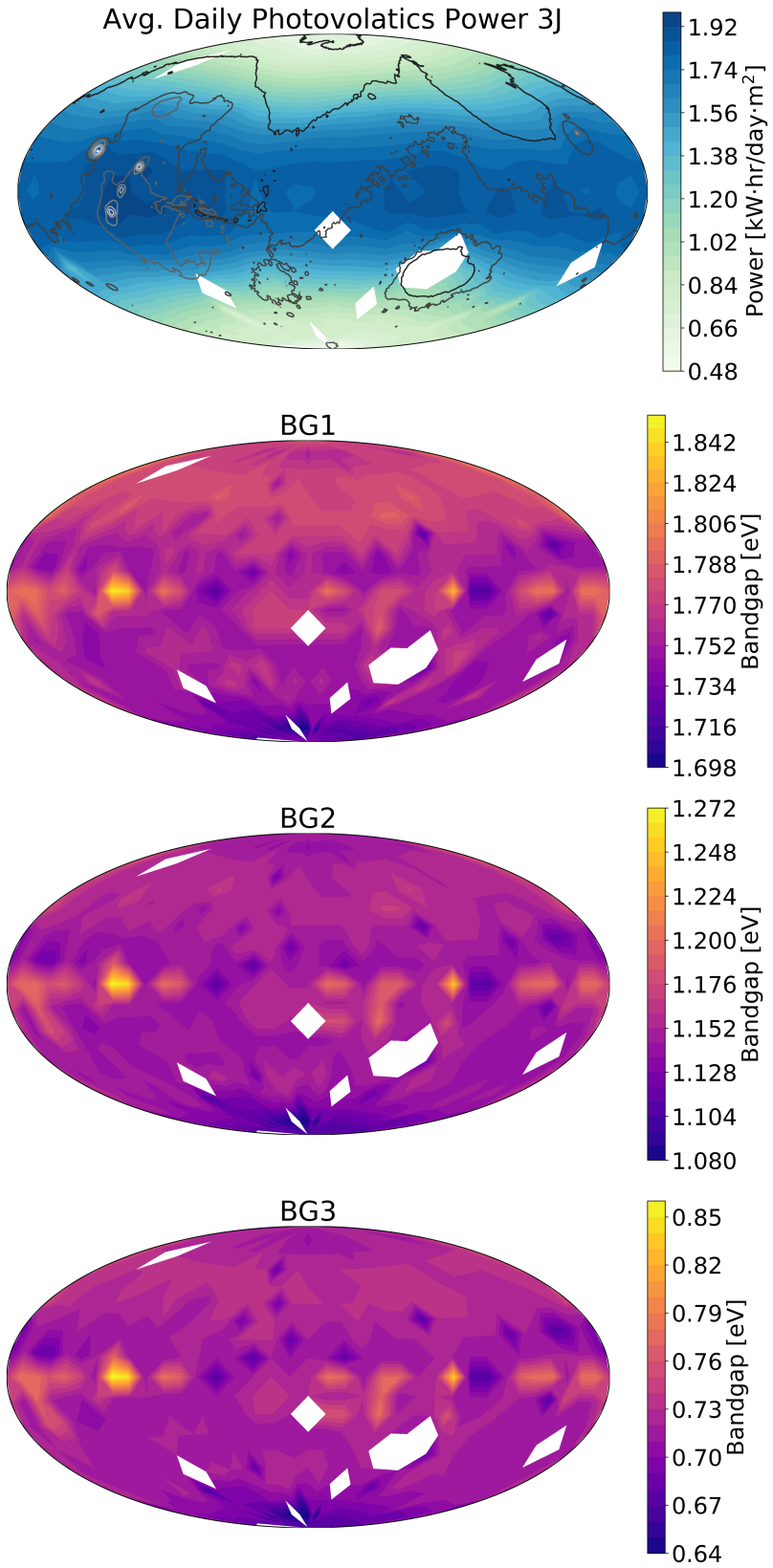

Figure S9: Three Junction Photovoltaic Power Production and Optimal Bandgaps distributed over the Martian Grid

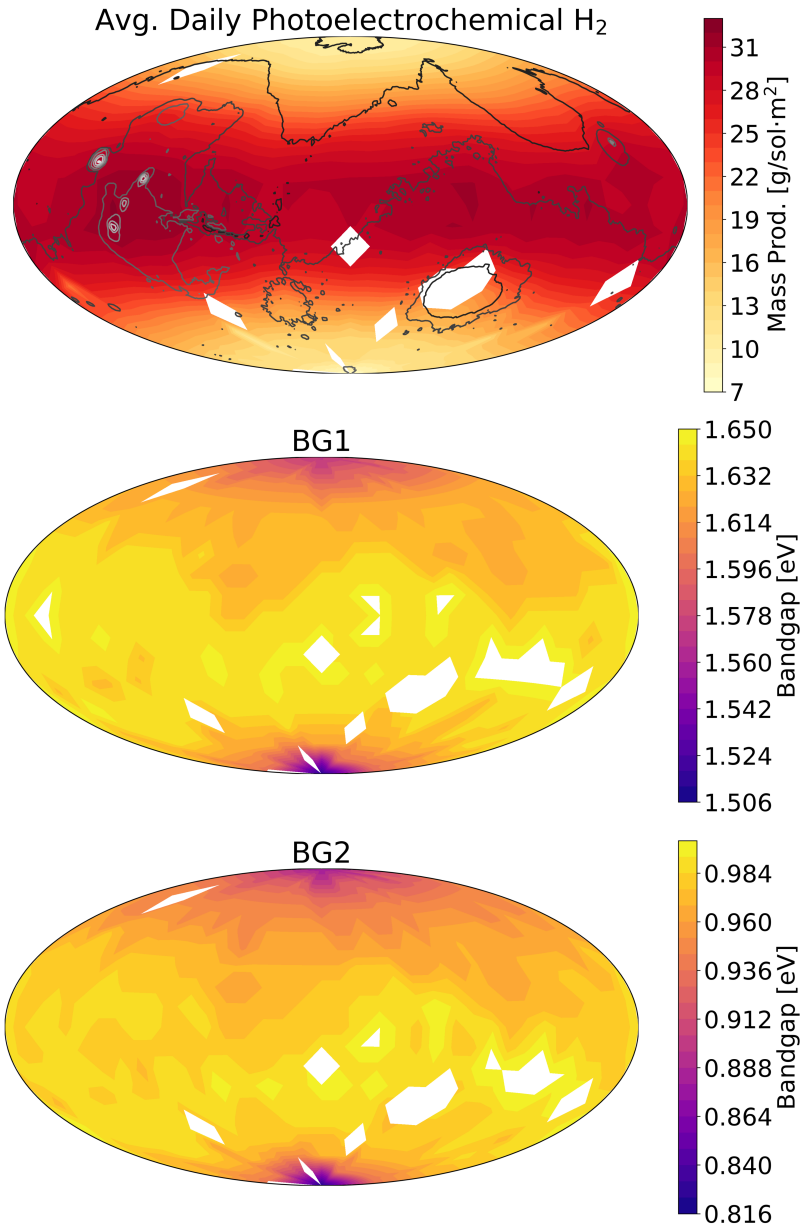

Figure S10: Two Junction Photoelectrochemical H_2 Production and Optimal Bandgaps distributed over the Martian Grid

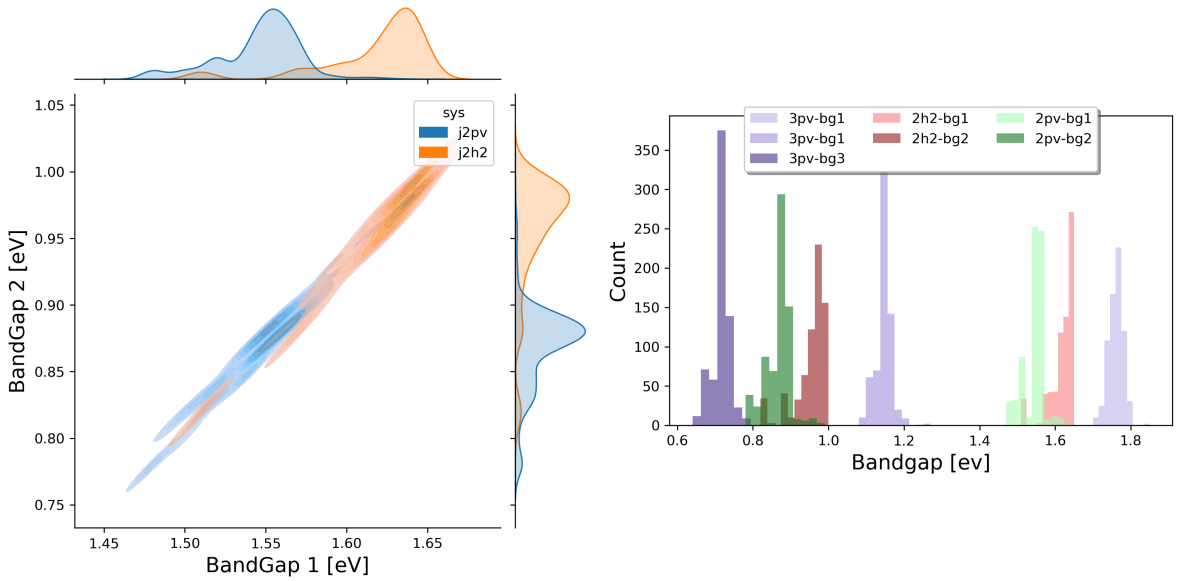

Figure S11: Optimal Bandgap Distributions.

Technoeconomic Calculations

Primary Power and Energy Demands

We consider four different power production and energy storage scenarios for comparison (Fig. S12): (1) Nuclear power generation with the Kilopower system; (2) Photovoltaic power generation with battery energy storage; (3) Photovoltaic power generation with compressed H_2 energy storage, and (4) Photoelectrochemical H_2 generation with compressed H_2 energy storage.

In all cases, power and/or energy demand is driven by continuous power required for habitat operations, including lighting, heating/cooling, pressurization, power draw for ISRU processes, and power draw for rover travel, and by materials demand for ISRU manufacturing. We assume that ammonia, methane, and plastics are produced using H_2 as the starting material (along with N_2 and CO_2 sourced from the atmosphere), which we use to calculate power demands based on water electrolysis to produce H_2. We note that methane could be diverted for bioprocess production (dashed lines in Fig. S12), although we don't explicitly consider this scenario here since it would not change the relative mass requirements of the four systems we consider.

To compare the carry-along mass necessary for each system, we include the mass of elements unique to or uniquely sized for a given energy supply scenario. For example, we consider the mass of photovoltaic cells because the area of cells necessary to power the habitat and ISRU manufacturing will be different depending on the strategy for energy

storage. However, we don't include the mass of the Sabatier reactor for methane production, since this mass will be equivalent regardless of the upstream processes producing H_2 and

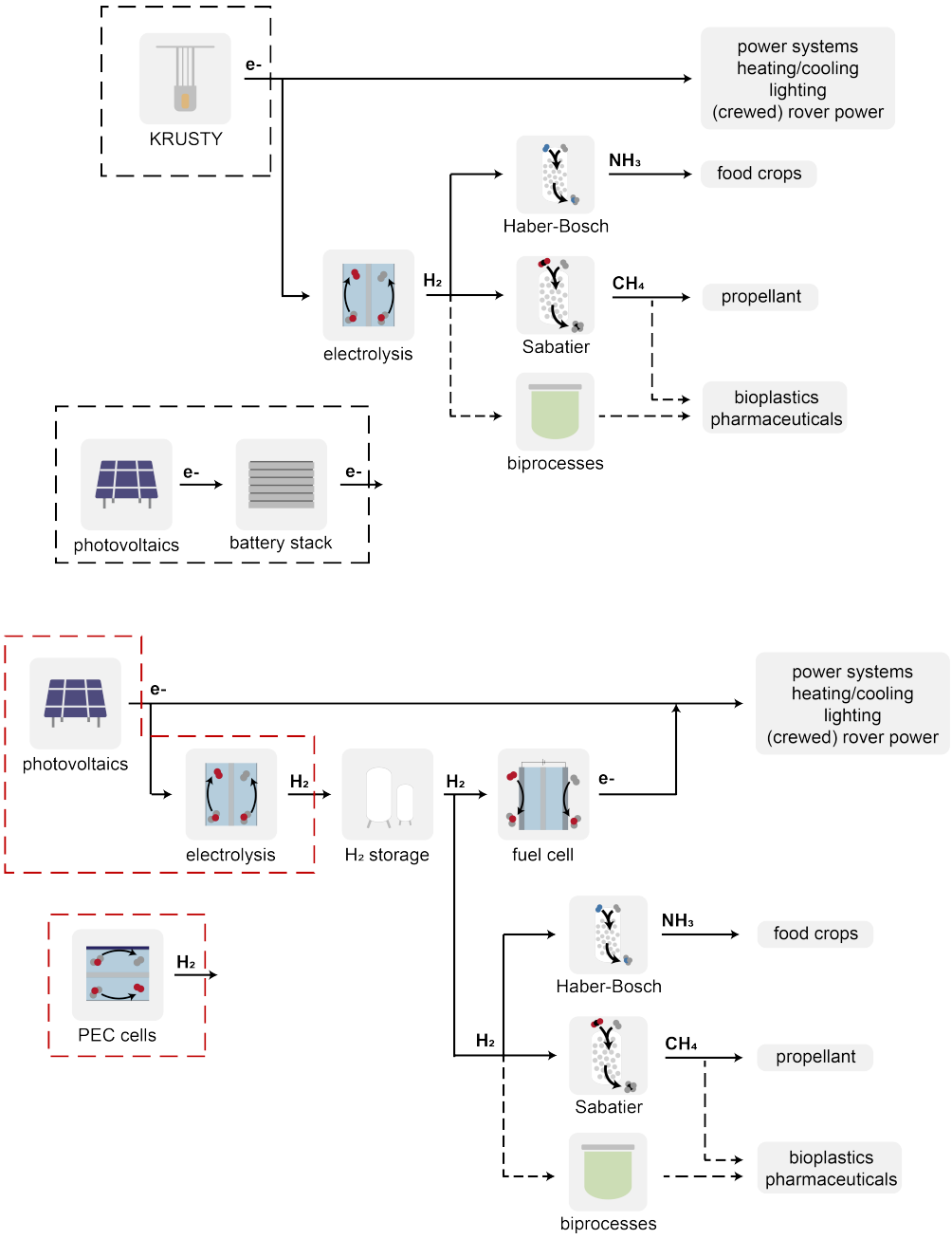

Figure S12: Power generation systems options. Habitat power systems and ammonia, propellant, and bioplastics production can be powered by nuclear power generation (KRUSTY), photovoltaics with battery storage (PV+B), photovoltaics with H2 energy storage from hydrolysis (PV+E), or photoelectrochemical H2 generation and storage (PEC).

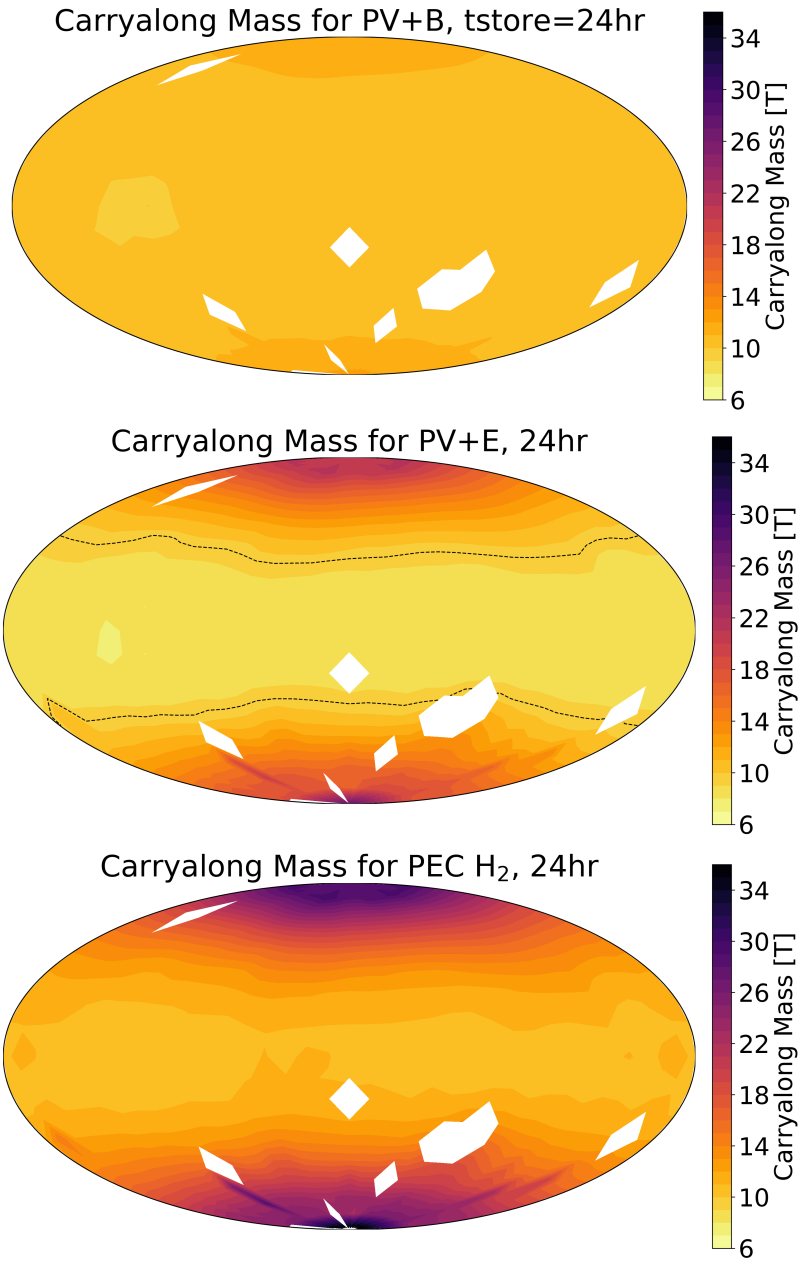

Figure S13: Carry-along mass for different power generation scenarios. Carry-along mass across the Martian surface for PV+B, PV+E, and PEC power generation systems. PV+B and PEC systems cannot reach parity with nuclear power generation in terms of carry along mass (no locations at which the projected mass of the PV+B or PEC systems is less than the projected mass of the nuclear system).

collecting CO_2 from the atmosphere. In this way, we can determine the mass contributions only of the uniquely necessary components for each energy supply scenario. The carry along masses are provided in Figure S13.

Nuclear Power

Power derived from the Kilopower nuclear reactor system is fed directly to habitat power systems and to an electrolyzer producing H_2 for ISRU manufacturing. Hence, the power draw is given by:

$$P_{\mathrm{K}} = P_{\mathrm{Hab}} + \alpha_{\mathrm{E}} \left(\dot{N}\alpha_{\mathrm{HB}} + \dot{M}\alpha_{\mathrm{S}} + \dot{B}\alpha_{\mathrm{HB}} \right) \tag{11.22}$$

$$P_{\mathrm{K}} = P_{\mathrm{Hab}} + \alpha_{\mathrm{E}}\Lambda \tag{11.23}$$

where P_{K} is the total power draw for Kilopower nuclear reactor system, P_{Hab} is the power draw for the habitat, α_{E} is the energy demand per unit of H_2 produced for the electrolyzer, $\dot{N}$ is the ammonia demand rate, $\dot{M}$ is the methane demand rate, $\dot{B}$ is the bioplastic demand rate, and α_i is the conversion factor between, e.g., the ammonia demand rate and the H_2 demand rate for the Haber-Bosch process. We also define $\Lambda = \dot{N}\alpha_{\mathrm{HB}} + \dot{M}\alpha_{\mathrm{S}} + \dot{B}\alpha_{\mathrm{HB}}$.

The carry-along mass requirements for this scenario is given by

$$M_{\mathrm{K}} = \frac{P_{\mathrm{K}}}{p_{\mathrm{K}}} + \frac{\Lambda}{p_{\mathrm{E}}} \tag{11.24}$$

where p_{K} is the specific power of the Kilopower reactor (6.25 W/kg) and p_{E} is the specific productivity of the electrolyzer (kg H_2/h/kg).

Photovoltaic power with battery energy storage (PV+B)

Power generated by photovoltaic cells can be transferred either directly to power-drawing systems (habitat systems, water electrolysis) or diverted to battery stacks for storage to enable continuous operation either at night or during low-sunlight days (due to high dust conditions). We define the fraction of power supplied directly to power systems as χ, which, for photovoltaic systems, can be thought of as the fraction of the day that solar cells produce equal or more power than what is consumed by power-drawing systems. Unless otherwise stated, we assume in our calculations $\chi = 1/3$. Hence, the total power draw for the PV+B system is given by:

$$P_{\mathrm{PV+B}} = \chi P_{\mathrm{Hab}} + \frac{1-\chi}{\eta_{\mathrm{B}}} P_{\mathrm{Hab}} + \chi\alpha_{\mathrm{E}}\Lambda + \frac{1-\chi}{\eta_{\mathrm{B}}}\alpha_{\mathrm{E}}\Lambda \tag{11.25}$$

where $P_{\mathrm{PV+B}}$ is the total power draw for the PV+B system and η_{B} is the energy efficiency of the battery storage system. More compactly,

$$P_{\mathrm{PV+B}} = \left(\chi + \frac{1-\chi}{\eta_{\mathrm{B}}} \right) (P_{\mathrm{Hab}} + \alpha_{\mathrm{E}}\Lambda) \tag{11.26}$$

The carry-along mass required for the PV+B scenario is given by

$$M_{\mathrm{PV+B}} = \frac{P_{\mathrm{PV+B}}}{p_{\mathrm{PV}}} + \frac{(P_{\mathrm{Hab}} + \alpha_{\mathrm{E}}\Lambda)}{e_{\mathrm{B}}} t_{\mathrm{store}} + \frac{\Lambda}{p_{\mathrm{E}}} \tag{11.27}$$

where p_{PV} is the specific power of photovoltaic cells, t_{store} is the desired back-up power availability time, and e_{B} is the specific energy of the battery stack (units of energy per mass).

Parameter	Value	Unit	Reference
Power and Material Demands			
P_{Hab}	40	kW	Note 11.2
$\dot{N}$	8.33×10^{-3}	kg h^{-1}	Note 11.2
$\dot{M}$	0.61	kg h^{-1}	Note 11.2
$\dot{B}$	0.1	kg h^{-1}	Note 11.2
Conversion Factors			
α_{HB}	0.196	$\mathrm{kgH_2\ kgNH_3^{-1}}$	Note 11.2
α_{S}	0.554	$\mathrm{kgH_2\ kgCH_4^{-1}}$	Note 11.2
α_{BP}	0.155	$\mathrm{kgH_2\ kgAA^{-1}}$	Note 11.2
α_{E}	54.13	$\mathrm{kWh\ kgH_2^{-1}}$	Note 11.2
α_{FC}	0.064	$\mathrm{kgH_2\ kWh^{-1}}$	Note 11.2
α_{HS}	3.39	$\mathrm{kWh\ kgH_2^{-1}}$	Note 11.2
Power[212] and Energy Density[159]			
p_{K}	6.25×10^{-3}	kW kg^{-1}	Note 11.2
η_{B}	80	%	Note 11.2
p_{E}	1.14×10^{-2}	$\mathrm{kgH_2\ h^{-1}\ kg^{-1}}$	Note 11.2
e_{B}	0.16	kWh kg^{-1}	Note 11.2
p_{FC}	0.365	kW kg^{-1}	Note 11.2
e_{HS}	7.18×10^{-2}	$\mathrm{kgH_2\ kg^{-1}}$	Note 11.2
Solar Cell Array Mess			
M_{PV}	2	kg m^{-2}	Note 11.2
M_{PEC}	2.4	kg m^{-2}	Note 11.2
Other Parameters			
χ	0.33	–	Assumed
t_{store}	24.6	h	Assumed

Table S9: Additional PV/Power Parameters and Conversion Factors.

Photovoltaic power with H_2 energy storage

In this scenario, power generated by photovoltaic cells can either be directly fed to habitat systems or to an electrolyzer, which produces H_2 for consumption in ISRU manufacturing and for consumption by fuel cells the supply power to the habitat and other demands when direct power cannot (e.g., at night). Here, the total power demand for the system is given by

$$P_{\mathrm{PV+E}} = \chi P_{\mathrm{Hab}} + \alpha_{\mathrm{E}} \dot{m}_{\mathrm{H_2}} \tag{11.28}$$

where $P_{\mathrm{PV+E}}$ is the total power draw for the PV+E system and $\dot{m}_{\mathrm{H_2}}$ is the flow rate of H_2 necessary to support the remaining system requirements. This flow rate is written as

$$\dot{m}_{\mathrm{H_2}} = \frac{(1-\chi)P_{\mathrm{Hab}}\alpha_{\mathrm{FC}} + \Lambda}{1 - \alpha_{\mathrm{HS}}\alpha_{\mathrm{FC}}} \tag{11.29}$$

where α_{FC} is the H_2 consumed per unit of energy produced by the fuel cell and α_{HS} is the energy consumed per unit of H_2 stored by the H_2 storage tanks (driven by compression of H_2).

The carry-along mass required for the PV+E scenario is given by

$$M_{\mathrm{PV+E}} = \frac{P_{\mathrm{PV+E}}}{p_{\mathrm{PV}}} + \frac{\dot{m}_{\mathrm{H_2}}}{p_{\mathrm{E}}} + \frac{P_{\mathrm{Hab}} + \alpha_{\mathrm{HS}}\dot{m}_{\mathrm{H_2}}}{p_{\mathrm{FC}}} + \frac{(P_{\mathrm{Hab}}\alpha_{\mathrm{FC}} + \Lambda)t_{\mathrm{store}}}{e_{\mathrm{HS}}} \tag{11.30}$$

where p_{FC} is the specific power of the fuel cell and e_{HS} is the specific mass of the H_2 storage tanks (in units $\mathrm{kgH_2/kg_{tank}}$).

Photoelectrochemical (PEC) H_2 generation with H_2 energy storage

This scenario uses an H_2 demand as opposed to a power demand to size the PEC array. The total H_2 demand rate is given by

$$\dot{m}_{\mathrm{H_2}} = \frac{P_{\mathrm{Hab}}\alpha_{\mathrm{FC}} + \Lambda}{1 - \alpha_{\mathrm{HS}}\alpha_{\mathrm{FC}}} \tag{11.31}$$

The carry-along mass required for the PEC scenario is given by

$$M_{\mathrm{PEC}} = \frac{\dot{m}_{\mathrm{H_2}}}{m_{\mathrm{PEC}}} + \frac{P_{\mathrm{Hab}} + \alpha_{\mathrm{HS}}\dot{m}_{\mathrm{H_2}}}{p_{\mathrm{FC}}} + \frac{(P_{\mathrm{Hab}}\alpha_{\mathrm{FC}} + \Lambda)t_{\mathrm{store}}}{e_{\mathrm{HS}}} \tag{11.32}$$

where m_{PEC} is the specific productivity ($\mathrm{kgH_2/h/kg}$) of PEC cells. All parameters for these calculations are compiled in Table S9.

Secondary Power and Energy Demands

Habitat Power Demand

Continuous power demand estimates for a Martian habitat range between 4 and ∼100 kW. We use 40 kW as a baseline value following the NASA Baseline Values and Assumptions Document (BVAD)[16]. This value includes ISRU power demands, including for crop growth, so we only calculated additional power demands for H_2 production for the ISRU processes considered.

Ammonia Demand

To calculate an upper-bound ammonia demand, we followed the optimization strategy by Do *et al.* assuming no recycling of nitrogen via urea recovery[143]. Briefly, we assumed that the metabolic demands for six crew members would be met entirely by food crops grown in hydroponic chambers. We used values from the BVAD and related literature to calculate nitrogen demand per nutrient availability for a given crop[16, 562]. The optimization function was defined to balance minimization of area necessary for crop growth with maximization of crop variability for human morale as

$$f = w_1 \sum_i A_i + w_2 \sigma(\boldsymbol{A}) \tag{11.33}$$

$$s.t. : \sum_i A_i r_i x_{i,j} > X_j \tag{11.34}$$

where f is the optimization function, A_i is the growth area for crop i, σ is the standard deviation of the vector of crop areas ($\boldsymbol{A}$), r_i is the static growth rate, $x_{i,j}$ is the nutritional content of crop i for nutrient j, and X_j is the crew member demand for nutrient j. The relative weights w_1 and w_2 are related by

$$w_2 = 1 - w_1 \tag{11.35}$$

and w_1 was varied between 0 and 1. Using $w_1 = 0.25$, all 5 crops we considered (soybeans, wheat, lettuce, potatoes, peanuts) were included, resulting in a total crop growth area of ∼421 m^2 and an ammonia demand of ∼205 g/sol, which we converted to 8.33 g/h for consistent units in Table S9. The nitrogen demand ranged between ∼285 g/sol and ∼194 g/sol for $0 < w_1 < 1$.

We assume ammonia is produced via the Haber-Bosch process with the characteristic reaction

$$N_2 + 3H_2 \rightarrow 2NH_3 \tag{11.36}$$

Hence, the H_2:NH_3 conversion factor is 0.196 $kgH_2/kgNH_3$ assuming 90% conversion of H_2.

Methane Demand

Resupply and crew member return to Earth from Mars will require that interplanetary transit vehicles can be refueled on Mars. We use the estimate by Kleinhenz and Paz[291] that such refueling requires 6978 kgCH_4 produced every 480 sols, corresponding to a CH_4 production rate of 0.61 kg/h. We assume this methane is produced via the Sabatier reaction:

$$CO_2 + 4H_2 \rightarrow CH_4 + 2H_2O \tag{11.37}$$

resulting in an H_2:CH_4 conversion factor of 0.554 kg H_2/kgCH_4 assuming 90% conversion efficiency.

Bioplastics and Biopharmaceutical Demand

Bioplastics and pharmaceutical demands for a Martian habitat are not well-defined in the literature. For a system where 50% of spare parts necessary for a habitat are generated via additive manufacturing based on ISRU, Owens *et al.* estimated that 9800 kg of spare parts mass would be necessary over 260 months (an extremely long duration with multiple resupplies and crew member exchanges)[418] Assuming these spares are generated from bioplastics, which are in turn produced from acetic acid at 50% yield by C_2 feedstock-utilizing microorganisms[44], this corresponds to ∼0.1 kg/h acetic acid demand. We assume acetic acid is produced by acetogens with a molar ratio of 4.2:1 (corresponding to 95% of H_2 reducing power diversion to acetic acid production, a common value for acetogens), this corresponds to an H_2:CH_3COOH ratio of 0.155 kgH_2/kg CH_3COOH assuming 90% conversion.

Pharmaceutical demand is not expected to exceed 1 g/sol, so we neglect this amount for the purposes of our calculations here.

Water electrolyzer, H_2 fuel cell, and H_2 storage systems

Water electrolysis and H_2 fuel cell power demands are based on commercially available, low-weight fuel cell systems designed for transportation vehicles[2]. The electrolyzer requires 54.13 kWh/kgH_2, while the fuel cell requires 0.064 kgH_2/kWh. We assume H_2 storage is accomplished with Type IV compression chambers at 350 bar, which stores H_2 at 20.77 kgH_2/m^3 with a tank mass of 289.23 kg/m^3, corresponding to a H_2 storage density of 0.0718 kgH_2/kg[141, 34]. For these systems, 3.39 kWh/kgH_2 is required to compress H_2 to 350 bar, which we account for in the total power demand[141].

Solar Cell Array Mass

Commercial low-weight, flexible solar cell arrays have an installed mass of 2.0 kg/m^2[3]. We are not aware of similarly commercial PEC arrays, so we assume that the installed mass is

[2] G-HFCS-6kW Hydrogen Fuel Cell Power Generator (Fuel Cell Store, Product Code: 1035012)

[3] MiaSolé Flex-03W Series Module with adhesive

driven primarily by the absorber material as opposed to the catalyst layers or ion exchange membrane. We therefore estimate an installed mass of 2.4 kg/m^2 by assuming the absorber and housing components comprise 80% of the installed mass.

11.3 SI: Case Study 3

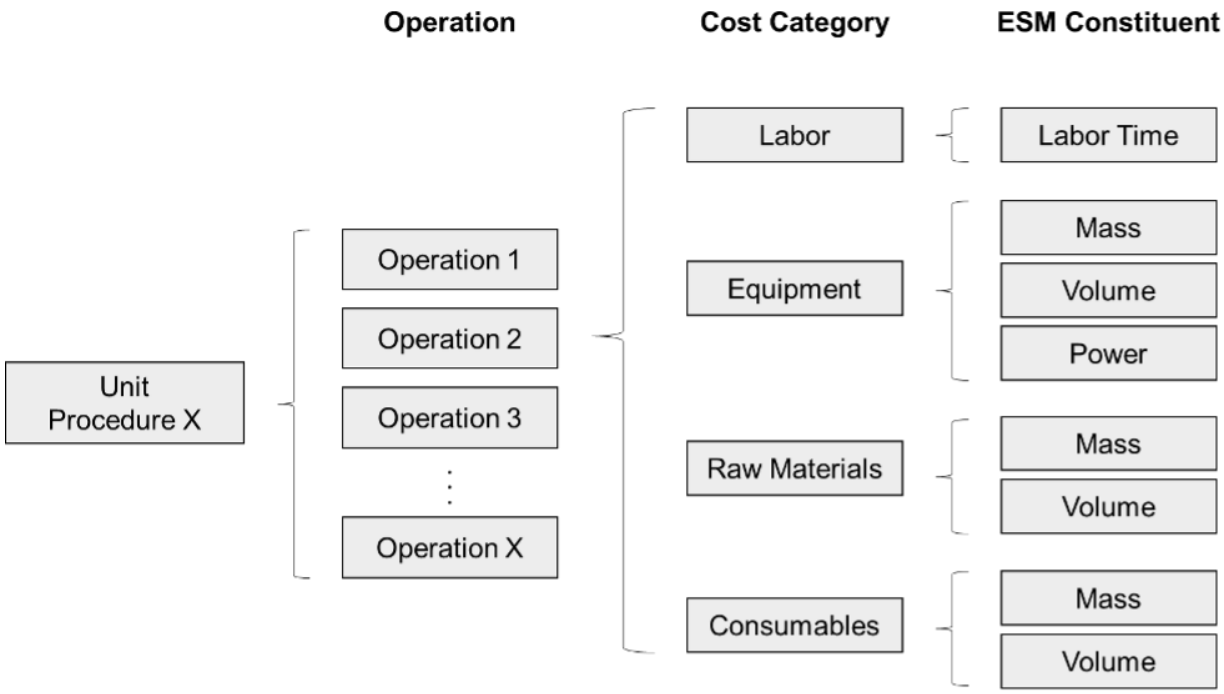

Figure S14: Schematic of deterministic unit procedure model construction grouped by operation, cost category, and equivalent system mass (ESM) constituent.

mAb	Indication	Dose	Need Basis
Erenumab-aooe (FDA Label)	Migraine headache prevention	70 mg (or 140 mg)	1 dose/month
Romosozumab (FDA Label)	Bone regeneration	210 mg	1 dose/month
Gemtuzumab ozogamicin*	Acute myeloid leukemia	6 mg/m2; 3 mg/m^2; 2 mg/m^2	day 1/day 8/every 4 weeks; 1 course/year

Table S10: Example commercially approved monoclonal antibody (mAb) therapies of relevance to human health in space that have been considered in the determination of the reference mission pharmaceutical demand. Need basis is defined per the listed indication and FDA label. Demand estimates are derived by multiplying the FDA-approved need basis by the crew size and the duration of the demand. Asterisk (*) denotes an antibody drug conjugate.

Unit Procedure	Code	mAb Binding Capacity	Maximal Feed Stream Volume
Pre-packed chromatography	CHM	30 mg/mL resin	N/A
Spin column	SPN	1 mg/column	0.6 mL
Magnetic bead	MAG	27 mg/mL bead slurry	0.3 mL
Plant virus-based nanoparticle	VIN	4 mg/mL stock solution	2 mL*
Elastin-like polypeptide	ELP	0.42 mg/mL stock solution	0.8 mL$^{*,\alpha}$
Oilbody-oleosin	OLE	6.74 mg/mL stock solution	0.1 mL$^{*,\gamma}$

Table S11: Unit procedure assumptions for maximal feed stream volume and monoclonal antibody (mAb) binding capacity. ***** based on 2 mL unit volume; actual feed stream volume added is based on the amount of stock solution required and thus mAb quantity in the feed stream. α reduced from 2 mL maximal to account for volume needed for salt solution addition (0.4 mL) and required 1:1 volume ratio of ELP:mAb. γ reduced from 2 mL maximal to account for required 1:20 volume ratio of OLE:mAb.

Operation	Value	Unit
Monitoring	0.05	labor hour/hour
Preparation (incubation + centrifugation)	1	min/effective batch
Pipetting liquid	0.5	min/solution type
	0.1	min/additional unit/effective batch
Resuspending pellet	1	min/unit

Table S12: Labor time standardizations applied to common operations across unit procedures.

Segment	Leq (kg/kg)	Meq (kg/kg)	Veq (kg/m^3)	Peq (kg/kW)	Ceq (kg/kW)	Teq (kg/CM-h)
Pre-deployment (Pd)	2.77	1	9.16	237	40	0.7
Transit to Mars (Tr1)	10	1	133.8	136	50	0.7
Surface Operation (Su)	1	1	9.16	228	145	0.7
Return Transit (Tr2)	10	1	133.8	136	50	0.7

Table S13: Equivalency factor values used to generate equivalent system mass values from constituents of mass, volume, power, cooling, and labor.

Unit procedure	Optimal number of batches per mission
CHM	342
SPN	948
MAG	5670
VIN	360
ELP	2058
OLE	846

Table S14: Optimal number of batches per mission in the base case scenario for each unit procedure, as determined via minimization of equivalent system mass.

Segment	Meq (kg/kg)	Veq (kg/m^3)	Peq (kg/kW)	Ceq (kg/kW)	Teq (kg/CM-h)
Surface Operation (Su)	1	215.5	87	146	0.465

Table S15: Mars surface mission equivalency factor values used by Zabel[581] of a space greenhouse.

mg/mL	0.1	0.2	0.35	0.5	75	1	1.5	2	5
CHM	342	342	342	342	342	342	342	342	342
SPN	9450	4728	2700	1896	1260	948	630	568	568
MAG	56694	28350	16200	11340	7560	5670	3780	2838	1134
VIN	2910	1494	882	639	450	360	264	216	132
ELP	7092	3546	2058	2058	2058	2058	2058	2058	2058
OLE	2988	1494	854	846	846	846	846	846	846

Table S16: Optimal number of effective batches per mission in the mAb stream composition scenario analysis conditions for each unit procedure, as determined via minimization of equivalent system mass.

Demand $\times 10^3$ (mg mAb/mission)	1	2	3.5	5	7.5	10	15	20	30
CHM	36	70	120	172	257	342	512	682	1022
SPN	96	192	336	474	714	948	1422	1890	2844
MAG	568	1134	1988	2838	4260	5670	8508	11340	17010
VIN	36	72	126	180	270	360	533	714	1068
ELP	210	414	726	1032	1548	2058	3090	4116	6174
OLE	86	170	300	422	632	846	1264	1692	2532

Table S17: Optimal number of batches per mission in the mAb demand scenario analysis conditions for each unit procedure, as determined via minimization of equivalent system mass.

Model	**Vendor**	**Capacity**	**Mass (kg)**	**Dimensions (cm)**	**Power (kW)**
MiniSpin	Eppendorf	12	3.7	22.5×23.0×13.0	0.085
5418R	Eppendorf	18	22	0.0345	0.32
5427R	Eppendorf	48	30	31.9×54.0×25.4	0.55

Table S18: List of centrifuge models used in the alternative centrifuge scenario.

Centrifuge model	**MiniSpin**	**5418R**	**5427R**
SPN	1422	948	360
VIN	533	360	137
ELP	3090	2058	774
OLE	1264	846	317

Table S19: Optimal number of effective batches per mission in the centrifuge model alternative scenario conditions for each analyzed unit procedure, as determined via minimization of equivalent system mass.

11.4 SI: Space Biomanufacturing

Assumptions and Methodology of Inventory Analysis

In order to construct a set of comparable mission profile scenarios for preliminary techno-economic analysis, we leveraged the NASA 'Advanced Life Support Sizing Analysis Tool' (ALSSAT)[317]; an analysis of cargo inventory broken down for each scenario and compared by means of Equivalent Systems Mass (ESM)[314] was conducted. In its current form[312], the total ESM M is defined only for the operations at a specific location as the sum over the set of all systems as:

$$M = L_{\text{eq}} \sum_{i=1}^{\mathcal{A}} [\underbrace{(M_i \cdot M_{\text{eq}}) + (V_i \cdot V_{\text{eq}}) + (P_i \cdot P_{\text{eq}}) + (C_i \cdot C_{\text{eq}})}_{M_{\text{NCT}}} + \underbrace{(CT_i \cdot D \cdot CT_{eq})}_{M_{\text{CT}}}] \tag{11.38}$$

for subsystem $i \in \mathcal{A}$ of the ESM excluding crew-time M_{NCT} and the ESM including crew-time M_{CT} where M_i, V_i, P_i, C_i are the initial mass [kg], volume [m^3], power requirement [kW$_e$], and cooling requirement [kg/kW$_{\text{th}}$], D is the duration of the mission segment [sol], T_i is the crew-time requirement based on an astronaut crew-member (CM) [CM-h/sol], M_{eq} is the stowage factor accounting for additional structural masses for a subsystem such as shelving [kg/kg], V_{eq} is the mass equivalency factor for the pressurized volume support infrastructure [kg/m^3], P_{eq} is the mass equivalency factor for the power generation support infrastructure [kg/kW$_e$], C_{eq} is the mass equivalency factor for the cooling infrastructure [kg/kW$_{\text{th}}$], CT_{eq} is the mass equivalency factor for the crew-time [kg/CM-h], and L_{eq} is the location factor for the mission segment [kg/kg] which accounts for the cost to transport mass from one location in space to another (such as Earth-orbit to Mars-orbit). Mass equivalency factors (V_{eq}, P_{eq}, C_{eq}, CT_{eq}) are used to convert the non-mass parameters to mass.

Inventory Analysis by Equivalent Systems Mass

Using values sourced from literature, the ALSSAT, and the NASA 'Baseline Values and Assumptions Documentation'[17], we constructed our scenario definitions and parameters as outlined in Table S20. Table 1 includes the Scenario Identifier (A-E), duration of surface mission operations in days, primary surface operation destination (Moon or Mars), and sortie number S_{num}. The sortie number corresponds to the number of "trips" for a given scenario. Also included are the equivalency factors (M_{eq}, V_{eq}, P_{eq}, C_{eq}, CT_{eq}) and location factor L_{eq}, which allow for the comparable calculation of ESM M.

The ALSSAT was then used to generate an exemplar set of inventory elements for all systems and subsystems ($i \in \mathcal{A}$) as shown in Table S21. Table S21 includes a uniformized breakdown for all inventory elements by system, subsystem, and item name – as well as the ESM terms (M, V, P, C, CT) for each element in each scenario. Using the data from Tables S20 and S21, we calculated the total ESM M_t for each scenario using the form $M_t = S_{\text{num}} M_{S_{\text{num}}=1}$.

Table S20: Parameter description of exemplar scenarios—scenarios 'A' and 'B' correspond to single sorties ($N = 1$) to Moon and Mars respectively using standard surface operation duration[17], while scenarios 'C' and 'D' correspond to multi-sortie campaigns with the same 5,400 days of surface operation as the single-sortie scenario 'E'. All scenarios consider a crew-strength of four astronauts. These parameters can be used to calculate the ESM cost and include equivalency factors for volume (V_{eq}), power (P_{eq}), cooling (C_{eq}), crew-time (CT_{eq}), and location (L_{eq}).

Scenario	**Duration**	**Destination**	$S_{\textbf{num}}$	$V_{\textbf{eq}}$	$P_{\textbf{eq}}$	$C_{\textbf{eq}}$	$CT_{\textbf{eq}}$	$L_{\textbf{eq}}$
A	180	Moon	1	126	136	55.4	0.7	7.2
B	540	Mars	1	117.7	162	96	0.7	30
C	180	Moon	30	126	136	55.4	0.7	7.2
D	540	Mars	10	117.7	162	96	0.7	30
E	5,400	Mars	1	117.7	162	96	0.7	30

Inventory Analysis by Elemental Composition

The inventory element composition analysis was carried out by first creating a set of composition classes: Structural Metal, Plastic, Electronics, Fabric, Glass, Rubber, Ceramics, Gas, Biomass, Water, Other. These classes were created as *prima facie* estimates. Next, we estimated the fractional composition for each inventory element as shown in Table S22. We note that these estimates were carried out as approximations and based on a number of factors such as literature and other official NASA resources. However, we acknowledge that often our estimates amount to assumptions and educated guestimations, due to the lack of exact data. That being said, we argue that exact values are not required in these calculations which should be considered an important first step in defining the order of magnitude envelope for a mission inventory's elemental composition.

Table S21: ESM parameters for all inventory items broken down by system and subsystem for each scenario described in Table S20. Parameters included are mass M [kg], V [m^3], power P [kW], cooling C [kW], and crew-time CT [hr][17, 317]. The ESM values correspond to a single sortie $S_{\text{num}} = 1$. (ORU = Orbital Replacement Unit)

			A					B					C					D					E				
System	**Subsystem**	**Item**	**M**	**V**	**P**	**C**	**CT**	**M**	**V**	**P**	**C**	**CT**	**M**	**V**	**P**	**C**	**CT**	**M**	**V**	**P**	**C**	**CT**	**M**	**V**	**P**	**C**	**CT**
Air	APC	Vent/Relief Valve	5.40	0.01	0.00	0.00	0.00	5.40	0.01	0.00	0.00	0.00	5.40	0.01	0.00	0.00	0.00	5.40	0.01	0.00	0.00	0.00	5.40	0.01	0.00	0.00	0.00
Air	APC	Pressure Control Panel	11.20	0.03	18.00	18.00	0.00	11.20	0.03	18.00	18.00	0.00	11.20	0.03	18.00	18.00	0.00	11.20	0.03	18.00	18.00	0.00	11.20	0.03	18.00	18.00	0.00
Air	APC	Manual Pressure Equalization Valve	9.60	0.01	0.00	0.00	0.00	9.60	0.01	0.00	0.00	0.00	9.60	0.01	0.00	0.00	0.00	9.60	0.01	0.00	0.00	0.00	9.60	0.01	0.00	0.00	0.00
Air	APC	Positive Pressure Relief Valve	1.80	0.00	0.00	0.00	0.00	1.80	0.00	0.00	0.00	0.00	1.80	0.00	0.00	0.00	0.00	1.80	0.00	0.00	0.00	0.00	1.80	0.00	0.00	0.00	0.00
Air	APC	Negative Pressure Relief Valve	3.00	0.01	0.00	0.00	0.00	3.00	0.01	0.00	0.00	0.00	3.00	0.01	0.00	0.00	0.00	3.00	0.01	0.00	0.00	0.00	3.00	0.01	0.00	0.00	0.00
Air	APC	Nitrogen Interface Assembly	7.50	0.01	5.50	5.50	0.00	7.50	0.01	5.50	5.50	0.00	7.50	0.01	5.50	5.50	0.00	7.50	0.01	5.50	5.50	0.00	7.50	0.01	5.50	5.50	0.00
Air	APC	Vacuum Access Jumper 5-ft	0.70	0.00	0.00	0.00	0.00	0.70	0.00	0.00	0.00	0.00	0.70	0.00	0.00	0.00	0.00	0.70	0.00	0.00	0.00	0.00	0.70	0.00	0.00	0.00	0.00
Air	APC	Vacuum Access Jumper 35-ft	3.20	0.00	0.00	0.00	0.00	3.20	0.00	0.00	0.00	0.00	3.20	0.00	0.00	0.00	0.00	3.20	0.00	0.00	0.00	0.00	3.20	0.00	0.00	0.00	0.00
Air	ACMA	Verification Gas Assembly	5.40	0.01	0.10	0.10	0.00	5.40	0.01	0.10	0.10	0.00	5.40	0.01	0.10	0.10	0.00	5.40	0.01	0.10	0.10	0.00	5.40	0.01	0.10	0.10	0.00
Air	ACMA	Mass Spectrometer	13.90	0.02	31.80	31.80	0.00	13.90	0.02	31.80	31.80	0.00	13.90	0.02	31.80	31.80	0.00	13.90	0.02	31.80	31.80	0.00	13.90	0.02	31.80	31.80	0.00
Air	ACMA	Sample Pump	3.40	0.00	4.00	4.00	0.00	3.40	0.00	4.00	4.00	0.00	3.40	0.00	4.00	4.00	0.00	3.40	0.00	4.00	4.00	0.00	3.40	0.00	4.00	4.00	0.00
Air	ACMA	Sample Distributor	2.10	0.00	0.10	0.10	0.00	2.10	0.00	0.10	0.10	0.00	2.10	0.00	0.10	0.10	0.00	2.10	0.00	0.10	0.10	0.00	2.10	0.00	0.10	0.10	0.00
Air	ACMA	Data + Control	8.00	0.01	34.90	34.90	0.00	8.00	0.01	34.90	34.90	0.00	8.00	0.01	34.90	34.90	0.00	8.00	0.01	34.90	34.90	0.00	8.00	0.01	34.90	34.90	0.00
Air	ACMA	Low Voltage Power Supply	5.70	0.01	30.80	30.80	0.00	5.70	0.01	30.80	30.80	0.00	5.70	0.01	30.80	30.80	0.00	5.70	0.01	30.80	30.80	0.00	5.70	0.01	30.80	30.80	0.00
Air	ACMA	Chassis	15.80	0.02	0.00	0.00	0.00	15.80	0.02	0.00	0.00	0.00	15.80	0.02	0.00	0.00	0.00	15.80	0.02	0.00	0.00	0.00	15.80	0.02	0.00	0.00	0.00
Air	ACMA	Inlet Valve Assembly	0.00	0.00	0.00	0.00	0.00	0.00	0.00	0.00	0.00	0.00	0.00	0.00	0.00	0.00	0.00	0.00	0.00	0.00	0.00	0.00	0.00	0.00	0.00	0.00	0.00
Air	ACMA	EMI Filter	0.00	0.00	1.80	1.80	0.00	0.00	0.00	1.80	1.80	0.00	0.00	0.00	1.80	1.80	0.00	0.00	0.00	1.80	1.80	0.00	0.00	0.00	1.80	1.80	0.00
Air	SDS	3-way Solenoid Valves	31.50	0.03	0.00	0.00	0.00	31.50	0.03	0.00	0.00	0.00	31.50	0.03	0.00	0.00	0.00	31.50	0.03	0.00	0.00	0.00	31.50	0.03	0.00	0.00	0.00
Air	SDS	Manual Valves	2.53	0.01	0.00	0.00	0.00	2.53	0.01	0.00	0.00	0.00	2.53	0.01	0.00	0.00	0.00	2.53	0.01	0.00	0.00	0.00	2.53	0.01	0.00	0.00	0.00

Table S21: ESM parameters for all inventory items broken down by system and subsystem for each scenario described in Table S20. Parameters included are mass M [kg], V [m^3], power P [kW], cooling C [kW], and crew-time CT [hr][17, 317]. The ESM values correspond to a single sortie $S_{\text{num}} = 1$. (ORU = Orbital Replacement Unit)

			A					B					C					D					E				
Sys-tem	**Sub-system**	**Item**	**M**	**V**	**P**	**C**	**CT**	**M**	**V**	**P**	**C**	**CT**	**M**	**V**	**P**	**C**	**CT**	**M**	**V**	**P**	**C**	**CT**	**M**	**V**	**P**	**C**	**CT**
Air	SDS	Sample probes	1.08	0.00	0.00	0.00	0.00	1.08	0.00	0.00	0.00	0.00	1.08	0.00	0.00	0.00	0.00	1.08	0.00	0.00	0.00	0.00	1.08	0.00	0.00	0.00	0.00
Air	CO_2	Air Selector Valve	12.81	0.01	0.70	0.70	0.99	12.81	0.01	0.70	0.70	0.99	12.75	0.01	0.70	0.70	0.99	12.65	0.01	0.68	0.68	2.74	12.60	0.01	0.68	0.68	29.59
Air	CO_2	Desiccant Bed	24.29	0.25	0.00	0.00	0.24	24.29	0.25	0.00	0.00	0.24	24.07	0.25	0.00	0.00	0.24	23.69	0.24	0.00	0.00	0.66	23.50	0.24	0.00	0.00	7.10
Air	CO_2	Adsorbent Bed	33.13	0.00	578.45	578.40	0.00	33.13	0.00	578.45	578.40	0.00	32.83	0.00	573.15	573.10	0.00	32.32	0.00	564.26	564.20	0.00	32.06	0.00	559.75	559.70	0.00
Air	CO_2	Air Check Valve	0.16	0.00	0.00	0.00	0.00	0.16	0.00	0.00	0.00	0.00	0.16	0.00	0.00	0.00	0.00	0.16	0.00	0.00	0.00	0.00	0.16	0.00	0.00	0.00	0.00
Air	CO_2	Heater Controller	6.60	0.00	38.00	38.00	0.01	6.60	0.00	38.00	38.00	0.01	6.60	0.00	38.00	38.00	0.01	6.60	0.00	38.00	38.00	0.03	6.60	0.00	38.00	38.00	0.30
Air	CO_2	Air Blower	0.82	0.02	40.71	40.71	0.06	0.82	0.02	40.71	40.71	0.06	0.82	0.02	40.34	40.34	0.06	0.81	0.02	39.72	39.72	0.18	0.81	0.02	39.40	39.40	1.92
Air	CO_2	Pre-cooler	2.22	0.00	0.00	0.00	0.00	2.22	0.00	0.00	0.00	0.00	2.21	0.00	0.00	0.00	0.00	2.19	0.00	0.00	0.00	0.00	2.18	0.00	0.00	0.00	0.00
Air	CO_2	Blower/Pre-cooler Motor Controller	1.30	0.00	5.00	5.00	0.00	1.30	0.00	5.00	5.00	0.00	1.30	0.00	5.00	5.00	0.00	1.30	0.00	5.00	5.00	0.00	1.30	0.00	5.00	5.00	0.00
Air	CO_2	CO_2 Pump	6.73	0.00	13.34	13.34	0.04	6.73	0.00	13.34	13.34	0.04	6.70	0.00	13.22	13.22	0.04	6.65	0.00	13.01	13.01	0.11	6.62	0.00	12.91	12.91	1.18
Air	CO_2	CO_2 Pump Motor Controller	1.30	0.01	2.00	2.00	0.00	1.30	0.01	2.00	2.00	0.00	1.30	0.01	2.00	2.00	0.00	1.30	0.01	2.00	2.00	0.01	1.30	0.01	2.00	2.00	0.15
Air	CO_2	Temperature Sensor	0.40	0.00	1.00	1.00	0.00	0.40	0.00	1.00	1.00	0.00	0.40	0.00	1.00	1.00	0.00	0.40	0.00	1.00	1.00	0.00	0.40	0.00	1.00	1.00	0.00
Air	CO_2	Differential Pressure Sensor	0.20	0.00	1.00	1.00	0.00	0.20	0.00	1.00	1.00	0.00	0.20	0.00	1.00	1.00	0.00	0.20	0.00	1.00	1.00	0.00	0.20	0.00	1.00	1.00	0.00
Air	CO_2	Absolute Pressure Sensor	0.20	0.00	1.00	1.00	0.00	0.20	0.00	1.00	1.00	0.00	0.20	0.00	1.00	1.00	0.00	0.20	0.00	1.00	1.00	0.00	0.20	0.00	1.00	1.00	0.00
Air	CO_2	Electrical Harness	4.50	0.00	0.00	0.00	0.00	4.50	0.00	0.00	0.00	0.00	4.50	0.00	0.00	0.00	0.00	4.50	0.00	0.00	0.00	0.00	4.50	0.00	0.00	0.00	0.00
Air	CO_2	Plumbing	4.85	0.00	0.00	0.00	0.00	4.85	0.00	0.00	0.00	0.00	4.82	0.00	0.00	0.00	0.00	4.78	0.00	0.00	0.00	0.00	4.76	0.00	0.00	0.00	0.00
Air	CO_2	Support Structure	29.64	0.00	0.00	0.00	0.00	29.64	0.00	0.00	0.00	0.00	29.51	0.00	0.00	0.00	0.00	29.27	0.00	0.00	0.00	0.00	29.15	0.00	0.00	0.00	0.00
Air	CO_2	Fluid Disconnects	1.97	0.00	0.00	0.00	0.00	1.97	0.00	0.00	0.00	0.00	1.96	0.00	0.00	0.00	0.00	1.95	0.00	0.00	0.00	0.00	1.94	0.00	0.00	0.00	0.00
Air	CO_2	Electronics Cold-Plate	2.71	0.00	0.00	0.00	0.00	2.71	0.00	0.00	0.00	0.00	2.70	0.00	0.00	0.00	0.00	2.68	0.00	0.00	0.00	0.00	2.67	0.00	0.00	0.00	0.00
Air	CO_2	Electronics Interface Plate	1.60	0.00	0.00	0.00	0.00	1.60	0.00	0.00	0.00	0.00	1.60	0.00	0.00	0.00	0.00	1.60	0.00	0.00	0.00	0.00	1.60	0.00	0.00	0.00	0.00

Table S21: ESM parameters for all inventory items broken down by system and subsystem for each scenario described in Table S20. Parameters included are mass M [kg], V [m^3], power P [kW], cooling C [kW], and crew-time CT [hr][17, 317]. The ESM values correspond to a single sortie $S_{\text{num}} = 1$. (ORU = Orbital Replacement Unit)

			A					B					C					D					E				
System	**Subsystem**	**Item**	**M**	**V**	**P**	**C**	**CT**	**M**	**V**	**P**	**C**	**CT**	**M**	**V**	**P**	**C**	**CT**	**M**	**V**	**P**	**C**	**CT**	**M**	**V**	**P**	**C**	**CT**
Air	N_2	MD Shield Instl	0.00	0.00	0.00	0.00	0.00	0.00	0.00	0.00	0.00	0.00	0.00	0.00	0.00	0.00	0.00	0.00	0.00	0.00	0.00	0.00	0.00	0.00	0.00	0.00	0.00
Air	N_2	Multilayer Insulation Assembly-T #1	0.00	0.00	0.00	0.00	0.00	0.00	0.00	0.00	0.00	0.00	0.00	0.00	0.00	0.00	0.00	0.00	0.00	0.00	0.00	0.00	0.00	0.00	0.00	0.00	0.00
Air	N_2	Multilayer Insulation Assembly-T #2	0.00	0.00	0.00	0.00	0.00	0.00	0.00	0.00	0.00	0.00	0.00	0.00	0.00	0.00	0.00	0.00	0.00	0.00	0.00	0.00	0.00	0.00	0.00	0.00	0.00
Air	N_2	Primary Structure Assembly-HPG ORU	0.00	0.00	0.00	0.00	0.00	0.00	0.00	0.00	0.00	0.00	0.00	0.00	0.00	0.00	0.00	0.00	0.00	0.00	0.00	0.00	0.00	0.00	0.00	0.00	0.00
Air	N_2	Tank ORU Assembly	0.00	0.00	0.00	0.00	0.00	0.00	0.00	0.00	0.00	0.00	0.00	0.00	0.00	0.00	0.00	0.00	0.00	0.00	0.00	0.00	0.00	0.00	0.00	0.00	0.00
Air	N_2	Utilities Installation - O_2/N_2 Tank	0.00	0.00	0.00	0.00	0.00	0.00	0.00	0.00	0.00	0.00	0.00	0.00	0.00	0.00	0.00	0.00	0.00	0.00	0.00	0.00	0.00	0.00	0.00	0.00	0.00
Air	N_2	N_2 Bare Tank	80.37	0.00	0.00	0.00	0.00	80.37	0.00	0.00	0.00	0.00	80.43	0.00	0.00	0.00	0.00	163.98	0.00	0.00	0.00	0.00	1443.26	0.00	0.00	0.00	0.00
Air	N_2	HPGA Fluid	81.74	0.00	0.00	0.00	0.00	81.74	0.00	0.00	0.00	0.00	81.83	0.00	0.00	0.00	0.00	144.73	0.00	0.00	0.00	0.00	1107.91	0.00	0.00	0.00	0.00
Air	N_2	Handhold, top mounted	0.22	0.00	0.00	0.00	0.00	0.22	0.00	0.00	0.00	0.00	0.22	0.00	0.00	0.00	0.00	0.38	0.00	0.00	0.00	0.00	2.92	0.00	0.00	0.00	0.00
Air	N_2	Handrail 21.941 in custom	0.38	0.00	0.00	0.00	0.00	0.38	0.00	0.00	0.00	0.00	0.38	0.00	0.00	0.00	0.00	0.67	0.00	0.00	0.00	0.00	5.12	0.00	0.00	0.00	0.00
Air	N_2	Handrail, top mounted	0.40	0.00	0.00	0.00	0.00	0.40	0.00	0.00	0.00	0.00	0.40	0.00	0.00	0.00	0.00	0.70	0.00	0.00	0.00	0.00	5.36	0.00	0.00	0.00	0.00
Air	N_2	Grapple Fixture, flt releasable	11.11	0.00	0.00	0.00	0.00	11.11	0.00	0.00	0.00	0.00	11.13	0.00	0.00	0.00	0.00	19.68	0.00	0.00	0.00	0.00	150.63	0.00	0.00	0.00	0.00
Air	N_2	Accessories	4.02	0.00	0.00	0.00	0.00	4.02	0.00	0.00	0.00	0.00	4.03	0.00	0.00	0.00	0.00	8.21	0.00	0.00	0.00	0.00	72.24	0.00	0.00	0.00	0.00
Air	O_2	MD Shield Instl	0.00	0.00	0.00	0.00	0.00	0.00	0.00	0.00	0.00	0.00	0.00	0.00	0.00	0.00	0.00	0.00	0.00	0.00	0.00	0.00	0.00	0.00	0.00	0.00	0.00
Air	O_2	Multilayer Insulation Assembly-T #1	0.00	0.00	0.00	0.00	0.00	0.00	0.00	0.00	0.00	0.00	0.00	0.00	0.00	0.00	0.00	0.00	0.00	0.00	0.00	0.00	0.00	0.00	0.00	0.00	0.00
Air	O_2	Multilayer Insulation Assembly-T #2	0.00	0.00	0.00	0.00	0.00	0.00	0.00	0.00	0.00	0.00	0.00	0.00	0.00	0.00	0.00	0.00	0.00	0.00	0.00	0.00	0.00	0.00	0.00	0.00	0.00
Air	O_2	Primary Structure Assembly-HPG ORU	0.00	0.00	0.00	0.00	0.00	0.00	0.00	0.00	0.00	0.00	0.00	0.00	0.00	0.00	0.00	0.00	0.00	0.00	0.00	0.00	0.00	0.00	0.00	0.00	0.00
Air	O_2	Tank ORU Assembly	0.00	0.00	0.00	0.00	0.00	0.00	0.00	0.00	0.00	0.00	0.00	0.00	0.00	0.00	0.00	0.00	0.00	0.00	0.00	0.00	0.00	0.00	0.00	0.00	0.00
Air	O_2	Utilities Installation - O_2/N_2 Tank	0.00	0.00	0.00	0.00	0.00	0.00	0.00	0.00	0.00	0.00	0.00	0.00	0.00	0.00	0.00	0.00	0.00	0.00	0.00	0.00	0.00	0.00	0.00	0.00	0.00
Air	O_2	O_2 Bare Tank	56.08	0.00	0.00	0.00	0.00	56.08	0.00	0.00	0.00	0.00	53.53	0.00	0.00	0.00	0.00	112.19	0.00	0.00	0.00	0.00	1010.36	0.00	0.00	0.00	0.00

Table S21: ESM parameters for all inventory items broken down by system and subsystem for each scenario described in Table S20. Parameters included are mass M [kg], V [m^3], power P [kW], cooling C [kW], and crew-time CT [hr][17, 317]. The ESM values correspond to a single sortie $S_{\text{num}} = 1$. (ORU = Orbital Replacement Unit)

			A					B					C					D					E				
System	**Subsystem**	**Item**	**M**	**V**	**P**	**C**	**CT**	**M**	**V**	**P**	**C**	**CT**	**M**	**V**	**P**	**C**	**CT**	**M**	**V**	**P**	**C**	**CT**	**M**	**V**	**P**	**C**	**CT**
Air	O_2	HPGA Fluid	48.00	0.00	0.00	0.00	0.00	48.00	0.00	0.00	0.00	0.00	44.47	0.00	0.00	0.00	0.00	72.80	0.00	0.00	0.00	0.00	506.64	0.00	0.00	0.00	0.00
Air	O_2	Handhold, top mounted	0.13	0.00	0.00	0.00	0.00	0.13	0.00	0.00	0.00	0.00	0.12	0.00	0.00	0.00	0.00	0.19	0.00	0.00	0.00	0.00	1.34	0.00	0.00	0.00	0.00
Air	O_2	Handrail 21.941 in custom	0.22	0.00	0.00	0.00	0.00	0.22	0.00	0.00	0.00	0.00	0.21	0.00	0.00	0.00	0.00	0.34	0.00	0.00	0.00	0.00	2.34	0.00	0.00	0.00	0.00
Air	O_2	Handrail, top mounted	0.23	0.00	0.00	0.00	0.00	0.23	0.00	0.00	0.00	0.00	0.22	0.00	0.00	0.00	0.00	0.35	0.00	0.00	0.00	0.00	2.45	0.00	0.00	0.00	0.00
Air	O_2	Grapple Fixture, flt releasable	6.53	0.00	0.00	0.00	0.00	6.53	0.00	0.00	0.00	0.00	6.05	0.00	0.00	0.00	0.00	9.90	0.00	0.00	0.00	0.00	68.88	0.00	0.00	0.00	0.00
Air	O_2	Accessories	2.81	0.00	0.00	0.00	0.00	2.81	0.00	0.00	0.00	0.00	2.68	0.00	0.00	0.00	0.00	5.62	0.00	0.00	0.00	0.00	50.57	0.00	0.00	0.00	0.00
Air	Sabatier	Condensing Heat Exchanger	1.47	0.00	0.00	0.00	0.00	1.47	0.00	0.00	0.00	0.00	1.49	0.00	0.00	0.00	0.00	1.48	0.00	0.00	0.00	0.00	1.48	0.00	0.00	0.00	0.00
Air	Sabatier	AAA Heat Exchanger	2.47	0.00	0.00	0.00	0.00	2.47	0.00	0.00	0.00	0.00	2.50	0.00	0.00	0.00	0.00	2.49	0.00	0.00	0.00	0.00	2.49	0.00	0.00	0.00	0.00
Air	Sabatier	ITCS Coolant Water Inlet QD	0.47	0.00	0.00	0.00	0.00	0.47	0.00	0.00	0.00	0.00	0.48	0.00	0.00	0.00	0.00	0.48	0.00	0.00	0.00	0.00	0.48	0.00	0.00	0.00	0.00
Air	Sabatier	ITCS Coolant Water Outlet QD	0.36	0.00	0.00	0.00	0.00	0.36	0.00	0.00	0.00	0.00	0.36	0.00	0.00	0.00	0.00	0.36	0.00	0.00	0.00	0.00	0.36	0.00	0.00	0.00	0.00
Air	Sabatier	Heat Exchanger Inlet Temp	0.36	0.00	0.00	0.00	0.00	0.36	0.00	0.00	0.00	0.00	0.36	0.00	0.00	0.00	0.00	0.36	0.00	0.00	0.00	0.00	0.36	0.00	0.00	0.00	0.00
Air	Sabatier	Heat Exchanger Outlet Temp	0.36	0.00	0.00	0.00	0.00	0.36	0.00	0.00	0.00	0.00	0.36	0.00	0.00	0.00	0.00	0.36	0.00	0.00	0.00	0.00	0.36	0.00	0.00	0.00	0.00
Air	Sabatier	Manifold, CO_2	4.72	0.00	0.00	0.00	0.00	4.72	0.00	0.00	0.00	0.00	4.80	0.00	0.00	0.00	0.00	4.77	0.00	0.00	0.00	0.00	4.76	0.00	0.00	0.00	0.00
Air	Sabatier	CO_2 Inlet Check Valve	0.10	0.00	0.00	0.00	0.00	0.10	0.00	0.00	0.00	0.00	0.11	0.00	0.00	0.00	0.00	0.11	0.00	0.00	0.00	0.00	0.11	0.00	0.00	0.00	0.00
Air	Sabatier	CO_2 Inlet Filter	0.05	0.00	0.00	0.00	0.00	0.05	0.00	0.00	0.00	0.00	0.06	0.00	0.00	0.00	0.00	0.06	0.00	0.00	0.00	0.00	0.06	0.00	0.00	0.00	0.00
Air	Sabatier	Pressure Sensor, CO_2 Inlet	0.41	0.00	0.00	0.00	0.00	0.41	0.00	0.00	0.00	0.00	0.41	0.00	0.00	0.00	0.00	0.41	0.00	0.00	0.00	0.00	0.41	0.00	0.00	0.00	0.00
Air	Sabatier	CO_2 Inlet QD	0.47	0.00	0.00	0.00	0.00	0.47	0.00	0.00	0.00	0.00	0.48	0.00	0.00	0.00	0.00	0.48	0.00	0.00	0.00	0.00	0.48	0.00	0.00	0.00	0.00
Air	Sabatier	CO_2 Inlet Regulator	0.92	0.00	0.00	0.00	0.00	0.92	0.00	0.00	0.00	0.00	0.93	0.00	0.00	0.00	0.00	0.93	0.00	0.00	0.00	0.00	0.93	0.00	0.00	0.00	0.00
Air	Sabatier	CO_2 Inlet NC Solenoid	0.47	0.00	0.00	0.00	0.00	0.47	0.00	0.00	0.00	0.00	0.48	0.00	0.00	0.00	0.00	0.48	0.00	0.00	0.00	0.00	0.48	0.00	0.00	0.00	0.00
Air	Sabatier	CO_2 Inlet Flow Control	2.15	0.00	0.00	0.00	0.00	2.15	0.00	0.00	0.00	0.00	2.18	0.00	0.00	0.00	0.00	2.17	0.00	0.00	0.00	0.00	2.17	0.00	0.00	0.00	0.00

Table S21: ESM parameters for all inventory items broken down by system and subsystem for each scenario described in Table S20. Parameters included are mass M [kg], V [m^3], power P [kW], cooling C [kW], and crew-time CT [hr][17, 317]. The ESM values correspond to a single sortie $S_{\text{num}} = 1$. (ORU = Orbital Replacement Unit)

			A					B					C					D					E				
System	**Subsystem**	**Item**	**M**	**V**	**P**	**C**	**CT**	**M**	**V**	**P**	**C**	**CT**	**M**	**V**	**P**	**C**	**CT**	**M**	**V**	**P**	**C**	**CT**	**M**	**V**	**P**	**C**	**CT**
Air	Sabatier	CO_2 Flow Control Orifice	0.05	0.00	0.00	0.00	0.00	0.05	0.00	0.00	0.00	0.00	0.05	0.00	0.00	0.00	0.00	0.05	0.00	0.00	0.00	0.00	0.05	0.00	0.00	0.00	0.00
Air	Sabatier	Delta P Sensor, Flow Sensor CO_2	0.91	0.00	0.00	0.00	0.00	0.91	0.00	0.00	0.00	0.00	0.91	0.00	0.00	0.00	0.00	0.91	0.00	0.00	0.00	0.00	0.91	0.00	0.00	0.00	0.00
Air	Sabatier	CO_2 Flow Meter Orifice	0.03	0.00	0.00	0.00	0.00	0.03	0.00	0.00	0.00	0.00	0.03	0.00	0.00	0.00	0.00	0.03	0.00	0.00	0.00	0.00	0.03	0.00	0.00	0.00	0.00
Air	Sabatier	Manifold, Hydrogen	4.38	0.00	0.00	0.00	0.00	4.38	0.00	0.00	0.00	0.00	4.45	0.00	0.00	0.00	0.00	4.43	0.00	0.00	0.00	0.00	4.42	0.00	0.00	0.00	0.00
Air	Sabatier	Water Outlet Quick Disconnect	0.47	0.00	0.00	0.00	0.00	0.47	0.00	0.00	0.00	0.00	0.48	0.00	0.00	0.00	0.00	0.48	0.00	0.00	0.00	0.00	0.48	0.00	0.00	0.00	0.00
Air	Sabatier	Hydrogen Inlet Check Valve	0.10	0.00	0.00	0.00	0.00	0.10	0.00	0.00	0.00	0.00	0.11	0.00	0.00	0.00	0.00	0.11	0.00	0.00	0.00	0.00	0.11	0.00	0.00	0.00	0.00
Air	Sabatier	Hydrogen Inlet Filter	0.05	0.00	0.00	0.00	0.00	0.05	0.00	0.00	0.00	0.00	0.06	0.00	0.00	0.00	0.00	0.06	0.00	0.00	0.00	0.00	0.06	0.00	0.00	0.00	0.00
Air	Sabatier	H_2O Outlet Pressure Sensor	0.82	0.00	0.00	0.00	0.00	0.82	0.00	0.00	0.00	0.00	0.82	0.00	0.00	0.00	0.00	0.82	0.00	0.00	0.00	0.00	0.82	0.00	0.00	0.00	0.00
Air	Sabatier	Hydrogen Inlet Quick Disconnect	0.47	0.00	0.00	0.00	0.00	0.47	0.00	0.00	0.00	0.00	0.48	0.00	0.00	0.00	0.00	0.48	0.00	0.00	0.00	0.00	0.48	0.00	0.00	0.00	0.00
Air	Sabatier	Hydrogen Inlet NC Solenoid	0.94	0.00	0.00	0.00	0.00	0.94	0.00	0.00	0.00	0.00	0.96	0.00	0.00	0.00	0.00	0.95	0.00	0.00	0.00	0.00	0.95	0.00	0.00	0.00	0.00
Air	Sabatier	Delta P Sensor, Flow Sensor H_2	0.91	0.00	0.00	0.00	0.00	0.91	0.00	0.00	0.00	0.00	0.91	0.00	0.00	0.00	0.00	0.91	0.00	0.00	0.00	0.00	0.91	0.00	0.00	0.00	0.00
Air	Sabatier	H_2 Flow Meter Orifice	0.03	0.00	0.00	0.00	0.00	0.03	0.00	0.00	0.00	0.00	0.03	0.00	0.00	0.00	0.00	0.03	0.00	0.00	0.00	0.00	0.03	0.00	0.00	0.00	0.00
Air	Sabatier	Manifold, Vent	5.06	0.00	0.00	0.00	0.00	5.06	0.00	0.00	0.00	0.00	5.14	0.00	0.00	0.00	0.00	5.12	0.00	0.00	0.00	0.00	5.10	0.00	0.00	0.00	0.00
Air	Sabatier	Liquid Sensor	1.09	0.00	0.00	0.00	0.00	1.09	0.00	0.00	0.00	0.00	1.09	0.00	0.00	0.00	0.00	1.09	0.00	0.00	0.00	0.00	1.09	0.00	0.00	0.00	0.00
Air	Sabatier	Vent Pressure Sensor	0.82	0.00	0.00	0.00	0.00	0.82	0.00	0.00	0.00	0.00	0.82	0.00	0.00	0.00	0.00	0.82	0.00	0.00	0.00	0.00	0.82	0.00	0.00	0.00	0.00
Air	Sabatier	Vent Outlet Quick Disconnect	0.47	0.00	0.00	0.00	0.00	0.47	0.00	0.00	0.00	0.00	0.48	0.00	0.00	0.00	0.00	0.48	0.00	0.00	0.00	0.00	0.48	0.00	0.00	0.00	0.00
Air	Sabatier	Vent Regulator	0.92	0.00	0.00	0.00	0.00	0.92	0.00	0.00	0.00	0.00	0.93	0.00	0.00	0.00	0.00	0.93	0.00	0.00	0.00	0.00	0.93	0.00	0.00	0.00	0.00
Air	Sabatier	Vent Relief/Check #1	0.16	0.00	0.00	0.00	0.00	0.16	0.00	0.00	0.00	0.00	0.16	0.00	0.00	0.00	0.00	0.16	0.00	0.00	0.00	0.00	0.16	0.00	0.00	0.00	0.00
Air	Sabatier	Vent Relief/Check #2	0.16	0.00	0.00	0.00	0.00	0.16	0.00	0.00	0.00	0.00	0.16	0.00	0.00	0.00	0.00	0.16	0.00	0.00	0.00	0.00	0.16	0.00	0.00	0.00	0.00
Air	Sabatier	Vent Outlet NO Solenoid	0.94	0.00	0.00	0.00	0.00	0.94	0.00	0.00	0.00	0.00	0.96	0.00	0.00	0.00	0.00	0.95	0.00	0.00	0.00	0.00	0.95	0.00	0.00	0.00	0.00

Table S21: ESM parameters for all inventory items broken down by system and subsystem for each scenario described in Table S20. Parameters included are mass M [kg], V [m^3], power P [kW], cooling C [kW], and crew-time CT [hr][17, 317]. The ESM values correspond to a single sortie $S_{\text{num}} = 1$. (ORU = Orbital Replacement Unit)

			A					B					C					D					E				
System	**Subsystem**	**Item**	**M**	**V**	**P**	**C**	**CT**	**M**	**V**	**P**	**C**	**CT**	**M**	**V**	**P**	**C**	**CT**	**M**	**V**	**P**	**C**	**CT**	**M**	**V**	**P**	**C**	**CT**
Air	Sabatier	Water Pressure Sensor	0.82	0.00	0.00	0.00	0.00	0.82	0.00	0.00	0.00	0.00	0.82	0.00	0.00	0.00	0.00	0.82	0.00	0.00	0.00	0.00	0.82	0.00	0.00	0.00	0.00
Air	Sabatier	Water Relief	0.16	0.00	0.00	0.00	0.00	0.16	0.00	0.00	0.00	0.00	0.16	0.00	0.00	0.00	0.00	0.16	0.00	0.00	0.00	0.00	0.16	0.00	0.00	0.00	0.00
Air	Sabatier	Water Outlet NC Solenoid	0.47	0.00	0.00	0.00	0.00	0.47	0.00	0.00	0.00	0.00	0.48	0.00	0.00	0.00	0.00	0.48	0.00	0.00	0.00	0.00	0.48	0.00	0.00	0.00	0.00
Air	Sabatier	Rotary Water Separator Assembly	4.04	0.00	22.66	22.66	0.00	4.04	0.00	22.66	22.66	0.00	4.10	0.00	22.93	22.93	0.00	4.08	0.00	22.84	22.84	0.00	4.07	0.00	22.80	22.80	0.00
Air	Sabatier	Sabatier Reactor Assembly	2.52	0.00	3.24	3.24	0.00	2.52	0.00	3.24	3.24	0.00	2.56	0.00	3.28	3.28	0.00	2.55	0.00	3.26	3.26	0.00	2.54	0.00	3.26	3.26	0.00
Air	Sabatier	Structure (A/R)	9.15	0.00	0.00	0.00	0.00	9.15	0.00	0.00	0.00	0.00	9.30	0.00	0.00	0.00	0.00	9.25	0.00	0.00	0.00	0.00	9.23	0.00	0.00	0.00	0.00
Air	Sabatier	Miscellaneous Hardware (clamps, bolts, etc.) (A/R)	1.77	0.00	0.00	0.00	0.00	1.77	0.00	0.00	0.00	0.00	1.77	0.00	0.00	0.00	0.00	1.77	0.00	0.00	0.00	0.00	1.77	0.00	0.00	0.00	0.00
Air	Sabatier	Air Cooling NC Solenoid	0.63	0.00	0.00	0.00	0.00	0.63	0.00	0.00	0.00	0.00	0.64	0.00	0.00	0.00	0.00	0.64	0.00	0.00	0.00	0.00	0.63	0.00	0.00	0.00	0.00
Air	Sabatier	Air Inlet Filter	0.11	0.00	0.00	0.00	0.00	0.11	0.00	0.00	0.00	0.00	0.11	0.00	0.00	0.00	0.00	0.11	0.00	0.00	0.00	0.00	0.11	0.00	0.00	0.00	0.00
Air	Sabatier	Air Sabatier Orifice	0.05	0.00	0.00	0.00	0.00	0.05	0.00	0.00	0.00	0.00	0.05	0.00	0.00	0.00	0.00	0.05	0.00	0.00	0.00	0.00	0.05	0.00	0.00	0.00	0.00
Air	Sabatier	Heat Exchanger Inlet Duct	0.10	0.00	0.00	0.00	0.00	0.10	0.00	0.00	0.00	0.00	0.11	0.00	0.00	0.00	0.00	0.11	0.00	0.00	0.00	0.00	0.11	0.00	0.00	0.00	0.00
Air	Sabatier	Heat Exchanger Outlet Duct	0.10	0.00	0.00	0.00	0.00	0.10	0.00	0.00	0.00	0.00	0.11	0.00	0.00	0.00	0.00	0.11	0.00	0.00	0.00	0.00	0.11	0.00	0.00	0.00	0.00
Air	Sabatier	Reactor Inlet Duct	0.21	0.00	0.00	0.00	0.00	0.21	0.00	0.00	0.00	0.00	0.21	0.00	0.00	0.00	0.00	0.21	0.00	0.00	0.00	0.00	0.21	0.00	0.00	0.00	0.00
Air	Sabatier	Reactor Outlet Duct	0.10	0.00	0.00	0.00	0.00	0.10	0.00	0.00	0.00	0.00	0.11	0.00	0.00	0.00	0.00	0.11	0.00	0.00	0.00	0.00	0.11	0.00	0.00	0.00	0.00
Air	Sabatier	Tubing (A/R)	0.68	0.00	0.00	0.00	0.00	0.68	0.00	0.00	0.00	0.00	0.69	0.00	0.00	0.00	0.00	0.69	0.00	0.00	0.00	0.00	0.69	0.00	0.00	0.00	0.00
Air	Sabatier	Harnesses	11.45	0.00	0.00	0.00	0.00	11.45	0.00	0.00	0.00	0.00	11.45	0.00	0.00	0.00	0.00	11.45	0.00	0.00	0.00	0.00	11.45	0.00	0.00	0.00	0.00
Air	Sabatier	Valves + Sensors' total power	0.00	0.00	7.37	7.37	0.00	0.00	0.00	7.37	7.37	0.00	0.00	0.00	7.76	7.76	0.00	0.00	0.00	7.63	7.63	0.00	0.00	0.00	7.57	7.57	0.00
Air	Sabatier	Mechanical Compressor ORU	18.88	0.00	45.32	45.32	0.00	18.88	0.00	45.32	45.32	0.00	19.18	0.00	45.86	45.86	0.00	19.09	0.00	45.69	45.69	0.00	19.04	0.00	45.60	45.60	0.00
Air	Sabatier	Compressor Manifold Assembly	4.62	0.00	0.00	0.00	0.00	4.62	0.00	0.00	0.00	0.00	4.69	0.00	0.00	0.00	0.00	4.67	0.00	0.00	0.00	0.00	4.65	0.00	0.00	0.00	0.00

Table S21: ESM parameters for all inventory items broken down by system and subsystem for each scenario described in Table S20. Parameters included are mass M [kg], V [m^3], power P [kW], cooling C [kW], and crew-time CT [hr][17, 317]. The ESM values correspond to a single sortie $S_{\text{num}} = 1$. (ORU = Orbital Replacement Unit)

			A					B					C					D					E				
Sys-tem	**Sub-system**	**Item**	**M**	**V**	**P**	**C**	**CT**	**M**	**V**	**P**	**C**	**CT**	**M**	**V**	**P**	**C**	**CT**	**M**	**V**	**P**	**C**	**CT**	**M**	**V**	**P**	**C**	**CT**
Air	Sabatier	Controller Assembly	28.59	0.00	55.00	55.00	0.00	28.59	0.00	55.00	55.00	0.00	28.59	0.00	55.00	55.00	0.00	28.59	0.00	55.00	55.00	0.00	28.59	0.00	55.00	55.00	0.00
Air	Sabatier	CO_2 Accumulator	10.03	0.01	0.00	0.00	0.00	10.03	0.01	0.00	0.00	0.00	10.19	0.01	0.00	0.00	0.00	10.14	0.01	0.00	0.00	0.00	10.11	0.01	0.00	0.00	0.00
Air	O_2-gen	Deionizing Bed ORU (Inlet)	7.79	0.01	0.00	0.00	0.00	7.79	0.01	0.00	0.00	0.00	8.19	0.01	0.00	0.00	0.00	8.07	0.01	0.00	0.00	0.00	8.00	0.01	0.00	0.00	0.00
Air	O_2-gen	Deionizing Bed ORU (Recirculating)	7.79	0.01	0.00	0.00	0.00	7.79	0.01	0.00	0.00	0.00	8.19	0.01	0.00	0.00	0.00	8.07	0.01	0.00	0.00	0.00	8.00	0.01	0.00	0.00	0.00
Air	O_2-gen	Oxygen/Water ORU	36.40	0.02	0.00	0.00	0.00	36.40	0.02	0.00	0.00	0.00	37.01	0.03	0.00	0.00	0.00	36.82	0.03	0.00	0.00	0.00	36.72	0.02	0.00	0.00	0.00
Air	O_2-gen	Pump ORU	6.46	0.01	23.33	23.33	0.00	6.46	0.01	23.33	23.33	0.00	6.56	0.01	24.53	24.53	0.00	6.53	0.01	24.15	24.15	0.00	6.51	0.01	23.96	23.96	0.00
Air	O_2-gen	Oxygen Phase Separator ORU	21.83	0.01	0.00	0.00	0.00	21.83	0.01	0.00	0.00	0.00	22.20	0.01	0.00	0.00	0.00	22.08	0.01	0.00	0.00	0.00	22.02	0.01	0.00	0.00	0.00
Air	O_2-gen	Hydrogen ORU	95.46	0.05	30.78	30.78	0.00	95.46	0.05	30.78	30.78	0.00	97.07	0.05	32.37	32.37	0.00	96.56	0.05	31.87	31.87	0.00	96.30	0.05	31.61	31.61	0.00
Air	O_2-gen	Hydrogen Sensor ORU	4.59	0.00	0.00	0.00	0.00	4.59	0.00	0.00	0.00	0.00	4.59	0.00	0.00	0.00	0.00	4.59	0.00	0.00	0.00	0.00	4.59	0.00	0.00	0.00	0.00
Air	O_2-gen	Process Controller	40.09	0.14	148.00	148.00	0.00	40.09	0.14	148.00	148.00	0.00	40.09	0.14	148.00	148.00	0.00	40.09	0.14	148.00	148.00	0.00	40.09	0.14	148.00	148.00	0.00
Air	O_2-gen	Power Supply Module (PSM)	13.45	0.02	1069.25	0.00	0.00	13.45	0.02	1069.25	0.00	0.00	14.14	0.02	1124.56	62.18	0.00	13.92	0.02	1106.55	53.47	0.00	13.81	0.02	1098.50	49.02	0.00
Air	Fire-det-sup	Fire Detection Assembly	1.50	0.00	1.48	1.48	0.03	1.50	0.00	1.48	1.48	0.03	1.50	0.00	1.48	1.48	0.03	1.50	0.00	1.48	1.48	0.08	1.50	0.00	1.48	1.48	0.89
Air	Fire-det-sup	Portable Fire Extinguisher	6.80	0.04	0.00	0.00	0.00	6.80	0.04	0.00	0.00	0.00	6.80	0.04	0.00	0.00	0.00	6.80	0.04	0.00	0.00	0.00	6.80	0.04	0.00	0.00	0.00
Air	ACO_2R	Regenerator 1	45.30	0.17	397.00	397.00	0.00	45.30	0.17	397.00	397.00	0.00	45.30	0.17	397.00	397.00	0.00	45.30	0.17	397.00	397.00	0.00	45.30	0.17	397.00	397.00	0.00
Air	ACO_2R	Metox Canisters	136.00	0.06	0.00	0.00	0.00	136.00	0.06	0.00	0.00	0.00	136.00	0.06	0.00	0.00	0.00	136.00	0.06	0.00	0.00	0.00	136.00	0.06	0.00	0.00	0.00
Air	TCCS-ISS	Activated Charcoal Bed	4.63	0.01	0.00	0.00	0.00	4.63	0.01	0.00	0.00	0.00	4.63	0.01	0.00	0.00	0.00	12.87	0.03	0.00	0.00	0.00	139.02	0.29	0.00	0.00	0.00
Air	TCCS-ISS	Blower Assembly	2.49	0.00	30.39	30.39	0.00	2.49	0.00	30.39	30.39	0.00	2.49	0.00	30.39	30.39	0.00	2.49	0.00	30.39	30.39	0.00	2.49	0.00	30.39	30.39	0.00
Air	TCCS-ISS	Flow Meter Assembly	1.10	0.00	11.50	11.50	0.00	1.10	0.00	11.50	11.50	0.00	1.10	0.00	11.50	11.50	0.00	1.10	0.00	11.50	11.50	0.00	1.10	0.00	11.50	11.50	0.00
Air	TCCS-ISS	Catalytic Oxidizer Assembly	8.46	0.02	92.19	92.19	0.00	8.46	0.02	92.19	92.19	0.00	8.46	0.02	92.19	92.19	0.00	8.46	0.02	92.19	92.19	0.00	8.46	0.02	92.19	92.19	0.00
Air	TCCS-ISS	LiOH Sorbent Bed Assembly	0.31	0.00	0.00	0.00	0.00	0.31	0.00	0.00	0.00	0.00	0.31	0.00	0.00	0.00	0.00	0.87	0.00	0.00	0.00	0.00	9.43	0.02	0.00	0.00	0.00

Table S21: ESM parameters for all inventory items broken down by system and subsystem for each scenario described in Table S20. Parameters included are mass M [kg], V [m^3], power P [kW], cooling C [kW], and crew-time CT [hr][17, 317]. The ESM values correspond to a single sortie $S_{\text{num}} = 1$. (ORU = Orbital Replacement Unit)

			A					B					C					D					E				
System	**Subsystem**	**Item**	**M**	**V**	**P**	**C**	**CT**	**M**	**V**	**P**	**C**	**CT**	**M**	**V**	**P**	**C**	**CT**	**M**	**V**	**P**	**C**	**CT**	**M**	**V**	**P**	**C**	**CT**
Air	TCCS-ISS	Electrical Interface Assembly	4.50	0.00	7.60	7.60	0.00	4.50	0.00	7.60	7.60	0.00	4.50	0.00	7.60	7.60	0.00	4.50	0.00	7.60	7.60	0.00	4.50	0.00	7.60	7.60	0.00
Waste	PMWC	Aluminum Compaction Cylinder	9.40	0.02	0.00	0.00	180.00	9.40	0.02	0.00	0.00	180.00	9.41	0.02	0.00	0.00	180.00	9.41	0.02	0.00	0.00	500.00	9.41	0.02	0.00	0.00	5400.00
Waste	PMWC	Band-type Heating Unit	0.00	0.00	136.34	0.00	0.00	0.00	0.00	136.34	0.00	0.00	0.00	0.00	162.58	0.00	0.00	0.00	0.00	162.39	0.00	0.00	0.00	0.00	162.29	0.00	0.00
Waste	PMWC	Lightweight, Oil-Less, Compressor/Vacuum Pump	0.00	0.00	2.71	0.00	0.00	0.00	0.00	2.71	0.00	0.00	0.00	0.00	3.23	0.00	0.00	0.00	0.00	3.22	0.00	0.00	0.00	0.00	3.22	0.00	0.00
Waste	PMWC	Temperature Sensor	0.22	0.00	0.00	0.00	0.00	0.22	0.00	0.00	0.00	0.00	0.22	0.00	0.00	0.00	0.00	0.22	0.00	0.00	0.00	0.00	0.22	0.00	0.00	0.00	0.00
Waste	PMWC	Pressure Sensor	0.30	0.00	0.33	0.00	0.00	0.30	0.00	0.33	0.00	0.00	0.30	0.00	0.33	0.00	0.00	0.30	0.00	0.33	0.00	0.00	0.30	0.00	0.33	0.00	0.00
Waste	PMWC	Housing + Mounting Equipment	23.86	0.48	0.00	0.00	0.00	23.86	0.48	0.00	0.00	0.00	23.89	0.48	0.00	0.00	0.00	23.89	0.48	0.00	0.00	0.00	23.89	0.48	0.00	0.00	0.00
Waste	PMWC	Condensing Heat Exchanger	1.91	0.00	0.00	0.00	0.00	1.91	0.00	0.00	0.00	0.00	2.86	0.01	0.00	0.00	0.00	2.86	0.01	0.00	0.00	0.00	2.85	0.01	0.00	0.00	0.00
Waste	PMWC	Cooling system	0.00	0.00	0.00	0.00	0.00	0.00	0.00	0.00	0.00	0.00	0.00	0.00	145.14	145.14	0.00	0.00	0.00	144.97	144.97	0.00	0.00	0.00	144.89	144.89	0.00
Waste	Waste-storage	Low Density PolyEthylene Box	17.70	0.49	0.00	0.00	0.00	17.70	0.49	0.00	0.00	0.00	17.70	0.49	0.00	0.00	0.00	49.18	1.37	0.00	0.00	0.00	531.15	14.75	0.00	0.00	0.00
Waste	Waste-col	Commode/Urinal	58.40	0.30	0.00	0.00	29.59	58.40	0.30	0.00	0.00	29.59	58.40	0.30	0.00	0.00	29.59	58.40	0.30	0.00	0.00	82.19	58.40	0.30	0.00	0.00	887.67
Waste	Waste-col	Fan	0.00	0.00	102.00	102.00	0.00	0.00	0.00	102.00	102.00	0.00	0.00	0.00	102.00	102.00	0.00	0.00	0.00	102.00	102.00	0.00	0.00	0.00	102.00	102.00	0.00
Waste	Waste-col	Urine Separator	0.00	0.00	125.00	125.00	0.00	0.00	0.00	125.00	125.00	0.00	0.00	0.00	125.00	125.00	0.00	0.00	0.00	125.00	125.00	0.00	0.00	0.00	125.00	125.00	0.00
Waste	Waste-col	Urine Vent Heater	0.00	0.00	14.00	14.00	0.00	0.00	0.00	14.00	14.00	0.00	0.00	0.00	14.00	14.00	0.00	0.00	0.00	14.00	14.00	0.00	0.00	0.00	14.00	14.00	0.00
Waste	Waste-col	Fecal Bags	19.64	0.22	0.00	0.00	0.00	19.64	0.22	0.00	0.00	0.00	19.64	0.22	0.00	0.00	0.00	54.55	0.61	0.00	0.00	0.00	589.09	6.58	0.00	0.00	0.00
Waste	Waste-col	Wipes, Dry	6.55	0.09	0.00	0.00	0.00	6.55	0.09	0.00	0.00	0.00	6.55	0.09	0.00	0.00	0.00	18.18	0.25	0.00	0.00	0.00	196.36	2.65	0.00	0.00	0.00
Waste	Waste-col	Wipes, Wet	10.23	0.05	0.00	0.00	0.00	10.23	0.05	0.00	0.00	0.00	10.23	0.05	0.00	0.00	0.00	28.41	0.15	0.00	0.00	0.00	306.82	1.59	0.00	0.00	0.00
Waste	Waste-col	Wipes, Toilet Tissue	3.53	0.04	0.00	0.00	0.00	3.53	0.04	0.00	0.00	0.00	3.53	0.04	0.00	0.00	0.00	9.82	0.12	0.00	0.00	0.00	106.04	1.29	0.00	0.00	0.00
Waste	Waste-col	Gloves	5.60	0.03	0.00	0.00	0.00	5.60	0.03	0.00	0.00	0.00	5.60	0.03	0.00	0.00	0.00	15.55	0.07	0.00	0.00	0.00	167.80	0.76	0.00	0.00	0.00

Table S21: ESM parameters for all inventory items broken down by system and subsystem for each scenario described in Table S20. Parameters included are mass M [kg], V [m^3], power P [kW], cooling C [kW], and crew-time CT [hr][17, 317]. The ESM values correspond to a single sortie $S_{\text{num}} = 1$. (ORU = Orbital Replacement Unit)

			A					B					C					D					E				
System	**Subsystem**	**Item**	**M**	**V**	**P**	**C**	**CT**	**M**	**V**	**P**	**C**	**CT**	**M**	**V**	**P**	**C**	**CT**	**M**	**V**	**P**	**C**	**CT**	**M**	**V**	**P**	**C**	**CT**
Waste	Waste-col	Fecal Bags Odor Lids	29.45	0.28	0.00	0.00	0.00	29.45	0.28	0.00	0.00	0.00	29.45	0.28	0.00	0.00	0.00	81.82	0.77	0.00	0.00	0.00	883.64	8.26	0.00	0.00	0.00
Waste	Waste-col	Fecal Collection Canisters	35.06	0.46	0.00	0.00	0.00	35.06	0.46	0.00	0.00	0.00	35.06	0.46	0.00	0.00	0.00	97.40	1.28	0.00	0.00	0.00	1051.19	13.77	0.00	0.00	0.00
Waste	Waste-col	Fecal collection Canisters lids	17.53	0.07	0.00	0.00	0.00	17.53	0.07	0.00	0.00	0.00	17.53	0.07	0.00	0.00	0.00	48.70	0.20	0.00	0.00	0.00	525.92	2.15	0.00	0.00	0.00
Waste	Waste-col	Urine Prefilters	30.68	0.17	0.00	0.00	0.00	30.68	0.17	0.00	0.00	0.00	30.68	0.17	0.00	0.00	0.00	85.23	0.46	0.00	0.00	0.00	920.45	5.01	0.00	0.00	0.00
Waste	Waste-col	Urine Filters	4.38	0.04	0.00	0.00	0.00	4.38	0.04	0.00	0.00	0.00	4.38	0.04	0.00	0.00	0.00	12.18	0.10	0.00	0.00	0.00	131.49	1.06	0.00	0.00	0.00
Waste	Waste-col	Urine Funnels	0.00	0.00	0.00	0.00	0.00	0.00	0.00	0.00	0.00	0.00	1.16	0.01	0.00	0.00	0.00	1.16	0.01	0.00	0.00	0.00	1.16	0.01	0.00	0.00	0.00
Waste	Waste-col	Flush Water Transfer Bags	5.61	0.08	0.00	0.00	0.00	5.61	0.08	0.00	0.00	0.00	5.61	0.08	0.00	0.00	0.00	15.58	0.22	0.00	0.00	0.00	168.32	2.35	0.00	0.00	0.00
Waste	TCCS-ISS-x3	Activated charcoal bed	9.27	0.02	0.00	0.00	0.00	9.27	0.02	0.00	0.00	0.00	9.27	0.02	0.00	0.00	0.00	25.74	0.05	0.00	0.00	0.00	278.04	0.57	0.00	0.00	0.00
Waste	TCCS-ISS-x4	Blower Assembly	4.97	0.01	60.79	60.79	0.00	4.97	0.01	60.79	60.79	0.00	4.97	0.01	60.79	60.79	0.00	4.97	0.01	60.79	60.79	0.00	4.97	0.01	60.79	60.79	0.00
Waste	TCCS-ISS-x5	Flow Meter Assembly	2.20	0.00	23.00	23.00	0.00	2.20	0.00	23.00	23.00	0.00	2.20	0.00	23.00	23.00	0.00	2.20	0.00	23.00	23.00	0.00	2.20	0.00	23.00	23.00	0.00
Waste	TCCS-ISS-x6	Catalytic Oxidizer Assembly	16.91	1.04	184.38	184.38	0.00	16.91	1.04	184.38	184.38	0.00	16.91	1.04	184.38	184.38	0.00	16.91	1.04	184.38	184.38	0.00	16.91	1.04	184.38	184.38	0.00
Waste	TCCS-ISS-x7	LiOH Sorbent Bed Assembly	0.63	0.00	0.00	0.00	0.00	0.63	0.00	0.00	0.00	0.00	0.63	0.00	0.00	0.00	0.00	1.75	0.00	0.00	0.00	0.00	18.86	0.04	0.00	0.00	0.00
Waste	TCCS-ISS-x8	Electrical Interface Assembly	9.00	0.01	15.20	15.20	0.00	9.00	0.01	15.20	15.20	0.00	9.00	0.01	15.20	15.20	0.00	9.00	0.01	15.20	15.20	0.00	9.00	0.01	15.20	15.20	0.00
Water	H_2O-rec	MLS Filter ORU	3.32	0.00	0.00	0.00	0.00	3.32	0.00	0.00	0.00	0.00	3.96	0.01	0.00	0.00	0.00	10.97	0.02	0.00	0.00	0.00	118.21	0.17	0.00	0.00	0.00
Water	H_2O-rec	Particulate Filter ORU	17.22	0.04	0.00	0.00	0.00	17.22	0.04	0.00	0.00	0.00	20.54	0.05	0.00	0.00	0.00	56.83	0.14	0.00	0.00	0.00	612.48	1.56	0.00	0.00	0.00
Water	H_2O-rec	Multifiltration Bed #1 + #2 ORUs	0.00	0.00	0.00	0.00	0.00	0.00	0.00	0.00	0.00	0.00	167.74	0.22	0.00	0.00	0.00	464.08	0.60	0.00	0.00	0.00	5001.68	6.51	0.00	0.00	0.00
Water	H_2O-rec	Sensor ORU	3.64	0.01	2.13	2.13	0.00	3.64	0.01	2.13	2.13	0.00	3.64	0.01	2.13	2.13	0.00	3.64	0.01	2.13	2.13	0.00	3.64	0.01	2.13	2.13	0.00
Water	H_2O-rec	Piping	5.37	0.01	0.00	0.00	0.00	5.37	0.01	0.00	0.00	0.00	0.74	0.00	0.00	0.00	0.00	0.74	0.00	0.00	0.00	0.00	0.74	0.00	0.00	0.00	0.00
Water	H_2O-rec	Pump/MLS ORU	30.28	0.09	51.17	51.17	0.00	30.28	0.09	51.17	51.17	0.00	18.42	0.06	19.62	19.62	0.00	18.40	0.06	19.54	19.54	0.00	18.38	0.06	19.50	19.50	0.00
Water	H_2O-rec	Catalytic Reactor + Preheeater ORU	0.00	0.00	0.00	0.00	0.00	0.00	0.00	0.00	0.00	0.00	0.00	0.00	107.90	107.90	0.00	0.00	0.00	107.47	107.47	0.00	0.00	0.00	107.25	107.25	0.00

Table S21: ESM parameters for all inventory items broken down by system and subsystem for each scenario described in Table S20. Parameters included are mass M [kg], V [m^3], power P [kW], cooling C [kW], and crew-time CT [hr][17, 317]. The ESM values correspond to a single sortie $S_{\text{num}} = 1$. (ORU = Orbital Replacement Unit)

			A					B					C					D					E				
System	**Subsystem**	**Item**	**M**	**V**	**P**	**C**	**CT**	**M**	**V**	**P**	**C**	**CT**	**M**	**V**	**P**	**C**	**CT**	**M**	**V**	**P**	**C**	**CT**	**M**	**V**	**P**	**C**	**CT**
Water	H_2O-rec	Oxygen Filter	0.00	0.00	0.00	0.00	0.00	0.00	0.00	0.00	0.00	0.00	0.00	0.00	0.00	0.00	0.00	0.00	0.00	0.00	0.00	0.00	0.00	0.00	0.00	0.00	0.00
Water	H_2O-rec	Microbial Check Valve	0.00	0.00	0.00	0.00	0.00	0.00	0.00	0.00	0.00	0.00	5.16	0.01	0.00	0.00	0.00	5.13	0.01	0.00	0.00	0.00	5.12	0.01	0.00	0.00	0.00
Water	H_2O-rec	Gas Separator ORU	43.11	0.09	132.33	132.33	0.00	43.11	0.09	132.33	132.33	0.00	26.24	0.06	50.73	50.73	0.00	26.20	0.06	50.53	50.53	0.00	26.17	0.06	50.43	50.43	0.00
Water	H_2O-rec	Hygiene H_2O Tank	95.90	0.18	7.05	7.05	0.00	95.90	0.18	7.05	7.05	0.00	58.36	0.11	4.72	4.72	0.00	58.27	0.11	4.71	4.71	0.00	58.22	0.11	4.71	4.71	0.00
Water	H_2O-rec	Product H_2O Tank	53.97	0.19	7.85	7.85	0.00	53.97	0.19	7.85	7.85	0.00	32.84	0.12	5.25	5.25	0.00	32.79	0.12	5.24	5.24	0.00	32.76	0.12	5.24	5.24	0.00
Water	H_2O-rec	Process Controller	36.91	0.08	156.18	156.18	0.00	36.91	0.08	156.18	156.18	0.00	36.91	0.08	156.18	156.18	0.00	36.91	0.08	156.18	156.18	0.00	36.91	0.08	156.18	156.18	0.00
Water	H_2O-rec	Reactor Health Sensor	8.64	0.04	4.72	4.72	0.00	8.64	0.04	4.72	4.72	0.00	8.64	0.04	4.72	4.72	0.00	8.64	0.04	4.72	4.72	0.00	8.64	0.04	4.72	4.72	0.00
Water	H_2O-rec	H_2O Delivery System	42.97	0.11	2.88	2.88	0.00	42.97	0.11	2.88	2.88	0.00	26.15	0.06	1.93	1.93	0.00	26.11	0.06	1.93	1.93	0.00	26.09	0.06	1.92	1.92	0.00
Water	WRS	Ion Exchange Bed	2.78	0.00	0.00	0.00	0.00	2.78	0.00	0.00	0.00	0.00	2.78	0.00	0.00	0.00	0.00	7.70	0.01	0.00	0.00	0.00	83.02	0.11	0.00	0.00	0.00
Water	Urine-proc	Pressure Control + Pump (PCPA)	27.14	0.04	5.73	5.73	0.00	27.14	0.04	5.73	5.73	0.00	33.73	0.05	9.83	9.83	0.00	33.64	0.05	9.77	9.77	0.00	33.60	0.05	9.75	9.75	0.00
Water	Urine-proc	Fluid Control + Pump (FCPA)	27.63	0.04	8.30	8.30	0.00	27.63	0.04	8.30	8.30	0.00	34.35	0.05	14.26	14.26	0.00	34.26	0.05	14.18	14.18	0.00	34.21	0.05	14.14	14.14	0.00
Water	Urine-proc	Recycle Filter Tank (RFTA)	11.55	0.06	0.00	0.00	0.00	11.55	0.06	0.00	0.00	0.00	14.35	0.08	0.00	0.00	0.00	14.32	0.08	0.00	0.00	0.00	14.30	0.08	0.00	0.00	0.00
Water	Urine-proc	Wastewater Storage Tank Assembly (WSTA)	28.95	0.02	0.08	0.08	0.00	28.95	0.02	0.08	0.08	0.00	35.98	0.03	0.14	0.14	0.00	35.89	0.03	0.14	0.14	0.00	35.84	0.03	0.14	0.14	0.00
Water	Urine-proc	Distillation Assembly (DA)	45.81	0.09	79.35	79.35	0.00	45.81	0.09	79.35	79.35	0.00	56.94	0.11	136.22	136.22	0.00	56.79	0.11	135.46	135.46	0.00	56.72	0.11	135.08	135.08	0.00
Water	Urine-proc	Separator Plumbing Assembly (SPA)	9.87	0.02	0.00	0.00	0.00	9.87	0.02	0.00	0.00	0.00	12.27	0.02	0.00	0.00	0.00	12.24	0.02	0.00	0.00	0.00	12.22	0.02	0.00	0.00	0.00
Water	Urine-proc	Power Module (Included in FCA)	0.00	0.00	0.00	0.00	0.00	0.00	0.00	0.00	0.00	0.00	0.00	0.00	0.00	0.00	0.00	0.00	0.00	0.00	0.00	0.00	0.00	0.00	0.00	0.00	0.00
Water	Urine-proc	Firmware Controller Assembly (Data Module, Power Module)	24.09	0.03	150.09	150.09	0.00	24.09	0.03	150.09	150.09	0.00	24.09	0.03	150.09	150.09	0.00	24.09	0.03	150.09	150.09	0.00	24.09	0.03	150.09	150.09	0.00
Water	Urine-proc	Piping	7.55	0.01	0.00	0.00	0.00	7.55	0.01	0.00	0.00	0.00	9.38	0.02	0.00	0.00	0.00	9.36	0.02	0.00	0.00	0.00	9.34	0.02	0.00	0.00	0.00
Water	Volatile-rem	Catalytic Reactor + Preheater ORU	0.00	0.00	90.48	90.48	0.00	0.00	0.00	90.48	90.48	0.00	0.00	0.00	90.48	90.48	0.00	0.00	0.00	90.48	90.48	0.00	0.00	0.00	90.48	90.48	0.00

Table S21: ESM parameters for all inventory items broken down by system and subsystem for each scenario described in Table S20. Parameters included are mass M [kg], V [m^3], power P [kW], cooling C [kW], and crew-time CT [hr][17, 317]. The ESM values correspond to a single sortie $S_{\text{num}} = 1$. (ORU = Orbital Replacement Unit)

			A					B					C					D					E				
System	**Subsystem**	**Item**	**M**	**V**	**P**	**C**	**CT**	**M**	**V**	**P**	**C**	**CT**	**M**	**V**	**P**	**C**	**CT**	**M**	**V**	**P**	**C**	**CT**	**M**	**V**	**P**	**C**	**CT**
Water	Volatile-rem	Gas Separator ORU	24.54	0.05	42.54	42.54	0.00	24.54	0.05	42.54	42.54	0.00	24.54	0.05	42.54	42.54	0.00	24.54	0.05	42.54	42.54	0.00	24.54	0.05	42.54	42.54	0.00
Water	Volatile-rem	Oxygen Filter	0.00	0.00	0.00	0.00	0.00	0.00	0.00	0.00	0.00	0.00	0.00	0.00	0.00	0.00	0.00	0.00	0.00	0.00	0.00	0.00	0.00	0.00	0.00	0.00	0.00
Water	Volatile-rem	Piping	1.26	0.00	0.00	0.00	0.00	1.26	0.00	0.00	0.00	0.00	1.26	0.00	0.00	0.00	0.00	1.26	0.00	0.00	0.00	0.00	1.26	0.00	0.00	0.00	0.00
Water	Tank	Product H_2O Tank	101.1	1236	13.65	13.65	0.00	101.1	1236	13.65	13.65	0.00	84.82	0.30	11.64	11.64	0.00	137.0	1949	18.07	18.07	0.00	937.4	3333	116.4	116.4	0.00
Water	Tank	H_2O Stored	256.9	9000	0.00	0.00	0.00	256.9	9000	0.00	0.00	0.00	205.5	5600	0.00	0.00	0.00	370.5	5500	0.00	0.00	0.00	2897	0000	0.00	0.00	0.00
Food	Food-storage	Packaging	0.00	0.00	0.00	0.00	0.00	0.00	0.00	0.00	0.00	0.00	990.0	0000	0.00	0.00	0.00	2707	0300	0.00	0.00	0.00	2900	4.85	0.00	0.00	0.00
Food	Food-storage	Lockers/Storage	218.8	3605	0.00	0.00	0.00	218.8	3605	0.00	0.00	0.00	242.7	7639	0.00	0.00	0.00	663.8	8826	0.00	0.00	0.00	7112	9324	0.00	0.00	0.00
Food	Food-processing	Rehydration Unit and Conduction Oven	36.30	0.09	960.0	960.0	0.00	36.30	0.09	960.0	960.0	0.00	36.30	0.09	10.00	10.00	0.00	36.30	0.09	10.00	10.00	0.00	36.30	0.09	10.00	10.00	0.00
Thermal	CCAA	Inlet ORU	0.00	0.00	312.6	312.6	0.00	0.00	0.00	312.6	312.6	0.00	0.00	0.00	299.2	299.2	0.00	0.00	0.00	299.0	299.0	0.00	0.00	0.00	299.0	299.0	0.00
Thermal	CCAA	Condensing Heat Exchanger	37.69	0.07	0.00	0.00	0.00	37.69	0.07	0.00	0.00	0.00	34.91	0.07	0.00	0.00	0.00	34.90	0.07	0.00	0.00	0.00	34.89	0.07	0.00	0.00	0.00
Thermal	CCAA	Water Separator	6.41	0.04	10.19	10.19	0.00	6.41	0.04	10.19	10.19	0.00	5.31	0.04	3.38	3.38	0.00	5.30	0.04	3.35	3.35	0.00	5.30	0.04	3.34	3.34	0.00
Thermal	CCAA	Temp. Control + Check Valve	4.09	0.03	0.06	0.06	0.00	4.09	0.03	0.06	0.06	0.00	3.89	0.03	0.06	0.06	0.00	3.89	0.03	0.06	0.06	0.00	3.89	0.03	0.06	0.06	0.00
Thermal	CCAA	Electrical Interface Box (EIB)	4.10	0.01	8.00	8.00	0.00	4.10	0.01	8.00	8.00	0.00	4.10	0.01	8.00	8.00	0.00	4.10	0.01	8.00	8.00	0.00	4.10	0.01	8.00	8.00	0.00
Thermal	CCAA	Temp. Sensor	0.24	0.00	0.01	0.01	0.00	0.24	0.00	0.01	0.01	0.00	0.24	0.00	0.01	0.01	0.00	0.24	0.00	0.01	0.01	0.00	0.24	0.00	0.01	0.01	0.00
Thermal	CCAA	Liquid Sensor	0.47	0.00	0.01	0.01	0.00	0.47	0.00	0.01	0.01	0.00	0.47	0.00	0.01	0.01	0.00	0.47	0.00	0.01	0.01	0.00	0.47	0.00	0.01	0.01	0.00

Table S21: ESM parameters for all inventory items broken down by system and subsystem for each scenario described in Table S20. Parameters included are mass M [kg], V [m^3], power P [kW], cooling C [kW], and crew-time CT [hr][17, 317]. The ESM values correspond to a single sortie $S_{\text{num}} = 1$. (ORU = Orbital Replacement Unit)

			A					B					C					D					E				
System	**Subsystem**	**Item**	**M**	**V**	**P**	**C**	**CT**	**M**	**V**	**P**	**C**	**CT**	**M**	**V**	**P**	**C**	**CT**	**M**	**V**	**P**	**C**	**CT**	**M**	**V**	**P**	**C**	**CT**
Thermal	CCAA	Fan Delta P Sensor	0.40	0.00	0.20	0.20	0.00	0.40	0.00	0.20	0.20	0.00	0.40	0.00	0.20	0.20	0.00	0.40	0.00	0.20	0.20	0.00	0.40	0.00	0.20	0.20	0.00
Thermal	CCAA	Pressure Sensor	0.30	0.00	0.20	0.20	0.00	0.30	0.00	0.20	0.20	0.00	0.30	0.00	0.20	0.20	0.00	0.30	0.00	0.20	0.20	0.00	0.30	0.00	0.20	0.20	0.00
Thermal	Atmoscont	HEPA Filter Element	49.22	0.19	0.00	0.00	0.99	49.22	0.19	0.00	0.00	0.99	49.22	0.19	0.00	0.00	0.99	49.22	0.19	0.00	0.00	2.74	49.22	0.19	0.00	0.00	29.59
Thermal	Atmoscont	Catalytic Filter Element	54.00	0.08	0.00	0.00	0.00	54.00	0.08	0.00	0.00	0.00	54.00	0.08	0.00	0.00	0.00	54.00	0.08	0.00	0.00	0.00	54.00	0.08	0.00	0.00	0.00
Thermal	Atmosphere-circ	IMV Fan	4.77	0.01	55.00	55.00	0.00	4.77	0.01	55.00	55.00	0.00	4.77	0.01	55.00	55.00	0.00	4.77	0.01	55.00	55.00	0.00	4.77	0.01	55.00	55.00	0.00
Thermal	Atmosphere-circ	IMV Valve	5.10	0.01	6.00	6.00	0.00	5.10	0.01	6.00	6.00	0.00	5.10	0.01	6.00	6.00	0.00	5.10	0.01	6.00	6.00	0.00	5.10	0.01	6.00	6.00	0.00
Thermal	AAA	Avionics Air Assembly	12.40	0.03	175.00	175.00	0.00	12.40	0.03	175.00	175.00	0.00	12.40	0.03	175.00	175.00	0.00	12.40	0.03	175.00	175.00	0.00	12.40	0.03	175.00	175.00	0.00
Thermal	ITCS	ITCS	211.83	0.36	2585.25	2585.00	0.00	211.83	0.36	2585.25	2585.00	0.00	211.83	0.36	2585.25	2585.00	0.00	212.49	0.36	2595.25	2595.00	0.00	217.23	0.36	2669.25	2669.00	0.00

Table S22: Estimation of inventory items into exemplar classes broken down by system and subsystem for each scenario described in Table S20. Classes include: Structural Metal, Plastic, Electronics, Fabric, Glass, Rubber, Ceramics, Gas, Biomass, Water, Other. (ORU = Orbital Replacement Unit)

System	**Subsystem**	**Item**	**Structural Metal**	**Plastic**	**Electronics**	**Fabric**	**Glass**	**Rubber**	**Ceramics**	**Gas**	**Biomass**	**Water**	**Other**
Air	APC	Vent/Relief Valve	1	0	0	0	0	0	0	0	0	0	0
Air	APC	Pressure Control Panel	0.2	0.1	0.7	0	0	0	0	0	0	0	0
Air	APC	Manual Pressure Equalization Valve	1	0	0	0	0	0	0	0	0	0	0
Air	APC	Positive Pressure Relief Valve	1	0	0	0	0	0	0	0	0	0	0

Table S22: Estimation of inventory items into exemplar classes broken down by system and subsystem for each scenario described in Table S20. Classes include: Structural Metal, Plastic, Electronics, Fabric, Glass, Rubber, Ceramics, Gas, Biomass, Water, Other. (ORU = Orbital Replacement Unit)

System	Subsystem	Item	Structural Metal	Plastic	Electronics	Fabric	Glass	Rubber	Ceramics	Gas	Biomass	Water	Other
Air	APC	Negative Pressure Relief Valve	1	0	0	0	0	0	0	0	0	0	0
Air	APC	Nitrogen Interface Assembly	1	0	0	0	0	0	0	0	0	0	0
Air	APC	Vacuum Access Jumper 5-ft	0	0	1	0	0	0	0	0	0	0	0
Air	APC	Vacuum Access Jumper 35-ft	0	0	1	0	0	0	0	0	0	0	0
Air	ACMA	Verification Gas Assembly	0.5	0	0	0	0	0	0	0.5	0	0	0
Air	ACMA	Mass Spectrometer	0.5	0	0.5	0	0	0	0	0	0	0	0
Air	ACMA	Sample Pump	1	0	0	0	0	0	0	0	0	0	0
Air	ACMA	Sample Distributor	0.95	0	0	0.05	0	0	0	0	0	0	0
Air	ACMA	Data + Control	0.5	0	0.5	0	0	0	0	0	0	0	0
Air	ACMA	Low Volt. Power supply	0.7	0	0	0	0	0.1	0.1	0	0	0	0.1
Air	ACMA	Chassis	1	0	0	0	0	0	0	0	0	0	0
Air	ACMA	Inlet Valve Assembly	0.9	0	0	0.01	0	0	0	0	0	0.09	0
Air	ACMA	EMI Filter	0.98	0.02	0	0	0	0	0	0	0	0	0
Air	SDS	3-way Solenoid Valves	1	0	0	0	0	0	0	0	0	0	0
Air	SDS	Manual Valves	1	0	0	0	0	0	0	0	0	0	0
Air	SDS	Sample Probes	1	0	0	0	0	0	0	0	0	0	0
Air	CO_2-rem	Air Selector Valve	0.9	0	0	0	0	0	0	0.1	0	0	0
Air	CO_2-rem	Desiccant Bed	0.4	0	0	0	0	0	0.6	0	0	0	0
Air	CO_2-rem	Adsorbent Bed	0.5	0	0	0.2	0	0	0.3	0	0	0	0
Air	CO_2-rem	Air Check Valve	1	0	0	0	0	0	0	0	0	0	0
Air	CO_2-rem	Heater Controller	0.8	0	0.2	0	0	0	0	0	0	0	0
Air	CO_2-rem	Air Blower	1	0	0	0	0	0	0	0	0	0	0
Air	CO_2-rem	Pre-cooler	1	0	0	0	0	0	0	0	0	0	0
Air	CO_2-rem	Blower/Pre-cooler Motor Controller	0.6	0	0.4	0	0	0	0	0	0	0	0
Air	CO_2-rem	CO_2 Pump	0.99	0	0	0	0	0	0	0	0	0	0.01
Air	CO_2-rem	CO_2 Pump Motor Controller	0.3	0	0.7	0	0	0	0	0	0	0	0
Air	CO_2-rem	Temperature Sensor	0	0	0.6	0	0.4	0	0	0	0	0	0
Air	CO_2-rem	Differential Pressure Sensor	0.1	0.25	0.65	0	0	0	0	0	0	0	0
Air	CO_2-rem	Absolute Pressure Sensor	0.75	0	0	0	0	0	0.25	0	0	0	0
Air	CO_2-rem	Electrical Harness	0.9	0.05	0	0.05	0	0	0	0	0	0	0
Air	CO_2-rem	Plumbing	1	0	0	0	0	0	0	0	0	0	0
Air	CO_2-rem	Support Structure	1	0	0	0	0	0	0	0	0	0	0
Air	CO_2-rem	Fluid Disconnects	1	0	0	0	0	0	0	0	0	0	0
Air	CO_2-rem	Electronics Cold-Plate	1	0	0	0	0	0	0	0	0	0	0
Air	CO_2-rem	Electronics Interface Plate	1	0	0	0	0	0	0	0	0	0	0
Air	N_2	MD Shield Instl	1	0	0	0	0	0	0	0	0	0	0
Air	N_2	Multilayer Insulation Assembly-T #1	1	0	0	0	0	0	0	0	0	0	0
Air	N_2	Multilayer Insulation Assembly-T #2	1	0	0	0	0	0	0	0	0	0	0
Air	N_2	Primary Structure Assembly-HPG ORU	0.5	0	0	0	0	0	0	0.5	0	0	0

Table S22: Estimation of inventory items into exemplar classes broken down by system and subsystem for each scenario described in Table S20. Classes include: Structural Metal, Plastic, Electronics, Fabric, Glass, Rubber, Ceramics, Gas, Biomass, Water, Other. (ORU = Orbital Replacement Unit)

System	Subsystem	Item	Structural Metal	Plastic	Electronics	Fabric	Glass	Rubber	Ceramics	Gas	Biomass	Water	Other
Air	N_2	Tank ORU Assembly	1	0	0	0	0	0	0	0	0	0	0
Air	N_2	Utilities Installation - O_2/N_2 Tank	0.5	0	0	0	0	0	0	0.5	0	0	0
Air	N_2	N_2 Bare Tank	0.9	0	0	0	0	0.05	0	0.05	0	0	0
Air	N_2	HPGA Fluid	0	0	0	0	0	0	0	0	0	1	0
Air	N_2	Handhold, top mounted	0	1	0	0	0	0	0	0	0	0	0
Air	N_2	Handrail 21.941 in custom	0	1	0	0	0	0	0	0	0	0	0
Air	N_2	Handrail, top mounted	0	1	0	0	0	0	0	0	0	0	0
Air	N_2	Grapple Fixture, flt releasable	0.5	0	0.5	0	0	0	0	0	0	0	0
Air	N_2	Accessories	0	0	0	0	0	0	0	0	0	0	0
Air	O_2	MD Shield Instl	1	0	0	0	0	0	0	0	0	0	0
Air	O_2	Multilayer Insulation Assembly-T #1	1	0	0	0	0	0	0	0	0	0	0
Air	O_2	Multilayer Insulation Assembly-T #2	1	0	0	0	0	0	0	0	0	0	0
Air	O_2	Primary Structure Assembly-HPG ORU	0.5	0	0	0	0	0	0	0.5	0	0	0
Air	O_2	Tank ORU Assembly	1	0	0	0	0	0	0	0	0	0	0
Air	O_2	Utilities Installation - O_2/N_2 Tank	0.5	0	0	0	0	0	0	0.5	0	0	0
Air	O_2	O_2 Bare Tank	0.95	0	0	0	0	0	0	0.05	0	0	0
Air	O_2	HPGA Fluid	0	0	0	0	0	0	0	0	0	1	0
Air	O_2	Handhold, top mounted	0	1	0	0	0	0	0	0	0	0	0
Air	O_2	Handrail 21.941 in custom	0	1	0	0	0	0	0	0	0	0	0
Air	O_2	Handrail, top mounted	0	1	0	0	0	0	0	0	0	0	0
Air	O_2	Grapple Fixture, flt releasable	0.5	0	0.5	0	0	0	0	0	0	0	0
Air	O_2	Accessories	0	0	0	0	0	0	0	0	0	0	0
Air	Sabatier	Condensing Heat Exchanger	0.9	0	0.1	0	0	0	0	0	0	0	0
Air	Sabatier	AAA Heat Exchanger	1	0	0	0	0	0	0	0	0	0	0
Air	Sabatier	ITCS Coolant Water Inlet QD	1	0	0	0	0	0	0	0	0	0	0
Air	Sabatier	ITCS Coolant Water Outlet QD	1	0	0	0	0	0	0	0	0	0	0
Air	Sabatier	Heat Exchanger Inlet Temp	1	0	0	0	0	0	0	0	0	0	0
Air	Sabatier	Heat Exchanger Outlet Temp	1	0	0	0	0	0	0	0	0	0	0
Air	Sabatier	Manifold, CO_2	0.95	0.05	0	0	0	0	0	0	0	0	0
Air	Sabatier	CO_2 Inlet Check Valve	0.9	0.1	0	0	0	0	0	0	0	0	0
Air	Sabatier	CO_2 Inlet Filter	1	0	0	0	0	0	0	0	0	0	0
Air	Sabatier	Pressure Sensor, CO_2 Inlet	0	0	0.6	0	0.4	0	0	0	0	0	0
Air	Sabatier	CO_2 Inlet QD	1	0	0	0	0	0	0	0	0	0	0
Air	Sabatier	CO_2 Inlet Regulator	0.9	0.05	0	0	0.05	0	0	0	0	0	0
Air	Sabatier	CO_2 Inlet NC Solenoid	1	0	0	0	0	0	0	0	0	0	0
Air	Sabatier	CO_2 Inlet Flow Control	0.85	0.05	0	0	0.1	0	0	0	0	0	0
Air	Sabatier	CO_2 Flow Control Orifice	1	0	0	0	0	0	0	0	0	0	0
Air	Sabatier	Delta P Sensor, Flow Sensor CO_2	0	0	0.6	0	0.4	0	0	0	0	0	0

Table S22: Estimation of inventory items into exemplar classes broken down by system and subsystem for each scenario described in Table S20. Classes include: Structural Metal, Plastic, Electronics, Fabric, Glass, Rubber, Ceramics, Gas, Biomass, Water, Other. (ORU = Orbital Replacement Unit)

System	Subsystem	Item	Structural Metal	Plastic	Electronics	Fabric	Glass	Rubber	Ceramics	Gas	Biomass	Water	Other
Air	Sabatier	CO_2 Flow Meter Orifice	1	0	0	0	0	0	0	0	0	0	0
Air	Sabatier	Manifold, Hydrogen	0.95	0.05	0	0	0	0	0	0	0	0	0
Air	Sabatier	Water Outlet Quick Disconnect	1	0	0	0	0	0	0	0	0	0	0
Air	Sabatier	Hydrogen Inlet Check Valve	0.9	0.1	0	0	0	0	0	0	0	0	0
Air	Sabatier	Hydrogen Inlet Filter	1	0	0	0	0	0	0	0	0	0	0
Air	Sabatier	H_2O Outlet Pressure Sensor	0	0	0.6	0	0.4	0	0	0	0	0	0
Air	Sabatier	Hydrogen Inlet Quick Disconnect	1	0	0	0	0	0	0	0	0	0	0
Air	Sabatier	Hydrogen Inlet NC Solenoid	1	0	0	0	0	0	0	0	0	0	0
Air	Sabatier	Delta P Sensor, Flow Sensor H_2	0	0	0.6	0	0.4	0	0	0	0	0	0
Air	Sabatier	H_2 Flow Meter Orifice	1	0	0	0	0	0	0	0	0	0	0
Air	Sabatier	Manifold, Vent	0.95	0.05	0	0	0	0	0	0	0	0	0
Air	Sabatier	Liquid Sensor	0	0.5	0.5	0	0	0	0	0	0	0	0
Air	Sabatier	Vent Pressure Sensor	0	0	0.6	0	0.4	0	0	0	0	0	0
Air	Sabatier	Vent Outlet Quick Disconnect	1	0	0	0	0	0	0	0	0	0	0
Air	Sabatier	Vent Regulator	0.9	0.05	0	0	0.05	0	0	0	0	0	0
Air	Sabatier	Vent Relief/Check #1	1	0	0	0	0	0	0	0	0	0	0
Air	Sabatier	Vent Relief/Check #2	1	0	0	0	0	0	0	0	0	0	0
Air	Sabatier	Vent Outlet NO Solenoid	1	0	0	0	0	0	0	0	0	0	0
Air	Sabatier	Water Pressure Sensor	0	0	0.6	0	0.4	0	0	0	0	0	0
Air	Sabatier	Water Relief	1	0	0	0	0	0	0	0	0	0	0
Air	Sabatier	Water Outlet NC Solenoid	1	0	0	0	0	0	0	0	0	0	0
Air	Sabatier	Rotary Water Separator Assembly	1	0	0	0	0	0	0	0	0	0	0
Air	Sabatier	Sabatier Reactor Assembly	0.9	0	0.1	0	0	0	0	0	0	0	0
Air	Sabatier	Structure (A/R)	1	0	0	0	0	0	0	0	0	0	0
Air	Sabatier	Miscellaneous Hardware (clamps, bolts, etc.) (A/R)	1	0	0	0	0	0	0	0	0	0	0
Air	Sabatier	Air Cooling NC Solenoid	1	0	0	0	0	0	0	0	0	0	0
Air	Sabatier	Air Inlet Filter	1	0	0	0	0	0	0	0	0	0	0
Air	Sabatier	Air Sabatier Orifice	1	0	0	0	0	0	0	0	0	0	0
Air	Sabatier	Heat Exchanger Inlet Duct	1	0	0	0	0	0	0	0	0	0	0
Air	Sabatier	Heat Exchanger Outlet Duct	1	0	0	0	0	0	0	0	0	0	0
Air	Sabatier	Reactor Inlet Duct	1	0	0	0	0	0	0	0	0	0	0
Air	Sabatier	Reactor Outlet Duct	1	0	0	0	0	0	0	0	0	0	0
Air	Sabatier	Tubing (A/R)	1	0	0	0	0	0	0	0	0	0	0
Air	Sabatier	Harnesses	0.9	0.05	0	0.05	0	0	0	0	0	0	0
Air	Sabatier	Valves + Sensors' Total Power	0	0	1	0	0	0	0	0	0	0	0
Air	Sabatier	Mechanical Compressor ORU	0.9	0.1	0	0	0	0	0	0	0	0	0.001
Air	Sabatier	Compressor Manifold Assembly	0.95	0.05	0	0	0	0	0	0	0	0	0

Table S22: Estimation of inventory items into exemplar classes broken down by system and subsystem for each scenario described in Table S20. Classes include: Structural Metal, Plastic, Electronics, Fabric, Glass, Rubber, Ceramics, Gas, Biomass, Water, Other. (ORU = Orbital Replacement Unit)

System	Subsystem	Item	Structural Metal	Plastic	Electronics	Fabric	Glass	Rubber	Ceramics	Gas	Biomass	Water	Other
Air	Sabatier	Controller Assembly	0	0.2	0.8	0	0	0	0	0	0	0	0
Air	Sabatier	CO_2 Accumulator	1	0	0	0	0	0	0	0	0	0	0
Air	O_2-gen	Deionizing Bed ORU (Inlet)	0.05	0.15	0	0	0	0	0	0	0	0	0.8
Air	O_2-gen	Deionizing Bed ORU (Recirculating)	0.05	0.15	0	0	0	0	0	0	0	0	0.8
Air	O_2-gen	Oxygen/Water ORU	0.33	0	0	0	0	0	0	0.33	0	0.33	0
Air	O_2-gen	Pump ORU	1	0	0	0	0	0	0	0	0	0	0
Air	O_2-gen	Oxygen Phase Separator ORU	1	0	0	0	0	0	0	0	0	0	0
Air	O_2-gen	Hydrogen ORU	1	0	0	0	0	0	0	0	0	0	0
Air	O_2-gen	Hydrogen Sensor ORU	1	0	0	0	0	0	0	0	0	0	0
Air	O_2-gen	Process Controller	0.3	0.001	0.7	0	0	0	0	0	0	0	0
Air	O_2-gen	Power Supply Module (PSM)	0.7	0	0	0	0	0.1	0.1	0	0	0	0.1
Air	Fire-det-sup	Fire Detection Assembly	0.05	0.9	0.05	0	0	0	0	0	0	0	0
Air	Fire-det-sup	Portable Fire Extinguisher	0.6	0	0	0	0	0	0	0.2	0	0	0.2
Air	ACO_2R	Regenerator 1	0.98	0.01	0	0	0.01	0	0	0	0	0	0
Air	ACO_2R	Metox Canisters	1	0	0	0	0	0	0	0	0	0	0
Air	TCCS-ISS	Activated Charcoal Bed	0	0.5	0	0	0	0	0.5	0	0	0	0
Air	TCCS-ISS	Blower Assembly	0.8	0	0.2	0	0	0	0	0	0	0	0
Air	TCCS-ISS	Flow Meter Assembly	0.7	0.1	0.1	0	0.1	0	0	0	0	0	0
Air	TCCS-ISS	Catalytic Oxidizer Assembly	1	0	0	0	0	0	0	0	0	0	0
Air	TCCS-ISS	LiOH Sorbent Bed Assembly	0.07	0.03	0	0	0	0	0.9	0	0	0	0
Air	TCCS-ISS	Electrical interface assembly	0	0	1	0	0	0	0	0	0	0	0
Waste	PMWC	Aluminum Compaction cylinder	1	0	0	0	0	0	0	0	0	0	0
Waste	PMWC	Band-type heating unit	0.9	0	0	0	0	0	0.1	0	0	0	0
Waste	PMWC	Lightweight, Oil-Less, Compressor/-Vacuum Pump	0.9	0	0.1	0	0	0	0	0	0	0	0
Waste	PMWC	Temperature Sensor	0	0	0.6	0	0.4	0	0	0	0	0	0
Waste	PMWC	Pressure Sensor	0.1	0.25	0.65	0	0	0	0	0	0	0	0
Waste	PMWC	Housing + Mounting Equipment	1	0	0	0	0	0	0	0	0	0	0
Waste	PMWC	Condensing Heat Exchanger	1	0	0	0	0	0	0	0	0	0	0
Waste	PMWC	Cooling system	1	0	0	0	0	0	0	0	0	0	0

Table S22: Estimation of inventory items into exemplar classes broken down by system and subsystem for each scenario described in Table S20. Classes include: Structural Metal, Plastic, Electronics, Fabric, Glass, Rubber, Ceramics, Gas, Biomass, Water, Other. (ORU = Orbital Replacement Unit)

System	Subsystem	Item	Structural Metal	Plastic	Electronics	Fabric	Glass	Rubber	Ceramics	Gas	Biomass	Water	Other
Waste	Waste-storage	Low Density PolyEthylene Box	0	1	0	0	0	0	0	0	0	0	0
Waste	Waste-col	Commode/Urinal	0	1	0	0	0	0	0	0	0	0	0
Waste	Waste-col	Fan	1	0	0	0	0	0	0	0	0	0	0
Waste	Waste-col	Urine Separator	0.9	0	0.09	0.01	0	0	0	0	0	0	0
Waste	Waste-col	Urine Vent Heater	1	0	0	0	0	0	0	0	0	0	0
Waste	Waste-col	Fecal Bags	0	0	0	1	0	0	0	0	0	0	0
Waste	Waste-col	Wipes, Dry	0	0	0	1	0	0	0	0	0	0	0
Waste	Waste-col	Wipes, Wet	0	0	0	0.6	0	0	0	0	0	0.4	0
Waste	Waste-col	Wipes, Toilet Tissue	0	0	0	0	0	0	0	0	0	0	1
Waste	Waste-col	Gloves	0	1	0	0	0	0	0	0	0	0	0
Waste	Waste-col	Fecal Bags Odor Lids	0	1	0	0	0	0	0	0	0	0	0
Waste	Waste-col	Fecal collection Canisters	0	0.9	0	0.1	0	0	0	0	0	0	0
Waste	Waste-col	Fecal collection Canisters lids	0	1	0	0	0	0	0	0	0	0	0
Waste	Waste-col	Urine Prefilters	1	0	0	0	0	0	0	0	0	0	0
Waste	Waste-col	Urine Filters	0	0	0	1	0	0	0	0	0	0	0
Waste	Waste-col	Urine Funnels	1	0	0	0	0	0	0	0	0	0	0
Waste	Waste-col	Flush Water Transfer Bags	0	0.3	0	0.7	0	0	0	0	0	0	0
Waste	TCCS-ISS-x3	Activated Charcoal Bed	0	0.5	0	0	0	0	0	0	0	0	0.5
Waste	TCCS-ISS-x4	Blower Assembly	0.8	0	0.2	0	0	0	0	0	0	0	0
Waste	TCCS-ISS-x5	Flow Meter Assembly	0.7	0.1	0.1	0	0.1	0	0	0	0	0	0
Waste	TCCS-ISS-x6	Catalytic Oxidizer Assembly	1	0	0	0	0	0	0	0	0	0	0
Waste	TCCS-ISS-x7	LiOH Sorbent Bed Assembly	0.07	0.03	0	0	0	0	0.9	0	0	0	0
Waste	TCCS-ISS-x8	Electrical Interface Assembly	0	0	1	0	0	0	0	0	0	0	0
Water	Water-rec	MLS Filter ORU	0.5	0	0.5	0	0	0	0	0	0	0	0
Water	Water-rec	Particulate Filter ORU	0.9	0	0	0	0	0	0	0	0	0	0.1
Water	Water-rec	Multifiltration Bed #1 + #2 ORUs	0.07	0.03	0	0	0	0	0	0	0	0.9	0
Water	Water-rec	Sensor ORU	0	0.6	0.2	0	0.2	0	0	0	0	0	0
Water	Water-rec	Piping	1	0	0	0	0	0	0	0	0	0	0
Water	Water-rec	Pump/MLS ORU	0.5	0	0.5	0	0	0	0	0	0	0	0
Water	Water-rec	Catalytic Reactor + Preheater ORU	1	0	0	0	0	0	0	0	0	0	0
Water	Water-rec	Oxygen Filter	0.5	0.5	0	0	0	0	0	0	0	0	0
Water	Water-rec	Microbial Check Valve	0.99	0	0	0	0	0	0	0	0	0	0.01

Table S22: Estimation of inventory items into exemplar classes broken down by system and subsystem for each scenario described in Table S20. Classes include: Structural Metal, Plastic, Electronics, Fabric, Glass, Rubber, Ceramics, Gas, Biomass, Water, Other. (ORU = Orbital Replacement Unit)

System	Subsystem	Item	Structural Metal	Plastic	Electronics	Fabric	Glass	Rubber	Ceramics	Gas	Biomass	Water	Other
Water	Water-rec	Gas Separator ORU	0.9	0.1	0	0	0	0	0	0	0	0	0.001
Water	Water-rec	Hygiene H_2O Tank	0	1	0	0	0	0	0	0	0	0	0
Water	Water-rec	Product H_2O Tank	0	1	0	0	0	0	0	0	0	0	0
Water	Water-rec	Process Controller	0.3	0.001	0.7	0	0	0	0	0	0	0	0
Water	Water-rec	Reactor Health Sensor	0.1	0.2	0.6	0	0	0	0.1	0	0	0	0
Water	Water-rec	H_2O Delivery System	0.9	0	0	0	0	0.1	0	0	0	0	0
Water	Urine-proc	Pressure Control + Pump (PCPA)	0.7	0.2	0.1	0	0	0	0	0	0	0	0
Water	Urine-proc	Fluid Control + Pump (FCPA)	0.7	0.2	0.1	0	0	0	0	0	0	0	0
Water	Urine-proc	Recycle Filter Tank (RFTA)	0	1	0	0	0	0	0	0	0	0	0
Water	Urine-proc	Wastewater Storage Tank Assembly (WSTA)	1	0	0	0	0	0	0	0	0	0	0
Water	Urine-proc	Distillation Assembly (DA)	0.6	0	0.1	0	0.3	0	0	0	0	0	0
Water	Urine-proc	Separator Plumbing Assembly (SPA)	0.99	0.01	0	0	0	0	0	0	0	0	0
Water	Urine-proc	Power Module (Included in FCA)	0	0	0	0	0	0	0	0	0	0	0
Water	Urine-proc	Firmware Controller Assembly (Data Module, Power Module)	0.8	0	0.2	0	0	0	0	0	0	0	0
Water	Urine-proc	Piping	1	0	0	0	0	0	0	0	0	0	0
Water	Volatile-rem	Catalytic Reactor + Preheater ORU	1	0	0	0	0	0	0	0	0	0	0
Water	Volatile-rem	Gas Separator ORU	0.9	0.1	0	0	0	0	0	0	0	0	0.001
Water	Volatile-rem	Oxygen Filter	0.5	0.5	0	0	0	0	0	0	0	0	0
Water	Volatile-rem	Piping	1	0	0	0	0	0	0	0	0	0	0
Water	Tank	Product H_2O Tank	0	1	0	0	0	0	0	0	0	0	0
Water	Tank	H_2O Stored	0	0	0	0	0	0	0	0	0	1	0
Food	Food-stor	Lockers	0.25	0.25	0	0	0	0	0	0	0.5	0	0
Food	Food-proc	Rehydration Unit and Conduction Oven	0.7	0.05	0.25	0	0	0	0	0	0	0	0

Table S22: Estimation of inventory items into exemplar classes broken down by system and subsystem for each scenario described in Table S20. Classes include: Structural Metal, Plastic, Electronics, Fabric, Glass, Rubber, Ceramics, Gas, Biomass, Water, Other. (ORU = Orbital Replacement Unit)

System	Subsystem	Item	Structural Metal	Plastic	Electronics	Fabric	Glass	Rubber	Ceramics	Gas	Biomass	Water	Other
Thermal	CCAA	Inlet ORU	1	0	0	0	0	0	0	0	0	0	0
Thermal	CCAA	Condensing Heat Exchanger	1	0	0	0	0	0	0	0	0	0	0
Thermal	CCAA	Water Separator	0.99	0	0	0	0	0	0	0	0	0	0.01
Thermal	CCAA	Temp Control + Check Valve	0.8	0.15	0	0.05	0	0	0	0	0	0	0
Thermal	CCAA	Electrical Interface Box (EIB)	0.9	0	0.1	0	0	0	0	0	0	0	0
Thermal	CCAA	Temp Sensor	0	0	0.6	0	0.4	0	0	0	0	0	0
Thermal	CCAA	Liquid Sensor	0	0.5	0.5	0	0	0	0	0	0	0	0
Thermal	CCAA	Fan Delta P Sensor	0.9	0	0.1	0	0	0	0	0	0	0	0
Thermal	CCAA	Pressure Sensor	0.1	0.25	0.65	0	0	0	0	0	0	0	0
Thermal	Atmoscon	HEPA Filter Element	0.7	0	0	0	0.3	0	0	0	0	0	0
Thermal	Atmoscon	Catalytic Filter Element	0	0.7	0	0.3	0	0	0	0	0	0	0
Thermal	Atmoscirc	IMV Fan	0.9	0.05	0	0.05	0	0	0	0	0	0	0
Thermal	Atmoscirc	IMV Valve	1	0	0	0	0	0	0	0	0	0	0
Thermal	AAA	Avionics Air Assembly	0.8	0.1	0	0.1	0	0	0	0	0	0	0

Opportunities for Biomanufacturing-based 3D- and bio-printing in Space

Bioprinting for Medical Applications

Advancing manufacturing and application concepts now aim to enable non-terran medical therapeutics beyond conventional pharmacological and medical device design, production, and treatment strategies translated from Earth deployment[387]. Among these developments are *in vitro* biofabrication models being prepared and tested in Space for the reduction to practice of bioficial tissue and organ manufacturing capable of supporting on-demand personalized medicine through autologous organs and systems repair or replacement. Nearly two-decades of Earth-based demonstrations show that 3D bio-printing of live cells provides feasible physical healthcare solutions in nonsurgical and surgical settings[509, 571, 353]. The constraints of Space and extraterrestrial environments, however, demand specialized standards for bio-printing, bio-product utilization, and medical/surgical procedures that currently restrict the near-term state-of-art to high positive-outcome healthcare interventions, such as bone and skin repair, which are more easily performed by suitably trained spaceflight surgeons and assistive medical staff using portable biomedical technologies and additional infrastructure in microgravity[462, 566, 189].

Despite these constraints, existing in-Space manufacturing technologies and methods outpace the readiness to practice sophisticated Earth medical and surgical procedures in off-Earth scenarios. For example, the Russian Space Agency and partners printed the first live tissue, a mouse thyroid, aboard the ISS using self-assembly magnetic manipulation, eliminating the need for traditional bio-compatible scaffolding techniques to organize and support cell structure, proliferation, differentiation, and extracellular matrix production[101, 421]. Alternate scaffold-free preparations, such as those employing hydrogels and metallic needles or electrostatic, acoustic, and gravitational forces, also offer practical solutions for implementing tissue and organ bio-printing in Space. NASA's Centennial Vascular Tissue Challenge will evaluate two of these methods, gel- and gravity-directed organ assembly, using the ISS BioFabrication Facility (BFF). The BFF is a collaboration between private industry and NASA that was launched to study and perfect the printing of human cells and organ-like tissues in microgravity.

Although human joint menisci with simple vascular zones have been already constructed on the ISS, technical obstacles remain for the bio-printing of sustainably viable complex organs believed necessary to replace astronaut anatomy, which may become damaged or diseased from long-duration space-travel and habitation. Th winners of the Centennial Vascular Tissue Challenge will, for instance, focus on improving organotypic vascular engineering of artificial liver -– the building of vascular networks that perfuse cells with nutrients and oxygen while removing metabolic waste and other biological toxins and debris[210]. Achieving naturalistic blood supplies for artificial organ systems continues to be a major limitation for both Earth and Space science and such manufacturing endeavors will help realize cell-

differentiated organ bio-printing for Space regenerative medicine, complementing a range of other envisioned off-Earth cell and tissue medical bio-printing applications, including the recent European Space Agency demonstration of skin-wound patching and accelerated healing with use of the hand-held Bioprint First Aid. Importantly, because 3D bio-printing presumably benefits from a near weightless manufacturing environment with atomic-level low mechanical stresses and viscosity[484], orbital facilities similar to the BFF may become significant supply-chain contributors to the Earth-based regenerative medicine industry, improving the health, wellness, and longevity of millions or more patients worldwide by catalyzing technology innovation and application [185].

Fabricating Finished Goods

In 2014, the first three-dimensional (3-D) printed object in space was produced on the ISS Additive Manufacturing Facility (AMF). Since then, additive manufacturing is actively being explored and developed in LEO as proving-ground for various off-world scenarios, as also exemplified by fused filament fabrication (FFF) of ABS (acrylnitril-butadien-styrol), conducted on the ISS in 2016[438]. The tests showed that 3D-printing of synthetic polymers in microgravity is reliable, because of automation, which privileges new material exploration: public and private sector alike have 3D-printed hundreds of parts aboard the ISS made from polymers of various classes[589]. Also the Space-based additive manufacturing of non-polymeric materials is being explored: flight-demo technology has featured flexible electronics, including laser-sintering of copper, printed ceramic sensors, batteries, and antennas[127]. A build-to-print RF antenna was successfully produced through additive manufacturing, reducing up-mass and enabling in-Space design customization[187]. Private companies provide hardware and printing solutions for conductors and dielectrics through stand-alone R&D printers as well as OEM print-heads that can be integrated with other additive manufacturing tools and robotic arms, even enabling plasma jet printing.

Potential applications and benefits are manifold and range from ISM to commercialization of on-Orbit manufacturing techniques. The Redwire Regolith Print study, for example, optimized on-orbit construction of civil infrastructure with an adoption plan for the Artemis Program. Material sources are a hybrid of locally (on the Moon) available regolith and Earth-made binder whose performance holds promise to be matched by biologically-produced adhesives of macromolecular nature[163]. While theoretically an abundant resource for construction at destination Moon, Lunar regolith is characteristically unlike any Earth material. Without wind and rain, Lunar regolith particles stay sharp, instead of eroding smooth [422]. This unique topology in combination with small size not only poses significant respiratory risk to astronauts, as observed during the Apollo missions, but also causes frictional damage of mechanical equipment[74], which must be accounted for in hardware development.

Aside from applications in ISM, the partial gravity of Space is being explored as a potentially advantageous environment for additive manufacturing of premium goods, because of suspected benefits in crystallographic consistency, and therefore enhanced performance of certain products. The first step is to “space-optimize” material processing windows to

account for gravity-mediated changes in sedimentation, rheology, crystallographic organization, and thermodynamics [544]. If successful, microgravity theoretically promotes the more uniform solidification of materials, which transforms the microstructure-dependent performance of space forged materials. However, the fabrication of high-fidelity optical ZBLAN fibers in 2017 [108], for example, found less crystallization, resulting in reduced optical performance of the microgravity-manufactured product [526]. Nevertheless, platforms like the Turbine Ceramics Manufacturing Module (Turbine CMM) and the Turbine Superalloy Casting Module (Turbine SCM) for microgravity-based production of ceramics and metal alloys build on this work and explore microgravity similarly, as means to increase the microhardness of Space-made parts. Overall, the exploration of material processing in Space does not only serve the advancement of ISM, but translates discoveries back to improve terrestrial applications[520].

Supplementary Display Items

Table S23: Qualitative comparison of biotic vs. abiotic *in situ* (bio)manufacturing approaches across different destinations in the Solar-system (excluding cis-Lunar, which can be considered as an in-between of Earth Orbit and destination Moon).

Destinations		abiotic	biological
Earth Orbit[191]	advantage	in certain cases manufacturing in microgravity may yield a premium product	bioprinting without structural stabilization and scaffold-free tissue engineering
		re-use/-purposing of infrastructure on-orbit for strategic reduction of up-mass	more extensive recycling allows for tighter loop-closure
	drawback	no *in situ* resource utilization possible	no *in situ* resource utilization possible
		in many cases ability to re-supply outweighs infrastructure-investment	in many cases ability to re-supply outweighs infrastructure-investment
		microgravity makes certain processes more difficult	microgravity makes aqueous processes challenging
Lunar[495]	advantage	strategic outpost for infrastructure as stepping stone to the solar system	allows resources to be exploit that are not accessible otherwise
		gravity, may allow certain processes to be adopted more readily	gravity, allows gas/liquid separation → operation of aqueous processes
		may in some cases save mass/cost of re-supply	may in some cases expand mission capabilities
	drawback	limited portfolio and amount/density of available resources	resources are limited and processes are largely dependent on abiotic ISRU
		ability to re-supply and delivery may often outweigh infrastructure investment	ability to re-supply and delivery may outweigh infrastructure investment
Interplanetary[558]	advantage	re-supply not feasible → recycling and loop-closure compulsory	increased redundancy through flexibility: can allow *ad hoc* solution of complex incidental problems
		systems proven in LEO are readily transferable/adaptable	may allow more complete loop-closure and recycling
	drawback	no *in situ* resources available (only recycling/production from stock)	no *in situ* resources available (only recycling/production from stock)
		microgravity makes certain processes more difficult	microgravity makes aqueous processes challenging
Martian[151]	advantage	no supply-chain, just-in-time response not feasible → ISRU, LC and ISM compulsory	especially suited to leverage the available *in situ* resources to expand capabilities
			allows resources to be exploit that are not accessible otherwise
		gravity, may allow certain processes to be adopted more readily	gravity, allows gas/liquid separation → operation of aqueous processes
	drawback	high infrastructure investment	high maintenance
		not as resilient	more susceptible to drift

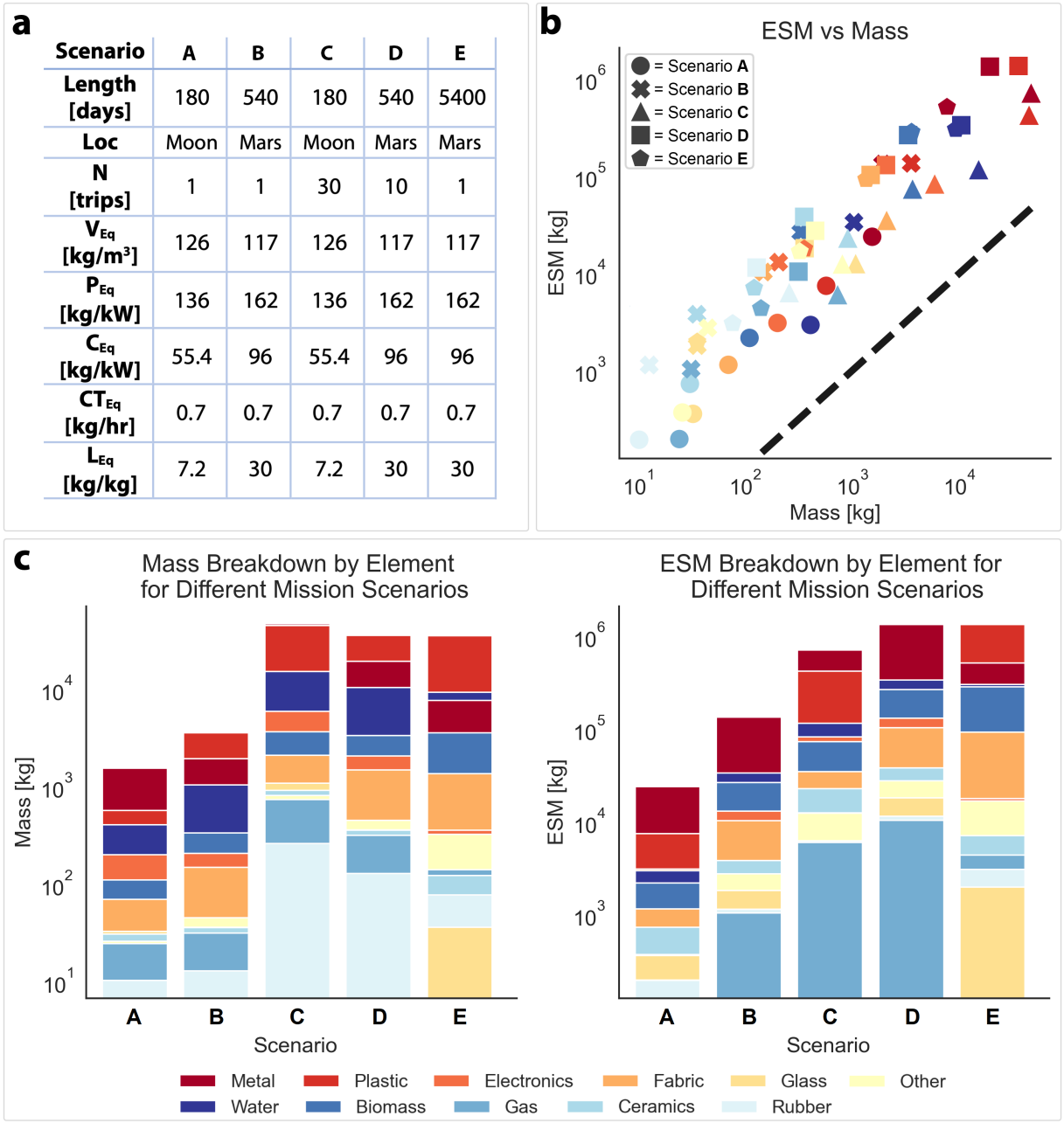

Scenario	A	B	C	D	E
Length [days]	180	540	180	540	5400
Loc	Moon	Mars	Moon	Mars	Mars
N [trips]	1	1	30	10	1
V_{Eq} [kg/m³]	126	117	126	117	117
P_{Eq} [kg/kW]	136	162	136	162	162
C_{Eq} [kg/kW]	55.4	96	55.4	96	96
CT_{Eq} [kg/hr]	0.7	0.7	0.7	0.7	0.7
L_{Eq} [kg/kg]	7.2	30	7.2	30	30

Figure S15: Alternate visualization of scenario-dependent inventory-breakdown. The parameter description of exemplar mission-design scenarios is given in panel **a**: scenarios 'A' and 'B' correspond to single sorties (N) to the Moon and Mars respectively using standard surface-operation duration[17], while scenarios 'C' and 'D' correspond to multi-sortie campaigns with the same (total) 5,400 days of surface operation as for scenario 'E'. These parameters can be used to calculate the ESM cost and include equivalency factors for Volume (V_{eq}), Power (P_{eq}), Cooling (C_{eq}), Crew-Time (CT_{eq}), and Location (L_{eq}).
A comparison of ESM and carry-along mass (both in kg) is presented in the scatter-plot **b**; the dotted line represents a 1:1 correspondence between ESM and carry-along mass to show the trade-offs in systems grouped by element in terms of non-standard mass components (volume, power, etc.) contributing to cost as compared to only mass. Color-coding of **b** corresponds to the bar-charts in **c**, where the carry-along and ESM are broken down by material-composition. Note that the carry-along and/or ESM for each scenario are plotted on a log scale. The maximum visible edge of each bar in a stack represents the corresponding component's carry-along or ESM value.

11.5 SI: Sustainability

UN SDGs	NASA STGC: Expand Human Presence In Space	NASA STGC: Manage In-space Resources	NASA STGC: Enable Transformational Space Exploration And Scientific Discovery
2,3	Molecular pharming is a perspective wherein plants are viewed as chemical factories, synthesizing desirable compounds with minimal inputs. In space, it would be used to allow astronauts to quickly respond to unanticipated disease states and decrease the need to bring or resupply large stockpiles of medication for longer missions[366]. Terrestrially, advances in molecular pharming can create healthier communities with more robust responses to sudden changes in medical needs[393].	Space agriculture has led to advances in the practice of vertical farming, a system which minimizes the amount of water, fertilizer, and pesticides needed to grow crops[483]. Besides the efficient use of resources, vertical farming allows crops to grow anywhere a controlled environment can be established, meaning that using vertical farming would allow densely populated urban areas to have readier access to locally grown fresh produce[45].	The Photobioreactor chamber on the ISS cultivates microalgae in order to create hybrid life support systems, combining biological and physicochemical processes to, for instance, grow *Chlorella vulgaris*[410], a microalgae rich in folate, iron, and vitamins D and B_{12}, the latter of which are notably absent from many traditional plant-based foods[50] . Advances in the Photobioreactor chamber have made it feasible to use it for advanced wastewater treatment and to cultivate nutrient-laden biomass over marine water instead of land[379].
6	The Microbial Check Valve developed for the Space Shuttle passively kills viable microorganisms within water to prevent cross-contamination[27]. In 2012, a water tank based on the ECLSS Water Recovery System was installed in Kendala, Iraq, a city whose population dropped 85% due to a deep-water well failure, and this tank uses the Microbial Check Valve to keep the water clean[274].	The Urine Processor Assembly on the ISS collects urine and processes it to potable standards[543], recovering much of the water available, but because urine can theoretically supply over 60% of the crew's water demand and the brine can be used as fertilizer, researchers continue to study how this system can be improved[543] Meanwhile on Earth, urine recovery systems are being implemented throughout wastewater systems in Europe, including by the European Space Agency[547], for use as fertilizer. Projections of a hypothetical urine-diversion system show that communities could lower their greenhouse gas emissions by up to 47%, energy consumption by up to 41%, and approximately halve their freshwater usage[225].	The ability to make ultra-pure water is extremely important for scientific research as well as for cooling the Extravehicular Mobility Unit (EMU) space suit. Aquaporin-based filtration, inspired by the aquaporin proteins found in almost every organism, is incredibly efficient and highly specific to filtering out water[224], and including it in the EMU design increases astronaut mobility. As clean freshwater resources are increasingly strained, there is a pressing need to improve filtration methods through non-energy intensive means, and aquaporins are eyed for their ability to fulfill this need[196].

UN SDGs	NASA STGC: Expand Human Presence In Space	NASA STGC: Manage In-space Resources	NASA STGC: Enable Transformational Space Exploration And Scientific Discovery
7	81.4% of human wastewater in space is urine, and transporting fresh water to space is expensive. Thus, the Urea Biochemical Reactor unit (UBR) is being studied as a way to combine wastewater treatment to separate urea from urine via forward osmosis, convert urea into ammonia in a bioreactor, and finally to convert that ammonia into energy, for use in space colonization. Results from studying the UBR show that it would work in any wastewater treatment containing urine and/or ammonia[409], potentially providing a new, non-energy or -resource intensive method for producing energy on Earth.	Using nutrients from wastewater, CO_2, and solar power, the algae studied in the NASA OMEGA project cleaned the wastewater and produced biomass that could be used for aviation fuel[586]. Coupled with advances made in using urine as a wastewater source for algae[245], with increased efficiency, this could provide a way for astronauts to produce *in situ* fuel rather than rely on resupply. The project renewed interest in using biomass as a fuel source, developed protocols for harvesting algae, and demonstrated that NASA has the motivation and the resources to study technological systems that are applicable both to rocket science and the search for efficient, affordable, and renewable energy.	At an optimal altitude for fuel conservation, the ISS expends about 8000 pounds of propellant a year[281]. Advances in bio-crude oil manufacturing by pre-treating microalgae with NaOH and urea[240] would mean that astronauts on the ISS would be able to conserve the amount of propellant brought and resupplied. As the environment is destroyed to mine natural oil, this technology presents an alternative way to manufacture crude oil and make it closer to becoming a renewable resource.
8,9	Phytoremediation is defined as the use of plants for remediation of contaminants[93]. In the 1980s, NASA studied closed-system applications of phytoremediation to create a healthy environment for astronauts off-world, and studies afterwards validated the idea that phytoremediation can effectively remove particulate matter, volatile organic compounds, and inorganic pollutants with minimal inputs[206]. This knowledge has been used to develop living walls, which have increased insulation and promote social and physical health using fewer inputs than traditional methods of urban construction[490].	Concrete production, especially making the boiled limestone that acts as a binding agent, accounts for 5% of anthropogenic carbon emissions[378]. Due to radiation and micrometeorites on the Moon and Mars, long-term human settlement on either will necessitate high amounts of concrete[405], but shipping tons of concrete to either location is not feasible, and traditional methods of making concrete are too energy-intensive, at least initially, to use off-world. To solve this issue, environmental engineers developed a method to harvest the binder from organisms[14] that could be shipped to other planets relatively cheaply and used in place of boiled limestone on Earth, lowering carbon emissions from concrete production.	The original purpose of Biosphere 2 (B2), a miniaturized version of Earth's ecological environments, was to establish a baseline for designing structures for long-term human habituation in space[14]. The B2 experiment informed other initiatives to simulate what life on the Moon and Mars would look like, such as HI-SEAS or PISCES[459]. Today, experiments in B2 are focused on improving ecology and eco-technology on Earth[408].

UN SDGs	NASA STGC: Expand Human Presence In Space	NASA STGC: Manage In-space Resources	NASA STGC: Enable Transformational Space Exploration And Scientific Discovery
11,12	One goal of MELiSSA is to create a closed-loop system in deep space which supplies astronauts with fresh air, water, and food using microbial recycling of human waste[548]. As the population grows and real estate becomes more limited, human-centered and sustainability-minded design philosophies are being used in cities. MELiSSA offers a potential blueprint for such design, by internalizing the complex relationships between humans and their environment while prioritizing sustainability.	Polyhydroxyalkanoate (PHA) polymers produced by bacteria and archaea are able to be used as biodegradable thermoplastics[432, 525], and have already tapped by NASA for use in long-term extraterrestrial missions precisely because they make production of needed materials possible even in space[90]. They have been studied for their use as a potential replacement for polyolefins in single-use plastics, in the hopes that in areas where single-use plastic is unavoidable (e.g. in medicine or research), PHAs would create less non-degradable waste[432]. Considering that the requirements for plastic production in space include producing minimal useless waste and that the plastics would have to meet the high standards of a top-of-the-line lab, perfecting the technology for NASA would mean that terrestrially, citizens would have access to plastics that are degradable but still safe enough for use in laboratory or medical environments.	So-called 'sick building syndrome' is a phenomenon wherein workers, especially if there are many of them, experience various health problems as a result of staying in a poorly ventilated building[450]. NASA has funded experiments which showed that houseplants in conjunction with activated charcoal efficiently cleaned indoor air pollutants[569, 570], and this research may be used to design space stations and terrestrial buildings which are conducive to the good health of their occupants.
13	Biofuels derived from cellulosic feedstocks (e.g. switchgrass, wood residues, etc.) have lower lifetime greenhouse gas emissions than those of petroleum fuels[288]. NASA has studied cellulosic biofuels for their potential as an *in situ* way of manufacturing fuel off-world[496] and developed enzyme structures which could facilitate access to biomass and biofuels[382]. On Earth, researchers are studying potentially carbon-negative biofuel production utilizing cellulosic feedstocks[288], which would require highly efficient processes potentially aided by NASA's research in enzymes to improve biomass production.	The Haber-Bosch process, which produces ammonia to be used in fertilizers and pharmaceuticals, requires large energy inputs[78] and releases 1.2% of global anthropogenic CO_2 emissions[494]. For space exploration, which thrusts astronauts into incredibly resource-limited environments, alternatives such as bacterial nitrogen fixation and urine ammonia extraction have been studied[302]. Methods which efficiently produce the ammonia astronauts need, using minimal energy inputs and recycled materials as feedstock, provides industrial chemical synthesizers strategies for ammonia production with a much smaller carbon footprint.	NASA's Surface Adhering BioReactor has a low energy and water input for cultivating microalgae. Microalgae can grow in extreme environments including microgravity[550], high temperature, solar radiation[423], and high salinity[8], to produce essential consumables and biofuels[533], making cultivation even on Earth relatively simple. Microalgae can be used for efficient CO_2 scrubbing, which would make significant progress towards cleaning the roughly 75% of greenhouse gas emissions that is CO_2[500, 413].

Table S24: Space Bioprocess Engineering technologies in the context of NASA's Space Technology Grand Challenges (STGCs) and United Nations Sustainability Development Goals (SDGs). Extended Version.

Bibliography

[1] *2001 Mars Odyssey Arrival Press Kit*. 2001. URL: https://mars.nasa.gov/files/odyssey/odysseyarrival1.pdf.

[2] *A Midterm Assessment of Implementation of the Decadal Survey on Life and Physical Sciences Research at NASA*. Tech. rep. National Academy of Sciences, 2018.

[3] Anthony J Abel and Douglas S Clark. "A comprehensive modeling analysis of formate-mediated microbial electrosynthesis". In: *ChemSusChem* (2020). ISSN: 1864-5631.

[4] Anthony J Abel et al. "Photovoltaics-Driven Power Production Can Support Human Exploration on Mars". In: *Frontiers in Astronomy and Space Sciences* 9 (2022). ISSN: 2296-987X. DOI: 10.3389/fspas.2022.868519. URL: https://www.frontiersin.org/articles/10.3389/fspas.2022.868519.

[5] Anthony J Abel et al. "Systems-informed genome mining for electroautotrophic microbial production". In: *bioRxiv* (2020).

[6] Morgan B Abney et al. "Comparison of Exploration Oxygen Recovery Technology Options Using ESM and LSMAC". In: *49th International Conference on Environmental Systems*. 2020.

[7] Morgan B Abney et al. "Ongoing Development of a Series Bosch Reactor System". In: *43rd International Conference on Environmental Systems*. 2013, p. 3512.

[8] Orit Adar, Ruth N Kaplan-Levy, and Gabi Banet. "High temperature Chlorellaceae (Chlorophyta) strains from the Syrian-African Rift Valley: the effect of salinity and temperature on growth, morphology and sporulation mode". In: *European Journal of Phycology* 51.4 (2016), pp. 387–400. DOI: 10.1080/09670262.2016.1193772. URL: https://doi.org/10.1080/09670262.2016.1193772.

[9] Rajani Adiga et al. "Point-of-care production of therapeutic proteins of good-manufacturing-practice quality". In: *Nature Biomedical Engineering* 2.9 (Sept. 2018), pp. 675–686. ISSN: 2157-846X. DOI: 10.1038/s41551-018-0259-1.

[10] Rien Aerts and F Stuart Chapin III. "The mineral nutrition of wild plants revisited: a re-evaluation of processes and patterns". In: *Advances in ecological research*. Vol. 30. Elsevier, 1999, pp. 1–67. ISBN: 0065-2504.

[11] Ebrahim Afshinnekoo et al. "Fundamental biological features of spaceflight: Advancing the field to enable deep-space exploration". In: *Cell* 183.5 (2020), pp. 1162–1184. ISSN: 0092-8674.

[12] *Agile Biofoundry Metabolic Map*. URL: https://agilebiofoundry.org/metabolic-map-3/.

[13] Göran I Ågren. "Theory for growth of plants derived from the nitrogen productivity concept". In: *Physiologia plantarum* 64.1 (1985), pp. 17–28. ISSN: 0031-9317.

[14] John Allen and Mark Nelson. "Overview and Design Biospherics and Biosphere 2, mission one (1991–1993)". In: *Ecological Engineering* 13.1 (1999), pp. 15–29. ISSN: 0925-8574. DOI: https://doi.org/10.1016/S0925-8574(98)00089-5. URL: https://www.sciencedirect.com/science/article/pii/S0925857498000895.

[15] Preetam Anbukarasu, Dominic Sauvageau, and Anastasia Elias. "Tuning the properties of polyhydroxybutyrate films using acetic acid via solvent casting". In: *Scientific reports* 5 (2015), p. 17884. ISSN: 2045-2322.

[16] Molly S Anderson, Michael K Ewert, and John F Keener. "Life support baseline values and assumptions document". In: (2018), p. 233. DOI: NTRS:NASA/TP-2015-218570/REV1. URL: https://ntrs.nasa.gov/api/citations/20210024855/downloads/BVAD_2.15.22-final.pdf.

[17] Molly S Anderson, Michael K Ewert, and John F Keener. *Life support baseline values and assumptions document*. Tech. rep. Washington DC: NASA, 2022, p. 233. DOI: NTRS:NASA/TP-2015-218570/REV1. URL: https://ntrs.nasa.gov/api/citations/20210024855/downloads/BVAD_2.15.22-final.pdf.

[18] Aaron C Anselmo, Yatin Gokarn, and Samir Mitragotri. "Non-invasive delivery strategies for biologics". In: *Nature Reviews Drug Discovery* 18.1 (Jan. 2019), pp. 19–40. ISSN: 1474-1776. DOI: 10.1038/nrd.2018.183.

[19] E Antonsen et al. "Evidence report: risk of adverse health outcomes and decrements in performance due to in-flight medical conditions". In: *National Aeronautics and Space Administration, Houston, TX, USA. Approved for public release: May8* (2017).

[20] George Apostolakis. "The distinction between aleatory and epistemic uncertainties is important: an example from the inclusion of aging effects into PSA". In: *Proceedings of PSA '99, International Topical Meeting on Probabilistic Safety Assessment*. 1999, pp. 135–142.

[21] Evan Appleton et al. "Design automation in synthetic biology". In: *Cold Spring Harbor perspectives in biology* 9.4 (2017), a023978. ISSN: 1943-0264.

[22] Onur Apul et al. "Divided Perception of Drinking Water Safety: Another Manifestation of America's Racial Gap". In: *ACS ES&T Water* 1.1 (Jan. 2021), pp. 6–7. DOI: 10.1021/acsestwater.0c00022. URL: https://doi.org/10.1021/acsestwater.0c00022.

[23] Natthiporn Aramrueang, Joshua Rapport, and Ruihong Zhang. "Effects of hydraulic retention time and organic loading rate on performance and stability of anaerobic digestion of {\textbackslash}textit{\{}Spirulina{\}}". In: *Bioresource Technology* 147 (2016), pp. 174–182. URL: https://www.sciencedirect.com/science/article/pii/S1537511015304670.

[24] Asieh Aramvash, Fatemeh Moazzeni Zavareh, and Narges Gholami Banadkuki. "Comparison of different solvents for extraction of polyhydroxybutyrate from Cupriavidus necator". In: *Engineering in Life Sciences* 18.1 (2018), pp. 20–28. ISSN: 1618-0240.

[25] G Araniti, I Bisio, and M De Sanctis. "Interplanetary Networks: Architectural Analysis, Technical Challenges and Solutions Overview". In: *2010 IEEE International Conference on Communications*. 2010, pp. 1–5. DOI: 10.1109/ICC.2010.5502491.

[26] Adam P Arkin et al. "KBase: the United States department of energy systems biology knowledgebase". In: *Nature biotechnology* 36.7 (2018), pp. 566–569. ISSN: 1546-1696.

[27] James E Atwater and Richard R Wheeler. "Advanced Development of the Regenerative Microbial Check Valve". In: *International Conference On Environmental Systems*. SAE International, July 1993. DOI: https://doi.org/10.4271/932175. URL: https://doi.org/10.4271/932175.

[28] Thomas R Aunins et al. "Spaceflight Modifies Escherichia coli Gene Expression in Response to Antibiotic Exposure and Reveals Role of Oxidative Stress Response". In: *Frontiers in Microbiology* 9 (2018), p. 310. ISSN: 1664-302X. DOI: 10.3389/fmicb.2018.00310. URL: https://www.frontiersin.org/article/10.3389/fmicb.2018.00310.

[29] Nils J H Averesch and Lynn J Rothschild. "Metabolic engineering of Bacillus subtilis for production of para-aminobenzoic acid – unexpected importance of carbon source is an advantage for space application". In: *Microbial Biotechnology* 12.4 (2019), pp. 703–714. DOI: https://doi.org/10.1111/1751-7915.13403. URL: https://sfamjournals.onlinelibrary.wiley.com/doi/abs/10.1111/1751-7915.13403.

[30] Nils J H Averesch et al. "Biocatalytic Formation of Novel Polyesters with para-Hydroxyphenyl groups in the Backbone {\textendash} Engineering Cupriavidus necator for production of high-performance materials from CO2 and electricity". In: *bioRxiv* (2021). DOI: 10.1101/2021.12.12.472320. URL: https://www.biorxiv.org/content/early/2021/12/13/2021.12.12.472320.

[31] Nils Jonathan Helmuth Averesch. "Choice of Microbial System for In-Situ Resource Utilization on Mars". In: *Frontiers in Astronomy and Space Sciences* 8 (2021), p. 116. ISSN: 2296-987X. DOI: 10.3389/fspas.2021.700370. URL: https://www.frontiersin.org/article/10.3389/fspas.2021.700370.

[32] Maurice M Averner. "The NASA CELSS program". In: (1990).

[33] Emily Baldwin et al. *ExoMars 2016: analysing atmospheric gases for signs of active biological or geological processes on Mars, and testing key landing technologies*. 2016. URL: https://sci.esa.int/documents/33431/35950/1567260281560-EXOMARS_Mediakit_2016-03-09.pdf.

[34] Hervé Barthélémy, Mathilde Weber, and Françoise Barbier. "Hydrogen storage: recent improvements and industrial perspectives". In: *International Journal of Hydrogen Energy* 42.11 (2017), pp. 7254–7262. ISSN: 0360-3199.

[35] Krystal Batelaan. "'It's not the science we distrust; it's the scientists': Reframing the anti-vaccination movement within Black communities". In: *Global Public Health* 17.6 (2022), pp. 1099–1112. DOI: 10.1080/17441692.2021.1912809. URL: https://doi.org/10.1080/17441692.2021.1912809.

[36] Mark R Bell et al. "To fuse or not to fuse: What is your purpose?" In: *Protein Science* 22.11 (Nov. 2013), pp. 1466–1477. ISSN: 0961-8368. DOI: 10.1002/pro.2356.

[37] Mia A Benevolenza and LeaAnne DeRigne. "The impact of climate change and natural disasters on vulnerable populations: A systematic review of literature". In: *Journal of Human Behavior in the Social Environment* 29.2 (2019), pp. 266–281. DOI: 10.1080/10911359.2018.1527739. URL: https://doi.org/10.1080/10911359.2018.1527739.

[38] Mark Benton. "Crew and Cargo Landers for Human Exploration of Mars-Vehicle System Design". In: *44th AIAA/ASME/SAE/ASEE Joint Propulsion Conference {\&} Exhibit*. 2008, p. 5156.

[39] Alexander J Benvenuti et al. "Design of Anaerobic Digestion Systems for Closed Loop Space Biomanufacturing". In: *50th International Conference on Environmental Systems (ICES)*. 2020.

[40] A J Berliner et al. "Towards a Biomanufacturing-Driven Reference Mission Architecture for Long-Term Human Mars Exploration". In: *LPICo* 2089 (2019), p. 6261. ISSN: 0161-5297.

[41] Aaron Berliner, George Makrygiorgos, and Avery Hill. "Extension of Equivalent System Mass for Human Exploration Missions on Mars". In: *preprints.org* (2021). DOI: doi:10.20944/preprints202101.0363.v1.

[42] Aaron Berliner et al. "Towards a Biomanufactory on Mars". In: *preprints.org* (2020). DOI: doi:10.20944/preprints202012.0714.v1.

[43] Aaron J Berliner et al. "Space bioprocess engineering on the horizon". In: *Communications Engineering* 1.1 (2022), p. 13. ISSN: 2731-3395. DOI: 10.1038/s44172-022-00012-9. URL: https://doi.org/10.1038/s44172-022-00012-9.

[44] Aaron J Berliner et al. "Towards a Biomanufactory on Mars". In: *Frontiers in Astronomy and Space Sciences* 8 (2021), p. 120. ISSN: 2296-987X. DOI: 10.3389/fspas.2021.711550. URL: https://www.frontiersin.org/article/10.3389/fspas.2021.711550.

[45] Fred H Besthorn. "Vertical Farming: Social Work and Sustainable Urban Agriculture in an Age of Global Food Crises". In: *Australian Social Work* 66.2 (2013), pp. 187–203. DOI: 10.1080/0312407X.2012.716448. URL: https://doi.org/10.1080/0312407X.2012.716448.

[46] BidenJoseph. *Budget of the U.S. Government: Fiscal Year 2023*. Tech. rep. Washington DC: Office of Management and Budget, 2022, pp. 1–158. URL: https://www.whitehouse.gov/wp-content/uploads/2022/03/budget_fy2023.pdf.

[47] Lorenz T Biegler, Ignacio E Grossmann, and Arthur W Westerberg. "Systematic methods for chemical process design". In: (1997).

[48] S J Bingham et al. "The Mars Climate Database". In: (2003).

[49] Deborah L Bishop et al. "Seedborne fungal contamination: consequences in space-grown wheat". In: *Phytopathology* 87.11 (1997), pp. 1125–1133. ISSN: 0031-949X.

[50] Tomohiro Bito et al. "Potential of Chlorella as a Dietary Supplement to Promote Human Health." eng. In: *Nutrients* 12.9 (Aug. 2020). ISSN: 2072-6643 (Electronic). DOI: 10.3390/nu12092524.

[51] A Biwer and E Heinzle. "Environmental assessment in early process development". In: *Journal Of Chemical Technology And Biotechnology* 79.6 (June 2004), pp. 597–609. ISSN: 0268-2575. DOI: 10.1002/jctb.1027.

[52] Mariano Bizzarri et al. "Journey to Mars: A Biomedical Challenge. Perspective on future human space flight". In: *Organisms. Journal of Biological Sciences* 1.2 (2017), pp. 15–26. ISSN: 2532-5876.

[53] Rebecca S Blue et al. "Supplying a pharmacy for NASA exploration spaceflight: challenges and current understanding". In: *Npj microgravity* 5.1 (2019), pp. 1–12. ISSN: 2373-8065.

[54] Space Studies Board and National Research Council. *Pathways to exploration: rationales and approaches for a US program of human space exploration*. National Academies Press, 2014. ISBN: 0309305101.

[55] Marianne R Bobskill and Mark L Lupisella. "The role of cis-lunar space in future global space exploration". In: *Global Space Exploration Conference*. GLEX-2012.05. 5.4 x12270. 2012.

[56] Anna-Sophia Boguraev et al. "Successful amplification of DNA aboard the International Space Station". In: *npj Microgravity* 3.1 (2017), p. 26. ISSN: 2373-8065. DOI: 10.1038/s41526-017-0033-9. URL: https://doi.org/10.1038/s41526-017-0033-9.

[57] Giorgio Boscheri et al. "SCALISS: An European Tool for Automated Scaling of Life Support Systems". In: 47th International Conference on Environmental Systems, 2017.

[58] Agathe Kathia Boutaud. *Multi-mission sizing and selection methodology for space habitat subsystems*. 2019.

[59] Wernher von Braun. "Manned Mars Landing Presentation to the Space Task Group". In: *presentation materials* 4 (1969).

[60] Ulysse Brémond et al. "Biological pretreatments of biomass for improving biogas production: an overview from lab scale to full-scale". In: *Renewable and Sustainable Energy Reviews* 90 (2018), pp. 583–604. URL: https://www.sciencedirect.com/science/article/pii/S1364032118301990.

[61] Drake G Bret et al. *Human Exploration of Mars Design Reference Architecture 5.0 Addendum# 2. NASA*. Tech. rep. NASA, 2014. DOI: NASA/SP-2009-566-ADD2,S-1037,JSC-CN-35516. URL: http://hdl.handle.net/2060/20160003093.

[62] R F Brodsky. "The Time Has Come for the BS in Astronautical Engineering." In: *Engineering Education* 76.3 (1985), pp. 149–152.

[63] Jean Brunet et al. "Alisse: Advanced life support system evaluator". In: *38th COSPAR Scientific Assembly* 38 (2010), p. 2.

[64] Kristi Budzinski et al. "Introduction of a process mass intensity metric for biologics". In: *New Biotechnology* 49 (Mar. 2019), pp. 37–42. ISSN: 1871-6784. DOI: 10.1016/j.nbt.2018.07.005.

[65] Bruce Bugbee. "Economics of LED Lighting". In: *Light Emitting Diodes for Agriculture: Smart Lighting*. Ed. by S Dutta Gupta. Singapore: Springer Singapore, 2017, pp. 81–99. ISBN: 978-981-10-5807-3. DOI: 10.1007/978-981-10-5807-3{_}5. URL: https://doi.org/10.1007/978-981-10-5807-3_5.

[66] V V Bukhmirov, N F Kokarev, and A V Sadchikov. "Installation of separation of methane-containing gas mixtures of the bioenergy station "Eco-Volt-Agro"". In: *Journal of Physics: Conference Series* 1111 (Dec. 2018), p. 12058. DOI: 10.1088/1742-6596/1111/1/012058. URL: https://doi.org/10.1088/1742-6596/1111/1/012058.

[67] Aaron S Burton et al. "Off Earth Identification of Bacterial Populations Using 16S rDNA Nanopore Sequencing". In: *Genes* 11.1 (2020). ISSN: 2073-4425. DOI: 10.3390/genes11010076. URL: https://www.mdpi.com/2073-4425/11/1/76.

[68] *Bush Unveils Plan to Return Humans to Moon and on to Mars | PBS NewsHour*. 2014. URL: https://www.pbs.org/newshour/science/science-jan-june04-moon_01-14.

[69] Ben Bussey and Stephen J Hoffman. "Human Mars landing site and impacts on Mars surface operations". In: *2016 IEEE Aerospace Conference*. IEEE, 2016, pp. 1–21. ISBN: 1467376760.

[70] Kathryne G Byrne-Bailey and John D Coates. "Complete genome sequence of the anaerobic perchlorate-reducing bacterium Azospira suillum strain PS". In: *Journal of bacteriology* 194.10 (2012), pp. 2767–2768. ISSN: 0021-9193.

[71] Kathryn F Bywaters and R C Quinn. "Perchlorate-Reducing Bacteria: Evaluating The Potential For Growth Utilizing Nutrient Sources Identified On Mars". In: *Lunar and Planetary Science Conference*. Vol. 47. 2016, p. 2946.

[72] Daniel F Caddell, Siwen Deng, and Devin Coleman-Derr. "Role of the plant root microbiome in abiotic stress tolerance". In: *Seed Endophytes*. Springer, 2019, pp. 273–311.

[73] F Cain. "Artificial meat could be grown on a large scale". In: *Universe Today* (2005).

[74] John R Cain. "Lunar dust: the hazard and astronaut exposure risks". In: *Earth, Moon, and Planets* 107.1 (2010), pp. 107–125.

[75] Riccardo Campa, Konrad Szocik, and Martin Braddock. "Why space colonization will be fully automated". In: *Technological Forecasting and Social Change* 143 (2019), pp. 162–171. ISSN: 0040-1625. DOI: https://doi.org/10.1016/j.techfore.2019.03.021. URL: https://www.sciencedirect.com/science/article/pii/S0040162518317281.

[76] Kevin M Cannon and Daniel T Britt. "Feeding one million people on Mars". In: *New Space* 7.4 (2019), pp. 245–254. ISSN: 2168-0256.

[77] Barry Canton, Anna Labno, and Drew Endy. "Refinement and standardization of synthetic biological parts and devices". In: *Nature biotechnology* 26.7 (2008), pp. 787–793. ISSN: 1546-1696.

[78] Marcal Capdevila-Cortada. "Electrifying the Haber–Bosch". In: *Nature Catalysis* 2.12 (2019), p. 1055. ISSN: 2520-1158. DOI: 10.1038/s41929-019-0414-4. URL: https://doi.org/10.1038/s41929-019-0414-4.

[79] Anne J Caraccio et al. "Trash-to-gas: Converting space trash into useful products". In: *43rd International Conference on Environmental Systems (ICES)*. AIAA 2013-3440. 2013. DOI: 10.2514/6.2013-3440.

[80] Pablo Carbonell. "Getting on the Path to Engineering Biology". In: *Metabolic Pathway Design*. Springer, 2019, pp. 3–10.

[81] ELIZABETE CARMO-SILVA et al. "Optimizing Rubisco and its regulation for greater resource use efficiency". In: *Plant, Cell & Environment* 38.9 (2015), pp. 1817–1832. DOI: https://doi.org/10.1111/pce.12425. URL: https://onlinelibrary.wiley.com/doi/abs/10.1111/pce.12425.

[82] Susana Carranza, Darby B Makel, and Brandon Blizman. "In situ manufacturing of plastics and composites to support H{\&}R exploration". In: *AIP Conference Proceedings*. Vol. 813. 1. American Institute of Physics, 2006, pp. 1122–1129. ISBN: 0735403058.

[83] Sofie M Castelein et al. "Iron can be microbially extracted from Lunar and Martian regolith simulants and 3D printed into tough structural materials". In: *PLOS ONE* 16.4 (2021), pp. 1–21. DOI: 10.1371/journal.pone.0249962. URL: https://doi.org/10.1371/journal.pone.0249962.

[84] Francesco Castellini et al. "A mars communication constellation for human exploration and network science". In: *Advances in Space Research* 45.1 (2010), pp. 183–199. ISSN: 0273-1177. DOI: https://doi.org/10.1016/j.asr.2009.10.019. URL: https://www.sciencedirect.com/science/article/pii/S0273117709006826.

[85] Sarah L. Castro, David J. Smith, and Martk Ott. *Researcher's Guide to: International Space Station Microbial Research*. Tech. rep. Houston, TX: National Aeronautics and Space Administration, Johnson Space Center, 2014.

[86] D C Catling et al. "Atmospheric origins of perchlorate on Mars and in the Atacama". In: *Journal of Geophysical Research: Planets* 115.E1 (2010). ISSN: 0148-0227.

[87] Manned Spacecraft Center and John Glenn. *Results of the First US Manned Orbital Space Flight, February 20, 1962*. Manned Spacecraft Center, National Aeronautics and Space Administration, 1962.

[88] Stefano Cestellos-Blanco, Hao Zhang, and Peidong Yang. "Solar-driven carbon dioxide fixation using photosynthetic semiconductor bio-hybrids". In: *Faraday Discuss.* 215.0 (2019), pp. 54–65. DOI: 10.1039/C8FD00187A. URL: http://dx.doi.org/10.1039/C8FD00187A.

[89] Stefano Cestellos-Blanco et al. "Photosynthetic biohybrid coculture for tandem and tunable CO₂ and N₂ fixation". In: *Proceedings of the National Academy of Sciences* 119.26 (2022), e2122364119. DOI: 10.1073/pnas.2122364119. URL: https://www.pnas.org/doi/abs/10.1073/pnas.2122364119.

[90] Stefano Cestellos-Blanco et al. "Production of PHB From CO2-Derived Acetate With Minimal Processing Assessed for Space Biomanufacturing". In: *Frontiers in Microbiology* 12 (2021), p. 2126. ISSN: 1664-302X. DOI: 10.3389/fmicb.2021.700010. URL: https://www.frontiersin.org/article/10.3389/fmicb.2021.700010.

[91] John-Marc Chandonia et al. *CORAL Prototype Implementation (CORAL) v0. 1*. Tech. rep. 2020.

[92] Gail Chapline and Steven Sullivan. "Systems engineering for Lifecycle of Complex Systems". In: *Engineering Innovations (NASA)* (2010).

[93] Khushboo Chaudhary, Sumira Jan, and Suphiya Khan. "Chapter 23 - Heavy Metal ATPase (HMA2, HMA3, and HMA4) Genes in Hyperaccumulation Mechanism of Heavy Metals". In: *Plant Metal Interaction*. Ed. by Parvaiz Ahmad. Elsevier, 2016, pp. 545–556. ISBN: 978-0-12-803158-2. DOI: https://doi.org/10.1016/B978-0-12-803158-2.00023-0. URL: https://www.sciencedirect.com/science/article/pii/B9780128031582000230.

[94] Jing Chen et al. "Metabolic engineering of Escherichia coli for the synthesis of polyhydroxyalkanoates using acetate as a main carbon source". In: *Microbial cell factories* 17.1 (2018), p. 102. ISSN: 1475-2859.

[95] Jingguang G Chen et al. "Beyond fossil fuel–driven nitrogen transformations". In: *Science* 360.6391 (2018). ISSN: 0036-8075.

[96] Xiangbin Chen et al. "Engineering Halomonas bluephagenesis TD01 for non-sterile production of poly (3-hydroxybutyrate-co-4-hydroxybutyrate)". In: *Bioresource technology* 244 (2017), pp. 534–541. ISSN: 0960-8524.

[97] Allen A Cheng and Timothy K Lu. "Synthetic biology: an emerging engineering discipline". In: *Annual review of biomedical engineering* 14 (2012), pp. 155–178. ISSN: 1523-9829.

[98] Wen-Hui Cheng et al. "Monolithic photoelectrochemical device for direct water splitting with 19% efficiency". In: *ACS Energy Letters* 3.8 (2018), pp. 1795–1800. ISSN: 2380-8195.

[99] Weonu Choe, Trishaladevi A Durgannavar, and Sang J Chung. "Fc-Binding Ligands of Immunoglobulin G: An Overview of High Affinity Proteins and Peptides". In: *Materials* 9.12 (Dec. 2016). ISSN: 1996-1944. DOI: 10.3390/ma9120994.

[100] So Young Choi et al. "One-step fermentative production of poly (lactate-co-glycolate) from carbohydrates in Escherichia coli". In: *Nature biotechnology* 34.4 (2016), pp. 435–440. ISSN: 1546-1696.

[101] Deepak Choudhury, Shivesh Anand, and May Win Naing. "The arrival of commercial bioprinters–Towards 3D bioprinting revolution!" In: *International journal of bioprinting* 4.2 (2018).

[102] Hassane Chraibi. "Resilience Assessment of Interconnected Critical Infrastructures with PyCATSHOO". In: *11th international conference on mathematical methods in reliability (MMR), Hong Kong, China*. 2019.

[103] Hassane Chraibi, J C Houbedine, and Alain Sibler. "Pycatshoo: Toward a new platform dedicated to dynamic reliability assessments of hybrid systems". In: *PSAM congress*. 2016.

[104] Timothy Cichan et al. "Mars base camp: An architecture for sending humans to Mars by 2028". In: *2017 IEEE Aerospace Conference*. IEEE, 2017, pp. 1–18. ISBN: 1509016139.

[105] I Cinelli and L Brown. "Innovation in Medical Technology Driven by Advances in Aerospace". In: *2018 40th Annual International Conference of the IEEE Engineering in Medicine and Biology Society (EMBC)*. July 2018, pp. 941–944. DOI: 10.1109/EMBC.2018.8512444.

[106] William Cirillo et al. "Supportability for beyond low earth orbit missions". In: *AIAA SPACE 2011 Conference & Exposition*. 2011, p. 7231.

[107] David Clark and David Clark. "In-situ propellant production on Mars-A Sabatier/-electrolysis demonstration plant". In: *33rd Joint Propulsion Conference and Exhibit*. 1997, p. 2764.

[108] Jan Kenneth Clawson, Matthew Christopher Napoli, and Michael P Snyder. "Optical Fiber Production in Microgravity". In: (2019). URL: https://www.nasa.gov/mission_pages/station/research/experiments/explorer/Investigation.html?#id=7388.

[109] C S Cockell and R Santomartino. "Mining and microbiology for the solar system silicate and basalt economy". In: *Space manufacturing resources: earth and planetary exploration applications. Wiley, Hoboken* (2021).

[110] Charles S Cockell. "Bridging the gap between microbial limits and extremes in space: space microbial biotechnology in the next 15 years". In: *Microbial Biotechnology* 15.1 (2022), pp. 29–41. DOI: https://doi.org/10.1111/1751-7915.13927. URL: https://sfamjournals.onlinelibrary.wiley.com/doi/abs/10.1111/1751-7915.13927.

[111] Charles S Cockell et al. "Space station biomining experiment demonstrates rare earth element extraction in microgravity and Mars gravity". In: *Nature communications* 11.1 (2020), pp. 1–11. ISSN: 2041-1723.

[112] Jacques Cohen. "The crucial role of CS in systems and synthetic biology". In: *Communications of the ACM* 51.5 (2008), pp. 15–18. ISSN: 0001-0782.

[113] Marc M Cohen. "First Mars Habitat Architecture". In: *AIAA SPACE 2015 Conference and Exposition*. 2015, p. 4517.

[114] William Colglazier. "Sustainable development agenda: 2030". In: *Science* 349.6252 (2015), pp. 1048–1050. ISSN: 0036-8075.

[115] Charles A R Cotton et al. "Renewable methanol and formate as microbial feedstocks". In: *Current Opinion in Biotechnology* 62 (2020), pp. 168–180. ISSN: 0958-1669. DOI: https://doi.org/10.1016/j.copbio.2019.10.002. URL: https://www.sciencedirect.com/science/article/pii/S0958166919301004.

[116] National Research Council. *Advanced technology for human support in space*. National Academies Press, 1997. ISBN: 0309057442.

[117] Robert Sidney Cox et al. "Synthetic biology open language (SBOL) version 2.2. 0". In: *Journal of integrative bioinformatics* 15.1 (2018). ISSN: 1613-4516.

[118] Ian A Crawford. "Lunar resources: A review". In: *Progress in Physical Geography* 39.2 (2015), pp. 137–167. ISSN: 0309-1333.

[119] Steve Creech, John Guidi, and Darcy Elburn. "Artemis: An Overview of NASA's Activities to Return Humans to the Moon". In: *IEEE Aerospace Conference*. Big Sky, MT: IEEE, 2022. DOI: 10.1109/AERO47225.2020.9172323. URL: https://ntrs.nasa.gov/citations/20210026673.

[120] *Criteria for Accrediting Engineering Programs, 2020 – 2021 | ABET*. Aug. 2021. URL: https://www.abet.org/accreditation/accreditation-criteria/criteria-for-accrediting-engineering-programs-2020-2021/.

[121] Laura E Crowell et al. "On-demand manufacturing of clinical-quality biopharmaceuticals". In: *Nature biotechnology* 36.10 (2018), pp. 988–995. ISSN: 1546-1696.

[122] Jason Crusan et al. "NASA's Gateway: An Update on Progress and Plans for Extending Human Presence to Cislunar Space". In: *2019 IEEE Aerospace Conference*. IEEE, 2019, pp. 1–19. ISBN: 1538668548.

[123] Pablo Cruz-Morales et al. "Biosynthesis of polycyclopropanated high energy biofuels". In: *Joule* (July 2022). ISSN: 2542-4785. DOI: 10.1016/j.joule.2022.05.011. URL: https://doi.org/10.1016/j.joule.2022.05.011.

[124] *Cubesat 101: basic concepts and processes for first-time CubeSat developers*. Tech. rep. 2017, p. 96.

[125] Selby C Cull et al. "Concentrated perchlorate at the Mars Phoenix landing site: Evidence for thin film liquid water on Mars". In: *Geophysical Research Letters* 37.22 (2010). ISSN: 0094-8276.

[126] Su Curley et al. "Deep space habitat ECLSS design concept". In: *42nd International Conference on Environmental Systems*. 2012, p. 3417.

[127] Hill Curtis et al. *FY21 On-Demand Manufacturing of Electronics (ODME)*. Aug. 2021. URL: https://ntrs.nasa.gov/citations/20210020977.

[128] M Czupalla et al. "An environmentally sensitive dynamic human model for LSS robustness studies with the V-HAB simulation". In: *Advances in space research* 44.12 (2009), pp. 1413–1427. ISSN: 0273-1177.

[129] Markus Czupalla et al. "Dynamic life support system simulations with the virtual habitat". In: *41st International Conference on Environmental Systems*. 2011, p. 5038.

[130] Markus Czupalla et al. "The Virtual Habitat–A tool for dynamic life support system simulations". In: *Advances in Space Research* 55.11 (2015), pp. 2683–2707. ISSN: 0273-1177.

[131] Arne Dahlback and Knut Stamnes. "A new spherical model for computing the radiation field available for photolysis and heating at twilight". In: *Planetary and Space Science* 39.5 (1991), pp. 671–683. ISSN: 0032-0633.

[132] Alfonso F Davila et al. "Perchlorate on Mars: a chemical hazard and a resource for humans". In: *International Journal of Astrobiology* 12.04 (2013), pp. 321–325. ISSN: 1475-3006.

[133] Charles DeLisi et al. "The Role of Synthetic Biology in Atmospheric Greenhouse Gas Reduction: Prospects and Challenges". In: *BioDesign Research* 2020 (2020), p. 1016207. ISSN: null. DOI: 10.34133/2020/1016207. URL: https://doi.org/10.34133/2020/1016207.

[134] Victor K. Der. *Clean Coal Technology Programs: Program Update 2009*. Tech. rep. Washington DC: U.S. Department of Energy, 2009, pp. 1–100. DOI: 10.2172/970830. URL: https://www.osti.gov/biblio/970830.

[135] Loïc Desgeorges et al. "Formalism and semantics of PyCATSHOO: A simulator of distributed stochastic hybrid automata." In: *Reliab. Eng. Syst. Saf.* 208 (2021), p. 107384.

[136] Gisela Detrell and Stefan Belz. "ELISSA–a comprehensive software package for ECLSS technology selection, modelling and simulation for human spaceflight missions". In: 47th International Conference on Environmental Systems, 2017.

[137] Gisela Detrell, Stefan Belz, and Jochen Keppler. "ELISSA: A Life Support System (LSS) technology selection, modelling and simulation tool for human spaceflight missions". In: *42nd COSPAR Scientific Assembly*. Vol. 42. 2018.

[138] Gisela Detrell, Ernst Messerschmid, and Eulàlia Gríful Ponsati. "ECLSS reliability analysis tool for long duration spaceflight". In: *46th International Conference on Environmental Systems*. 2016.

[139] Homayoon Dezfuli et al. "Bayesian inference for NASA probabilistic risk and reliability analysis". In: (2009).

[140] Homayoon Dezfuli et al. "NASA Risk-Informed Decision Making Handbook". In: (2010).

[141] Pietro Di Profio et al. "Comparison of hydrogen hydrates with existing hydrogen storage technologies: Energetic and economic evaluations". In: *International Journal of Hydrogen Energy* 34.22 (2009), pp. 9173–9180. ISSN: 0360-3199.

[142] Sydney Do, Andrew Owens, and Olivier de Weck. "HabNet–An Integrated Habitation and Supportability Architecting and Analysis Environment". In: 45th International Conference on Environmental Systems, 2015.

[143] Sydney Do et al. "An independent assessment of the technical feasibility of the Mars One mission plan–Updated analysis". In: *Acta Astronautica* 120 (2016), pp. 192–228. ISSN: 0094-5765.

[144] *DOE Announces New $60 Million Investment to Increase Energy Efficiency in Manufacturing*. 2021. URL: https://www.energy.gov/articles/doe-announces-new-60-million-investment-increase-energy-efficiency-manufacturing.

[145] Anna Doloman and Lance C Seefeldt. "An Experimentally Evaluated Thermodynamic Approach to Estimate Growth of Photoheterotrophic Purple Non-Sulfur Bacteria". In: *Frontiers in Microbiology* 11 (2020), p. 2163. ISSN: 1664-302X.

[146] H Döscher et al. "Sunlight absorption in water–efficiency and design implications for photoelectrochemical devices". In: *Energy & Environmental Science* 7.9 (2014), pp. 2951–2956. ISSN: 1754-5706.

[147] Bret G Drake, Stephen J Hoffman, and David W Beaty. "Human exploration of Mars, design reference architecture 5.0". In: *Aerospace Conference, 2010 IEEE*. IEEE, 2010, pp. 1–24. ISBN: 142443887X.

[148] Saige Drecksler et al. "Effects of Space Biomanufacturing on Fuel Production Alternatives for Mars Exploration". In: *50th International Conference on Environmental Systems (ICES)*. 2020 International Conference on Environmental Systems, 2020.

[149] Kai Dresia et al. "Nonlinear control of an expander-bleed rocket engine using reinforcement learning". In: (2021).

[150] A E Drysdale. "The effect of resource cost on life support selection". In: *SAE Technical Paper* 951492 (1995), p. 25.

[151] A E Drysdale, M K Ewert, and A J Hanford. "Life support approaches for Mars missions". In: *Advances in Space Research* 31.1 (2003), pp. 51–61. ISSN: 0273-1177.

[152] Alan Drysdale. *Esm history, capability, and methods*. Tech. rep. 2003.

[153] Alan Drysdale. *Metrics and system analysis*. Tech. rep. 1998.

[154] Alan Drysdale et al. "Use of sunlight for plant lighting in a bioregenerative life support system–equivalent system mass calculations". In: *Advances in Space Research* 42.12 (2008), pp. 1929–1943. ISSN: 0273-1177.

[155] Alan E Drysdale, Mike Ewert, and Anthony J Hanford. *Equivalent system mass studies of missions and concepts*. Tech. rep. 1999.

[156] Brian Du et al. "Evaluation of physical and chemical changes in pharmaceuticals flown on space missions". In: *The AAPS journal* 13.2 (2011), pp. 299–308. ISSN: 1550-7416.

[157] Kevin D Earle et al. "Strategic Framework for NASA's Space Technology Mission Directorate". In: *2018 AIAA SPACE and Astronautics Forum and Exposition*. DOI: 10.2514/6.2018-5136. URL: https://arc.aiaa.org/doi/abs/10.2514/6.2018-5136.

[158] Marybeth A Edeen et al. "Control of air revitalization using plants: Results of the early human testing initiative Phase I Test". In: *SAE transactions* (1996), pp. 781–795. ISSN: 0096-736X.

[159] Ali Eftekhari. "Energy efficiency: a critically important but neglected factor in battery research". In: *Sustainable Energy & Fuels* 1.10 (2017), pp. 2053–2060. ISSN: 2398-4902.

[160] Alex Ellery. "Supplementing Closed Ecological Life Support Systems with In-Situ Resources on the Moon". In: *Life* 11.8 (2021). ISSN: 2075-1729. DOI: 10.3390/life11080770. URL: https://www.mdpi.com/2075-1729/11/8/770.

[161] Claudia Emde et al. "The libRadtran software package for radiative transfer calculations (version 2.0. 1)". In: *Geoscientific Model Development* 9.5 (2016), pp. 1647–1672. ISSN: 1991-959X.

[162] H A Engle and D L Christensen. "Identification and evaluation of educational uses and users for the STS. Educational planning for utilization of space shuttle ED-PLUSS". In: (1974).

[163] Lynn Epstein and Ralph Nicholson. "Adhesion and adhesives of fungi and oomycetes". In: *Biological adhesives*. Springer, 2016, pp. 25–55.

[164] Christine Escobar and James Nabity. "Past, present, and future of closed human life support ecosystems-a review". In: *47th International Conference on Environmental Systems*. Charleston, SC: 47th International Conference on Environmental Systems, 2017, pp. 1–18. DOI: ICES-2017-311. URL: https://ttu-ir.tdl.org/handle/2346/73083.

[165] Christine Escobar, James Nabity, and David Klaus. "Defining ECLSS Robustness for Deep Space Exploration". In: 47th International Conference on Environmental Systems, 2017.

[166] *Establishing Biomanufacturing Processes for Human Systems in Remote Environments*. URL: https://www.nasa.gov/mission_pages/station/research/experiments/explorer/Investigation.html?#id=8306.

[167] John R Evans. "Photosynthesis and nitrogen relationships in leaves of C 3 plants". In: *Oecologia* 78.1 (1989), pp. 9–19. ISSN: 0029-8549.

[168] Sarah K Everton et al. "Review of in-situ process monitoring and in-situ metrology for metal additive manufacturing". In: *Materials & Design* 95 (2016), pp. 431–445. ISSN: 0264-1275.

[169] Maria Felicia Faienza et al. "Monoclonal antibodies for treating osteoporosis". In: *Expert Opinion On Biological Therapy* 18.2 (2018), pp. 149–157. ISSN: 1471-2598. DOI: 10.1080/14712598.2018.1401607.

[170] Tom Farmer. "A STEM Brainstorm at NASA." In: *Techniques: Connecting Education and Careers (J1)* 84.1 (2009), pp. 42–43. ISSN: 1527-1803.

[171] Andreas Feigel. "Advancement of a Trade-off Tool for Life Support Technologies and its Application in Proposing a Life Support Architecture for the Gateway". In: (2019).

[172] John W Fisher, Julie A Levri, and Harry W Jones. *The Effect of Mission Location on Mission Costs and Equivalent System Mass*. Tech. rep. 2003.

[173] John W Fisher et al. "Waste Management Technology and the Drivers for Space Missions". In: *SAE international Journal of Aerospace* 1.2008-01-2047 (2008), pp. 207–227. ISSN: 1946-3855.

[174] L S Fletcher and R H Page. "Technology transfer: The key to successful space engineering education". In: *Acta Astronautica* 29.2 (1993), pp. 141–146. ISSN: 0094-5765. DOI: https://doi.org/10.1016/0094-5765(93)90032-R. URL: https://www.sciencedirect.com/science/article/pii/009457659390032R.

[175] Ginger Flores et al. "Deep Space Habitation: Establishing a Sustainable Human Presence on the Moon and Beyond". In: *2021 IEEE Aerospace Conference (50100)*. IEEE, 2021, pp. 1–7. DOI: https://doi.org/10.1109/AERO50100.2021.9438260. URL: https://ieeexplore.ieee.org/document/9438260.

[176] Michael Flynn et al. "Planetary Water Recycling Systems Trade Study". In: 49th International Conference on Environmental Systems, 2019.

[177] James M. Free and Ralph Roe. *NASA's Management Of The Artemis Missions*. Tech. rep. Washington DC: National Aeronautics and Space Administration, 2021, pp. 1–73. URL: https://oig.nasa.gov/docs/IG-22-003.pdf.

[178] K E French. "Harnessing synthetic biology for sustainable development". In: *Nature Sustainability* 2.4 (2019), pp. 250–252. ISSN: 2398-9629. DOI: 10.1038/s41893-019-0270-x. URL: https://doi.org/10.1038/s41893-019-0270-x.

[179] Margaret A Frerking and Patricia M Beauchamp. "JPL technology readiness assessment guideline". In: *2016 IEEE Aerospace Conference*. IEEE, 2016, pp. 1–10. ISBN: 1467376760.

[180] Malcolm Fridlund and Helmut Lammer. "The astrobiology habitability primer". In: *Astrobiology* 10.1 (2010), pp. 1–4. ISSN: 1531-1074.

[181] N Friedland et al. "Fine-tuning the photosynthetic light harvesting apparatus for improved photosynthetic efficiency and biomass yield". In: *Scientific reports* 9.1 (2019), pp. 1–12. ISSN: 2045-2322.

[182] Jonathan Matthew Galazka, Asif Rahman, and Samantha Therese Fleury. *Methylotrophic microorganisms expressing soluble methane monooxygenase proteins*. Mar. 2020. URL: https://patents.google.com/patent/US20200095611A1.

[183] Thomas Galtier. "Accelerated Monte-Carlo methods for Piecewise Deterministic Markov Processes for a faster reliability assessment of power generation systems within the PyCATSHOO toolbox". PhD thesis. Université de Paris, 2019.

[184] Thomas Gassler et al. "The industrial yeast Pichia pastoris is converted from a heterotroph into an autotroph capable of growth on CO2". In: *Nature Biotechnology* 38.2 (2020), pp. 210–216. ISSN: 1546-1696. DOI: 10.1038/s41587-019-0363-0. URL: https://doi.org/10.1038/s41587-019-0363-0.

[185] Joel Gaston. *BFF Assembled Next-gen Development of Collagenous Allograft Meniscal Prosthetics aboard the International Space Station*. 2019. URL: https://www.nasa.gov/mission_pages/station/research/experiments/explorer/Investigation.html?#id=8274.

[186] J F Geisz et al. "High-efficiency GaInPGaAsInGaAs triple-junction solar cells grown inverted with a metamorphic bottom junction". In: *Applied Physics Letters* 91.2 (2007), p. 23502. DOI: 10.1063/1.2753729. URL: https://doi.org/10.1063/1.2753729.

[187] Geldzahler Barry and Jason A Soloff. "On-Orbit Validation of Additive Manufacturing of High Frequency Microwave Components in Microgravity". In: (2016). URL: https://www.nasa.gov/mission_pages/station/research/experiments/explorer/Investigation.html?#id=7518.

[188] Kelly Whealan George. "The Economic Impacts of the Commercial Space Industry". In: *Space Policy* 47 (Feb. 2019), pp. 181–186. ISSN: 0265-9646. DOI: 10.1016/j.spacepol.2018.12.003.

[189] Tommaso Ghidini. "Regenerative medicine and 3D bioprinting for human space exploration and planet colonisation". In: *Journal of Thoracic Disease* 10.20 (2018). ISSN: 2077-6624. DOI: 10.21037/jtd.2018.03.19. URL: https://jtd.amegroups.com/article/view/21895.

[190] Tracy R Gill. "Expanding Human Presence into the Solar System Starting with the Lunar Gateway". In: (2019).

[191] Marc Giulianotti et al. "Opportunities for Biomanufacturing in Low Earth Orbit: Current Status and Future Directions". In: *Preprints* (Aug. 2021). DOI: 10.20944/PREPRINTS202108.0044.V1. URL: https://www.preprints.org/manuscript/202108.0044/v1.

[192] Shmuel Gleizer et al. "Conversion of Escherichia coli to Generate All Biomass Carbon from CO2". In: *Cell* 179.6 (2019), pp. 1255–1263. ISSN: 0092-8674. DOI: https://doi.org/10.1016/j.cell.2019.11.009. URL: https://www.sciencedirect.com/science/article/pii/S0092867419312309.

[193] Al Globus. *Sourcing-and Sustaining-Optimum Financing*. 2018. URL: https://space.nss.org/settlement/nasa/spaceresvol4/references.html.

[194] F Godia et al. "MELISSA: a loop of interconnected bioreactors to develop life support in space". In: *Journal of biotechnology* 99.3 (2002), pp. 319–330. ISSN: 0168-1656.

[195] James W Goding. *Monoclonal antibodies: principles and practice*. Elsevier, 1996. ISBN: 0080536956.

[196] Gaurav Goel et al. "A bibliometric study on biomimetic and bioinspired membranes for water filtration". In: *npj Clean Water* 4.1 (2021), p. 41. ISSN: 2059-7037. DOI: 10.1038/s41545-021-00131-4. URL: https://doi.org/10.1038/s41545-021-00131-4.

[197] Angel Goñi-Moreno et al. "An implementation-focused bio/algorithmic workflow for synthetic biology". In: *ACS synthetic biology* 5.10 (2016), pp. 1127–1135. ISSN: 2161-5063.

[198] Robert D Green and Julie E Kleinhenz. "In-situ resource utilization (ISRU) Living off the Land on the Moon and Mars". In: *American Chemical Society National Meeting & Exposition*. Cleveland, OH: National Aeronautics and Space Administration, 2019, pp. 1–41. DOI: GRC-E-DAA-TN67217. URL: https://ntrs.nasa.gov/citations/20190025283.

[199] Jean-Christophe Grenouilleau, Oliver Housseini, and Francois Pérès. "In-Situ Rapid Spares Manufacturing and Its Application to Human Space Missions". In: *Space 2000*. 2000, pp. 42–48.

[200] Michael D. Griffin. *The Space Economy*. Washington DC, 2007. URL: https://www.nasa.gov/pdf/189537main_mg_space_economy_20070917.pdf.

[201] Paul Grogan, Olivier De Weck, and Chairwoo Lee. "Comparative usability study of two space logistics analysis tools". In: *AIAA SPACE 2011 Conference {\&} Exposition*. 2011, p. 7345.

[202] Paul T Grogan, Afreen Siddiqi, and Olivier L De Weck. "Matrix methods for optimal manifesting of multinode space exploration systems". In: *Journal of Spacecraft and Rockets* 48.4 (2011), pp. 679–690. ISSN: 0022-4650.

[203] J Gruenwald. "Human outposts on Mars: engineering and scientific lessons learned from history". In: *CEAS Space Journal* 6.2 (2014), pp. 73–77. ISSN: 1868-2510.

[204] Mike Gruntman. "The Time for Academic Departments in Astronautical Engineering". In: *AIAA SPACE 2007 Conference & Exposition*. 2007. DOI: 10.2514/6.2007-6042. URL: https://arc.aiaa.org/doi/abs/10.2514/6.2007-6042.

[205] Yosephine Gumulya, Luis Zea, and Anna H Kaksonen. "In situ resource utilisation: The potential for space biomining". In: *Minerals Engineering* 176 (2022), p. 107288. ISSN: 0892-6875. DOI: 10.1016/j.mineng.2021.107288. URL: https://www.sciencedirect.com/science/article/pii/S0892687521005173.

[206] Kanchane Gunawardena and Koen Steemers. "Living walls in indoor environments". In: *Building and Environment* 148 (2019), pp. 478–487. ISSN: 0360-1323. DOI: https://doi.org/10.1016/j.buildenv.2018.11.014. URL: https://www.sciencedirect.com/science/article/pii/S0360132318307091.

[207] Robert M Haberle et al. "Documentation of the NASA/Ames Legacy Mars Global Climate Model: Simulations of the present seasonal water cycle". In: *Icarus* 333 (2019), pp. 130–164. ISSN: 0019-1035.

[208] Lydia Asrat Haile et al. "Detection of Innate Immune Response Modulating Impurities in Therapeutic Proteins". In: *PLOS ONE* 10.4 (Apr. 2015). ISSN: 1932-6203. DOI: 10.1371/journal.pone.0125078.

[209] Loura Hall. "The Center for the Utilization of Biological Engineering in Space (CUB". In: (2017). URL: https://www.nasa.gov/directorates/spacetech/strg/stri/cubes/.

[210] Jason J Han. "Teams successfully 3D print vascularized liver tissue to win NASA's vascular tissue challenge". In: *Artificial Organs* 45.8 (2021), pp. 802–803. DOI: https://doi.org/10.1111/aor.14012. URL: https://onlinelibrary.wiley.com/doi/abs/10.1111/aor.14012.

[211] M C Hanna and A J Nozik. "Solar conversion efficiency of photovoltaic and photoelectrolysis cells with carrier multiplication absorbers". In: *Journal of Applied Physics* 100.7 (2006), p. 74510. ISSN: 0021-8979.

[212] Mahammad A Hannan et al. "State-of-the-art and energy management system of lithium-ion batteries in electric vehicle applications: Issues and recommendations". In: *Ieee Access* 6 (2018), pp. 19362–19378. ISSN: 2169-3536.

[213] Matthew Hardy et al. "Providing photons for food in regenerative life support: A comparative analysis of solar fiber optic and electric light systems". In: *50th International Conference on Environmental Systems (ICES)*. 2020.

[214] Roger G Harrison et al. *Bioseparations science and engineering*. Topics in Chemical Engineering, 2015. ISBN: 0195391810.

[215] M Amine Hassani, Paloma Durán, and Stéphane Hacquard. "Microbial interactions within the plant holobiont". In: *Microbiome* 6.1 (2018), p. 58. ISSN: 2049-2618.

[216] Malcolm Hawkesford et al. "Functions of macronutrients". In: *Marschner's mineral nutrition of higher plants*. Elsevier, 2012, pp. 135–189.

[217] C Hayes. *Video: Garver on NASA Exploration Policy and Budgets, posted by Keith Cowing, NASA Watch, December 6, 2014*. 2016.

[218] Christiane Heinicke et al. "Equipping an extraterrestrial laboratory: Overview of open research questions and recommended instrumentation for the Moon". In: *Advances in Space Research* 68.6 (2021), pp. 2565–2599. ISSN: 0273-1177. DOI: https://doi.org/10.1016/j.asr.2021.04.047. URL: https://www.sciencedirect.com/science/article/pii/S0273117721003653.

[219] Harald Helisch et al. "Close the gap–Potential of microalgal biomass for closed ECLSS and future in-situ resource utilization in space". In: *49th International Conference on Environmental Systems*. 49th International Conference on Environmental Systems, 2019.

[220] Stephen R Heller and Alan D McNaught. "The IUPAC international chemical identifier (InChI)". In: *Chemistry International* 31.1 (2009), p. 7. ISSN: 0193-6484.

[221] Larissa Hendrickx et al. "Microbial ecology of the closed artificial ecosystem MELiSSA (Micro-Ecological Life Support System Alternative): reinventing and compartmentalizing the Earth's food and oxygen regeneration system for long-haul space exploration missions". In: *Research in microbiology* 157.1 (2006), pp. 77–86. ISSN: 0923-2508.

[222] J Nicolas Hernandez-Aguilera et al. "Supporting interdisciplinary careers for sustainability". In: *Nature Sustainability* 4.5 (2021), pp. 374–375. ISSN: 2398-9629. DOI: 10.1038/s41893-020-00679-y. URL: https://doi.org/10.1038/s41893-020-00679-y.

[223] Henry R Hertzfeld. "Measuring the economic returns from successful NASA life sciences technology transfers." eng. In: *The Journal of technology transfer* 27.4 (Dec. 2002), pp. 311–320. ISSN: 0892-9912 (Print). DOI: 10.1023/a:1020207506064.

[224] Terry Hill and Brandon Taylor. "Use of Aquaporins to Achieve Needed Water Purity on the International Space Station for the Extravehicular Mobility Unit Space Suit System". In: *42nd International Conference on Environmental Systems*. International Conference on Environmental Systems (ICES). San Diego, CA: American Institute of Aeronautics and Astronautics, July 2012. DOI: doi:10.2514/6.2012-3436. URL: https://doi.org/10.2514/6.2012-3436.

[225] Stephen P Hilton et al. "Life Cycle Assessment of Urine Diversion and Conversion to Fertilizer Products at the City Scale". In: *Environmental Science & Technology* 55.1 (Jan. 2021), pp. 593–603. ISSN: 0013-936X. DOI: 10.1021/acs.est.0c04195. URL: https://doi.org/10.1021/acs.est.0c04195.

[226] Aditya Hindupur et al. "BioNutrients-1: On-Demand Production of Nutrients in Space". In: (2019).

[227] Paul Hintze, Anne Meier, and Malay Shah. "Sabatier System Design Study for a Mars ISRU Propellant Production Plant". In: 48th International Conference on Environmental Systems, 2018.

[228] Paul E Hintze et al. "Trash-to-gas: using waste products to minimize logistical mass during long duration space missions". In: *AIAA SPACE 2013 Conference and Exposition*. 2013, p. 5326.

[229] Steven Hirshorn and Sharon Jefferies. "Final report of the NASA Technology Readiness Assessment (TRA) study team". In: (2016).

[230] Steven R Hirshorn, Linda D Voss, and Linda K Bromley. "Nasa systems engineering handbook". In: (2017).

[231] Koki Ho et al. "Dynamic modeling and optimization for space logistics using time-expanded networks". In: *Acta Astronautica* 105.2 (2014), pp. 428–443. ISSN: 0094-5765.

[232] Stephen J Hoffman and David I Kaplan. *Human exploration of Mars: the reference mission of the NASA Mars exploration study team*. Vol. 6107. National Aeronautics and Space Administration, Lyndon B. Johnson Space Center, 1997.

[233] John Hogan et al. "A Simulation Study Comparing Incineration and Composting in a Mars-Based Advanced Life Support System". In: (2000).

[234] Maciej B Holowko et al. "Building a biofoundry". In: *Synthetic biology (Oxford, England)* 6.1 (2021), ysaa026. ISSN: 2397-7000. DOI: 10.1093/synbio/ysaa026. URL: https://europepmc.org/articles/PMC7998708.

[235] M Honan et al. "Feed additives as a strategic approach to reduce enteric methane production in cattle: modes of action, effectiveness and safety". In: *Animal Production Science* (2021). URL: https://doi.org/10.1071/AN20295.

[236] John H Honeycutt and Chris Cianciola. "NASA's Space Launch System: First Mission Hardware Nears Completion". In: *AIAA Propulsion and Energy 2019 Forum*. American Institute of Aeronautics and Astronautics, 2019, pp. 1–10. DOI: 10.2514/6.2019-4047. URL: https://doi.org/10.2514/6.2019-4047.

[237] Gerda Horneck, David M Klaus, and Rocco L Mancinelli. "Space Microbiology". In: *Microbiology and Molecular Biology Reviews* 74.1 (2010), pp. 121–156. DOI: 10.1128/MMBR.00016-09.

[238] J R Howard C. Stevenson. "The Psychology of Sexual Racism and Aids: An Ongoing Saga of Distrust and the "Sexual Other"". In: *Journal of Black Studies* 25.1 (1994), pp. 62–80. DOI: 10.1177/002193479402500104. URL: https://doi.org/10.1177/002193479402500104.

[239] Shu Hu et al. "An analysis of the optimal band gaps of light absorbers in integrated tandem photoelectrochemical water-splitting systems". In: *Energy & Environmental Science* 6.10 (2013), pp. 2984–2993.

[240] Yulin Hu et al. "Production of low-nitrogen bio-crude oils from microalgae pre-treated with pre-cooled NaOH/urea solution". In: *Fuel* 206 (2017), pp. 300–306. ISSN: 0016-2361. DOI: https://doi.org/10.1016/j.fuel.2017.06.021. URL: https://www.sciencedirect.com/science/article/pii/S0016236117307172.

[241] L Hua et al. "Assessment of an Anti-Alpha-Toxin Monoclonal Antibody for Prevention and Treatment of Staphylococcus aureus-Induced Pneumonia". In: *Antimicrobial Agents And Chemotherapy* 58.2 (Feb. 2014), pp. 1108–1117. ISSN: 0066-4804. DOI: 10.1128/AAC.02190-13.

[242] Bing Huang et al. "Effects of spaceflight and simulated microgravity on microbial growth and secondary metabolism". In: *Military Medical Research* 5.1 (2018), p. 18. ISSN: 2054-9369. DOI: 10.1186/s40779-018-0162-9. URL: https://doi.org/10.1186/s40779-018-0162-9.

[243] Kathryn Hurlbert et al. "Human Health, Life Support and Habitation Systems Technology Area 06". In: *NASA Sp. Technol. Roadmaps* (2012).

[244] Tahir Hussain. *Engineering economics*. Laxmi Publications, Ltd., 2010. ISBN: 9380386478.

[245] Ioannis Ieropoulos, John Greenman, and Chris Melhuish. "Urine utilisation by microbial fuel cells; energy fuel for the future". In: *Phys. Chem. Chem. Phys.* 14.1 (2012), pp. 94–98. DOI: 10.1039/C1CP23213D. URL: http://dx.doi.org/10.1039/C1CP23213D.

[246] Yukiko Iino et al. "Clinical efficacy of anti-IL-5 monoclonal antibody mepolizumab in the treatment of eosinophilic otitis media". In: *Auris Nasus Larynx* 46.2 (Apr. 2019), pp. 196–203. ISSN: 0385-8146. DOI: 10.1016/j.anl.2018.07.011.

[247] Torsten Ingestad. "Relative addition rate and external concentration; Driving variables used in plant nutrition research". In: *Plant, Cell \& Environment* 5.6 (1982), pp. 443–453. DOI: https://doi.org/10.1111/1365-3040.ep11611714. URL: https://onlinelibrary.wiley.com/doi/abs/10.1111/1365-3040.ep11611714.

[248] Maxim Isachenkov et al. "Regolith-based additive manufacturing for sustainable development of lunar infrastructure – An overview". In: *Acta Astronautica* 180 (2021), pp. 650–678. ISSN: 0094-5765. DOI: https://doi.org/10.1016/j.actaastro.2021.01.005. URL: https://www.sciencedirect.com/science/article/pii/S0094576521000060.

[249] Takuto Ishimatsu, Paul Grogan, and Olivier de Weck. "Interplanetary Trajectory Analysis and Logistical Considerations of Human Mars Exploration". In: *Journal of Cosmology* 12 (2010), pp. 3588–3600.

[250] Takuto Ishimatsu et al. "Generalized Multicommodity Network Flow Model for the Earth–Moon–Mars Logistics System". In: *Journal of Spacecraft and Rockets* 53.1 (2016), pp. 25–38. DOI: 10.2514/1.A33235. URL: https://doi.org/10.2514/1.A33235.

[251] Adam E Jakus et al. "Robust and Elastic Lunar and Martian Structures from 3D-Printed Regolith Inks". In: *Scientific Reports* 7.1 (2017), p. 44931. ISSN: 2045-2322. DOI: 10.1038/srep44931. URL: https://doi.org/10.1038/srep44931.

[252] Christer Jansson et al. "Crops for Carbon Farming". In: *Frontiers in Plant Science* 12 (2021). ISSN: 1664-462X. DOI: 10.3389/fpls.2021.636709. URL: https://www.frontiersin.org/articles/10.3389/fpls.2021.636709.

[253] Donald A Jaworske and Jerry G Myers. *Pharmaceuticals exposed to the space environment: Problems and prospects*. National Aeronautics and Space Administration, Glenn Research Center, 2016.

[254] Thomas Jedrey, Robert Lock, and Mika Matsumoto. *Conceptual Studies for the Next Mars Orbiter (NeMO)*. 2016. URL: http://images.spaceref.com/news/2016/NeMOIndustryDay.pdf.

[255] Jieyang Jia et al. "Solar water splitting by photovoltaic-electrolysis with a solar-to-hydrogen efficiency over 30%". In: *Nature communications* 7.1 (2016), pp. 1–6. ISSN: 2041-1723.

[256] JÉRÉMIE Joannès. "Feasibility Study of a DNA-Sequencing Cubesat Satellite". In: *Journal of the British Interplanetary Society* 70.8 (2017), pp. 287–299.

[257] Masahumi Johkan et al. "Blue Light-emitting Diode Light Irradiation of Seedlings Improves Seedling Quality and Growth after Transplanting in Red Leaf Lettuce". In: *HortScience horts* 45.12 (2010), pp. 1809–1814. DOI: 10.21273/HORTSCI.45.12.1809. URL: https://journals.ashs.org/hortsci/view/journals/hortsci/45/12/article-p1809.xml.

[258] Alan R Johnson. "Biodiversity requirements for self-sustaining space colonies". In: *Futures* 110 (2019), pp. 24–27. ISSN: 0016-3287. DOI: 10.1016/j.futures.2019.02.017. URL: https://doi.org/10.1016/j.futures.2019.02.017.

[259] Alicia Johnstone. *CubeSat design specification (1U-12U) rev 14 CP-CDS-R14*. Tech. rep. San Luis Obispo, CA: California Polytechnic State University, 2020. DOI: CP-CDS-R14.

[260] Harry Jones. "Comparison of Bioregenerative and Physical/Chemical Life Support Systems". In: *SAE Transactions* (2006), pp. 181–192. ISSN: 0096-736X.

[261] Harry Jones. *Equivalent mass versus life cycle cost for life support technology selection*. Tech. rep. 2003.

[262] Harry Jones. "Humans to Mars will cost about "half a trillion dollars" and life support roughly two billion dollars". In: *46th International Conference on Environmental Systems*. Vienna, Austria: 46th International Conference on Environmental Systems, 2016, pp. 1–11. DOI: ICES-2016-111. URL: https://ttu-ir.tdl.org/handle/2346/67531.

[263] Harry Jones. "Much Lower Launch Costs Make Resupply Cheaper Than Recycling for Space Life Support". In: 47th International Conference on Environmental Systems, 2017.

[264] Harry Jones. "Multiple Metrics for Advanced Life Support". In: *29th International Conference on Environmental Systems*. Denver, CO: SAE Technical Paper, 1999. ISBN: 0148-7191.

[265] Harry Jones. "Planning dynamic simulation of space life support". In: *39th International Conference on Environmental Systems*. Savannah, GA: SAE Technical Paper, 2009, p. 10. ISBN: 0148-7191.

[266] Harry Jones. "The recent large reduction in space launch cost". In: 48th International Conference on Environmental Systems, 2018.

[267] Harry Jones and Grant Anderson. "Need for Cost Optimization of Space Life Support Systems". In: 47th International Conference on Environmental Systems, 2017.

[268] Harry Jones, James Cavazzoni, and Paul Keas. *Crop models for varying environmental conditions*. Tech. rep. 2002.

[269] Harry W Jones. "Don't trust a management metric, especially in life support". In: *44th International Conference on Environmental Systems*. 44th International Conference on Environmental Systems, 2014. ISBN: 0692382208.

[270] Harry W Jones. "Impact of Lower Launch Cost on Space Life Support". In: *2018 AIAA SPACE and Astronautics Forum and Exposition*. 2018, p. 5286.

[271] Harry W Jones. *The cost and equivalent system mass of space crew time*. Tech. rep. 2001.

[272] Harry W Jones. "The System Complexity Metric (SCM) Predicts System Costs and Failure Rates". In: *49th International Conference on Environmental Systems*. 2020.

[273] Harry W Jones and Daniel J Rasky. "Advanced Life Support System Value Metric". In: *29th International Conference on Environmental Systems*. Denver, CO: SAE Technical Paper, 1999.

[274] Arun Joshi. *Advanced NASA Technology Supports Water Purification Efforts Worldwide*. 2012. URL: https://www.nasa.gov/mission_pages/station/research/benefits/water_purification.html.

[275] Collin Jugler, Jussi Joensuu, and Qiang Chen. "Hydrophobin-Protein A Fusion Protein Produced in Plants Efficiently Purified an Anti-West Nile Virus Monoclonal Antibody from Plant Extracts via Aqueous Two-Phase Separation". In: *International Journal Of Molecular Sciences* 21.6 (Mar. 2020). DOI: 10.3390/ijms21062140.

[276] Yu Kyung Jung et al. "Metabolic engineering of Escherichia coli for the production of polylactic acid and its copolymers". In: *Biotechnology and bioengineering* 105.1 (2010), pp. 161–171. ISSN: 0006-3592.

[277] Tae Hyun Kang and Sang Taek Jung. "Boosting therapeutic potency of antibodies by taming Fc domain functions". In: *Experimental And Molecular Medicine* 51 (Nov. 2019). ISSN: 1226-3613. DOI: 10.1038/s12276-019-0345-9.

[278] Pratistha Kansakar and Faisal Hossain. "A review of applications of satellite earth observation data for global societal benefit and stewardship of planet earth". In: *Space Policy* 36 (2016), pp. 46–54. ISSN: 0265-9646. DOI: https://doi.org/10.1016/j.spacepol.2016.05.005. URL: https://www.sciencedirect.com/science/article/pii/S0265964616300133.

[279] David Karl et al. "Sintering of ceramics for clay in situ resource utilization on Mars". In: *Open Ceramics* (2020), p. 100008. ISSN: 2666-5395.

[280] Fathi Karouia, Kianoosh Peyvan, and Andrew Pohorille. "Toward biotechnology in space: High-throughput instruments for in situ biological research beyond Earth". In: *Biotechnology advances* 35.7 (2017), pp. 905–932. ISSN: 0734-9750.

[281] Amiko Kauderer. *Higher Altitude Improves Station's Fuel Economy*. 2011. URL: https://www.nasa.gov/mission_pages/station/expeditions/expedition26/iss_altitude.html.

[282] Richard J R Kelwick, Alexander J Webb, and Paul S Freemont. "Biological Materials: The Next Frontier for Cell-Free Synthetic Biology". In: *Frontiers in Bioengineering and Biotechnology* 8 (2020). ISSN: 2296-4185. DOI: 10.3389/fbioe.2020.00399. URL: https://www.frontiersin.org/articles/10.3389/fbioe.2020.00399.

[283] A J Kempers and C J Kok. "Re-examination of the determination of ammonium as the indophenol blue complex using salicylate". In: *Analytica Chimica Acta* 221 (1989), pp. 147–155.

[284] Jochen Keppler et al. "The final configuration of the algae-based ISS experiment PBR@ LSR". In: *48th International Conference on Environmental Systems*. Albuquerque, NM: ICES, 2018.

[285] Mohd Atiqueuzzaman Khan et al. "Biohydrogen production from anaerobic digestion and its potential as renewable energy". In: *Renewable Energy* 129B (2018), pp. 754–768. URL: https://www.sciencedirect.com/science/article/pii/S0960148117303361.

[286] Christina L M Khodadad et al. "Microbiological and Nutritional Analysis of Lettuce Crops Grown on the International Space Station". In: *Frontiers in Plant Science* 11 (2020), p. 199. ISSN: 1664-462X.

[287] P Kidd et al. "Comparison of the crystalline quality of step-graded and continuously graded InGaAs buffer layers". In: *Journal of Crystal Growth* 169.4 (1996), pp. 649–659. ISSN: 0022-0248. DOI: https://doi.org/10.1016/S0022-0248(96)00665-3. URL: https://www.sciencedirect.com/science/article/pii/S0022024896006653.

[288] Seungdo Kim et al. "Carbon-Negative Biofuel Production". In: *Environmental Science & Technology* 54.17 (Sept. 2020), pp. 10797–10807. ISSN: 0013-936X. DOI: 10.1021/acs.est.0c01097. URL: https://doi.org/10.1021/acs.est.0c01097.

[289] David M Klaus. "Incorporating Bioastronautics into an Engineering Curriculum". In: 44th International Conference on Environmental Systems, 2014. ISBN: 0692382208.

[290] David M Klaus. "Microgravity and its implications for fermentation biotechnology". In: *Trends in Biotechnology* 16.9 (1998), pp. 369–373. ISSN: 0167-7799. DOI: https://doi.org/10.1016/S0167-7799(98)01197-4. URL: https://www.sciencedirect.com/science/article/pii/S0167779998011974.

[291] Julie E Kleinhenz and Aaron Paz. "An ISRU propellant production system for a fully fueled Mars Ascent Vehicle". In: *10th Symposium on Space Resource Utilization*. 2017, p. 423.

[292] David Kortenkamp and Scott Bell. "BioSim: Simulating Space Habitats for Artificial Intelligence Research". In: (2015).

[293] David Kortenkamp and Scott Bell. *Simulating advanced life support systems for integrated controls research*. Tech. rep. 2003.

[294] Adalbert Krawczyk et al. "Prevention of Herpes Simplex Virus Induced Stromal Keratitis by a Glycoprotein B-Specific Monoclonal Antibody". In: *PLOS ONE* 10.1 (Jan. 2015). ISSN: 1932-6203. DOI: 10.1371/journal.pone.0116800.

[295] Valdis Krumins, Richard Strayer, and Mary Hummerick. "Development of a fixed-film bioreactor for recycling of inedible plant nutrients in controlled biological systems". In: *2001 ASAE Annual Meeting*. American Society of Agricultural and Biological Engineers, 1998, p. 1. ISBN: 1940956196.

[296] Paul Kusuma, P Morgan Pattison, and Bruce Bugbee. "From physics to fixtures to food: current and potential LED efficacy". In: *Horticulture Research* 7.1 (2020), pp. 1–9. ISSN: 2052-7276.

[297] Kwang-Chul Kwon and Henry Daniell. "Low-cost oral delivery of protein drugs bioencapsulated in plant cells". In: *Plant Biotechnology Journal* 13.8, SI (Oct. 2015), pp. 1017–1022. ISSN: 1467-7644. DOI: 10.1111/pbi.12462.

[298] Marios C Kyriacou et al. "Microgreens as a component of space life support systems: A cornucopia of functional food". In: *Frontiers in Plant Science* 8 (2017), p. 1587. ISSN: 1664-462X.

[299] G A Landis. "Exploring mars with solar-powered rovers". In: *Conference Record of the Thirty-first IEEE Photovoltaic Specialists Conference, 2005.* 2005, pp. 858–861. DOI: 10.1109/PVSC.2005.1488268.

[300] Geoffrey Landis et al. "Mars solar power". In: *2nd International Energy Conversion Engineering Conference*. 2004, p. 5555.

[301] Geoffrey A Landis. "Solar cell selection for Mars". In: *IEEE Aerospace and Electronic Systems Magazine* 15.1 (2000), pp. 17–21. ISSN: 0885-8985.

[302] Noah J Langenfeld et al. "Optimizing Nitrogen Fixation and Recycling for Food Production in Regenerative Life Support Systems". In: *Frontiers in Astronomy and Space Sciences* 8 (2021), p. 105. ISSN: 2296-987X. DOI: 10.3389/fspas.2021.699688. URL: https://www.frontiersin.org/article/10.3389/fspas.2021.699688.

[303] Tomislav Laptos and Jasna Omersel. "The importance of handling high-value biologicals: Physico-chemical instability and immunogenicity of monoclonal antibodies". In: *Experimental And Therapeutic Medicine* 15.4 (Apr. 2018), pp. 3161–3168. ISSN: 1792-0981. DOI: 10.3892/etm.2018.5821.

[304] Wiley J Larson and James Richard Wertz. *Space mission analysis and design*. Tech. rep. 1992.

[305] Jan E Leach et al. "Plants, plant pathogens, and microgravity—A deadly trio". In: *Gravitational and Space Research* 14.2 (2007). ISSN: 2332-7774.

[306] Bandy X Lee et al. "Transforming our world: implementing the 2030 agenda through sustainable development goal indicators". In: *Journal of public health policy* 37.1 (2016), pp. 13–31. ISSN: 1745-655X.

[307] Gene Lee et al. "SpaceNet: Modeling and Simulating Space Logistics". In: *AIAA SPACE 2008 Conference {\&} Exposition*. 2008, p. 7747.

[308] Hyun Jeong Lee, Jong-Il Choi, and Han Min Woo. "Biocontainment of Engineered Synechococcus elongatus PCC 7942 for Photosynthetic Production of α-Farnesene from CO(2)." eng. In: *Journal of agricultural and food chemistry* 69.2 (Jan. 2021), pp. 698–703. ISSN: 1520-5118 (Electronic). DOI: 10.1021/acs.jafc.0c07020.

[309] Sang Yup Lee et al. "A comprehensive metabolic map for production of bio-based chemicals". In: *Nature Catalysis* 2.1 (2019), pp. 18–33. ISSN: 2520-1158. DOI: 10.1038/s41929-018-0212-4. URL: https://doi.org/10.1038/s41929-018-0212-4.

[310] Chunli Lei and Nicki J Engeseth. "Comparison of growth characteristics, functional qualities, and texture of hydroponically grown and soil-grown lettuce". In: *LWT* 150 (2021), p. 111931. ISSN: 0023-6438.

[311] Howard G. Levine and David A. Flowers. *Spectrum*. Tech. rep. Merritt Island, Florida: NASA Ames Research Center, Kennedy Space Center, 2019, p. 2.

[312] Julie Levri et al. "Advanced life support equivalent system mass guidelines document". In: (2003), pp. 1–47. DOI: NASA/TM-2003-212278. URL: https://ntrs.nasa.gov/citations/20040021355.

[313] Julie Levri et al. *Food system trade study for an early Mars mission*. Tech. rep. 2001.

[314] Julie A Levri, David A Vaccari, and Alan E Drysdale. *Theory and application of the equivalent system mass metric*. Tech. rep. 2000, p. 12. DOI: 10.4271/2000-01-2395. URL: https://doi.org/10.4271/2000-01-2395%0A.

[315] Han Li et al. "3D Printing and Solvent Dissolution Recycling of Polylactide–Lunar Regolith Composites by Material Extrusion Approach". In: *Polymers* 12.8 (2020). ISSN: 2073-4360. DOI: 10.3390/polym12081724. URL: https://www.mdpi.com/2073-4360/12/8/1724.

[316] Han Li et al. "Integrated electromicrobial conversion of CO2 to higher alcohols". In: *Science* 335.6076 (2012), p. 1596. ISSN: 0036-8075.

[317] Chin H Lin et al. "ALSSAT Development Status and Its Applications in Trade Studies". In: *International Conference On Environmental Systems*. SAE International, July 2004. DOI: https://doi.org/10.4271/2004-01-2438. URL: https://doi.org/10.4271/2004-01-2438.

[318] Myat T Lin et al. "A faster Rubisco with potential to increase photosynthesis in crops". In: *Nature* 513.7519 (2014), pp. 547–550. ISSN: 1476-4687. DOI: 10.1038/nature13776. URL: https://doi.org/10.1038/nature13776.

[319] Evan Linck et al. *Evaluation of a Human Mission to Mars by 2033*. IDA Science and Technology Policy Institute, 2019.

[320] Diane Linne et al. "Current NASA In-Situ Resource Utilization (ISRU) Strategic Vision". In: *Space Resources Roundtable Planetary & Terrestrial Mining and Sciences Symposium*. GRC-E-DAA-TN69644. 2019. URL: https://www.exploremars.org/wp-content/uploads/2021/09/0915_1200_Gerry-Sanders_ISRU.pdf.

[321] D R Liskowsky and W W Seitz. "Human integration design handbook". In: *Washington, DC, Rep. NASA/SP-2010-3407: NASA* (2010).

[322] Chao Liu et al. "Effect of organic loading rate on anaerobic digestion of food waste under mesophilic and thermophilic conditions". In: *Energy Fuels* 31.3 (2018), pp. 2976–2984. URL: https://pubs.acs.org/doi/full/10.1021/acs.energyfuels.7b00018.

[323] Chong Liu et al. "Nanowire-Bacteria Hybrids for Unassisted Solar Carbon Dioxide Fixation to Value-Added Chemicals". In: *Nano Letters* 15.5 (May 2015), pp. 3634–3639. ISSN: 1530-6984. DOI: 10.1021/acs.nanolett.5b01254. URL: http://dx.doi.org/10.1021/acs.nanolett.5b01254.

[324] Chong Liu et al. "Water splitting–biosynthetic system with CO2 reduction efficiencies exceeding photosynthesis". In: *Science* 352.6290 (2016), pp. 1210–1213. ISSN: 0036-8075.

[325] Dan Lockney. *NASA Spinoff | NASA Technology Transfer Program*. 2022. URL: https://spinoff.nasa.gov/.

[326] Bruce E Logan, Ruggero Rossi, and Pascal E Saikaly. "Electroactive microorganisms in bioelectrochemical systems". In: *Nature Reviews Microbiology* 17.5 (2019), pp. 307–319. ISSN: 1740-1534.

[327] Jenna M Loyd. "'Whitey on the Moon': Space, Race, and the Crisis of Black Mobility". In: *Mobile Desires: The Politics and Erotics of Mobility Justice*. Springer, 2015, pp. 41–52.

[328] Julius B Lucks et al. "Toward scalable parts families for predictable design of biological circuits". In: *Current opinion in microbiology* 11.6 (2008), pp. 567–573. ISSN: 1369-5274.

[329] Autumn Luna et al. "Protein structural changes on a CubeSat under rocket acceleration profile". In: *npj Microgravity* 6.1 (2020), p. 12. ISSN: 2373-8065. DOI: 10.1038/s41526-020-0102-3. URL: https://doi.org/10.1038/s41526-020-0102-3.

[330] Kathy Lynn, Katharine MacKendrick, and Ellen M Donoghue. "Social vulnerability and climate change: Synthesis of literature". In: *Gen. Tech. Rep. PNW-GTR-838. Portland, OR: US Department of Agriculture, Forest Service, Pacific Northwest Research Station. 70 p.* 838 (2011).

[331] Malaya Kumar Biswal M et al. "A Review on Human Interplanetary Exploration Challenges". In: *AIAA SCITECH 2022 Forum*. 2022. DOI: 10.2514/6.2022-2585. URL: https://arc.aiaa.org/doi/abs/10.2514/6.2022-2585.

[332] Robert D MacElroy and D Wang. "Waste recycling issues in bioregenerative life support". In: *Advances in Space Research* 9.8 (1989), pp. 75–84. ISSN: 0273-1177.

[333] Neil M Maher. "Grounding the space race". In: *Modern American History* 1.1 (2018), pp. 141–146. ISSN: 2515-0456. DOI: doi:10.1017/mah.2017.4. URL: https://doi.org/10.1017/mah.2017.4.

[334] Sahar Mahmoodi et al. "Current affinity approaches for purification of recombinant proteins". In: *Cogent Biology* 5.1 (2019), p. 1665406. ISSN: 2331-2025.

[335] Advenit Makaya et al. "Towards out of earth manufacturing: overview of the ESA materials and processes activities on manufacturing in space". In: *CEAS Space Journal* (2022). ISSN: 1868-2510. DOI: 10.1007/s12567-022-00428-1. URL: https://doi.org/10.1007/s12567-022-00428-1.

[336] Meghna R Malik et al. "Production of high levels of poly-3-hydroxybutyrate in plastids of C amelina sativa seeds". In: *Plant biotechnology journal* 13.5 (2015), pp. 675–688. ISSN: 1467-7644.

[337] Tariq Malik. *Trump Says Mars Is NASA's Big Target Because the Moon's 'Not So Exciting' | Space*. 2019. URL: https://www.space.com/trump-us-space-program-nasa-moon-mars-and-australia.html.

[338] Daniel J Mandell et al. "Biocontainment of genetically modified organisms by synthetic protein design." eng. In: *Nature* 518.7537 (Feb. 2015), pp. 55–60. ISSN: 1476-4687 (Electronic). DOI: 10.1038/nature14121.

[339] John C Mankins. "Technology readiness levels". In: *White Paper, April* 6 (1995), p. 1995.

[340] Lydia J Mapstone et al. "Cyanobacteria and microalgae in supporting human habitation on Mars". In: *Biotechnology Advances* 59 (2022), p. 107946. ISSN: 0734-9750. DOI: https://doi.org/10.1016/j.biotechadv.2022.107946. URL: https://www.sciencedirect.com/science/article/pii/S0734975022000428.

[341] Gregorio Marbán and Teresa Valdés-Solís. "Towards the hydrogen economy?" In: *International journal of hydrogen energy* 32.12 (2007), pp. 1625–1637. ISSN: 0360-3199.

[342] Robert H Marchessault and Ga-er Yu. "Crystallization and material properties of polyhydroxyalkanoates PHAs". In: *Biopolymers Online: Biology Chemistry Biotechnology Applications* 3 (2005).

[343] Jeannette Marrero, Orquidea Coto, and Axel Schippers. "11 Metal bioleaching: fundamentals and geobiotechnical application of aerobic and anaerobic acidophiles". In: *Biotechnological Applications of Extremophilic Microorganisms*. Ed. by Natuschka M Lee. De Gruyter, 2020, pp. 261–288. DOI: doi:10.1515/9783110424331-011. URL: https://doi.org/10.1515/9783110424331-011.

[344] *Mars 2020 Perseverance Launch Press Kit*. 2020. URL: https://www.jpl.nasa.gov/news/press_kits/mars_2020/download/mars_2020_launch_press_kit.pdf.

[345] *Mars Express: A Decade of Observing the Red Planet*. 2013. URL: http://esamultimedia.esa.int/docs/science/media/marsexpress_brochure.pdf.

[346] *Mars Helicopter/Ingenuity*. 2020. URL: https://mars.nasa.gov/files/mars2020/MarsHelicopterIngenuity_FactSheet.pdf.

[347] *Mars InSight Landing Press Kit*. 2018. URL: https://www.jpl.nasa.gov/news/press_kits/insight/landing/download/mars_insight_landing_presskit.pdf.

[348] *Mars Reconnaissance Orbiter Arrival Press Kit*. 2006. URL: https://www.jpl.nasa.gov/news/press_kits/mro-arrival.pdf.

[349] *Mars Science Laboratory Landing Press Kit*. 2012. URL: https://www.jpl.nasa.gov/news/press_kits/MSLLanding.pdf.

[350] *Marshall Space Flight Center Space Systems*. Tech. rep. Huntsville, AL: National Aeronautics and Space Administration, Marshall Space Flight Center, 2011. DOI: NP-2011-05-051-MSFC8âĂŞ477491b. URL: https://www.nasa.gov/sites/default/files/atoms/files/space_systems.pdf.

[351] Paolo Marzioli et al. "CultCube: Experiments in autonomous in-orbit cultivation onboard a 12-Units CubeSat platform". In: *Life Sciences in Space Research* 25 (2020), pp. 42–52. ISSN: 2214-5524. DOI: https://doi.org/10.1016/j.lssr.2020.02.005. URL: https://www.sciencedirect.com/science/article/pii/S2214552420300134.

[352] Gioia D Massa et al. "Plant-growth lighting for space life support: a review". In: *Gravitational and Space Research* 19.2 (2007). ISSN: 2332-7774.

[353] Ishita Matai et al. "Progress in 3D bioprinting technology for tissue/organ regenerative engineering". In: *Biomaterials* 226 (2020), p. 119536. ISSN: 0142-9612. DOI: https://doi.org/10.1016/j.biomaterials.2019.119536. URL: https://www.sciencedirect.com/science/article/pii/S0142961219306350.

[354] Maxie C Maultsby. "A Historical View of Blacks' Distrust of Psychiatry". In: *Behavior Modification in Black Populations: Psychosocial Issues and Empirical Findings*. Ed. by Samuel M Turner and Russell T Jones. Boston, MA: Springer US, 1982, pp. 39–55. ISBN: 978-1-4684-4100-0. DOI: 10.1007/978-1-4684-4100-0{_}3. URL: https://doi.org/10.1007/978-1-4684-4100-0_3.

[355] *MAVEN Press Kit*. 2013. URL: https://mars.nasa.gov/files/resources/MAVEN_PressKit_Final.pdf.

[356] Sabrina Maxwell and Alan E Drysdale. *Asssessment of Waste Processing Technologies for 3 Missions*. Tech. rep. 2001.

[357] Ana Mayela Ramos-de-la-Pena, Jose Gonzalez-Valdez, and Oscar Aguilar. "Protein A chromatography: Challenges and progress in the purification of monoclonal antibodies". In: *Journal Of Separation Science* 42.9 (May 2019), pp. 1816–1827. ISSN: 1615-9306. DOI: 10.1002/jssc.201800963.

[358] Bernhard Mayer and Arve Kylling. "The libRadtran software package for radiative transfer calculations-description and examples of use". In: *Atmospheric Chemistry and Physics* 5.7 (2005), pp. 1855–1877. ISSN: 1680-7316.

[359] Bernhard Mayer et al. "libRadtran user's guide". In: *Edition for libRadtran version* 1 (2012).

[360] E Pamela McGlothlin, H Y Yeh, and C H Lin. *Development of the ECLSS Sizing Analysis Tool and ARS Mass Balance Model using Microsoft® Excel*. Tech. rep. 1999.

[361] Alexa B R McIntyre et al. "Nanopore sequencing in microgravity". In: *npj Microgravity* 2.1 (2016), pp. 1–9. ISSN: 2373-8065.

[362] Christopher P McKay et al. "The Icebreaker Life Mission to Mars: a search for biomolecular evidence for life". In: *Astrobiology* 13.4 (2013), pp. 334–353. ISSN: 1531-1074.

[363] Michael D McLean et al. "Purification of the therapeutic antibody trastuzumab from genetically modified plants using safflower Protein A-oleosin oilbody technology". In: *Transgenic Research* 21.6 (Dec. 2012), pp. 1291–1301. ISSN: 0962-8819. DOI: 10.1007/s11248-012-9603-5.

[364] Claire L McLeod and Mark. P S Krekeler. "Sources of Extraterrestrial Rare Earth Elements: To the Moon and Beyond". In: *Resources* 6.3 (2017). ISSN: 2079-9276. DOI: 10.3390/resources6030040. URL: https://www.mdpi.com/2079-9276/6/3/40.

[365] Larry V Mclntire and Frederick B Rudolph. "NASA Specialized Center of Research and Training (NSCORT) in Gravitational Biology". In: (1996).

[366] Matthew J McNulty et al. "Molecular pharming to support human life on the moon, mars, and beyond". In: *Critical Reviews in Biotechnology* 0.0 (2021), pp. 1–16. DOI: 10.1080/07388551.2021.1888070. URL: https://www.preprints.org/manuscript/202009.0086/v1%20https://doi.org/10.1080/07388551.2021.1888070.

[367] Matthew J McNulty1 et al. "Evaluating the Cost of Pharmaceutical Purification for a Long-Duration Space Exploration Medical Foundry". In: *Frontiers in Microbiology* 12 (2021), p. 3056. ISSN: 1664302X. DOI: 10.3389/fmicb.2021.700863. URL: https://www.biorxiv.org/content/early/2021/06/22/2021.06.21.449300%20https://www.frontiersin.org/article/10.3389/fmicb.2021.700863.

[368] Jay N Meegoda et al. "A review of the processes, parameters, and optimization of anaerobic digestion". In: *International journal of environmental research and public health* 15.10 (2018), p. 2224.

[369] Anne Meier et al. "Mars atmospheric conversion to methane and water: An engineering model of the sabatier reactor with characterization of ru/al2o3 for long duration use on mars". In: 47th International Conference on Environmental Systems, 2017.

[370] A A Menezes. "Realizing a Self-Reproducing Space Factory with Engineered and Programmed Biology". In: *LPICo* 2063 (2018), p. 3145. ISSN: 0161-5297.

[371] Amor A Menezes et al. *Towards synthetic biological approaches to resource utilization on space missions*. Vol. 12. 102. The Royal Society, 2015, p. 20140715. DOI: doi.org/10.1098/rsif.2014.0715. URL: https://doi.org/10.1098/rsif.2014.0715.

[372] Amor A. Menezes et al. "Grand challenges in space synthetic biology". In: *Journal of The Royal Society Interface* 12.113 (2015), p. 20150803. ISSN: 1742-5689. DOI: 10.1098/rsif.2015.0803. URL: http://rsif.royalsocietypublishing.org/lookup/doi/10.1098/rsif.2015.0803.

[373] A Mesbah et al. "Stochastic nonlinear model predictive control with probabilistic constraints". In: *2014 American Control Conference*. June 2014, pp. 2413–2419. DOI: 10.1109/ACC.2014.6858851.

[374] Ali Mesbah. "Stochastic model predictive control: An overview and perspectives for future research". In: *IEEE Control Systems Magazine* 36.6 (2016), pp. 30–44.

[375] Ernst Messerschmid and Reinhold Bertrand. "Environmental control and life support system". In: *Space Stations*. Springer, 1999, pp. 109–145.

[376] A Miele and T Wang. "Optimal transfers from an Earth orbit to a Mars orbit". In: *Acta Astronautica* 45.3 (1999), pp. 119–133. ISSN: 0094-5765.

[377] Michael J Miglioranzi et al. "Project Ares: A systems engineering and operations architecture for the exploration of Mars". In: *NASA STI/Recon Technical Report N* 93 (1992), p. 18021.

[378] Hrvoje Mikulčić, Milan Vujanović, and Neven Duić. "Improving the sustainability of cement production by using numerical simulation of limestone thermal degradation and pulverized coal combustion in a cement calciner". In: *Journal of Cleaner Production* 88 (2015), pp. 262–271. ISSN: 0959-6526. DOI: https://doi.org/10.1016/j.jclepro.2014.04.011. URL: https://www.sciencedirect.com/science/article/pii/S0959652614003588.

[379] Min Min et al. "Cultivating Chlorella sp. in a Pilot-Scale Photobioreactor Using Centrate Wastewater for Microalgae Biomass Production and Wastewater Nutrient Removal". In: *Applied Biochemistry and Biotechnology* 165.1 (2011), pp. 123–137. ISSN: 1559-0291. DOI: 10.1007/s12010-011-9238-7. URL: https://doi.org/10.1007/s12010-011-9238-7.

[380] David Miranda. *2020 NASA Technology Taxonomy*. Tech. rep. Washington DC: National Aeronautics and Space Administration, 2020, pp. 1–239. DOI: HQ-E-DAA-TN76545. URL: https://ntrs.nasa.gov/citations/20200000399.

[381] Samir Mitragotri, Paul A Burke, and Robert Langer. "Overcoming the challenges in administering biopharmaceuticals: formulation and delivery strategies". In: *Nature Reviews Drug Discovery* 13.9 (Sept. 2014), pp. 655–672. ISSN: 1474-1776. DOI: 10.1038/nrd4363.

[382] Shigenobu Mitsuzawa et al. "The rosettazyme: A synthetic cellulosome". In: *Journal of Biotechnology* 143.2 (2009), pp. 139–144. ISSN: 0168-1656. DOI: https://doi.org/10.1016/j.jbiotec.2009.06.019. URL: https://www.sciencedirect.com/science/article/pii/S0168165609002673.

[383] M Jezri Mohideen, John D Perkins, and Efstratios N Pistikopoulos. "Optimal design of dynamic systems under uncertainty". In: *AIChE Journal* 42.8 (1996), pp. 2251–2272.

[384] Kurt Möller and Torsten Müller. "Effects of anaerobic digestion on digestate nutrient availability and crop growth: a review". In: *Engineering in Life Sciences* 12.3 (2012), pp. 242–257. ISSN: 1618-0240.

[385] Christopher L Moore. "Technology development for human exploration of Mars". In: *Acta Astronautica* 67.9-10 (2010), pp. 1170–1175. ISSN: 0094-5765. DOI: https://doi.org/10.1016/j.actaastro.2010.06.031. URL: https://www.sciencedirect.com/science/article/pii/S0094576510002225.

[386] J áB Morgan and E áL Connolly. "Plant-soil interactions: nutrient uptake". In: *Nature Education Knowledge* 4.8 (2013), p. 2.

[387] Lorenzo Moroni et al. "What can biofabrication do for space and what can space do for biofabrication?" In: *Trends in Biotechnology* 40.4 (Apr. 2022), pp. 398–411. ISSN: 0167-7799. DOI: 10.1016/j.tibtech.2021.08.008. URL: https://doi.org/10.1016/j.tibtech.2021.08.008.

[388] Robert C Morrow and Ross W Remiker. *A deployable salad crop production system for lunar habitats*. Tech. rep. 2009.

[389] Thomas Morrow and Linda Hull Felcone. "Defining the difference: What Makes Biologics Unique." In: *Biotechnology healthcare* 1.4 (Sept. 2004), pp. 24–29. ISSN: 1554-169X.

[390] Jenny C Mortimer and Matthew Gilliham. "SpaceHort: redesigning plants to support space exploration and on-earth sustainability". In: *Current Opinion in Biotechnology* 73 (2022), pp. 246–252. ISSN: 0958-1669. DOI: https://doi.org/10.1016/j.copbio.2021.08.018. URL: https://www.sciencedirect.com/science/article/pii/S0958166921001646.

[391] Robert W Moses and Dennis M Bushnell. "Frontier in-situ resource utilization for enabling sustained human presence on mars". In: (2016), pp. 1–55. DOI: NASA/TMâĂŞ2016-219182. URL: https://ntrs.nasa.gov/citations/20160005963.

[392] Hans-Martin Müller and Dieter Seebach. "Poly (hydroxyalkanoates): a fifth class of physiologically important organic biopolymers?" In: *Angewandte Chemie International Edition in English* 32.4 (1993), pp. 477–502. ISSN: 0570-0833.

[393] Sheeba Murad et al. "Molecular Pharming for low and middle income countries." eng. In: *Current opinion in biotechnology* 61 (Feb. 2020), pp. 53–59. ISSN: 1879-0429 (Electronic). DOI: 10.1016/j.copbio.2019.10.005.

[394] Elon Musk. "Making Humans a Multi-Planetary Species". In: *New Space* 5.2 (2017), pp. 46–61. ISSN: 2168-0256. DOI: 10.1089/space.2017.29009.emu. URL: https://www.liebertpub.com/doi/10.1089/space.2017.29009.emu.

[395] Elon Musk. "Making life multi-planetary". In: *New Space* 6.1 (2018), pp. 2–11. ISSN: 2168-0256.

[396] Jaewook Myung et al. "Expanding the range of polyhydroxyalkanoates synthesized by methanotrophic bacteria through the utilization of omega-hydroxyalkanoate co-substrates". In: *AMB Express* 7.1 (2017), p. 118. ISSN: 2191-0855.

[397] Jaewook Myung et al. "Production of nitrous oxide from nitrite in stable Type II methanotrophic enrichments". In: *Environmental science & technology* 49.18 (2015), pp. 10969–10975. ISSN: 0013-936X.

[398] Zoltan K Nagy and Richard D Braatz. "Open-loop and closed-loop robust optimal control of batch processes using distributional and worst-case analysis". In: *J. Process Control* 14.4 (2004), pp. 411–422. ISSN: 09591524. DOI: 10.1016/j.jprocont.2003.07.004.

[399] Surabhi Naik, S K Venu Gopal, and Priti Somal. "Bioproduction of polyhydroxyalkanoates from bacteria: a metabolic approach". In: *World Journal of Microbiology and Biotechnology* 24.10 (2008), p. 2307. ISSN: 0959-3993.

[400] Sidney N Nakahodo and Steven Gonzalez. "Creating Startups with NASA Technology". In: *New Space* 8.3 (2020), pp. 137–145. DOI: 10.1089/space.2020.0002. URL: https://doi.org/10.1089/space.2020.0002.

[401] Shannon N Nangle et al. "The case for biotech on Mars". In: *Nature Biotechnology* 38.4 (2020), pp. 401–407. ISSN: 1546-1696. DOI: 10.1038/s41587-020-0485-4. URL: https://doi.org/10.1038/s41587-020-0485-4%20https://www.nature.com/articles/s41587-020-0485-4.

[402] Shannon N Nangle et al. "Valorization of CO2 through lithoautotrophic production of sustainable chemicals in Cupriavidus necator". In: *Metabolic Engineering* 62 (2020), pp. 207–220. ISSN: 1096-7176. DOI: https://doi.org/10.1016/j.ymben.2020.09.002. URL: http://www.sciencedirect.com/science/article/pii/S1096717620301361.

[403] NASA. *NASA's Journey to Mars: Pioneering Next Steps in Space Exploration.* Tech. rep. 2015. DOI: NP-2015-08-2018-HQ.

[404] *NASA's Lunar Exploration Program Overview.* Tech. rep. 2020. URL: https://www.nasa.gov/sites/default/files/atoms/files/artemis_plan-20200921.pdf.

[405] M Z Naser. "Space-native construction materials for earth-independent and sustainable infrastructure". In: *Acta Astronautica* 155 (2019), pp. 264–273. ISSN: 0094-5765. DOI: https://doi.org/10.1016/j.actaastro.2018.12.014. URL: https://www.sciencedirect.com/science/article/pii/S0094576518307033.

[406] *National Aeronautics And Space Administration (NASA) Model Equal Employment Opportunity Program Status Report: FY 2019.* Tech. rep. NASA, 2020. URL: https://moon.nasa.gov/resources/23/apollo-11-landing-site/.

[407] Rafael Navarro-González et al. "Reanalysis of the Viking results suggests perchlorate and organics at midlatitudes on Mars". In: *Journal of Geophysical Research: Planets* 115.E12 (2010). ISSN: 0148-0227.

[408] Mark Nelson. "Biosphere 2's Lessons about Living on Earth and in Space". In: *Space: Science & Technology* 2021 (2021), p. 8067539. ISSN: null. DOI: 10.34133/2021/8067539. URL: https://doi.org/10.34133/2021/8067539.

[409] Eduardo Nicolau et al. "Evaluation of a Urea Bioelectrochemical System for Wastewater Treatment Processes". In: *ACS Sustainable Chemistry & Engineering* 2.4 (Apr. 2014), pp. 749–754. DOI: 10.1021/sc400342x. URL: https://doi.org/10.1021/sc400342x.

[410] Tobias Niederwieser, Patrick Kociolek, and David Klaus. "Spacecraft cabin environment effects on the growth and behavior of Chlorella vulgaris for life support applications". In: *Life Sciences in Space Research* 16 (2018), pp. 8–17. ISSN: 2214-5524. DOI: https://doi.org/10.1016/j.lssr.2017.10.002. URL: https://www.sciencedirect.com/science/article/pii/S2214552417300780.

[411] Per Halkjær Nielsen. "Microbial biotechnology and circular economy in wastewater treatment". In: *Microbial biotechnology* 10.5 (2017), pp. 1102–1105. ISSN: 1751-7915.

[412] Ahmed E S Nosseir, Angelo Cervone, and Angelo Pasini. "Modular Impulsive Green Monopropellant Propulsion System (MIMPS-G): For CubeSats in LEO and to the Moon". In: *Aerospace* 8.6 (2021). ISSN: 2226-4310. DOI: 10.3390/aerospace8060169. URL: https://www.mdpi.com/2226-4310/8/6/169.

[413] Jos G J Olivier et al. "Recent trends in global greenhouse gas emissions:regional trends 1970–2000 and spatial distributionof key sources in 2000". In: *Environmental Sciences* 2.2-3 (2005), pp. 81–99. DOI: 10.1080/15693430500400345. URL: https://doi.org/10.1080/15693430500400345.

[414] Carsten Olsen. "The Significance of Concentration for the Rate of Ion Absorption by Higher Plants in Water Culture". In: *Physiologia Plantarum* 3.2 (1950), pp. 152–164. DOI: https://doi.org/10.1111/j.1399-3054.1950.tb07498.x. URL: https://onlinelibrary.wiley.com/doi/abs/10.1111/j.1399-3054.1950.tb07498.x.

[415] C Olthoff, D Pütz, and J Schnaitmann. *Dynamic Life Support System Simulations with V-HAB*. Deutsche Gesellschaft für Luft-und Raumfahrt-Lilienthal-Oberth eV, 2015.

[416] Eiichi Ono and Joel L Cuello. *Photosynthetically Active Radiation (PAR) on Mars for Advanced Life Support*. Tech. rep. 2000.

[417] Andrew Owens and Olivier De Weck. "Systems Analysis of In-Space Manufacturing Applications for the International Space Station and the Evolvable Mars Campaign". In: *AIAA SPACE 2016*. 2016, p. 5394.

[418] Andrew Owens et al. "Benefits of additive manufacturing for human exploration of Mars". In: *45th International Conference on Environmental Systems*. Bellevue, WA: 45th International Conference on Environmental Systems, 2015, pp. 1–17. DOI: ICES-2015-287. URL: http://hdl.handle.net/2346/64526.

[419] Ramalho Tiago P et al. "Selection of Anabaena sp. PCC 7938 as a Cyanobacterium Model for Biological ISRU on Mars". In: *Applied and Environmental Microbiology* 0.0 (July 2022), pp. 00594–22. DOI: 10.1128/aem.00594-22. URL: https://doi.org/10.1128/aem.00594-22.

[420] Muthuraman Pandurangan and Doo Hwan Kim. "A novel approach for in vitro meat production". In: *Applied microbiology and biotechnology* 99.13 (2015), pp. 5391–5395. ISSN: 0175-7598.

[421] Vladislav A Parfenov et al. "Magnetic levitational bioassembly of 3D tissue construct in space". In: *Science Advances* 6.29 (2020), eaba4174. DOI: 10.1126/sciadv.aba4174. URL: https://www.science.org/doi/abs/10.1126/sciadv.aba4174.

[422] Jaesung Park et al. "Characterization of lunar dust for toxicological studies. I: Particle size distribution". In: *Journal of Aerospace Engineering* 21.4 (2008), pp. 266–271.

[423] Alok Patel et al. "A perspective on biotechnological applications of thermophilic microalgae and cyanobacteria". In: *Bioresource Technology* 278 (2019), pp. 424–434. ISSN: 0960-8524. DOI: https://doi.org/10.1016/j.biortech.2019.01.063. URL: https://www.sciencedirect.com/science/article/pii/S0960852419300768.

[424] M R Patel et al. "Annual solar UV exposure and biological effective dose rates on the Martian surface". In: *Advances in Space Research* 33.8 (2004), pp. 1247–1252. ISSN: 0273-1177.

[425] Mili Pathak and Anurag S Rathore. "Mechanistic understanding of fouling of protein A chromatography resin". In: *Journal Of Chromatography A* 1459 (Aug. 2016), pp. 78–88. ISSN: 0021-9673. DOI: 10.1016/j.chroma.2016.06.084.

[426] P M Pattison et al. "LEDs for photons, physiology and food". In: *Nature* 563.7732 (2018), pp. 493–500. ISSN: 1476-4687.

[427] Marilene Pavan et al. "Advances in systems metabolic engineering of autotrophic carbon oxide-fixing biocatalysts towards a circular economy". In: *Metabolic Engineering* 71 (2022), pp. 117–141. ISSN: 1096-7176. DOI: https://doi.org/10.1016/j.ymben.2022.01.015. URL: https://www.sciencedirect.com/science/article/pii/S1096717622000210.

[428] Ramón Pérez-Vara et al. *Overview of European Applications of EcosimPro to ECLSS, CELSS, and ATCS*. Tech. rep. 2003.

[429] Laurie J Peterson. "Environmental Control and Life Support System (ECLSS) System Engineering Workshop". In: (2009).

[430] Jennifer Piaseczny et al. "Atmospheric Dispersal of Contamination Sourced from a Putative Human Habitat on Mars". In: *AGUFM* 2019 (2019), P51C–08.

[431] Gregory P Pogue et al. "Making an ally from an enemy: plant virology and the new agriculture". In: *Annual Review of Phytopathology* 40.1 (2002), pp. 45–74. ISSN: 0066-4286.

[432] Yves Poirier et al. "Polyhydroxybutyrate, a Biodegradable Thermoplastic, Produced in Transgenic Plants". In: *Science* 256.5056 (1992), pp. 520–523. DOI: 10.1126/science.256.5056.520. URL: https://www.science.org/doi/abs/10.1126/science.256.5056.520.

[433] David Pollard, Mark Brower, and Douglas Richardson. "Progress toward automated single-use continuous monoclonal antibody manufacturing via the protein refinery operations lab". In: *Continuous Biomanufacturing-Innovative Technologies and Methods* (2017), pp. 107–130.

[434] David S F Portree. "Humans to Mars: Fifty years of mission planning, 1950-2000". In: (2001).

[435] L Poughon et al. "Simulation of the MELiSSA closed loop system as a tool to define its integration strategy". In: *Advances in Space Research* 44.12 (2009), pp. 1392–1403. ISSN: 0273-1177. DOI: https://doi.org/10.1016/j.asr.2009.07.021. URL: http://www.sciencedirect.com/science/article/pii/S0273117709005286.

[436] T J Prater, N J Werkheiser, and F E Ledbetter III. "Summary Report on Phase I and Phase II Results From the 3D Printing in Zero-G Technology Demonstration Mission. Volume II". In: (2018).

[437] T J Prater et al. "Summary report on phase I results from the 3D printing in zero g technology demonstration mission, volume I". In: (2016).

[438] Tracie Prater et al. "3D Printing in Zero G Technology Demonstration Mission: complete experimental results and summary of related material modeling efforts". In: *The International Journal of Advanced Manufacturing Technology* 101.1-4 (2019), pp. 391–417. ISSN: 0268-3768.

[439] Anastasiia Prysyazhnyuk and Carolyn McGregorAM. "Space as an Extreme Environment: Technical Considerations". In: *Engineering and Medicine in Extreme Environments*. Ed. by Tobias Cibis and Carolyn McGregor AM. Cham: Springer International Publishing, 2022, pp. 143–164. ISBN: 978-3-030-96921-9. DOI: 10.1007/978-3-030-96921-9{_}8. URL: https://doi.org/10.1007/978-3-030-96921-9_8.

[440] Daniel Pütz et al. "Development Status of the Virtual Habitat (V-HAB) Simulation System". In: 49th International Conference on Environmental Systems, 2019.

[441] Rüdiger Rackwitz. "Reliability analysis—a review and some perspectives". In: *Structural safety* 23.4 (2001), pp. 365–395.

[442] Javier C Ramirez-Perez, John A Hogan, and Peter F Strom. "Inedible biomass biodegradation for advanced life support systems: I. Composting reactor and kinetics". In: *Habitation* 11.3 (2007), pp. 105–122. ISSN: 1542-9660.

[443] Javier C Ramirez-Perez, John A Hogan, and Peter F Strom. "Inedible Biomass Biodegradation for Advanced Life Support Systems: II. Compost Quality and Resource Recovery". In: *Habitation* 11.4 (2008), pp. 163–172. ISSN: 1542-9660.

[444] Donald Rapp. "Mars ISRU technology". In: *Use of Extraterrestrial Resources for Human Space Missions to Moon or Mars*. Springer, 2013, pp. 31–90.

[445] D-N Rathi et al. "Polyhydroxyalkanoate biosynthesis and simplified polymer recovery by a novel moderately halophilic bacterium isolated from hypersaline microbial mats". In: *Journal of applied microbiology* 114.2 (2013), pp. 384–395. ISSN: 1364-5072.

[446] Anurag S Rathore et al. "Re-use of Protein A Resin: Fouling and Economics". In: *Biopharm International* 28.3 (Mar. 2015), pp. 28–33. ISSN: 1542-166X.

[447] Muhammad Razaq et al. "Influence of nitrogen and phosphorous on the growth and root morphology of Acer mono". In: *PLOS ONE* 12.2 (2017), pp. 1–13. DOI: 10.1371/journal.pone.0171321. URL: https://doi.org/10.1371/journal.pone.0171321.

[448] P L Read et al. "A GCM climate database for Mars: for mission planning and for scientific studies". In: *Advances in Space Research* 19.8 (1997), pp. 1213–1222. ISSN: 0273-1177.

[449] Vidya Sagar Reddy. "The spacex effect". In: *New Space* 6.2 (2018), pp. 125–134. ISSN: 2168-0256.

[450] Carrie A Redlich, Judy Sparer, and Mark R Cullen. "Sick-building syndrome". In: *The Lancet* 349.9057 (1997), pp. 1013–1016. ISSN: 0140-6736. DOI: https://doi.org/10.1016/S0140-6736(96)07220-0. URL: https://www.sciencedirect.com/science/article/pii/S0140673696072200.

[451] Manfred Hugh Rees. *Physics and chemistry of the upper atmosphere*. Cambridge University Press, 1989. ISBN: 0521368480.

[452] Bernd H A Rehm. "Bacterial polymers: biosynthesis, modifications and applications". In: *Nature Reviews Microbiology* 8.8 (2010), pp. 578–592. ISSN: 1740-1534. DOI: 10.1038/nrmicro2354. URL: https://doi.org/10.1038/nrmicro2354.

[453] Emmanuel D Revellame et al. "Microalgae cultivation for space exploration: Assessing the potential for a new generation of waste to human life-support system for long duration space travel and planetary human habitation". In: *Algal Research* 55 (2021), p. 102258. ISSN: 2211-9264. DOI: 10.1016/j.algal.2021.102258. URL: https://www.sciencedirect.com/science/article/pii/S2211926421000771.

[454] Christopher J Rhodes. "Only 12 years left to readjust for the 1.5-degree climate change option – Says International Panel on Climate Change report: Current commentary". In: *Science Progress* 102.1 (2019), pp. 73–87. DOI: 10.1177/0036850418823397. URL: https://doi.org/10.1177/0036850418823397.

[455] Russel E Rhodes, Edward M Henderson, and John W Robinson. "Choices for Long Term Sustainable Space Exploration and Habitation with Recommended Near Term Focus". In: *50th AIAA/ASME/SAE/ASEE Joint Propulsion Conference*. 2014, p. 3648.

[456] Bruce E Rittmann and Perry L McCarty. *Environmental biotechnology: principles and applications*. McGraw-Hill Education, 2001. ISBN: 1260440591.

[457] Andrew S Rivkin et al. "Asteroid Resource Utilization: Ethical Concerns and Progress". In: *arXiv preprint arXiv:2011.03369* (2020).

[458] K S Robinson. *Red Mars*. Mars Trilogy. HarperCollins, 1996. ISBN: 9780586213896. URL: https://books.google.com/books?id=IVxAAQAAIAAJ.

[459] Henk Rogers et al. "How to Build Moon Bases". In: *Europlanet Science Congress 2020*. Virtual: Copernicus Meetings, 2020. DOI: 10.5194/epsc2020-1026. URL: https://doi.org/10.5194/epsc2020-1026%0A.

[460] Elkin Romero and David Francisco. "The NASA human system risk mitigation process for space exploration". In: *Acta Astronautica* 175 (2020), pp. 606–615. ISSN: 0094-5765. DOI: https://doi.org/10.1016/j.actaastro.2020.04.046. URL: https://www.sciencedirect.com/science/article/pii/S0094576520302617.

[461] Lynn J Rothschild et al. *Urban biomining meets printable electronics: end-to-end at destination biological recycling and reprinting*. Tech. rep. Washington DC: National Aeronautics and Space Administration, 2017, p. 39. URL: https://ntrs.nasa.gov/api/citations/20170004558/downloads/20170004558.pdf.

[462] Lynn J. Rothschild. "Synthetic biology meets bioprinting: enabling technologies for humans on Mars (and Earth)". In: *Biochemical Society Transactions* 44.4 (2016), pp. 1158–1164. ISSN: 0300-5127. DOI: 10.1042/BST20160067. URL: http://www.biochemsoctrans.org/content/44/4/1158.

[463] Joseph Roy. "Engineering by the numbers". In: *American Society for Engineering Education*. American Society for Engineering Education, 2019, pp. 1–40.

[464] Marietta Ryba-White et al. "Growth in microgravity increases susceptibility of soybean to a fungal pathogen". In: *Plant and Cell Physiology* 42.6 (2001), pp. 657–664. ISSN: 1471-9053.

[465] Krishna Kalyani Sahoo, Gargi Goswami, and Debasish Das. "Biotransformation of Methane and Carbon Dioxide Into High-Value Products by Methanotrophs: Current State of Art and Future Prospects". In: *Frontiers in Microbiology* 12 (2021). ISSN: 1664-302X. DOI: 10.3389/fmicb.2021.636486. URL: https://www.frontiersin.org/article/10.3389/fmicb.2021.636486.

[466] Alexander F Sandahl et al. "On-demand synthesis of phosphoramidites". In: *Nature Communications* 12.1 (2021), p. 2760. ISSN: 2041-1723. DOI: 10.1038/s41467-021-22945-z. URL: https://doi.org/10.1038/s41467-021-22945-z.

[467] Gerald Sanders. "Current NASA Plans for Mars In Situ Resource Utilization". In: (2018).

[468] Rosa Santomartino, Luis Zea, and Charles S Cockell. "The smallest space miners: principles of space biomining". In: *Extremophiles* 26.1 (2022), p. 7. ISSN: 1433-4909. DOI: 10.1007/s00792-021-01253-w. URL: https://doi.org/10.1007/s00792-021-01253-w.

[469] Fabio Santoni et al. "GreenCube: microgreens cultivation and growth monitoring onboard a 3U CubeSat". In: *2020 IEEE 7th International Workshop on Metrology for AeroSpace (MetroAeroSpace)*. 2020, pp. 130–135. DOI: 10.1109/MetroAeroSpace48742.2020.9160063.

[470] Brian Sauser et al. "Determining system interoperability using an integration readiness level". In: *Stevens Institute of Technology, Systems Engineering and Engineering Management,* (2006).

[471] Brian Sauser et al. "Integration maturity metrics: Development of an integration readiness level". In: *Information Knowledge Systems Management* 9.1 (2010), pp. 17–46. ISSN: 1389-1995.

[472] Brian Sauser et al. "Optimization of system maturity and equivalent system mass for exploration systems development". In: *8th conference on systems engineering research, Hoboken, NJ, USA*. Citeseer, 2010.

[473] Brian Bruce Brian Sauser et al. *Optimization of System Maturity and Equivalent System Mass for Space Systems Engineering Management*. Tech. rep. 2010.

[474] A Schievano et al. "Two-Stage vs single-Stage thermophilic anaerobic digestion: Comparison of energy production and biodegradation efficiencies". In: *Environmental Science and Technology* 46.15 (2012), pp. 8502–8510. DOI: dx.doi.org/10.1021/es301376n.

[475] David Schlosberg and Lisette B Collins. "From environmental to climate justice: climate change and the discourse of environmental justice". In: *WIREs Climate Change* 5.3 (2014), pp. 359–374. DOI: https://doi.org/10.1002/wcc.275. URL: https://wires.onlinelibrary.wiley.com/doi/abs/10.1002/wcc.275.

[476] Lukas Schrenk. "Master Thesis Development of an In-Situ Resource Utilization (ISRU) Module for the Mission Analysis Environment HabNet". In: *Technische Universität München, Munich, Germany* (2015).

[477] Nathaniel M Schuster and Alan M Rapoport. "New strategies for the treatment and prevention of primary headache disorders". In: *Nature Reviews Neurology* 12.11 (Nov. 2016), pp. 635–650. ISSN: 1759-4758. DOI: 10.1038/nrneurol.2016.143.

[478] Gil Scott-Heron. *Whitey on the Moon*. New York, NY, Feb. 1970. URL: https://www.youtube.com/watch?v=goh2x_G0ct4.

[479] Corinne D Scown and Jay D Keasling. "Sustainable manufacturing with synthetic biology". In: *Nature Biotechnology* 40.3 (2022), pp. 304–307. ISSN: 1546-1696. DOI: 10.1038/s41587-022-01248-8. URL: https://doi.org/10.1038/s41587-022-01248-8.

[480] Ido Seginer. "A dynamic model for nitrogen-stressed lettuce." eng. In: *Annals of botany* 91.6 (May 2003), pp. 623–635. ISSN: 0305-7364 (Print). DOI: 10.1093/aob/mcg069.

[481] Giuliana Senatore et al. "Effect of microgravity & space radiation on microbes". In: *Future microbiology* 13.07 (2018), pp. 831–847. ISSN: 1746-0913.

[482] Michael Serio et al. *Pyrolysis of mixed solid food, paper, and packaging wastes*. Tech. rep. 2008.

[483] Malleshaiah SharathKumar, Ep Heuvelink, and Leo F M Marcelis. "Vertical Farming: Moving from Genetic to Environmental Modification". In: *Trends in Plant Science* 25.8 (2020), pp. 724–727. ISSN: 1360-1385. DOI: https://doi.org/10.1016/j.tplants.2020.05.012. URL: https://www.sciencedirect.com/science/article/pii/S1360138520301941.

[484] Arun Sharma et al. "Biomanufacturing in low Earth orbit for regenerative medicine." eng. In: *Stem cell reports* 17.1 (Jan. 2022), pp. 1–13. ISSN: 2213-6711 (Electronic). DOI: 10.1016/j.stemcr.2021.12.001.

[485] Gayatri Sharma and Patrick D Curtis. "The Impacts of Microgravity on Bacterial Metabolism". In: *Life* 12.6 (2022). ISSN: 2075-1729. DOI: 10.3390/life12060774. URL: https://www.mdpi.com/2075-1729/12/6/774.

[486] Stafford W Sheehan. "Electrochemical methane production from CO2 for orbital and interplanetary refueling". In: *iScience* 24.3 (2021), p. 102230. ISSN: 2589-0042. DOI: https://doi.org/10.1016/j.isci.2021.102230. URL: https://www.sciencedirect.com/science/article/pii/S258900422100198X.

[487] Roger A Sheldon. "The E factor: fifteen years on". In: *Green Chemistry* 9.12 (2007), pp. 1273–1283. ISSN: 1463-9262. DOI: 10.1039/b713736m.

[488] Rahul D Sheth et al. "Affinity Precipitation of a Monoclonal Antibody From an Industrial Harvest Feedstock Using an ELP-Z Stimuli Responsive Biopolymer". In: *Biotechnology And Bioengineering* 111.8 (Aug. 2014), pp. 1595–1603. ISSN: 0006-3592. DOI: 10.1002/bit.25230.

[489] Reshma P Shetty, Drew Endy, and Thomas F Knight. "Engineering BioBrick vectors from BioBrick parts". In: *Journal of biological engineering* 2.1 (2008), pp. 1–12. ISSN: 1754-1611.

[490] Samar Sheweka and Arch. Nourhan Magdy. "The Living walls as an Approach for a Healthy Urban Environment". In: *Energy Procedia* 6 (2011), pp. 592–599. ISSN: 1876-6102. DOI: https://doi.org/10.1016/j.egypro.2011.05.068. URL: https://www.sciencedirect.com/science/article/pii/S1876610211014792.

[491] Robert Shishko, Donald H Ebbeler, and George Fox. "NASA technology assessment using real options valuation". In: *Systems Engineering* 7.1 (2004), pp. 1–13. DOI: https://doi.org/10.1002/sys.10052. URL: https://onlinelibrary.wiley.com/doi/abs/10.1002/sys.10052.

[492] Sarah Shull and Olivier de Weck. "Modeling and Simulation of Lunar Campaign Logistics". In: *AIAA SPACE 2007 Conference \& Exposition*. 2007. DOI: 10.2514/6.2007-6244. URL: https://arc.aiaa.org/doi/abs/10.2514/6.2007-6244.

[493] Natasa Skalko-Basnet. "Biologics: the role of delivery systems in improved therapy". In: *Biologics-targets \& Therapy* 8 (2014), pp. 107–114. ISSN: 1177-5475. DOI: 10.2147/BTT.S38387.

[494] Collin Smith, Alfred K Hill, and Laura Torrente-Murciano. "Current and future role of Haber–Bosch ammonia in a carbon-free energy landscape". In: *Energy {\&} Environmental Science* 13.2 (2020), pp. 331–344.

[495] Gary C Smith. "Some Biological Considerations for a Permanent, Manned Lunar Base". In: *The American Biology Teacher* 57.2 (1995), pp. 92–98. ISSN: 0002-7685. DOI: 10.2307/4449930. URL: https://doi.org/10.2307/4449930.

[496] Jeffrey Smith, Deborah Bazar, and William Buchan. *Greenspace: Leveraging NASA Capabilities for a Cleaner, Greener Earth*. Denver, CO, 2012. DOI: 10.2514/6.2009-4583. URL: https://arc.aiaa.org/doi/abs/10.2514/6.2009-4583.

[497] Marshall Smith et al. "The Artemis Program: An Overview of NASA's Activities to Return Humans to the Moon". In: *2020 IEEE Aerospace Conference*. IEEE, 2020, pp. 1–10. ISBN: 1728127343. DOI: 10.1109/AERO47225.2020.9172323. URL: https://ieeexplore.ieee.org/document/9172323.

[498] Ricard Solé. "Bioengineering the biosphere?" In: *Ecological Complexity* 22 (2015), pp. 40–49. ISSN: 1476-945X. DOI: https://doi.org/10.1016/j.ecocom.2015.01.005. URL: https://www.sciencedirect.com/science/article/pii/S1476945X15000082.

[499] S Sommerfeld and J Strube. "Challenges in biotechnology production - generic processes and process optimization for monoclonal antibodies". In: *Chemical Engineering And Processing-process Intensification* 44.10 (Oct. 2005), pp. 1123–1137. ISSN: 0255-2701. DOI: 10.1016/j.cep.2005.03.006.

[500] Mohammad Songolzadeh et al. "Carbon Dioxide Separation from Flue Gases: A Technological Review Emphasizing Reduction in Greenhouse Gas Emissions". In: *The Scientific World Journal* 2014 (2014). Ed. by D.-W. Han and V A Rogov, p. 828131. ISSN: 2356-6140. DOI: 10.1155/2014/828131. URL: https://doi.org/10.1155/2014/828131.

[501] Gerald Sonnenfeld. "NASA Space Biology Research Associate Program for the 21st Century". In: (1999).

[502] Mathangi Soundararajan et al. "Phototrophic N2 and CO2 Fixation Using a Rhodopseudomonas palustris-H2 Mediated Electrochemical System With Infrared Photons". In: *Frontiers in microbiology* 10 (2019), p. 1817. ISSN: 1664-302X.

[503] Paul D Spudis. "An argument for human exploration of the Moon and Mars". In: *American Scientist* 80.3 (1992), pp. 269–277. ISSN: 0003-0996.

[504] Fabian Steinebach, Daniel Karst, and Massimo Morbidelli. "Design of integrated continuous processes for high-quality biotherapeutics". In: *Continuous Biomanufacturing-Innovative Technologies and Methods* (2017), pp. 457–480.

[505] P M Stella, R C Ewell, and J J Hoskin. "Design and performance of the MER (Mars Exploration Rovers) solar arrays". In: *Conference Record of the Thirty-first IEEE Photovoltaic Specialists Conference, 2005.* 2005, pp. 626–630. DOI: 10.1109/PVSC.2005.1488209.

[506] Giuseppe Strazzera et al. "Volatile fatty acids production from food wastes for biorefinery platforms: A review". In: *Journal of environmental management* 226 (2018), pp. 278–288. ISSN: 0301-4797.

[507] J Strube et al. "Process intensification in biologics manufacturing". In: *Chemical Engineering And Processing-process Intensification* 133 (Nov. 2018), pp. 278–293. ISSN: 0255-2701. DOI: 10.1016/j.cep.2018.09.022.

[508] Michael T. Suffredini. *Reference guide to the international space station.* Tech. rep. Houston, TX: National Aeronautics and Space Administration, Johnson Space Center, 2014. DOI: NP-2015-05-022-JSC.

[509] Wei Sun et al. "The bioprinting roadmap". In: *Biofabrication* 12.2 (Feb. 2020), p. 22002. DOI: 10.1088/1758-5090/ab5158. URL: https://doi.org/10.1088/1758-5090/ab5158.

[510] Akshita Swaminathan and Vinayak Malhotra. "A case study on the advancements in Mars colonization". In: *AIP Conference Proceedings.* Vol. 2341. 1. AIP Publishing LLC, 2021, p. 30019. ISBN: 0735440956.

[511] Michael Swickrath, Molly Anderson, and Robert Bagdigian. "Parametric analysis of life support systems for future space exploration missions". In: *41st International Conference on Environmental Systems.* 2011, p. 5039.

[512] Claire Sykes. "Time- and Temperature-Controlled Transport: Supply Chain Challenges and Solutions." In: *P \& T : a peer-reviewed journal for formulary management* 43.3 (Mar. 2018), pp. 154–170. ISSN: 1052-1372.

[513] Mohammad J Taherzadeh. "Bioengineering to tackle environmental challenges, climate changes and resource recovery". In: *Bioengineered* 10.1 (2019), pp. 698–699. DOI: 10.1080/21655979.2019.1705065. URL: https://doi.org/10.1080/21655979.2019.1705065.

[514] Tricia Talbert and Mike Green. *Space Technology Grand Challenges*. Tech. rep. Washington DC: National Aeronautics and Space Administration, 2010, p. 3. URL: https://www.nasa.gov/offices/oct/strategic_integration/grand_challenges_detail.html#.

[515] Dan Tan et al. "Unsterile and continuous production of polyhydroxybutyrate by Halomonas TD01". In: *Bioresource technology* 102.17 (2011), pp. 8130–8136. ISSN: 0960-8524.

[516] Frank Tavares et al. "Ethical Exploration and the Role of Planetary Protection in Disrupting Colonial Practices". In: *arXiv preprint arXiv:2010.08344* (2020).

[517] Shannon L Taylor et al. "Sintering of micro-trusses created by extrusion-3D-printing of lunar regolith inks". In: *Acta Astronautica* 143 (2018), pp. 1–8. ISSN: 0094-5765. DOI: https://doi.org/10.1016/j.actaastro.2017.11.005. URL: https://www.sciencedirect.com/science/article/pii/S0094576517310378.

[518] *Technology Drives Exploration*. Tech. rep. Washington DC: National Aeronautics and Space Administration, 2014, pp. 1–8. URL: https://www.nasa.gov/sites/default/files/atoms/files/stmd_technology_drives_exploration_508_8_11_2016.pdf.

[519] Edred Thorsson. *Futhark: A handbook of rune magic*. Weiser Books, 2020. ISBN: 1578637007.

[520] Tracy L Thumm et al. "International space station benefits for humanity". In: *63rd International Astronautical Congress (IAC2012)*. JSC-CN-25979. 2012.

[521] Rongzhen Tian et al. "Titrating bacterial growth and chemical biosynthesis for efficient N-acetylglucosamine and N-acetylneuraminic acid bioproduction." eng. In: *Nature communications* 11.1 (Oct. 2020), p. 5078. ISSN: 2041-1723 (Electronic). DOI: 10.1038/s41467-020-18960-1.

[522] Till Tiso et al. "The metabolic potential of plastics as biotechnological carbon sources – Review and targets for the future". In: *Metabolic Engineering* 71 (2022), pp. 77–98. ISSN: 1096-7176. DOI: https://doi.org/10.1016/j.ymben.2021.12.006. URL: https://www.sciencedirect.com/science/article/pii/S1096717621001920.

[523] Paul Todd. "Space Bioprocessing". In: *Bio/Technology* 3.9 (1985), pp. 786–790. ISSN: 1546-1696. DOI: 10.1038/nbt0985-786. URL: https://doi.org/10.1038/nbt0985-786.

[524] Jeff Tollefson. "IPCC says limiting global warming to 1.5 [degrees] C will require drastic action". In: *Nature* 562.7726 (2018), pp. 172–174. ISSN: 0028-0836.

[525] Chanaporn Trakunjae et al. "Enhanced polyhydroxybutyrate (PHB) production by newly isolated rare actinomycetes Rhodococcus sp. strain BSRT1-1 using response surface methodology". In: *Scientific Reports* 11.1 (2021), p. 1896. ISSN: 2045-2322. DOI: 10.1038/s41598-021-81386-2. URL: https://doi.org/10.1038/s41598-021-81386-2.

[526] Dennis S Tucker and Michael SanSoucie. "Production of ZBLAN Optical Fiber in Microgravity". In: *Optical Fiber Sensors*. Optical Society of America. 2020, T2B–1.

[527] Andrew Tylecote. "Biotechnology as a new techno-economic paradigm that will help drive the world economy and mitigate climate change". In: *Research Policy* 48.4, SI (May 2019), pp. 858–868. ISSN: 0048-7333. DOI: 10.1016/j.respol.2018.10.001.

[528] Kerstin Uhde-Holzem et al. "Production of Immunoabsorbent Nanoparticles by Displaying Single-Domain Protein A on Potato Virus X". In: *Macromolecular Bioscience* 16.2 (Feb. 2016), pp. 231–241. ISSN: 1616-5187. DOI: 10.1002/mabi.201500280.

[529] Sebastian Ulrich and Frank Ebel. "Monoclonal Antibodies as Tools to Combat Fungal Infections". In: *Journal Of Fungi* 6.1 (Mar. 2020). DOI: 10.3390/jof6010022.

[530] Jesica Urbina et al. "A new approach to biomining: Bioengineering surfaces for metal recovery from aqueous solutions". In: *Scientific Reports* 9.1 (2019), p. 16422. ISSN: 2045-2322. DOI: 10.1038/s41598-019-52778-2. URL: https://doi.org/10.1038/s41598-019-52778-2.

[531] Alfredo Ursua, Luis M Gandia, and Pablo Sanchis. "Hydrogen production from water electrolysis: current status and future trends". In: *Proceedings of the IEEE* 100.2 (2011), pp. 410–426. ISSN: 0018-9219.

[532] Jorge L Vago et al. "Habitability on Early Mars and the Search for Biosignatures with the ExoMars Rover". In: *Astrobiology* 17.6-7 (2017), pp. 471–510. ISSN: 1531-1074. DOI: 10.1089/ast.2016.1533. URL: https://doi.org/10.1089/ast.2016.1533.

[533] Marieke Vanthoor-Koopmans et al. "Biorefinery of microalgae for food and fuel". In: *Bioresource Technology* 135 (2013), pp. 142–149. ISSN: 0960-8524. DOI: https://doi.org/10.1016/j.biortech.2012.10.135. URL: https://www.sciencedirect.com/science/article/pii/S0960852412016446.

[534] Ramón Pérez Vara, Pedro Cobas Herrero, and Andrés García Parrilla. *Ecosim: A state-of-the-art continuous simulation tool for TCS and ECLSS*. Tech. rep. 1999.

[535] Venkat Venkatasubramanian et al. "A review of process fault detection and diagnosis: Part I: Quantitative model-based methods". In: *Computers \& chemical engineering* 27.3 (2003), pp. 293–311.

[536] Francesca Vergari, Arianna Tibuzzi, and Giovanni Basile. "An overview of the functional food market: from marketing issues and commercial players to future demand from life in space". In: *Bio-Farms for Nutraceuticals*. Springer, 2010, pp. 308–321.

[537] A W M Verkroost and M J Wassen. "A simple model for nitrogen-limited plant growth and nitrogen allocation". In: *Annals of Botany* 96.5 (2005), pp. 871–876. ISSN: 1095-8290.

[538] Cyprien Verseux et al. "Sustainable life support on Mars–the potential roles of cyanobacteria". In: *International Journal of Astrobiology* 15.1 (2016), pp. 65–92. ISSN: 1473-5504. DOI: 10.1017/S147355041500021X. URL: https://doi.org/10.1017/S147355041500021X.

[539] Vicente-Retortillo, Álvaro et al. "A model to calculate solar radiation fluxes on the Martian surface". In: *Journal of Space Weather and Space Climate* 5 (2015), A33. ISSN: 2115-7251. DOI: 10.1051/swsc/2015035. URL: https://doi.org/10.1051/swsc/2015035.

[540] Brian P Vickery et al. "AR101 Oral Immunotherapy for Peanut Allergy". In: *New England Journal Of Medicine* 379.21 (Nov. 2018), pp. 1991–2001. ISSN: 0028-4793. DOI: 10.1056/NEJMoa1812856.

[541] R Volger et al. "Theoretical bioreactor design to perform microbial mining activities on mars". In: *Acta Astronautica* 170 (2020), pp. 354–364. ISSN: 0094-5765. DOI: https://doi.org/10.1016/j.actaastro.2020.01.036. URL: https://www.sciencedirect.com/science/article/pii/S0094576520300564.

[542] Tyler Volk, Bruce Bugbee, and Raymond M Wheeler. "An approach to crop modeling with the energy cascade". In: *Life Support & Biosphere Science* 1.3-4 (1995), pp. 119–127. ISSN: 1069-9422.

[543] Federico Volpin et al. "Urine Treatment on the International Space Station: Current Practice and Novel Approaches." eng. In: *Membranes* 10.11 (Nov. 2020). ISSN: 2077-0375 (Print). DOI: 10.3390/membranes10110327.

[544] Martin Volz. "Materials Science on the International Space Station". In: (2018). URL: https://ntrs.nasa.gov/api/citations/20180002052/downloads/20180002052.pdf.

[545] Wernher Von Braun and Cornelius Ryan. "Can we get to Mars?" In: *Collier's* 30 (1954), pp. 22–29.

[546] Wernher Von Braun and Henry J White. *The Mars Project*. University of Illinois Press, 1953. ISBN: 0252062272.

[547] Chelsea Wald. *The urine revolution: how recycling pee could help to save the world.* eng. Feb. 2022. DOI: 10.1038/d41586-022-00338-6.

[548] Jeremy Walker and Céline Granjou. "MELiSSA the minimal biosphere: Human life, waste and refuge in deep space". In: *Futures* 92 (2017), pp. 59–69. ISSN: 0016-3287. DOI: https://doi.org/10.1016/j.futures.2016.12.001. URL: https://www.sciencedirect.com/science/article/pii/S0016328716301380.

[549] Mike Wall. "NASA's Shuttle Program Cost$209 Billion- Was it Worth It?" In: *Space News* 22.27 (2011), p. 14. ISSN: 1046-6940.

[550] G H Wang et al. "Real-time studies on microalgae under microgravity". In: *Acta Astronautica* 55.2 (2004), pp. 131–137. ISSN: 0094-5765. DOI: https://doi.org/10.1016/j.actaastro.2004.02.005. URL: https://www.sciencedirect.com/science/article/pii/S0094576504001006.

[551] Jan Weber and Jonas Schnaitmann. "A New Human Thermal Model for the Dynamic Life Support System Simulation V-HAB". In: 46th International Conference on Environmental Systems, 2016.

[552] Chris R Webster et al. "Isotope ratios of H, C, and O in CO2 and H2O of the Martian atmosphere". In: *Science* 341.6143 (2013), pp. 260–263. ISSN: 0036-8075.

[553] Cameron Kingsley Wehringer. "Spaceports–Waystations of Space". In: *Tex. L. Rev.* 40 (1961), p. 371.

[554] Niki Werkheiser. "In-space manufacturing: pioneering a sustainable path to Mars". In: (2015), pp. 1–14. DOI: NASA-M16-4949. URL: https://ntrs.nasa.gov/citations/20150022327.

[555] Stefan Werner et al. "Immunoabsorbent nanoparticles based on a tobamovirus displaying protein A". In: *Proceedings of the National Academy of Sciences* 103.47 (2006), pp. 17678–17683. ISSN: 0027-8424.

[556] James Richard Wertz, David F Everett, and Jeffery John Puschell. *Space mission engineering: the new SMAD*. Microcosm Press, 2011. ISBN: 1881883159.

[557] James Richard Wertz and Wiley J Larson. *Reducing space mission cost*. Microcosm Press Torrance, CA, 1996. ISBN: 1881883051.

[558] Paul Westgate et al. "Bioprocessing in space". In: *Enzyme and microbial technology* 14.1 (1992), pp. 76–79. ISSN: 0141-0229.

[559] Kelly M Wetmore et al. "Rapid Quantification of Mutant Fitness in Diverse Bacteria by Sequencing Randomly Bar-Coded Transposons". In: *mBio* 6.3 (2015), pp. 1–15. DOI: 10.1128/mBio.00306-15.Editor.

[560] Ruud A Weusthuis et al. "Microbial production of bulk chemicals: development of anaerobic processes". In: *Trends in Biotechnology* 29.4 (2011), pp. 153–158. ISSN: 0167-7799. DOI: https://doi.org/10.1016/j.tibtech.2010.12.007. URL: https://www.sciencedirect.com/science/article/pii/S0167779910002180.

[561] R M Wheeler et al. "Proximate composition of CELSS crops grown in NASA's biomass production chamber". In: *Advances in Space Research* 18.4-5 (1996), pp. 43–47. ISSN: 0273-1177.

[562] R. M. Wheeler et al. *Crop production for advanced life support systems-observations from the Kennedy Space Center Breadboard Project*. Tech. rep. Mountain View, CA: NASA Ames Research Center, 2003. DOI: NASA/TM-2003-211184.

[563] Raymond M Wheeler. "Agriculture for space: people and places paving the way". In: *Open agriculture* 2.1 (2017), pp. 14–32.

[564] Raymond M Wheeler. "Plants for human life support in space: from Myers to Mars". In: *Gravitational and Space Research* 23.2 (2010). ISSN: 2332-7774.

[565] Mihriban Whitmore, Jennifer Boyer, and Keith Holubec. "NASA-STD-3001, Space Flight Human-System Standard and the Human Integration Design Handbook". In: *Industrial and Systems Engineering Research Conference*. 2012.

[566] R Willians. *NASA Space Flight Human System Standard Volume 1: Crew Health*. Tech. rep. Washington DC: National Aeronautics and Space Administration, 2012. DOI: NASA-STD-3001VOL1. URL: https://standards.nasa.gov/standard/nasa/nasa-std-3001-vol-1.

[567] Jack T Wilson et al. "Equatorial locations of water on Mars: Improved resolution maps based on Mars Odyssey Neutron Spectrometer data". In: *Icarus* 299 (2018), pp. 148–160. ISSN: 0019-1035.

[568] Warren J Wiscombe. "Improved Mie scattering algorithms". In: *Applied optics* 19.9 (1980), pp. 1505–1509. ISSN: 2155-3165.

[569] Bill C Wolverton, Anne Johnson, and Keith Bounds. *Interior landscape plants for indoor air pollution abatement*. Tech. rep. Washington DC: National Aeronautics and Space Administration, 1989, pp. 1–30. DOI: NASA-TM-101766. URL: https://ntrs.nasa.gov/citations/19930073077.

[570] Bill C Wolverton and John D Wolverton. "Interior plants: their influence on airborne microbes inside energy-efficient buildings". In: *Journal of the Mississippi Academy of Sciences* 41.2 (1996), pp. 99–105.

[571] Yang Wu, Dino J Ravnic, and Ibrahim T Ozbolat. "Intraoperative Bioprinting: Repairing Tissues and Organs in a Surgical Setting". In: *Trends in Biotechnology* 38.6 (2020), pp. 594–605. ISSN: 0167-7799. DOI: https://doi.org/10.1016/j.tibtech.2020.01.004. URL: https://www.sciencedirect.com/science/article/pii/S016777992030007X.

[572] H Y Yeh et al. "ALSSAT Development Status and its Applications in Trade Studies". In: (2004).

[573] H Y Jannivine Yeh et al. *Advanced Life Support Sizing Analysis Tool (ALSSAT) Using Microsoft®Excel*. Tech. rep. 2001.

[574] H Y Jannivine Yeh et al. *ALSSAT development status*. Tech. rep. 2009.

[575] Hue-Hsia Yeh, Cheryl Brown, and Frank Jeng. "ALSSAT Version 6.0". In: (2012).

[576] Hue-Hsie Jannivine Yeh, Cheryl B Brown, and Frank J Jeng. "Tool for Sizing Analysis of the Advanced Life Support System". In: (2005).

[577] Shenghua Yin et al. "Copper Bioleaching in China: Review and Prospect". In: *Minerals* 8.2 (2018). ISSN: 2075-163X. DOI: 10.3390/min8020032. URL: https://www.mdpi.com/2075-163X/8/2/32.

[578] James L Young et al. "Direct solar-to-hydrogen conversion via inverted metamorphic multi-junction semiconductor architectures". In: *Nature Energy* 2.4 (2017), pp. 1–8. ISSN: 2058-7546.

[579] Laurence R Young and Alan Natapoff. "The Harvard-MIT PHD Program in Bioastronautics". In: *Life in Space for Life on Earth* 553 (2008), p. 90. ISSN: 9292212273.

[580] Laurence R Young and Jeffrey P Sutton. *Handbook of Bioastronautics*. Springer, 2020. ISBN: 3319101528.

[581] Paul Zabel. "Influence of crop cultivation conditions on space greenhouse equivalent system mass". In: *CEAS Space Journal* 13.1 (Jan. 2021), pp. 1–13. ISSN: 1868-2502. DOI: 10.1007/s12567-020-00317-5.

[582] David Zahavi and Louis Weiner. "Monoclonal Antibodies in Cancer Therapy". In: *Antibodies* 9.3 (Sept. 2020). DOI: 10.3390/antib9030034.

[583] Jhony Zavaleta et al. "An Automated Behavioral Analysis of Drosophila Melanogaster". In: *Annual Meeting of the American Society for Gravitational and Space Research*. 2019.

[584] Yittayih Zelalem, Joshua Drucker, and Zafer Sonmez. *National Aeronautics and Space Administration & Moon to Mars Program Economic Impact Study*. Tech. rep. Washington DC: National Aeronautics and Space Administration, 2020, pp. 1–2670. URL: https://www.nasa.gov/sites/default/files/atoms/files/nasa_economic_impact_study.pdf.

[585] Lizhan Zhang et al. "Effective production of Poly(3-hydroxybutyrate-co-4-hydroxybutyrate) by engineered Halomonas bluephagenesis grown on glucose and 1,4-Butanediol". In: *Bioresource Technology* 355 (2022), p. 127270. ISSN: 0960-8524. DOI: https://doi.org/10.1016/j.biortech.2022.127270. URL: https://www.sciencedirect.com/science/article/pii/S0960852422005995.

[586] Tian-Yuan Zhang et al. "Promising solutions to solve the bottlenecks in the large-scale cultivation of microalgae for biomass/bioenergy production". In: *Renewable and Sustainable Energy Reviews* 60 (2016), pp. 1602–1614. ISSN: 1364-0321. DOI: https://doi.org/10.1016/j.rser.2016.02.008. URL: https://www.sciencedirect.com/science/article/pii/S1364032116002161.

[587] Junli Zhao et al. "Therapeutic potential of an anti-high mobility group box-1 monoclonal antibody in epilepsy". In: *Brain Behavior And Immunity* 64 (Aug. 2017), pp. 308–319. ISSN: 0889-1591. DOI: 10.1016/j.bbi.2017.02.002.

[588] Zhu Zhongming et al. *The future is now: Science for achieving sustainable development*. Tech. rep. Global Sustainable Development Group, 2019, pp. 1–252. URL: https://sustainabledevelopment.un.org/content/documents/24797GSDR_report_2019.pdf.

[589] Andrea Zocca et al. "Challenges in the Technology Development for Additive Manufacturing in Space". In: *Chinese Journal of Mechanical Engineering: Additive Manufacturing Frontiers* (2022), p. 100018.

[590] Robert M Zubrin and David A Baker. "Mars direct: humans to the red planet by 1999". In: *Acta Astronautica* 26.12 (1992), pp. 899–912. ISSN: 0094-5765.